August 2014

Neurophysiological and Morphological Plasticity in Rat Hippocampus and Medial Prefrontal Cortex Following Trace Fear Conditioning

Chenghui Song
University of Wisconsin-Milwaukee

NEUROPHYSIOLOGICAL AND MORPHOLOGICAL PLASTICITY IN RAT

HIPPOCAMPUS AND MEDIAL PREFRONTAL CORTEX FOLLOWING TRACE

FEAR CONDITIONING

By

Chenghui Song

A Dissertation Submitted in

Partial Fulfillment of the

Requirements for the Degree of

Doctor of Philosophy

in Psychology

at

The University of Wisconsin-Milwaukee

August 2014

ABSTRACT

NEUROPHYSIOLOGICAL AND MORPHOLOGICAL PLASTICITY IN RAT

HIPPOCAMPUS AND MEDIAL PREFRONTAL CORTEX FOLLOWING TRACE

FEAR CONDITIONING

by

Chenghui Song

The University of Wisconsin-Milwaukee, 2014
Under the Supervision of Professor James R. Moyer, Jr.

Pavlovian fear conditioning provides a useful model system for investigating the mechanisms underlying associative learning. In recent years, there has been an increasing interest in "trace" fear conditioning, which requires conscious awareness of the contingency of CS and US therefore considered as a rodent model of explicit fear. Acquisition of trace fear conditioning requires an intact hippocampus and medial prefrontal cortex (mPFC), but the underlying mechanisms are still unclear. The current set of studies investigated how trace fear conditioning affects neuronal plasticity in both hippocampus and mPFC in adult rats. Trace fear conditioning significantly enhanced both intrinsic excitability and synaptic plasticity (LTP) in hippocampal CA1 neurons. Interestingly, intrinsic excitability and synaptic plasticity were significantly correlated with behavioral performance, suggesting that these changes were learning-specific. The next set of experiments investigated learning-related changes in mPFC. In order to study circuit-specific changes, only neurons that project to the basolateral nucleus of amygdala (BLA) were studied by injecting a retrograde tracer into BLA. Trace fear conditioning significantly enhanced the excitability the layer 5 (L5) projection neurons in the infralimbic

ii

(IL) subregion of mPFC whereas it decreased the excitability of L5 projection neurons in the prelimbic (PL) subregion. In both IL and PL, the conditioning effect was time-dependent because it was not observed following a retention (tested 10 days after conditioning). Furthermore, extinction reversed the conditioning effect in both IL and PL, suggesting that these changes are transient and plastic. For comparison, the effects of delay fear conditioning on mPFC neuronal excitability was also studied. These data demonstrated that in adult rats delay fear conditioning significantly enhanced the intrinsic excitability of IL but not PL neurons. However, this conditioning effect was only significant in response to stronger (e.g., larger magnitude) current injections, suggesting that this learning effect was weak. Finally, how trace fear conditioning and extinction modulate dendritic spine density of mPFC-BLA projection neurons was also studied. These data suggest that the spine density is significantly higher in L2/3 neurons than that of L5 neurons, and that extinction facilitates the elimination of spines within L2/3 neurons in both IL and PL. Together these data implicate that both neurophysiological and morphological changes within hippocampus and mPFC are critical for the acquisition and extinction of trace fear conditioning in rats.

TABLE OF CONTENTS

LIST OF FIGURES

LIST OF TABLES

LIST OF ABBREVIATIONS

General abbreviations

AHP: afterhyperpolarization

AMPA: alpha-amino-3-hydroxy-5-methyl-4-isoxazolepropionic acid

CaMKII: Ca2+/calmodulin-dependent protein kinase II

CR: Conditioned response

CREB: cAMP response element-binding

CS: conditioned stimulus

CLSM: confocal laser scanning microscopy

EPSP: excitatory postsynaptic potential

fMRI: functional magnetic resonance imaging

HCN channels: hyperpolarization-activated cyclic nucleotide-gated channels

HFS: high frequency stimulation

I_h**:** h current, an inward (depolarizing) current generated by HCN channels in response to hyperpolarization

IPSP: inhibitory postsynaptic potential

IR-DIC: infra-red differential interference contrast

ISI: Interstimulus interval

ITCs: Intercalated cells

ITI: Intertrial interval

KMeSO$_3$: potassium methylsulfonate

LTP: long term potentiation

LY: Lucifer Yellow

MAPK: mitogen-activated protein kinases

mGLuR5: Metabotropic glutamate receptor 5

MSBs: multiple synaptic boutons

MWM: Morris Water Maze

NMDA: N-methyl-D-aspartic acid

NMDAR: N-methyl-D-aspartic acid receptors

PB: phosphate buffer

PBS: Phosphate buffered saline

PFC: prefrontal cortex

PKA: protein kinase A

PKC: protein kinase C

PSD: postsynaptic density

PTSD: post-traumatic stress disorder

SK channel: small-conductance Ca^{2+}-activated K^+ channel

UR: unconditioned response

US: unconditioned stimulus

VDCC: voltage-dependent calcium cannels

VDSC: voltage-dependent sodium channels

WCR: whole-cell recording

Brain structure abbreviations

AB: accessory basal nucleus of amygdala

AC: anterior cingulate

AGm: medial agranular

BL: basolateral nucleus of amygdala

CE: central nucleus of amygdala

dmPFC: dorsal medial prefrontal cortex

FrA: frontal association cortex

IL: infralimbic subdivision of medial prefrontal cortex

LA: lateral amygdala

mPFC: medial prefrontal cortex

MTL: medial temporal lobe

PL: prelimbic subdivision of mPFC

vmPFC: ventral medial prefrontal cortex

ACKNOWLEGDEMENTS

DEDICATION

This dissertation is dedicated to my late mom Chunxiang Yu and my late brother Chengjie. I sincerely thank you both for your endless love and support while you were on this earth.

CHAPTER ONE: introduction

Pavlovian Fear Conditioning as a Model of Associative Learning

Pavlovian fear conditioning paradigms have been used extensively to study the neurobiology of learning and memory (Davis & Astrachan, 1978; Davis, Redmond, & Baraban, 1979; Doyere, Debiec, Monfils, Schafe, & LeDoux, 2007; Fanselow & Poulos, 2005; LeDoux, 2000; Moyer & Brown, 2006). In these paradigms, a neutral conditioned stimulus (CS, such as a tone) is paired with an aversive unconditioned stimulus (US, such as a footshock), which evokes an unconditioned response (URs, such as fear). After a few pairs of CS-US presentations, the CS alone elicits a variety of defensive responses that share characteristics of innate fear, such as freezing in rodents. Because these responses are not elicited by the CS before conditioning, they are referred to as learned or conditioned responses (CRs) (Blanchard & Blanchard, 1969).

Pavlovian fear conditioning has been investigated in laboratory rodents because the learned behavior (freezing) occurs in both laboratory situations and the natural environment. Furthermore, findings with rodents have been replicated with humans via functional magnetic resonance imaging (fMRI). For example, damage to the amygdala impairs fear conditioning in both humans and rodents (Bechara *et al.*, 1995; LaBar & LeDoux, 1996; LaBar, LeDoux, Spencer, & Phelps, 1995), and amygdala activity is increased during acquisition and recall of conditioned fear (Buchel, Morris, Dolan, & Friston, 1998; Cheng, Knight, Smith, Stein, & Helmstetter, 2003; Knight, Smith, Stein, & Helmstetter, 1999; LaBar, Gatenby, Gore, LeDoux, & Phelps, 1998). Clinically, Pavlovian fear conditioning has been studied as a model of post-traumatic stress disorder (PTSD), a

severe anxiety disorder that is characterized by intense fear and helplessness after being exposed to or witnessing a traumatic event such as military combat, violent personal assault, natural or manmade disaster (DSM–IV–TR. American Psychiatric Association, 2000). Thus, the study of Pavlovian fear conditioning in rodents may have important implications for understanding the mechanism and pathology of learning and memory in humans.

Paradigms and underlying mechanisms of Pavlovian fear conditioning – an overview. For cued fear conditioning, there are two commonly used paradigms depending on the timing of the predictive CS and the aversive US – delay and trace. In delay conditioning, the CS precedes and temporally overlaps with the US (see Figure 1A). In trace conditioning, however, a stimulus-free trace interval is interposed between the CS offset and the US onset (see Figure 1B). This subtle temporal variation between the two paradigms dramatically impacts the brain structures necessary for learning the CS-US relationship. The acquisition of delay fear conditioning requires intact amygdala and brainstem structures (for review see LeDoux, 2000). Whereas in the trace paradigm, in addition to the amygdala and brainstem structures, medial temporal lobe and higher cortical structures are also required for learning (Gilmartin & Helmstetter, 2010; Kholodar-Smith, Boguszewski, & Brown, 2008; McEchron, Bouwmeester, Tseng, Weiss, & Disterhoft, 1998; Quinn, Oommen, Morrison, & Fanselow, 2002; Suh, Rivest, Nakashiba, Tominaga, & Tonegawa, 2011). In either paradigm, the conditioned fear response can also be established to the context where the animals received the US presentations. Such contextual fear memory can be formed with or without the presence of the cue and requires both amygdala and hippocampus (Kim & Fanselow, 1992; LaBar *et al.*, 1995).

A. Delay fear conditioning paradigm

B. Trace fear conditioning paradigm
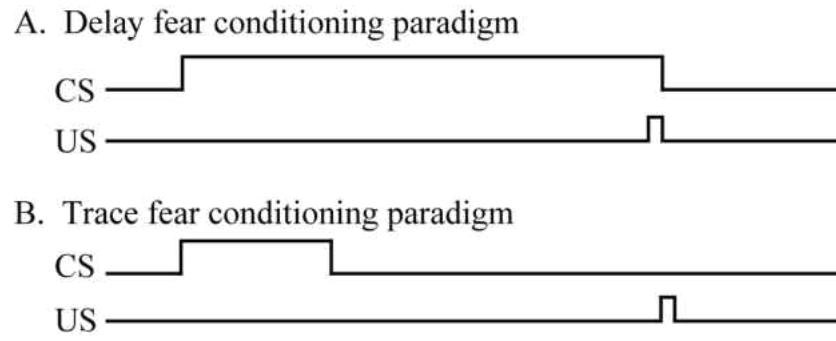
Figure 1. Two commonly used behavioral paradigms of Pavlovian fear conditioning. A, In delay fear conditioning, the CS precedes and temporally overlaps with the US. B, In trace fear conditioning, a stimulus-free trace interval is interposed between the CS offset and the US onset.

The brain circuits involved in the acquisition and recall of conditioned fear have been well studied and include critical brainstem structures in addition to higher cortical and subcortical structures (LeDoux 2000). The major higher brain regions include the amygdala, the hippocampus, and the medial prefrontal cortex (mPFC). Specifically, the amygdala is required for fear acquisition and fear memory expression (for review see LeDoux, 2000; Maren & Quirk, 2004). The hippocampus encodes contextual information (Kim & Fanselow, 1992; Phillips & LeDoux, 1992) and (along with other MTL structures) is required in the trace fear conditioning paradigm (McEchron et al., 1998). The mPFC is critical for acquisition of trace fear memory (Gilmartin & Helmstetter, 2010) and the retrieval of long term conditioned fear (Burgos-Robles, Vidal-Gonzalez, & Quirk, 2009; Runyan, Moore, & Dash, 2004).

Bidirectional modification of synaptic efficiency (synaptic plasticity) and intrinsic excitability (intrinsic plasticity) is thought to underlie the cellular basis of certain types of learning and memory, including Pavlovian fear conditioning (Bear & Abraham, 1996; Dudek & Bear, 1993; M. A. Lynch, 2004; Zhang & Linden, 2003). For example, a learning-specific enhancement of basal synaptic transmission or long-term potentiation (LTP) has been observed in amygdala (Nabavi et al., 2014) or hippocampus following fear conditioning (Doyere et al., 1995; Song, Detert, Sehgal, & Moyer, 2012). Interestingly, acquisition of Pavlovian fear conditioning also enhances the intrinsic excitability of hippocampal neurons, as evidenced by a reduced post-burst afterhyperpolarization (AHP) and a decrease in spike-frequency adaptation (Kaczorowski & Disterhoft, 2009; McKay, Matthews, Oliveira, & Disterhoft, 2009; Song et al., 2012). Furthermore, it has been hypothesized that the enhancement of synaptic plasticity emerges as a result of intrinsic

plasticity (Kramar *et al.*, 2004; Sah & Bekkers, 1996; Song *et al.*, 2012) and thus contributes to learning.

Trace fear conditioning as a model of declarative memory. Trace and delay fear conditioning have been used to study two types of memory – declarative and non-declarative respectively. Declarative (explicit) memory refers to memories that can be consciously recalled, such as facts and events (Eichenbaum, 1997). In contrast, non-declarative (implicit) memory refers to procedural memories that do not require conscious recollection. In human subjects, measuring the ability to recall the presented stimuli has been used to measure conscious awareness. Studies have demonstrated that awareness of the CS-US contingency is required for acquisition of trace but not delay fear conditioning (Clark & Squire, 1998; Knight, Cheng, Smith, Stein, & Helmstetter, 2004; Knight, Nguyen, & Bandettini, 2006; Weike, Schupp, & Hamm, 2007), and that the activity in hippocampus is stronger in the subjects that predicted the US more accurately during the trace interval than in the subjects that predicted poorly (Knight *et al.*, 2004). Thus, during trace fear conditioning, the subjects not only acquire the affective response to the CS but also acquire the explicit declarative knowledge of the CS–US contingencies (Weike *et al.*, 2007). Awareness requires multiple cortical areas including MTL, PFC and parietal cortex (for review, see Rees, 2007), all of which are also activated during trace fear conditioning (Knight *et al.*, 2004). Thus, trace fear conditioning may be an excellent paradigm for studying the mechanisms of explicit memory and learning-related changes in higher-order brain regions, including hippocampus and mPFC.

Extinction of Pavlovian fear memory as a model of cognitive flexibility. Following acquisition of conditioned fear, repeated exposure to the CS in the absence of

the US causes a weakening of the learned CR, a process known as extinction. Behavioral studies indicate that extinction does not simply erase conditioned memory but involves a new learning to inhibit the CR (Barrett, Shumake, Jones, & Gonzalez-Lima, 2003; Bouton, 1993; I. P. Pavlov, 1927; Quirk, 2002; Rescorla, 2001). Extinction of Pavlovian fear conditioning therefore has been studied as a model of cognitive flexibility, which is the ability of an organism to change or switch established behaviors in response to changes in environmental contingencies or rules (Kaczorowski, Davis, & Moyer, 2012; Miyake *et al.*, 2000; Moore & Malinowski, 2009).

Extinction deficits as a model of anxiety disorders. Poor cognitive flexibility leads to greater resistance to extinction and is associated with anxiety disorders such as PTSD, which is the failure to inhibit maladaptive responses following being exposed to traumatic events (Orr *et al.*, 2000; Peri, Ben-Shakhar, Orr, & Shalev, 2000; Wessa & Flor, 2007). The individual initially responds to the traumatic stimuli with intense fear, helplessness, or horror. The characteristic symptoms resulting from being exposed to the trauma include re-experiencing the traumatic event, avoiding reminders of the trauma, and increased anxiety and arousal. Neuroimaging studies in human PTSD patients indicate that the amygdala is more responsive whereas the mPFC is less responsive during the presentation of traumatic-related stimuli (Rauch *et al.*, 1996; Shin *et al.*, 2004). Furthermore, both mPFC and hippocampus are volumetrically smaller in PTSD patients than in trauma-exposed non-PTSD control subjects (Bremner *et al.*, 2003; Gurvits *et al.*, 1996; Rauch *et al.*, 2003; Yamasue *et al.*, 2003). These neuroimaging findings suggest that the traumatic stress may have damaged the hippocampus and the mPFC, thus impairing cognitive functions that depend on these brain areas (e.g., working memory and long-term

declarative memory). Consistent with these data, aged PTSD patients are found to have a higher risk of dementia, which is a serious loss of cognitive ability (Yaffe *et al.*, 2010). Because PTSD is characterized by intense fear to previous traumatic-related stimuli, elucidating the brain circuits responsible for acquisition and extinction of conditioned fear is not only critical for understanding the basic mechanisms of learning and memory, but also helpful in screening for the treatment of anxiety disorders such as PTSD and other age-related cognitive decline.

Major Brain Areas Involved in Pavlovian Fear Conditioning and Extinction

   The amygdala is essential for acquisition and expression of conditioned fear. The amygdaloid complex is an almond-shaped structure located within the medial temporal lobe, and it has at least 12 interconnected sub-regions (Krettek & Price, 1978; LeDoux, Cicchetti, Xagoraris, & Romanski, 1990; Romanski, Clugnet, Bordi, & LeDoux, 1993; Romanski & LeDoux, 1992; Turner & Zimmer, 1984). The areas that are thought to be most relevant to fear conditioning include the lateral (LA), basolateral (BL), accessory basal (AB), and central (CE) nuclei and their connections (see Figure 2). Sometimes LA, BL and AB are collectively termed the basolateral complex or BLA (LeDoux, 2000; Maren, 2011).

   During auditory fear conditioning, both the CS (e.g., a neutral tone) and the US (e.g., a nociceptive footshock) inputs terminate mainly in the LA. The CS comes from both the auditory thalamus and auditory cortex (LeDoux, Farb, & Ruggiero, 1990), and the US comes from both the thalamus and somatosensory cortex (LeDoux, Cicchetti, *et al.*, 1990; McDonald, 1998). The CS and US inputs converge in LA and induce synaptic plasticity such that after conditioning, the LA neurons are more responsive to the CS alone
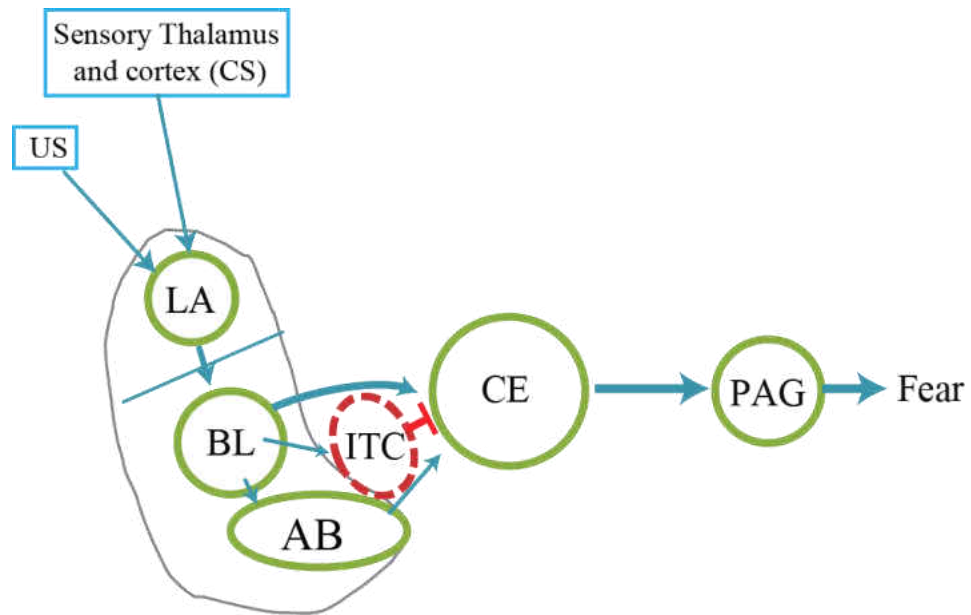
Figure 2. Major structures of the amygdala and the information flow. The amygdaloid complex (includes LA, BL, AB, ITC, CE and other nuclei) is the center of emotional control. Sensory information converges in LA and then is processed in the BL and AB. The information is finally integrated again in the CE, which in turn activates the periaqueductal gray area (PAG) and produce fear. The ITC masses is a collect of GABAergic interneurons located between the BLA and the CE and is critical for adjusting fear expression. LA, lateral; BL, basolateral; AB, accessory basal; CE, central nucleus of amygdala. LA, BL, and AB are usually collectively termed as basolateral complex of amygdala (BLA).

presentation and generate larger field potentials after conditioning (McKernan & Shinnick-Gallagher, 1997; Pare & Collins, 2000; Quirk, Repa, & LeDoux, 1995; Rogan, Staubli, & LeDoux, 1997). The integrated information is then fed into other amygdala nuclei (e.g., BL and AB) and finally converges again in the CE (Canteras & Swanson, 1992). The AB also receives contextual information from hippocampus (Bernard & Besson, 1990; Burstein & Potrebic, 1993). The CE integrates both intra- (e.g., LA, BL, and AB) and extra- (e.g., nociceptive stimuli) amygdala stimuli and is the major output of the whole amygdala. The CE produces both autonomic emotional responses (e.g., changes in heart rate, blood pressure, and respiration) through the output pathways to the hypothalamus and brain stem areas (Gray, Carney, & Magnuson, 1989; LeDoux, Iwata, Cicchetti, & Reis, 1988). In rodents, fear conditioning induces freezing through activation of the pathway from the CE to the periaqueductal gray (PAG). Thus, the acquisition and expression of conditioned fear involves the coordination of multiple subregions within amygdala in response to sensory inputs.

The aforementioned network within the amygdala uses glutamate as a neurotransmitter. In addition to these excitatory neurons, there are also inhibitory GABAergic interneurons that play important roles for normal amygdala functions (Royer, Martina, & Pare, 1999). Some GABAergic neurons are diversely distributed throughout the whole amygdala complex with higher concentration in the basolateral complex (Pare & Smith, 1993a). There are also clusters of GABAergic neurons located between the basolateral complex and CE, which are known as intercalated cells (ITCs). The GABAergic neurons in BL and the intercalated cell mass receive strong projections from infralimbic (IL) subregion of mPFC and is related to fear suppression during extinction

(McDonald & Augustine, 1993; Pare & Smith, 1993b). It has been shown that extinction is associated with potentiation of BLA inputs to ITC cells, which inhibits fear expression (Amano, Unal, & Pare, 2010). Thus, within the amygdala, the balance between the glutamatergic excitatory system and the GABAergic inhibitory system determines the level of fear expression.

Hippocampus is critical for emotional responses and memory formation. The hippocampus is a major component of the limbic system located in the medial temporal lobe. The critical role of the hippocampus is the formation and consolidation of new memories. This mnemonic function of the hippocampus was not unveiled until the report of patient H.M., who underwent bilateral resection of the medial temporal lobe (MTL) including most of the hippocampus, parahippocampal gyrus, and amygdala, in an attempt to stop his intractable epileptic seizures. After surgery, the seizures were controlled, but H.M. suffered severe anterograde amnesia (Scoville & Milner, 1957; Squire, 2009). Since then, a great deal of research has confirmed the critical role of hippocampus in memory acquisition and consolidation, especially for declarative memory. During declarative memory formation and retrieval, hippocampus is required for processing spatial information (i.e., the contextual information), temporal ordering (e.g., the temporal relation between the CS and US in trace fear conditioning) and sequential ordering of the environmental signals (Bangasser, Waxler, Santollo, & Shors, 2006; Fortin, Agster, & Eichenbaum, 2002; O'Keefe & Dostrovsky, 1971; Sweatt, 2004). Furthermore, recent studies suggest that the hippocampus is functionally differentiated along the dorsoventral (septotemporal) axis as evidenced by variations in its connections with other cortical and subcortical regions (M. B. Moser & Moser, 1998). In addition, according to studies in

rodents, the hippocampus only plays a transient role (up to 7 days) in memory acquisition (Kim & Fanselow, 1992; Moyer, Thompson, & Disterhoft, 1996). After memory consolidation, the mPFC but not hippocampus is required for memory retrieval (Corcoran & Quirk, 2007; Sierra-Mercado, Corcoran, Lebron-Milad, & Quirk, 2006).

   Anatomical and functional dissociation between dorsal and ventral hippocampus. It has been established that the hippocampus does not function uniformly but differently along the dorsal-ventral axis (Fanselow & Dong, 2011; M. B. Moser & Moser, 1998). The dorsal hippocampus, defined as the septal two-thirds of the hippocampus, performs primarily cognitive functions through the reciprocal innervations with auditory, visual and somatosensory cortices and thalamus. The ventral hippocampus, defined as the temporal one-third of the hippocampus, regulates stress, emotion, and affect through the reciprocal projections with the amygdala, the hypothalamus, and the nucleus accumbens (Czerniawski, Yoon, & Otto, 2009; M. B. Moser & Moser, 1998; M. B. Moser, Moser, Forrest, Andersen, & Morris, 1995; Witter, Groenewegen, Lopes da Silva, & Lohman, 1989). The study conducted by Moser and colleagues (1995) demonstrated that lesions to dorsal (but not the ventral) hippocampus impaired spatial memory. Furthermore, lesions in dorsal hippocampus impaired both contextual and trace fear conditioning (Chowdhury, Quinn, & Fanselow, 2005; Esclassan, Coutureau, Di Scala, & Marchand, 2009; Kim & Fanselow, 1992), perhaps because the ability of establishing the association between the CS and US is attenuated. Thus, dorsal hippocampus is crucial for the processing of spatial, temporal and relational associations between stimuli. The ventral hippocampus is involved in emotion-related processes, through the dense projections to the amygdala and hypothalamus. Lesions in ventral hippocampus impair most forms of fear

conditioning including contextual and trace fear conditioning, as well as delay fear conditioning (Bast, Zhang, & Feldon, 2001; Esclassan *et al.*, 2009; Richmond *et al.*, 1999). However, some controversial results exist regarding the role of ventral hippocampus in contextual fear conditioning, as ventral hippocampal lesions did not significantly attenuate conditioned fear (e.g., Kjelstrup *et al.*, 2002).

Transient role of hippocampus in memory acquisition and consolidation. In patient H.M., the detrimental effect of hippocampectomy on recent, but not remote memories has attracted a great deal of research interest (Scoville & Milner, 1957). This effect has been replicated in experiments from non-human primates and other lower mammals. For example, monkeys with hippocampal lesions showed retrograde amnesia that was more severe for recently learned than remotely learned memories (Zola-Morgan & Squire, 1990). Likewise, numerous studies in rodents have also demonstrated that hippocampal lesions only disrupt recent (e.g., 1 day after training), but not remote (e.g., 7 days or later) contextual or trace memory (Anagnostaras, Maren, & Fanselow, 1999; Bontempi, Laurent-Demir, Destrade, & Jaffard, 1999; Frankland *et al.*, 2004; Kim & Fanselow, 1992; Maren, Aharonov, & Fanselow, 1997; Teng & Squire, 1999). It has also been demonstrated that the neocortices, including prefrontal and anterior cingulate cortices, are critical for the storage and retrieval of remote memory (Bontempi *et al.*, 1999; Maviel, Durkin, Menzaghi, & Bontempi, 2004; Squire, 1992). Thus, it seems that memories are initially acquired in hippocampus, then stored in other cortical areas and transformed into permanent memories, a process known as consolidation (Dudai, 2004; Frankland & Bontempi, 2005).

Medial prefrontal cortex (mPFC) is critical for fear memory retrieval. The medial prefrontal cortex (mPFC) is important for working memory and a variety of executive functions, including emotional responses and decision making (Heidbreder & Groenewegen, 2003; Neafsey, 1990). In rats, the mPFC can be divided into the medial agranular (AGm), dorsal and ventral anterior cingulate (AC), the prelimbic (PL), and the infralimbic (IL) cortices (Heidbreder & Groenewegen, 2003; Ongur & Price, 2000; Vertes, 2004). According to anatomical and functional diversities, the mPFC can be roughly divided into dorsal and ventral portions. The dorsal part of mPFC (dmPFC, including AGm and AC) is associated with motor behaviors such as eye movements (Donoghue & Wise, 1982), while the ventral regions (vmPFC, including PL and IL) have been implicated in diverse emotional, cognitive, and mnemonic processes (Heidbreder & Groenewegen, 2003; Vertes, 2004). As illustrated in Figure 3, anatomical studies and *in vivo* recordings have demonstrated that ventral mPFC has reciprocal innervations with the amygdala (McDonald, 1991; McDonald, Mascagni, & Guo, 1996), the hippocampus (Parent, Wang, Su, Netoff, & Yuan, 2010), the nucleus accumbens (McGinty & Grace, 2008), the raphe nucleus (Baratta *et al.*, 2009) and other cortical and subcortical regions (Hoover & Vertes, 2007; Vertes, 2004). The anatomical connections between the mPFC and amygdala, hippocampus, and accumbens are particularly important for processing the emotional information.

Different roles of the PL and IL in fear regulation. A majority of studies suggests that the PL and IL cortices play opposing roles in emotional responses, such that activation of PL neurons facilitates fear expression and impairs extinction (Burgos-Robles *et al.*, 2009; Vidal-Gonzalez, Vidal-Gonzalez, Rauch, & Quirk, 2006), whereas activation IL
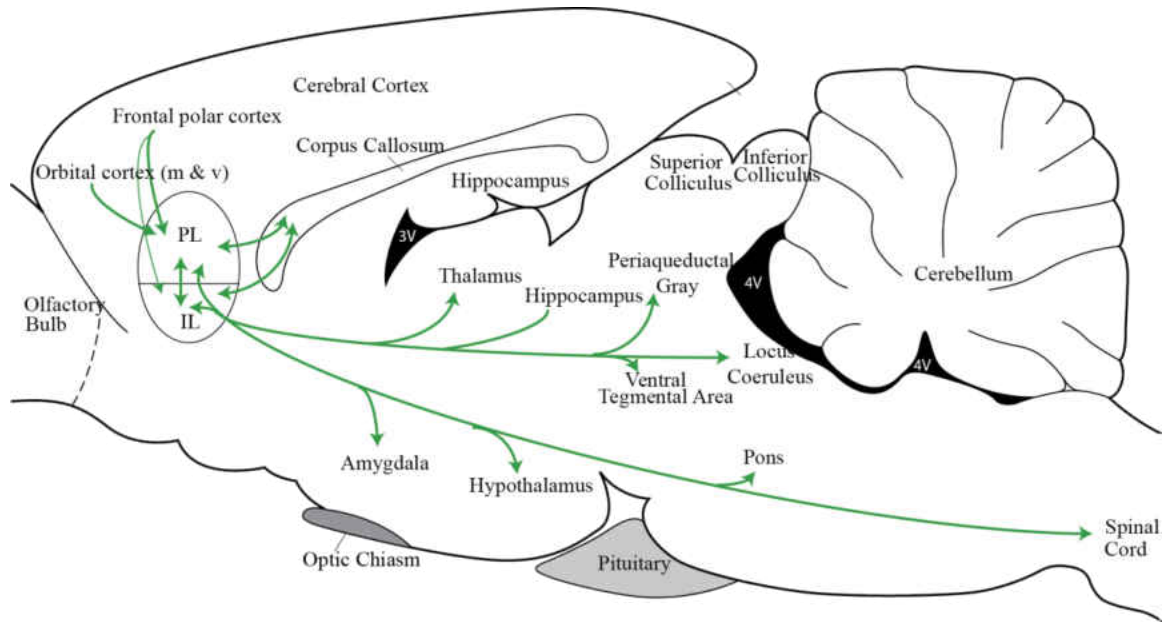
Figure 3. Anatomical location and the projections of ventral mPFC. PL and IL only receive adjacent cortical projections but have intense reciprocal projections with most subcortical brain regions. PL and IL also project to contralateral mPFC through corpus callosum. IL, infralimbic; mPFC, medial prefrontal cortex; PL, prelimbic. Illustration was modified from Paxinos & Watson (1998), with permission from *Elsevier*.

neurons reduces fear and facilitates extinction (Burgos-Robles, Vidal-Gonzalez, Santini, & Quirk, 2007; Chang & Maren, 2011; Milad & Quirk, 2002; Milad, Vidal-Gonzalez, & Quirk, 2004; Vidal-Gonzalez *et al.*, 2006). Consistent with the differential roles of PL and IL activation, pharmacological inactivation of PL neurons impairs fear memory recall (Blum, Hebert, & Dash, 2006), whereas lesions of IL neurons impair the expression of extinction memory (Quirk, Russo, Barron, & Lebron, 2000). Furthermore, in rodents PL lesions specifically impair the recall of conditioned fear memory, but not the acquisition of conditioned fear, nor any innate fear such as freezing in response to the presentation of a cat (Corcoran & Quirk, 2007), whereas IL lesions specifically impair the retention of extinction memory but not the acquisition of extinction (Burgos-Robles *et al.*, 2007; Lebron, Milad, & Quirk, 2004; Quirk *et al.*, 2000). Moreover, Lebron's study (2004) revealed that although lesions in IL impaired extinction memory when tested 1 day after extinction training, the animals displayed savings of extinction memory (residual low level of freezing) in the following 5 days. Thus, IL lesions do not abolish extinction memory, suggesting that IL is not the only location where the extinction memory is stored, instead it may be a part of a more distributed extinction memory circuit.

Consistent with the findings from mPFC stimulation and lesion studies, neuroimaging studies have also demonstrated that IL is more active during extinction memory recall. For example, metabolic mapping in mice with fluorodeoxyglucose (a radiolabeled glucose analog) revealed that IL activity was significantly increased during the retrieval of extinction memory (Barrett *et al.*, 2003). In human subjects, retrieval of extinction memory increases ventral mPFC activity as indicated in an fMRI study (Phelps, Delgado, Nearing, & LeDoux, 2004). The increase in IL activity during extinction memory

retrieval suggests that the function of IL is to inhibit the conditioned fear. Therefore, IL malfunction would lead to extinction deficits. Consistent with this, PTSD patients (characterized by extinction failure) have been found to have decreased metabolism in vmPFC compared to control subjects without PTSD (Bremner, Narayan, *et al.*, 1999; Bremner, Staib, *et al.*, 1999; Shin *et al.*, 2005). All these studies suggest that IL activation is necessary for extinction memory retrieval.

Although many studies support the model that PL facilitates fear expression and IL suppresses fear, there are studies that appear to contradict these findings. For example, LeDoux and colleagues (Morgan & LeDoux, 1995) have reported that lesions in dorsal mPFC including cingulate area 1 and dorsal PL enhanced the expression of conditioned fear, which is supported by a study by Thompson and colleagues (Garcia, Vouimba, Baudry, & Thompson, 1999) that demonstrated that the spontaneous activity of PL neurons was suppressed by CS presentations and that the unit activity was negatively correlated with the amount of freezing during memory test. There are also conflicting data regarding the role of IL in fear memory retrieval. For example, the work by Quirk and colleagues (Santini 2008) indicates that fear conditioning suppresses the excitability of IL neurons but has no effect on PL neurons. In contrast, an *in vivo* study of olfactory fear conditioning by Grace and colleagues (Laviolette, Lipski, & Grace, 2005) demonstrated that mPFC (both IL and PL) neurons that received monosynaptic and orthodromic inputs from the basolateral nucleus of amygdala (BL-responsive mPFC neurons) increased spontaneous activity in response to the odors that were previously paired with footshock. In another study, Grace and colleagues (McGinty & Grace, 2008) isolated the mPFC neurons that project to the nucleus accumbens (mPFC-NAcc) and the mPFC to mPFC (mPFC-mPFC)

projection neurons and found that BLA stimulation specifically excited the BLA-responsive mPFC-NAcc projection neurons but inhibited mPFC-NAcc nonresponsive neurons or mPFC-mPFC projection neurons. Furthermore, most mPFC-NAcc responsive neurons were located in IL and dorsal peduncular (DP) and displayed elevated spontaneous activity to conditioned odor compared to other neurons. However, no conditioning-induced effect was discovered when all neurons were analyzed together (McGinty & Grace, 2008). It is possible that these conflicting results stem from the fact that neurons that project to different targets have distinct physiological properties (i.e., heterogeneity) and play distinct roles during fear conditioning.

   Heterogeneity of mPFC projection neurons. Cortical neurons are heterogeneous in anatomical and physiological properties depending on their long-range projection targets (Dembrow, Chitwood, & Johnston, 2010; Hattox & Nelson, 2007; Larkman & Mason, 1990; Mason & Larkman, 1990; Xiao, Zikopoulos, & Barbas, 2009). For example, within PL, neurons that project to the pons (corticopontine neurons) display lower steady-state input resistance and lower intrinsic excitability compared to the neurons that project to the contralateral PL (commissural projection neurons), perhaps because of the differential expression of hyperpolarization-activated cyclic nucleotide-gated (HCN) channels (Dembrow *et al.*, 2010). This suggests that different projection neurons may respond differently to the same sensory input, and that elucidating how these neurons communicate within the local network may be important for understanding the mechanisms of learning and memory (Llano & Sherman, 2009; Molnar & Cheung, 2006). Consistent with this, corticopontine neurons are found to be more responsive to cholinergic modulation than commissural neurons, because they are more likely to fire persistently in response to the

cholinergic agonist carbachol (Dembrow *et al.*, 2010). Persistent firing activity is characterized by prolonged firing activity after the neurons have received suprathreshold stimulation. Because persistent activity occurs when the stimulation has ceased, it has been hypothesized as a cellular mechanism of working memory by holding the internally or externally driven sensory stimuli (Egorov, Hamam, Fransen, Hasselmo, & Alonso, 2002; Siegel, Kalmbach, Chitwood, & Mauk, 2011). In fact, recent studies have indicated that commissural projection neurons and subcortical projection neurons might have generated from distinct progenitors during development, therefore have different gene expression profiles and display distinct properties and functions (Molyneaux *et al.*, 2009; Molyneaux, Arlotta, Menezes, & Macklis, 2007). Moreover, the different projection neurons may play distinct roles during cognition. For example, it has been demonstrated that electrical stimulation of BLA or presentation of a Pavlovian fear conditioned odor to anesthetized rats selectively activates the IL neurons that project to the nucleus accumbens but not contralateral mPFC (McGinty & Grace, 2008). Although enough evidence has demonstrated the important role of mPFC neurons in Pavlovian fear conditioning and extinction, most studies have been carried out in unidentified neurons. Thus, to fully understand role of mPFC in Pavlovian fear conditioning and extinction, it might be necessary to identify the subpopulations of projection neurons and study their functions.

Functional Plasticity of Physiological Properties as a Mechanism of Associative Learning

  Synaptic plasticity. Hebb (1949) postulated that synaptic strength (or efficiency) increases when a postsynaptic neuron receives repeated and persistent stimulation from a presynaptic neuron. This theory is known as "cells that fire together, wire together" but it

was not demonstrated until the discovery of the phenomenon of long-term potentiation (LTP), which involves a robust and persistent enhancement of synaptic strength following high frequency stimulation (HFS). LTP was first discovered in the rabbit hippocampus (Bliss & Lomo, 1973). The hippocampus was studied because of its well-defined trisynaptic circuit and important roles in learning and memory. In the original study, Bliss and Lomo found a persistent potentiation (> 10 h) at the perforant path – granule cell synaptic transmission in the hippocampal dentate gyrus after a brief HFS. Since then, LTP has been observed in a variety of other neural structures including the prefrontal cortex, the visual cortex, the cerebellum, the amygdala, and many others that are known to participate in learning and higher cognitive function (e.g., Artola & Singer, 1987; Chapman, Kairiss, Keenan, & Brown, 1990; Laroche, Jay, & Thierry, 1990; Racine, Wilson, Gingell, & Sunderland, 1986). For example, Thomas Brown's lab (Chapman *et al.*, 1990) was the first to show LTP in cortical-LA pathways, which has been considered as a cellular mechanism of learning and memory of fear conditioning (LeDoux, 2000). In addition, a great deal of research has been focused on the correlation between LTP and learning, trying to demonstrate a causal link between LTP and learning (see discussion below).

The correlation between learning and LTP. The first demonstration that provided a possible causal link between LTP and behavioral learning utilized the Morris water maze (MWM) paradigm, a spatial memory task that depends upon the hippocampus. Blockade of NMDARs, shown to be critical for LTP induction at these synapses, was sufficient to impair both LTP and spatial learning *in vivo* (Morris, Anderson, Lynch, & Baudry, 1986). *In vitro* experiments in this same study also confirmed that NMDA receptor blockers impaired LTP induction on hippocampus slices.

Strong evidence of the correlation between behavioral learning and LTP comes from studies that conducted both behavioral training and electrophysiological recordings on the same animals. For example, field potential recordings performed in brain slices from rabbits that learned trace eyeblink conditioning demonstrated a learning-specific, time-dependent enhancement of baseline synaptic responses in CA1 evoked by Schaffer collateral stimulation (e.g., Power, Thompson, Moyer, & Disterhoft, 1997). Such enhancement of synaptic transmission was only observed in slices prepared 1 h (but not 24 h) after learning (Power *et al.*, 1997). Likewise, field recordings from the hippocampus of freely moving animals suggest that acquisition of trace eyeblink (e.g., Gruart, Munoz, & Delgado-Garcia, 2006) or fear (e.g., Doyere *et al.*, 1995) conditioning is accompanied by a facilitation of basal synaptic transmission. *In each case these LTP-like changes could be observed within 1 h after learning, and suggest* that an LTP-like change can occur during certain learning tasks, but that this change is transient and not observed 24 h later. Interestingly, studies have also demonstrated that after learning, LTP induction is facilitated (Barnes, 1979; Boric, Munoz, Gallagher, & Kirkwood, 2008; Gruart *et al.*, 2006) and that learning ability is positively correlated with the amount of hippocampal LTP after learning (Barnes, 1979; Boric *et al.*, 2008; Song *et al.*, 2012; Tombaugh, Rowe, Chow, Michael, & Rose, 2002). The enhancement of synaptic plasticity following behavioral learning strongly suggests that LTP is a biological substrate for learning and memory.

LTP saturation impairs learning. It has been predicted that LTP and learning should interfere with each other if they share the common cellular pathways. Thus, saturation of LTP in a given pathway should impair learning that depends on that pathway, and *vice versa* (M. A. Lynch, 2004). This has been demonstrated by Barnes and colleagues

(1989), who effectively induced LTP and saturated it by repeatedly delivering HFS in the dentate gyrus of hippocampus, followed by behavioral training in MWM. They found that LTP severely impaired spatial learning, but the learning ability tended to recover when the LTP has decayed to baseline levels. Likewise, Morris and his colleagues (E. I. Moser, Krobert, Moser, & Morris, 1998) found that animals that received repeated tetanization of hippocampal inputs were impaired in acquisition of MWM task if LTP was saturated. In contrast, if hippocampal LTP was not saturated, those animals were still capable of learning the task. These experiments suggest that LTP and learning share the same cellular mechanism because they compete with each other.

There is also evidence that associative learning blocks LTP induction. For example, using the inhibitory avoidance (IA) learning paradigm, in which rats acquire the association between entering the dark side of the training chamber and foot shock, Whitlock and colleagues (2006) showed that only a small portion (12/44) of recording electrodes (or pathways) in hippocampal CA1 were potentiated after learning. Furthermore, this learning-related fEPSP potentiation blocked additional LTP induction *in vivo* (tested with repeated HFS until no further potentiation): the pathways that were potentiated by IA learning had smaller increase in fEPSPs than the pathways that were not potentiated by learning. Again, the interference between LTP acquisition and learning suggests that learning shares some of the common pathways with LTP induction.

LTP induction and learning share common cellular mechanisms. The cellular mechanisms underlying LTP on excitatory synapses are well studied. Although it is difficult to establish a causal link between LTP and behavioral learning, significant advances have been made in understanding the cellular mechanisms of this form of

synaptic plasticity. In addition, there are largely two forms of LTP – NMDAR-dependent and non-NMDAR-dependent (Cavus & Teyler, 1996; Urban & Barrionuevo, 1996; Yeckel, Kapur, & Johnston, 1999). NMDAR-dependent LTP (known as Hebbian LTP) has been the most widely studied and is the focus of the following discussion.

Intracellular AMPA receptor trafficking. Alpha-amino-3-hydroxy-5-methyl-4-isoxazolepropionic acid (AMPA) receptors (AMPARs) and NMDARs are two important subtypes of glutamate receptors that have been widely studied in both synaptic plasticity and behavioral learning. AMPARs often co-exist with NMDARs at the synapse but are functionally different. The activation of AMPARs opens non-selective cationic channels that primarily allow the permeation of sodium and in some cases calcium ions (Hume, Dingledine, & Heinemann, 1991). The influx of sodium and calcium produces excitatory postsynaptic potentials (EPSPs). The number of functional AMPARs in the postsynaptic membrane is increased by LTP induction (Luscher, Nicoll, Malenka, & Muller, 2000; Malinow & Malenka, 2002; Park, Penick, Edwards, Kauer, & Ehlers, 2004), suggesting LTP is at least partially due to an upregulation of AMPARs in postsynaptic membrane. The number of AMPARs is also increased shortly (30 min) after IA training, which was associated with the phosphorylation of AMPAR (GluR1 subunit at Ser[831]) in the dorsal hippocampus (Whitlock *et al.*, 2006). This is consistent with a previous study that LTP induction involves the phosphorylation of the AMPA receptor subunit GluR1 at Ser[831] (Lee, Barbarosie, Kameyama, Bear, & Huganir, 2000). Thus, both LTP induction and learning increase synaptic strength through up-regulation of phosphorylated AMPRs of postsynaptic neurons.

NMDAR activation is required for both LTP induction and learning. At glutamatergic synapses, LTP depends on the influx of Ca^{2+} via NMDARs (Collingridge, Herron, & Lester, 1988; Collingridge, Kehl, & McLennan, 1983; G. Lynch, Larson, Kelso, Barrionuevo, & Schottler, 1983; S. Williams & Johnston, 1989). However, NMDARs are activated only when glutamate is bound to the receptor *and* the postsynaptic cell is depolarized. These properties – the dependence of presynaptic glutamate release *and* postsynaptic depolarization allow NMDARs to function as a "coincidence detector" for simultaneous presynaptic and postsynaptic activities. Such coincidence detection is one of the essential elements of Hebbian plasticity, as repeated pairings of pre- and post-synaptic stimulation are sufficient to activate NMDARs, which allows Ca^{2+} entry to the neurons and trigger a cascade of intracellular events (e.g., phosphorylation and insertion of AMPARs, gene activation and protein synthesis) that are necessary for LTP induction and maintenance (for review, see Kandel, 2001). Conversely, chelating residual calcium with intracellular injection of the EGTA (G. Lynch *et al.*, 1983) or BAPTA (S. Williams & Johnston, 1989) blocks LTP induction, and intracellular infusion of the NMDAR antagonist AP5 blocks LTP induction and impairs behavioral learning (Morris *et al.*, 1986).

Morphological modification of dendritic spines by LTP induction and learning. LTP can be induced not only by HFS, but also by direct glutamate iontophoresis onto postsynaptic neurons in hippocampal slices (Cormier & Kelly, 1996). Using a repetitive quantum-like photo release (uncaging) of glutamate, Matsuzaki and colleagues (2004) found that application of glutamate at single spines of hippocampal CA1 neurons induced a rapid and selective enlargement of the stimulated spines, and this enlargement is associated with an increase in AMPARs and relies on NMDA receptors, which also

depends on Ca^{2+}/calmodulin-dependent protein kinase II (CaMKII) activation and actin polymerization (Matsuzaki *et al.*, 2004). Furthermore, LTP induction and behavioral learning can also induce synaptogenesis – the formation of new spines (Fedulov *et al.*, 2007; Kleim *et al.*, 2002; Leuner, Falduto, & Shors, 2003; Ramirez-Amaya, Escobar, Chao, & Bermudez-Rattoni, 1999; Restivo, Vetere, Bontempi, & Ammassari-Teule, 2009). One mechanism that underlies synaptogenesis or spine enlargement by LTP induction and behavioral learning is the modification of actin dynamic through phosphorylation of cofilin (L. Y. Chen, Rex, Casale, Gall, & Lynch, 2007; Fedulov *et al.*, 2007; Yuste & Bonhoeffer, 2001). Cofilin is a family of actin-binding protein which binds and depolymerizes actin whereas phosphorylation of cofilin abolished its ability (N. Yang *et al.*, 1998). The LTP-induced enlargement of dendritic spines is associated with higher p-cofilin levels than their neighboring spines (L. Y. Chen *et al.*, 2007), suggesting that the regulation of actin dynamics underlies LTP induction. In fact, a recent study has revealed that LTP induction involves a sequence cofilin dephosphorylation and phosphorylation which underlies AMPAR trafficking and spine enlargement (Gu *et al.*, 2010). Taken together, LTP induction and behavioral learning involve spine enlargement via activation of NMDARs and cofilin phosphorylation.

Intracellular mechanisms of LTP induction and learning. In hippocampus, the maintenance of LTP is usually divided into two distinct phases (Kandel, 2001; M. A. Lynch, 2004). An early phase LTP is elicited by a moderate stimulation that activates NMDA receptors. The elevated Ca^{2+} in postsynaptic cells activates a set of second messengers, such as protein kinase C (PKC) and CAMKII that phosphorylate existing AMPARs. The insertion of phosphorylated AMPARs into postsynaptic membrane

enhances EPSPs (Kandel, 2001; Sweatt, 2003). This form of LTP decays within approximately 2 hours and does not require protein synthesis. A strong stimulation that induces more Ca^{2+} influx will elicit a late phase LTP, which lasts for hours to days. This late phase LTP depends upon activation of second messengers (e.g., cAMP) that trigger new gene expression. The underlying mechanisms of new gene expression include the activation of protein kinase A (PKA), mitogen-activated protein kinases (MAPK), and cAMP response element-binding (CREB). The activation of CREB finally promotes protein synthesis, which results in AMPAR insertion and synaptogenesis (Bolshakov, Golan, Kandel, & Siegelbaum, 1997; Engert & Bonhoeffer, 1999; Impey *et al.*, 1998; Nguyen, Abel, & Kandel, 1994).

Similar with the two phases of LTP (early and late), behavioral learning also occurs over two phases: initial acquisition and later consolidation. For fear conditioning, the initial acquisition takes minutes to hours whereas the later consolidation takes days to weeks (Dudai, 2004). Also similar to LTP expression, synthesis of new proteins is not required during initial acquisition but is necessary for memory consolidation, because protein synthesis inhibitors (e.g., anisomycin) or PKA inhibitors (e.g., Rp-cAMP) only disrupts long term memory but not initial learning (Rodrigues, Schafe, & LeDoux, 2004; Schafe & LeDoux, 2000). Thus, the dependence of protein synthesis of both late phase of LTP and the memory consolidation suggests that LTP and learning share common mechanisms.

Intrinsic plasticity. One possible explanation for the activity-dependent changes in synaptic plasticity is an alteration to the intrinsic excitability (intrinsic plasticity) of a postsynaptic neuron. Intrinsic excitability refers to the probability that the postsynaptic neuron fires action potentials in response to an input signal (see review in Beck & Yaari,

2008; Schulz, 2006). The enhancement of intrinsic excitability is manifested by a reduction in post-burst afterhyperpolarization (AHP) and a decrease in spike frequency adaptation (e.g., Moyer *et al.*, 1996; Thompson, Moyer, & Disterhoft, 1996b). In addition, intrinsic plasticity shares common properties with synaptic plasticity as being bi-directional, long lasting and learning specific. Such enhancement of intrinsic neuronal excitability is not only critical for memory consolidation but also facilitates LTP induction and subsequent learning (Kramar *et al.*, 2004; Moyer *et al.*, 1996; Sah & Bekkers, 1996; Song *et al.*, 2012; Zelcer *et al.*, 2006). In contrast, failure to modulate intrinsic neuronal excitability may impair the learning ability in adult animals, as well as learning deficits both in normal aging (Kaczorowski, Sametsky, Shah, Vassar, & Disterhoft, 2009; Moyer, Power, Thompson, & Disterhoft, 2000) and in a mouse model of Alzheimer's disease (Kaczorowski, Sametsky, Shah, Vassar, & Disterhoft, 2011).

Learning-induced plasticity of AHP. The post-burst AHP, especially the median (mAHP, defined as the AHP measured from 50 – 100 ms following the current injection) and slow component (sAHP, defined as the AHP measured beyond 100 ms following the current injection), are commonly used as an index of neuronal intrinsic excitability because it is correlated with the firing frequency of a neuron. For example, during a prolonged current injection, hippocampal pyramidal neurons first respond with a rapid action potential discharge which slows, or accommodates afterward, known as spike frequency adaptation or accommodation (Madison & Nicoll, 1984). In most cases, accommodation is reduced (more spikes) when a neuron has a smaller sAHP whereas accommodation is enhanced (less spikes) when a neuron has a larger sAHP.

Leaning-specific reductions in post-burst AHPs have been widely reported. For example, reduced AHPs in hippocampal neurons have been observed after trace fear conditioning (Kaczorowski & Disterhoft, 2009; McKay *et al.*, 2009; Song *et al.*, 2012), trace eyeblink conditioning (Moyer *et al.*, 2000; Moyer *et al.*, 1996), water maze learning (Oh, Kuo, Wu, Sametsky, & Disterhoft, 2003), and an olfactory discrimination task (Zelcer *et al.*, 2006). Furthermore, the learning-specific increase of intrinsic excitability is time-dependent. For example, in a trace eyeblink conditioning paradigm, a significant reduction in AHP was observed as early as 1 hour after training, which reached the asymptotic level 24 hours later, but returned to baseline level 7 days after initial learning. In contrast, the behavioral performance (conditioned response) remained at a high level over 6 months (Moyer *et al.*, 1996). Thus, such time course of increased intrinsic plasticity in hippocampal neurons may represent the transient role of hippocampus in acquisition of associative learning. After memory is consolidated, the enhanced intrinsic excitability in hippocampal neurons is not required for maintenance of conditioned response.

Learning-induced modulation of AHP is also bidirectional, which has been shown in IL neurons following fear conditioning and extinction (Santini, Quirk, & Porter, 2008). The excitability of IL pyramidal neurons was suppressed after a one-day session of fear conditioning, but reversed by the following extinction training on the next day. In addition, fear extinction did not simply reverse the suppression effect of fear conditioning on intrinsic excitability but also changed firing pattern of IL neurons with increased bursting activities after extinction (Santini *et al.*, 2008), which may be caused by the modulation in M-type potassium channels (Santini & Porter, 2010).

Cellular mechanisms underlying AHP modification. Previous studies suggest that

the AHP is primarily modulated by several currents that mediated by Ca^{2+}-activated K^+

channels (Sehgal, Song, Ehlers, & Moyer, 2013). Specifically, the mAHP is mediated by

several components including a voltage-and Ca^{2+}-activated current (I_C), a voltage-

dependent, muscarine-sensitive current (I_M), and a Ca^{2+}-dependent apamin-sensitive

current (I_{AHP}). In contrast, the sAHP is mediated by apamin-insensitive, Ca^{2+}-dependent

K^+ current (sI_{AHP}) (Gasparini & DiFrancesco, 1999; Sah, 1996; Storm, 1989). Thus, the

size and duration of AHP is greatly affected by the concentration of intracellular Ca^{2+}.

While an optimal level of intracellular Ca^{2+} is necessary for normal neuronal function,

excess Ca^{2+} in the cytoplasm may enhance the sAHP and impair LTP induction (for review,

see Foster, 2007), even lead to cell death (Farber, 1981). One source of intracellular Ca^{2+}

is rushing into the cell through voltage-dependent calcium channels (VDCC) when the

membrane is depolarized. It has been established that aged animals are associated with

increased density of L-type VDCC in hippocampal neurons, which may contribute to larger

AHPs (Power, Wu, Sametsky, Oh, & Disterhoft, 2002). Another source of excessive

intracellular Ca^{2+} in aged animals is from intracellular Ca^{2+} stores, because inhibition of

intracellular Ca^{2+} release significantly reduces the sAHP and facilitates LTP induction in

aged but not young animals (Kumar & Foster, 2004).

A recent study suggests that the sodium-potassium ATPase (the "sodium pump")

plays a critical role in mediating the sAHP and regulating intrinsic excitability (Gulledge

et al., 2013). The sodium pump generates a net outward current as it exchanges three

intracellular sodium for two extracellular potassium ions thus hyperpolarizes the cortical

pyramidal neurons (Koike, Mano, Okada, & Oshima, 1972). It has been shown that the

altered expression of sodium pump is associated with increased anxiety behavior and impaired spatial learning (Moseley *et al.*, 2007). However, it is not clear how the sodium pump is involved in the acquisition and expression of conditioned fear.

Previous studies suggest that the intracellular signals that are critical for synaptic plasticity are also important for intrinsic excitability. For instance, activation of PKC enhances intrinsic neuronal excitability through blocking calcium-dependent potassium channels and reduces the AHP (Baraban, Snyder, & Alger, 1985). In aged rabbits, the abnormal distribution of PKC isoforms − an increase in cytosolic PKC levels and a decrease in membrane-associated PKC levels are associated with aging-related learning deficits (Colombo, Wetsel, & Gallagher, 1997; Van der Zee *et al.*, 2004). Similar with PKC, activation of CaMKII reduces the AHP and spike frequency adaptation (Muller, Petrozzino, Griffith, Danho, & Connor, 1992; Ohno, Sametsky, Silva, & Disterhoft, 2006), but the contribution of CaMKII in intrinsic excitability is still unclear because CaMKII mutant mice that are impaired in learning still have reduced AHP (Ohno *et al.*, 2006).

Morphological Plasticity in Dendritic Spines as a Mechanism of Associative learning

In the central nervous system, most synapses occur on the dendritic spines, which are the small protrusions of the postsynaptic neuron. Dendritic spines receive most of the excitatory impulses (EPSPs) that enter a pyramidal cell. In the mature hippocampus and cortex, dendritic spines are highly heterogeneous and plastic both for their number and for their shape (Grutzendler, Kasthuri, & Gan, 2002; Trachtenberg *et al.*, 2002), which are dynamically modified by synaptic activity. Furthermore, recent studies have suggested that the number and shape of dendritic spines are associated with synaptic strength and

learning ability (Roberts, Tschida, Klein, & Mooney, 2010; Tschida & Mooney, 2012; T. Xu *et al.*, 2009).

Functional importance of spine structure and shape. Each spine has a head (volume $\sim 0.001\text{-}1$ μm^3) connected to the neuron by a thin (diameter < 0.1 μm) spine neck. According to the shape under light microscopy, spines can be classified as stubby, thin, or mushroom (Peters & Kaiserman-Abramof, 1970; Yuste & Bonhoeffer, 2004). During early development, stubby spines (lacking clear necks) are common. In the adult, mushroom spines (with large heads with thin neck) and thin spines (small heads with thin necks) are more common than stubby spines, although many stubby spines still exist. In addition, another type of long, thin dendritic protrusion named filopodia is also common during early development and is thought as immature predecessors of spines (Ethell & Pasquale, 2005; Yuste & Bonhoeffer, 2004).

Electron microscopy studies have revealed that the tip of the spine contains a thick electron dense region referred to as the "postsynaptic density" (PSD), which gives an asymmetrical appearance to the synaptic contact. The PSDs contain hundreds of components such as receptors, cytoskeletal proteins, and associated signaling molecules that are involved in synaptic plasticity (Husi, Ward, Choudhary, Blackstock, & Grant, 2000; Walikonis *et al.*, 2000). For example, the two major subtypes of glutamate receptors (AMPARs and NMDARs) are primarily distributed in the PSD (Kennedy, 1998, 2000). AMPARs mediate the postsynaptic depolarization that initiates neuronal firing and are the targets for multiple signaling pathways that regulate synaptic strength, whereas NMDARs initiate synaptic plasticity that regulates AMPAR trafficking and maintains the synaptic strength (Derkach, Oh, Guire, & Soderling, 2007). Interestingly, NMDARs are found in

all spines whereas some (12 - 25%) spines lack AMPA receptors. In the adult animal, such spines that lack of AMPARs are functionally "silent", but they have also been described as immature glutamate synapses (Nusser *et al.*, 1998; Racca, Stephenson, Streit, Roberts, & Somogyi, 2000; Takumi, Ramirez-Leon, Laake, Rinvik, & Ottersen, 1999). Moreover, the area of PSD is positively correlated with the spine volume, and the density of AMPAR is strongly correlated with the size of PSD within a certain type of synapses such as Schaffer collateral–commissural synapses in the hippocampus (Nusser *et al.*, 1998; Takumi *et al.*, 1999). The correlation between the synapse size and the number of NMDA receptors in Schaffer collateral–commissural synapses is also significant, but is much weaker (Racca *et al.*, 2000). Thus, the synaptic strength is determined by the size of the spine and the number of AMPARs in the postsynaptic membrane.

According to the PSD profile in electron micrograph of consecutive serial sections, axospinous synapses can be roughly divided into perforated and nonperforated conjunctions (Geinisman, 1993). Perforated synapses are characterized by the appearance of one or more discontinuities or perforations in the PSD and can be further divided into fenestrated, horseshoe, or segmented shape (Geinisman, 1993; Nicholson, Yoshida, Berry, Gallagher, & Geinisman, 2004). In contrast, nonperforated synapses are exclusively continuous in serial sections. In general, perforated synapses are larger and contain more AMPARs whereas nonperforated synapses are smaller and contain less or no AMPARs (Geinisman, 1993).

Structural plasticity induced by experience and synaptic stimulation. The number and shape of dendritic spines are highly dynamic and modulated by ongoing synaptic activity, which depends on afferent signals from local or distal brain regions. For

example, *in vivo* time-lapse imaging on individual pyramidal neurons in the mouse barrel

cortex suggests that the synapses undergo formation and elimination over time, although

the dendritic structure is stable (Trachtenberg *et al.*, 2002). The lifetime of dendritic spines

varies greatly: ~ 50% of the spines are stable for at least one month whereas the rest are

present only for a few days or less. Furthermore, the percent of spines that appear and

disappear over time (turnover ratio) was significantly increased after sensory deprivation

induced by whisker trimming (Trachtenberg *et al.*, 2002). These observations suggest that

sensory deprivation turns stable synapses into unstable synapses, which might then be

removed. This is consistent with earlier studies in visual cortex that the number of dendritic

spines was reduced when the afferent input was deprived either by rearing in total darkness

(Valverde, 1967) or by surgical lesions in the lateral geniculate body (Globus & Scheibel,

1966). In contrast, the number of dendritic spines in visual cortex was significantly

increased in animals reared in an enriched environment compared with animals reared in a

standard environment (Kozorovitskiy *et al.*, 2005).

In addition to sensory deprivation and environment enrichment, the induction of

LTP and LTD through synaptic stimulation also significantly alters the number of dendritic

spines. For example, recent time-lapse imaging studies have shown that LTP induction

significantly increased both spine volume and growth (Engert & Bonhoeffer, 1999;

Hosokawa, Rusakov, Bliss, & Fine, 1995; Lang *et al.*, 2004; Matsuzaki *et al.*, 2004;

Okamoto, Nagai, Miyawaki, & Hayashi, 2004). In contrast, LTD induction elicits long

lasting shrinkage of existing spines (Okamoto *et al.*, 2004). Furthermore, these structural

changes share the same mechanisms as functional changes (i.e., potentiation of synaptic

strength) in that they involve AMPAR insertion, are input specific, and are dependent on

activation of NMDA receptors and CAMKII (Engert & Bonhoeffer, 1999; Lang *et al.*, 2004; Matsuzaki *et al.*, 2004). Interestingly, the spine expansion involves actin polymerization (Okamoto *et al.*, 2004) which occurs before the AMPAR insertion (Kopec, Li, Wei, Boehm, & Malinow, 2006), suggesting that morphological changes precede functional changes. In addition, LTP induction primarily involves a persistent expansion or growth of small spines (Hosokawa *et al.*, 1995; Matsuzaki *et al.*, 2004), whereas the expansion of large spines is transient (Matsuzaki *et al.*, 2004). Taken together, these data suggest that bidirectional regulation of dendritic spine density and size is critical for synaptic function and is a mechanism underlying learning and memory.

Structural plasticity induced by behavioral learning. In addition to LTP induction, studies have revealed that behavioral learning also induces the formation of new dendritic spines, as well as the elimination and remodeling of existing spines (e.g., enlargement). Such learning-induced structural plasticity has been observed in a variety of learning tasks and brain areas. Although fear conditioning is the primary interest of the current study, a brief review of other learning paradigms is presented here in order to provide a general view of how learning affects the plasticity of dendritic spine.

Motor skill learning induces synaptogenesis in the motor cortex. Learning a simple skill to obtain food rewards (motor skill learning) temporarily increases the spine formation in motor cortical neurons (Kleim *et al.*, 2002; Kleim *et al.*, 2004; T. Xu *et al.*, 2009). The learning-induced synapse formation was long lasting and was significantly correlated with behavioral performance (T. Xu *et al.*, 2009; G. Yang, Pan, & Gan, 2009). Furthermore, when retraining the learned animals on another motor task, the spine formation and elimination were further increased with similar rates as naïve animals but

the newly formed spines were different from those formed in previous learning (T. Xu *et al.*, 2009), suggesting that different learning tasks involve different sets of synapses.

Water maze learning induces synaptogenesis in hippocampal neurons.   The MWM task has been widely used to measure hippocampal dependent spatial memory (Morris, Garrud, Rawlins, & O'Keefe, 1982). Several studies have found an increase in synaptogenesis in the dentate gyrus and CA3 neurons following acquisition of the MWM task (O'Malley, O'Connell, Murphy, & Regan, 2000; Ramirez-Amaya, Balderas, Sandoval, Escobar, & Bermudez-Rattoni, 2001; Ramirez-Amaya *et al.*, 1999). Interestingly, this increase of synaptogenesis was transient because it was only observed in the dentate gyrus at 6-9 hours after training but not 24 (Eyre, Richter-Levin, Avital, & Stewart, 2003) or 72 (O'Malley *et al.*, 2000) hours later. A similar time-dependent synaptogenesis may also exist in CA1 neurons after water maze training because a significant increase in mushroom synapses but not stubby or thin or filopodia was reported in rats that learned the task after 2 days of training (Hongpaisan & Alkon, 2007), although earlier studies didn't find a net increase in synapse formation following 5 days of training (Rusakov *et al.*, 1997).

Trace eyeblink conditioning induces synaptogenesis and synaptic remodeling in hippocampus.   Trace eyeblink conditioning is a form of hippocampus-dependent associative learning (Kim, Clark, & Thompson, 1995; Moyer, Deyo, & Disterhoft, 1990; Solomon, Vander Schaaf, Thompson, & Weisz, 1986). It has been reported that trace eyeblink conditioning induced an increase of synaptogenesis on basal dendrites (Leuner *et al.*, 2003) but not on apical dendrites of *stratum radiatum* in the CA1 area (Geinisman, 2000; Geinisman, Berry, Disterhoft, Power, & Van der Zee, 2001; Leuner *et al.*, 2003). However, on apical dendrites of CA1 neurons, an increase in PSD area and multiple

synaptic boutons (MSBs) in *stratum radiatum* was observed although no net increase in total synapse number was seen, indicating the involvement of a learning-specific remodeling of the synaptic network after acquisition of trace eyeblink conditioning (Geinisman, 2000; Geinisman *et al.*, 2001).

Fear conditioning and extinction induce bidirectional structural modification in the hippocampus, amygdala, and prefrontal cortex. The correlation between synaptogenesis and acquisition of fear conditioning has recently been reported in all of these brain areas. For example, acquisition of delay fear conditioning increases synapse density (Dalzell *et al.*, 2011) and synapse size (Ostroff, Cain, Jindal, Dar, & Ledoux, 2012) in the lateral amygdala (LA). Such learning-induced synapse modification may contribute to the observed increase in AMPAR mediated synaptic transmission in the LA (McKernan & Shinnick-Gallagher, 1997; Rogan *et al.*, 1997). In addition, contextual fear conditioning increases spine density on apical dendrites of hippocampal CA1 and anterior cingulate cortical (ACC) neurons in a time-dependent manner (Restivo *et al.*, 2009) – the learning induced synaptogenesis in hippocampus was only observed 1 day but not 36 days after learning. In contrast, the increase in spine density in ACC was observed at 36 days but not 1 day after conditioning, which is consistent with the transient role of the hippocampus in acquisition of fear conditioning (Restivo *et al.*, 2009). A follow-up study from the same group (Vetere *et al.*, 2011) revealed that contextual fear conditioning also facilitated spine formation in IL 36 days after conditioning. However, extinction reversed the effect of conditioning on spine formation in ACC but not in IL –spine density was reduced in ACC but remained high in IL after extinction. In IL, extinction decreased in spine size, which was not observed in ACC (Vetere *et al.*, 2011).

A bidirectional modulation of spine number through spine formation and elimination has also been observed in the frontal association cortex (FrA) in live animals after delay fear conditioning and extinction (Lai, Franke, & Gan, 2012). In that study, the spines in layer 5 pyramidal neurons in the dorsal medial region of the FrA were dynamically observed before and after the animals underwent fear conditioning, extinction, and reconditioning. Twenty-four hours after fear conditioning, the number of dendritic spines was significantly reduced – an effect that lasted at least 9 days. Interestingly, extinction reversed the effect of conditioning such that not only the number of spines was restored but also that the spines formed after extinction were located at the same sites (within 2 μm) as those that were eliminated during conditioning. Moreover, the spines that formed after extinction seem to be eliminated again after reconditioning with the same tone-shock pairings. However, a different set of spines (located more than 2 μm away from the spines formed after extinction) was eliminated if the animals were conditioned using a different tone CS (Lai *et al.*, 2012). Thus, this study demonstrated that within FrA, fear conditioning and extinction have the opposite effect on spine formation and that different learning experiences use different sets of dendritic spines.

Summary

Pavlovian fear conditioning is an excellent model system to study the mechanisms underlying associative learning. Although much progress has been made, the neural basis of fear conditioning is still unclear, including which brain regions are required and how they function during learning and memory retrieval. In addition, much of our understanding of the mechanisms of fear conditioning and extinction comes from studies using delay paradigm, whereas trace fear conditioning relatively poorly studied.

The goal of the present project was to investigate how the synaptic plasticity, intrinsic excitability, as well as spine density are modulated by trace fear conditioning in hippocampus and mPFC. We studied synaptic plasticity in hippocampus because of its well-defined tri-synaptic structure. We did not conduct synaptic studies in the mPFC because of its complex afferent and efferent connections. In addition, mPFC neurons are highly heterogeneous in term of morphology, electrophysiology, and interconnectivity depending on their long-range projection targets. Thus, we examined how trace fear conditioning affects both synaptic and intrinsic plasticity in hippocampal CA1 neurons, and conducted a set of studies to examine the role of mPFC in trace fear conditioning and extinction. We first characterized the basic membrane properties of randomly selected neurons by comparing the neurons between different cortical layers (layer 2/3 and layer 5) and between subregions (IL vs PL). We then characterized the membrane properties of mPFC-amygdala projection neurons by using a combination of retrograde labeling and whole-cell recording. Next, we studied the effect of trace fear conditioning and extinction on the intrinsic excitability of mPFC-amygdala projection neurons. Finally, we examined the effect of trace fear conditioning on spine density of mPFC-amygdala projection neurons. These experiments demonstrate that the trace fear conditioning enhances the intrinsic excitability in both hippocampal and infralimbic cortical neurons, whereas inhibits prelimbic neurons. We also demonstrate that the mPFC neurons are highly heterogeneous and recording from neurons with known projection targets is necessary for elucidating the cellular mechanisms of trace fear conditioning.

CHAPTER TWO: trace fear conditioning enhances synaptic and intrinsic plasticity in hippocampal CA1 neurons

Abstract

The current study utilized trace fear conditioning as a model system to examine how associative learning affects both synaptic and intrinsic plasticity of hippocampal CA1 neurons in the same behavioral characterized rats. Rats received a one-day 10-trial trace fear conditioning, followed by a brief memory test in a novel context the next day. Brain slices were prepared immediately after the test for electrophysiological recordings. Synaptic plasticity was studied by stimulating Schaffer collateral pathway and recorded in *stratum radiatum* in CA1 area. Intrinsic excitability of CA1 neurons was studied by using sharp electrode intracellular recording. Analysis with the data we found that the behavioral performance (percent freezing during memory test) was significantly correlated with the amount of LTP ($r = 0.64$, $p < 0.05$) and the size of post-burst AHP ($r = -0.55$, $p < 0.05$). The significant correlation was only observed in conditioned rats but not pseudoconditioned rats, suggesting it is learning specific. In addition, the rats that displayed higher level of freezing during memory test (good learners) had significantly greater LTP in hippocampus than the rats that displayed lower level of freezing (poor learners). Furthermore, neurons from good learners displayed enhanced intrinsic excitability than the neurons from poor learners and other control rats, as evidenced by smaller post-burst AHPs [$F(4,52) = 4.77$, $p < 0.01$] and reduced spike-frequency adaptation [$F(3,52) = 5.62$, $p < 0.01$]. Finally, the percent LTP was significantly correlated with the size of post-burst AHP ($r = -0.38$, $p < 0.05$). Thus these data suggest that within

hippocampus both synaptic and intrinsic plasticity are involved in the acquisition of trace fear conditioning.

Introduction

Bidirectional modification of synaptic efficiency by long-term potentiation (LTP) and long-term depression (LTD) is believed to underlie the cellular mechanisms of learning and memory (Bear & Abraham, 1996; Dudek & Bear, 1993; M. A. Lynch, 2004). For example, the learning-specific enhancement of baseline synaptic response has been observed in Schaffer collateral pathway in hippocampus following the acquisition of trace eyeblink conditioning (Power *et al.*, 1997) or fear conditioning (Doyere *et al.*, 1995). Interestingly, a facilitation of LTP induction has also been observed in hippocampus after acquisition of trace eyeblink conditioning (Gruart *et al.*, 2006), trace fear conditioning (Song *et al.*, 2012), and Morris water maze task (Boric *et al.*, 2008). Furthermore, the behavioral performance is significantly correlated with hippocampal LTP after learning Morris water maze task (Boric *et al.*, 2008), suggesting the important role of synaptic plasticity in learning. Such learning-induced facilitation of LTP induction has been coined "metaplasticity" by Abraham and colleagues (Abraham, 2008; Abraham & Bear, 1996). Metaplasticity is a high-order plasticity that greatly depends on previous synaptic activity and strongly affects subsequent synaptic plasticity (Abraham & Bear, 1996). Although metaplasticity is usually attributed to synaptic activity, recent evidence suggests that modification of intrinsic excitability may underlie such phenomenon (Sehgal *et al.*, 2013; Zhang & Linden, 2003). For example, the enhancement of intrinsic excitability has been observed in hippocampal neurons following acquisition of trace eyeblink conditioning (Moyer *et al.*, 1996), trace fear conditioning (Kaczorowski & Disterhoft, 2009; McKay *et*

al., 2009) Morris water maze training (Oh *et al.*, 2003). Thus, both intrinsic and synaptic plasticity are important for learning and that synaptic plasticity may arise from intrinsic plasticity.

The aim of the present study was to investigate how trace fear conditioning affects both synaptic and intrinsic plasticity in hippocampal CA1 neurons in the same behavioral characterized animals. The data suggest that acquisition of trace fear conditioning enhances both synaptic plasticity and intrinsic excitability, and supports the hypothesis that synaptic plasticity arises from intrinsic plasticity.

Methods

Subjects. The subjects were 51 adult male F344 rats (4.1 ± 0.1 mo). Rats were maintained in an Association for Assessment and Accreditation of Laboratory Animal Care (AAALAC) accredited facility on a 14 h light–10 h dark cycle and housed individually with food and water ad libitum. All rats were handled at least one week prior to experiments. Procedures were conducted in accordance with the University of Wisconsin-Milwaukee animal care and use committee (ACUC) and NIH guidelines.

Apparatus. *Fear conditioning chambers.* Trace fear conditioning was conducted in a Plexiglas and stainless steel chamber (30.5 X 25.4 X 30.5 cm; Coulbourn Instruments, Whitehall, PA), located in a sound-attenuating box. The chamber had a standard grid floor consisting of 26 parallel steel rods (5 mm diameter and 6 mm spacing). The floor was connected to a precision adjustable shock generator (Coulbourn Instruments) for delivery of a scrambled footshock US. Within the sound-attenuating box, a ventilation fan produced a constant background noise of about 58 dB (measured by a sound level meter, A scale; model #33-2050, Realistic, Fort Worth, TX). The chamber was illuminated by a miniature

incandescent white lamp (28V, type 1819) and was wiped with a 5% ammonium hydroxide solution prior to each training session. During training, the room lights were left on (illumination 20.9 lux) for the entire session.

CS testing chambers. An additional Plexiglas and stainless steel chamber was served as a novel context for the auditory cue test. This chamber was located within a separate sound-attenuating box located in the same room. The test chamber was physically different from the training chamber in that it had a curved wall, the floor was black-painted Plexiglas (instead of grid bars), and it was illuminated with an infrared light. In addition, the tray below the test chamber floor contained clean bedding and the test chamber was wiped with 2% acetic acid prior to each test session to provide a different olfactory stimulus from that used during training. The room lights were turned off (illumination 0.2 lux) for the entire testing session.

Behavioral training. Rats were randomly assigned into *trace fear conditioned* (n = 15), *pseudoconditioned* (n = 10), *chamber exposed* (n = 3), and *naïve* (21) groups. *Trace fear conditioned* rats received one 10-trial session of *auditory trace fear conditioning* using a 15 s CS (80 dB white noise) followed by a 30 s trace interval (stimulus-free period) and a 1 s footshock US (1 mA). A long (5.2 min ± 20 %) intertrial interval was used to maximize CS and minimize context (i.e., training chamber) conditioning (Blanchard & Blanchard, 1969). *Pseudoconditioned* rats received the same amount of CS and US presentations but explicitly unpaired. *Chamber exposed* were placed in the training chamber for the same amount of time as conditioned rats without receiving any stimuli. *Naïve* rats were never be exposed to the training or testing chambers. To assess learning in the conditioned and pseudoconditioned rats, the amount of time spent freezing during

the baseline and the 30 s intervals following CS offset was measured (see analysis below). A PC running FreezeFrame 2.04 (Actimetrics Software, Coulbourn Instruments, Whitehall, PA) controlled the delivery of all stimuli during training and testing.

Behavioral testing. Twenty-four hours after training, *trace conditioned* and *pseudoconditioned* rats received a brief CS test session in a novel context. After a 2 min baseline, trace and pseudoconditioned rats received two 15 s CS presentations with a 2.9 min ITI. Rats remained in the chamber for additional 2 min before they were removed from the chamber. To assess memory, the amount of time spent freezing during the baseline, the first CS, and the first trace interval (defined as the first 30 sec after CS offset) was measured (see analysis below). The *chamber exposed* rats were placed in the same novel context for the same amount of time but without any CS presentations.

Analysis of behavioral data. A remote CCTV video camera (model #WV-BP334; Panasonic Corp., Suzhou, China), mounted to the top of each behavioral chamber, was used to record the activity of each rat during training and testing. The video data were fed to a PC running FreezeFrame 2.04. Data were analyzed using FreezeView 2.04 (Actimetrics Software, Coulbourn Instruments) where a 1-sec bout of immobility was scored as freezing. Freezing was defined as the absence of all movement except that required for respiration (Blanchard & Blanchard, 1969). To correlate learning ability and synaptic plasticity and intrinsic excitability, conditioned rats were classified as good learners and poor learners according to their performance during CS test. Rats that froze more than 2 SD above the mean of chamber-exposed rats were defined as good learners (n = 8), and those below were defined as poor learners (n = 7). Figure 4 shows the freezing levels of conditioned and pseudoconditioned rats during training and testing.
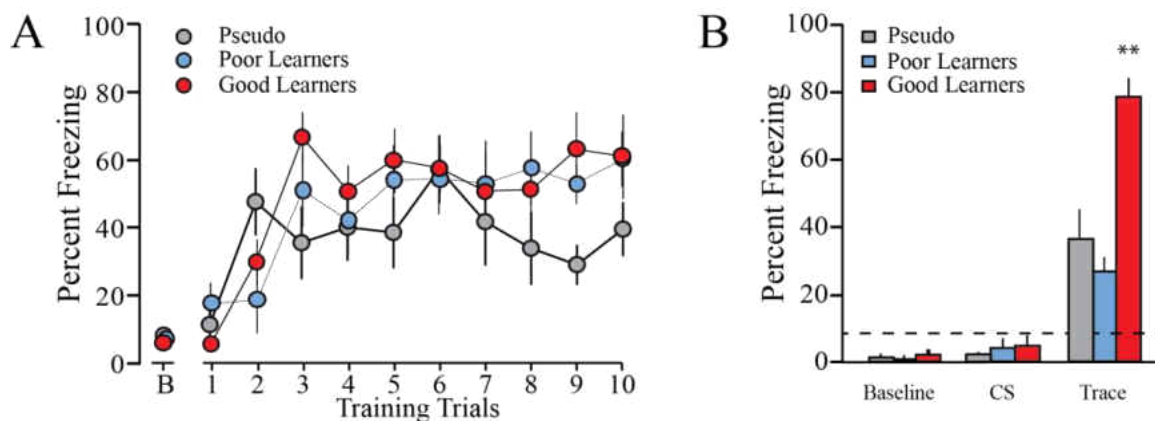
Figure 4. Behavioral performance of trace fear conditioned and pseudoconditioned rats during conditioning and testing. Conditioned rats were divided into good learners (rats that froze more than 2 SD of the chamber exposed rats, n = 8) and poor learners (the rest of the rats, n = 7) according the behavior performance during the probe test. A, Throughout training, good learners, poor learners, and pseudoconditioned rats froze at comparable levels during trace interval. B, during test, good learners froze significantly more than poor learners and pseudoconditioned rats (**$p < 0.01$ for all values) during the trace interval. The dashed line in B indicates the percent freeze of chamber exposed during test. (Adapted from Song *et al.*, 2012).

Slice preparation. Brain slices were prepared within 1 h of the test session by an individual blind to training condition. Rats were deeply anesthetized with isoflurane and decapitated. The brain was quickly removed and placed in ice-cold oxygenated (95% O_2/5% CO_2) aCSF (composition in mM: 124 NaCl, 2.8 KCl, 1.25 NaH_2PO_4, 2 $MgSO_4$, 2 $CaCl_2$, 26 $NaHCO_3$, and 20 dextrose, pH 7.4). The brain was then blocked and horizontal brain slices (400 µm) were cut in aCSF at ~ 0°C using a temperature-controlled vibratome 3000 (the Vibratome Company). Slices were then transferred to a holding chamber (Moyer *et al.*, 1996) containing oxygenated aCSF at room temperature (21-23°C). For experiments, slices were transferred as needed to an interface- type recording chamber (Warner Instrument, Hamden, CT) where they were perfused with oxygenated aCSF at 32°C and allowed to recover for at least one hour prior to starting an experiment.

Electrophysiological recordings. All recordings were obtained using a MultiClamp 700B amplifier system (Molecular Devices, Union City, CA). Experiments were controlled by PClamp 10 software (Molecular Devices) running on a PC, and the data were acquired using the Digidata 1440A acquisition system (Molecular Devices). All electrodes were pulled from thin-walled capillary glass (A-M Systems, Carlsborg, WA) using a Sutter Instruments P97 puller. For field potential recordings, voltage signals were filtered at 2 kHz and digitized at 50 kHz. For intracellular recordings, voltage signals were filtered at 0.5 – 2 kHz and digitized at 20 kHz.

Synaptic plasticity studies. Dendritic field excitatory postsynaptic potentials (fEPSPs) were obtained from the *stratum radiatum* of CA1 using aCSF-filled pipettes (R1; see Figure 5) with resistances of 2-6 MΩ. Two concentric bipolar stimulating electrodes (FHC, Brunswick, ME) were positioned in the *stratum radiatum*, one on each side of the
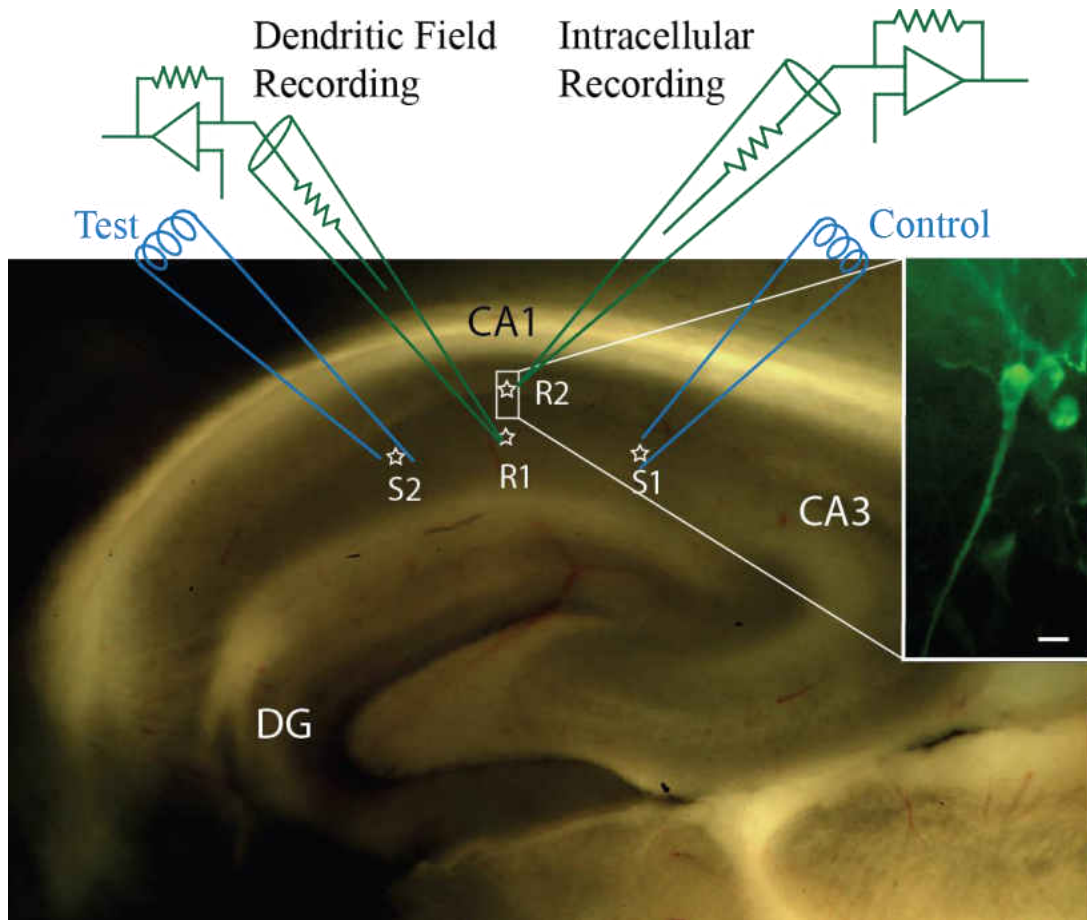
Figure 5. Hippocampal slice preparation used to study learning-related changes in synaptic and intrinsic plasticity. A photograph of hippocampal slice illustrating the location of stimulating electrodes for the test (S1) and control (S2) pathways and the location of recording electrodes for field (R1) and sharp intracellular (R2) recording. *Inset*: representative photograph of a biocytin-filled pyramidal neuron. Scale bar, 5 μm. (Adapted from Song *et al.*, 2012).

field electrode at a distance of ~500 μm. The stimulating electrode closest to CA3 (S1) was used as the test pathway (for inducing LTP) whereas the other stimulating electrode (S2) was used as the control pathway to test for input specificity (see Figure 5). Input-output (I-O) curves were used to find the stimulation intensity necessary to elicit an initial fEPSP slope that was 50% of the maximal fEPSP slope obtained in the absence of a population spike (see Figure 6A). After establishing a stable baseline for 10 min, LTP was induced in the test pathway by delivering a single tetanic stimulation (100 Hz for 1 s) to S1. Both pathways were monitored for at least 30 minutes by delivering a single stimulus every 30 s (alternating every 15 s between S1 and S2). The 30-min time frame was selected because pilot data (see Figure 7) indicated that stable LTP was observed within ~15 min following HFS, and the amount of LTP did not differ when compared at 30, 45, or 60 minutes, $F(2,6) = 0.22$, $p = 0.7$.

Intrinsic excitability studies. Somatic intracellular recordings were obtained from CA1 pyramidal neurons using sharp microelectrodes filled with 3M potassium acetate and 20 mM KCl (60-100 MΩ). Only cells with a stable resting membrane potential (V_{rest}) more negative than -60 mV, overshooting action potentials, and an input resistance (R_N) > 20 MΩ were used (Moyer *et al.*, 1996). To minimize the influence of voltage-dependent changes on membrane conductances, all cells were studied at rest and at a membrane potential near -65 mV (≤ 0.3 nA constant current injection, if necessary). Neurons were recorded under current clamp using the following protocol: (1) Voltage–current (V-I) relations were obtained using 400 ms current steps (range -1.0 to +0.2 nA) and plotting the plateau voltage deflection against current amplitude. Neuronal input resistance (R_N) was determined from the slope of the linear fit of that portion of the V-I plot where the voltage.
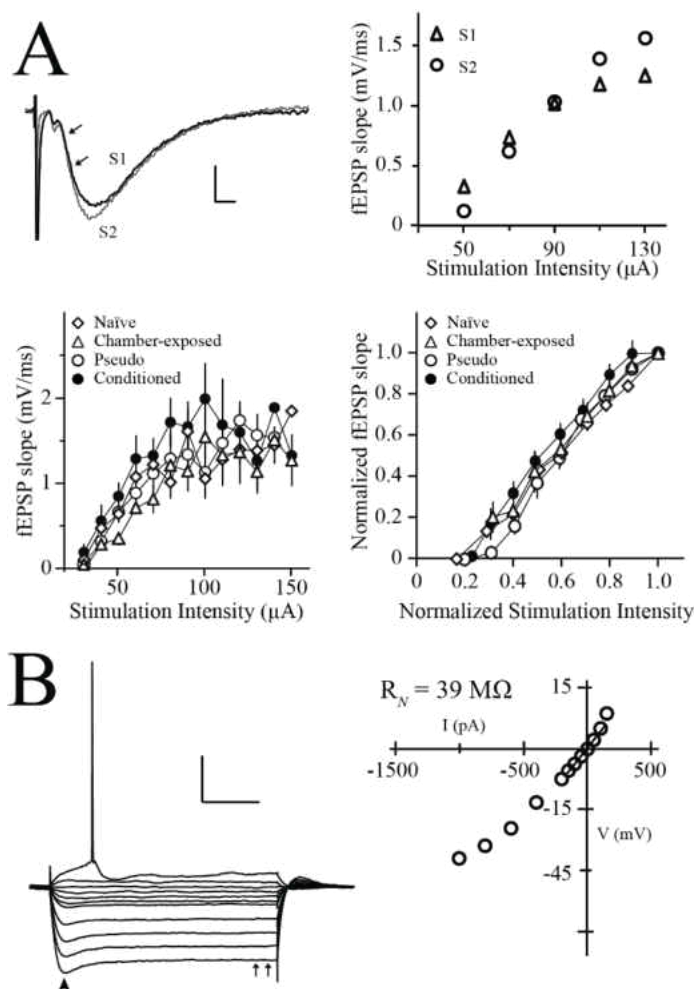
Figure 6. Study of synaptic and intrinsic properties of hippocampal neurons. A, Representative and averaged input-output (I-O) curves for extracellular field recordings. *Top left*: fEPSPs of test pathway (S1, black) and control pathway (S2, gray) were obtained by stimulating the Schaffer collaterals on either side of the recording electrode. The strength of synaptic transmission was measured as the initial slope indicated between the two arrows. Scale bar, 0.5 mV, 2 ms. *Top right*: example of an I-O curve used to calculate the stimulation intensity required to generate a 50% maximal fEPSP slope. *Bottom left*: averaged I-O curves of the test pathway for all groups. *Bottom right*: normalized I-O curves of the test pathway for each group. B, Voltage-current (V-I) relation used to calculate neuronal input resistance (R_N). Representative voltage responses to a series of current injections and the accompanying V-I plot used to measure R_N. Scale bar, 20 mV, 100 ms. Arrowhead shows peak voltage deflection (used in measuring the depolarizing sag) and double arrows show steady-state voltage near the end of the current injection. (Adapted from Song *et al.*, 2012).
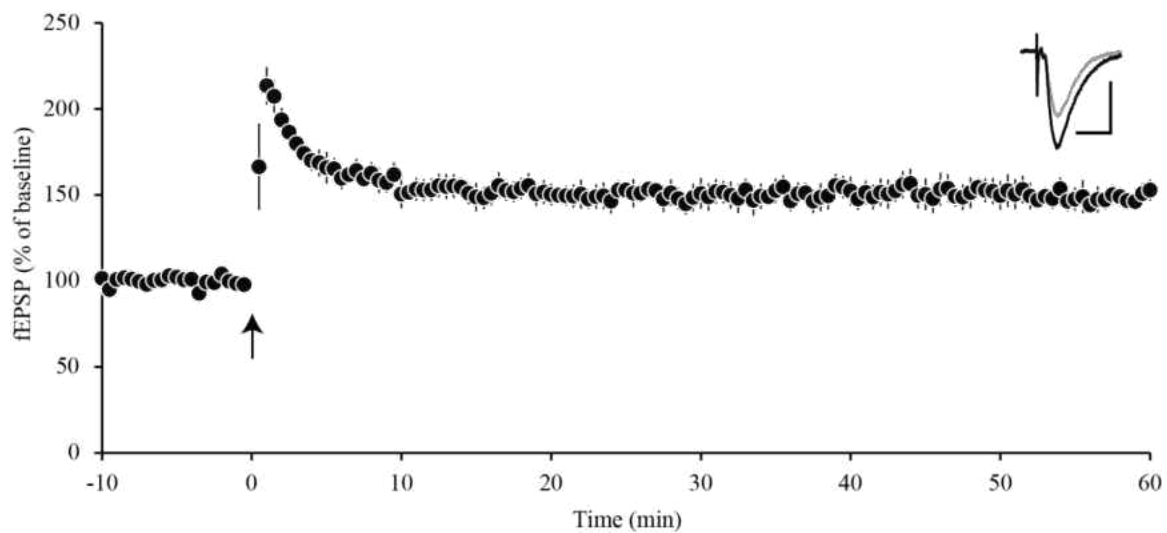
Figure 7. Stability of hippocampal LTP. LTP was induced in Shaffer-collateral pathway and fEPSPs were recorded in stratum radiatum of CA1. LTP did not differ between 30, 45, or 60 min [$F(2,6) = 0.22$, $p = 0.7$] following the high frequency stimulation (HFS) at time 0 (arrow). Inset shows representative traces obtained before (gray) and 60 min after (black) LTP induction. Scale bar, 1 mV, 10 ms.

sweeps did not exhibit sags or active conductance (see Figure 6B). (2) The post-burst afterhyperpolarization (AHP; 3X, at 20 s intervals) was evoked using a 100 ms depolarizing current injection sufficient to elicit a burst of four action potentials. The AHP amplitude, duration, and integrated area were measured. (3) Spike-frequency adaptation (accommodation; 3X, at 30 sec intervals) was studied using a 1 s depolarizing current injection of the same stimulus intensity used to study the AHP. For each sweep, the number of action potentials were counted. (4) Resting membrane potential (V_{rest}) was calculated as the difference in membrane potential before and after withdrawing the microelectrode from the cell.

Biocytin staining. A subset of neurons were filled with biocytin to confirm the position and identity of pyramidal cells in the CA1 area. For these recordings, sharp electrodes were filled with 2% (w/v) biocytin dissolved in 1 M potassium acetate (80 – 120 MΩ). After obtaining stable resting membrane potential, biocytin was injected iontophoretically by using 300 ms, 800 pA depolarizing current pulses delivered every 600 ms for 10 to 20 min. Slices were allowed to recover in the recording chamber for 30 min after biocytin injection (Yankova, Hart, & Woolley, 2001), and were then be fixed in 10% neutral-buffered formalin at 4 °C for 1 to 3 days before being visualized with streptavidin Alexa Fluor 488 (Invitrogen).

To visualize hippocampal neurons labeled by biocytin, the slices were incubated with 1% $NaBH_4$ for 30 min and washed with 0.1 M PBS for 10 min (three times). Slices were then incubated in 3% H_2O_2/10% methanol for 45 min, washed with PBS for 10 min (three times), followed by 0.25% Triton X-100/ 2% BSA for 60 min and 2% BSA for 10 min. The slices were then incubated with 1:500 streptavidin Alexa Fluor 488 (Invitrogen)

for 135 min in the dark, and washed with PBS for 10 min (three times), rinsed in dH_2O, incubated for 90 min in 10 mM $CuSO_4$, rinsed with dH_2O, and rinsed in PBS (15 min, three times). They were mounted onto slides, coverslipped with Ultra Cruz Mounting Medium (Santa Cruz Biotechnology, Santa Cruz, CA), and sealed with nail polish. The neurons were viewed under a fluorescence microscope (BX51WI, Olympus) at 20X and photographed. A representative biocytin-filled hippocampal CA1 pyramidal neuron and *V-I* relation are shown in Figure 5.

Statistical analyses. The overall treatment effects were examined using a one-way ANOVA or paired t-tests using SPSS 18.0 (SPSS, Chicago, IL). A repeated measures ANOVA was used to compare freezing levels across training trials and the AHP across time for each group of rats. For significant main effects (alpha 0.05), a Fisher's PLSD test was used for *post hoc* comparisons. All data were expressed as mean ± SEM.

Results

To assess the effect of trace fear conditioning on the synaptic and intrinsic plasticity of hippocampal neurons, rats received one-session trace fear conditioning or pseudoconditioning followed by a brief probe test the next day. Chamber-exposed rats were placed into the same conditioning and test context for the same amount of time as conditioned rats but no CS or US presented. Analysis of the behavioral data we found that there was heterogeneous for the conditioned rats during the probe test. We thus divided the conditioned rats into good learners (the rats that froze > 2SD than the mean of chamber-exposed, n = 8) and poor learners (the rest, n =7) before further analysis.

As shown in Figure 4A, both good and poor learners exhibited comparable levels of freezing throughout the training session. The pseudoconditioned rats also expressed a similar rapid increase in freezing, presumably due to contextual fear acquisition (Amano *et al.*, 2010). When memory was tested 24 h later, freezing levels were comparably low during the 2 min baseline and the 15 s CS (see Figure 4B). In contrast, a statistically significant group effect was observed during the 30 s trace interval following the CS offset [$F(2,23) = 12.11$, $p < 0.01$]. A *post hoc* analyses revealed that good learners froze significantly more than both poor learners ($p < 0.001$) and pseudoconditioned rats ($p < 0.001$).

Acquisition of trace fear conditioning enhances synaptic plasticity in hippocampus

To investigate the effect of trace fear conditioning on synaptic and intrinsic plasticity on hippocampal neurons, brain slices were prepared from behaviorally characterized or naïve rats. To evaluate the learning-specific effects of trace fear conditioning on synaptic plasticity, LTP was compared between brain slices prepared from different experimental groups. Two pathways were studied, but LTP was induced only in the test pathway. As shown in Figure 8, Although all groups exhibited LTP in the test pathway, the good learners showed significantly greater LTP compared to the other groups [$F(4,46) = 5.13$, $p < 0.01$]. In all groups, LTP was input specific because no changes were observed in the control pathway (see inset in Figure 8).

Interestingly, as shown in Figure 9A, the amount of LTP observed in the hippocampus of the trace fear conditioned rats was significantly correlated ($r = 0.64$, $p < 0.05$) with their behavioral performance. This correlation was learning-specific because it was not significant in the pseudoconditioned rats ($r = -0.05$, $p = 0.88$; see Figure 9B).
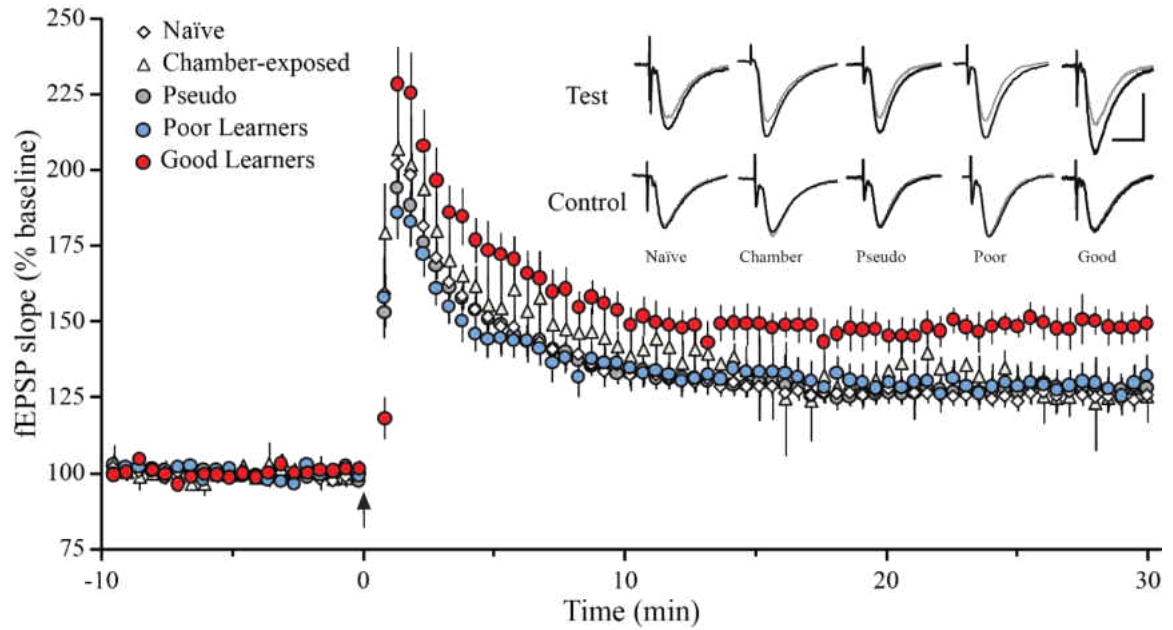
Figure 8. Acquisition of trace fear conditioning enhances synaptic plasticity in hippocampal CA1 area. One train of high frequency stimulation (100 Hz 1 s) induced LTP in slices from all groups. Good learners had hippocampal LTP that was significantly greater than all other groups ($p < 0.01$). *Inset*, representative fEPSP waveforms before (gray) and 30 min after (black) LTP induction. Scale bar, 1 mV, 10 ms. (Adapted from Song *et al.*, 2012).
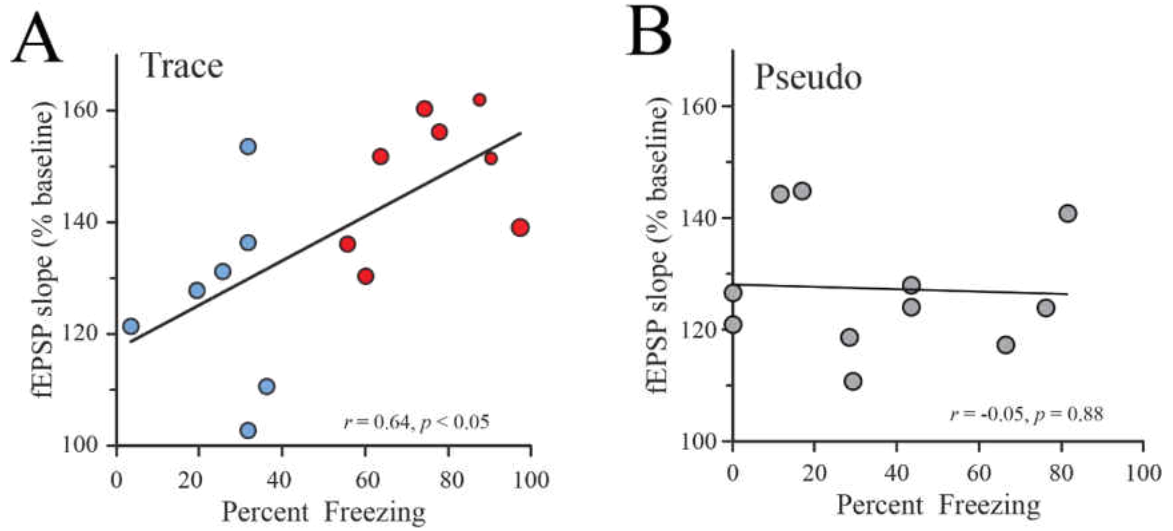
Figure 9. Acquisition of trace fear conditioning is significantly correlated with hippocampal synaptic plasticity. The percent of time spent freezing during the CS test session was significantly correlated with amount of LTP in slices taken from trace fear-conditioned (A; blue, poor learners; red, good learners) but not pseudoconditioned (B) rats. (Adapted from Song *et al.*, 2012).

Furthermore, acquisition of trace fear conditioning did not appear to alter basal synaptic transmission in the Schaffer collateral CA1 pathway – the average I/O curves did not differ between groups (for all individual intensities, $p > 0.25$ in raw I/O curves; see Figure 6A). In addition, the baseline fEPSP (measured prior to LTP induction, see Methods) was not significantly different in slices taken from naïve, chamber-exposed, pseudoconditioned, poor learners, or good learners [see Table 1; $F(4,46) = 0.40$, $p = 0.81$]. These data demonstrate that the enhanced synaptic plasticity following trace fear conditioning is learning-specific and does not involve enhanced basal transmission.

Effects of trace fear conditioning on hippocampal CA1 intrinsic neuronal excitability

Intracellular recordings revealed a significant reduction of the post-burst AHP in good learners compared with poor learners, pseudoconditioned, chamber-exposed and naïve rats (see representative traces in Figure 10A and average values in Figure 10B). The AHP amplitude was measured at different time points following offset of the somatic current injection (from 50 ms to 3 s). A repeated-measures ANOVA showed that good learners had significantly smaller AHPs than the other groups [main effect of group, $F(4,52) = 4.77$; $p < 0.01$]. There was also a significant effect of time point [within-subject effect, $F(2.0,103.8) = 210.9$; $p < 0.001$; Greenhouse-Geisser corrected] and a group by time point interaction [$F(8.0,103.8) = 3.36$; $p < 0.01$; Greenhouse-Geisser corrected]. Follow-up analyses using a one-way ANOVA revealed that from 0.1 s to 2 s following current offset, a statistically significant group effect on AHP amplitude was observed (all values, $p < 0.01$). *Post hoc* comparisons confirmed that the AHP was significantly smaller in CA1 neurons from good learners compared with those from poor learners, pseudoconditioned, chamber-exposed, and naïve rats ($p < 0.05$; see Figure 10B). Our findings indicate that

Table 1. Facilitation of LTP after trace fear conditioning is learning-specific

Group (number of rats)	Baseline fEPSP slope Mean (mV/ms)	Percent LTP Mean (% of baseline)
Naïve (21)	-0.63 ± 0.07	125.0 ± 3.0
Chamber-exposed (4)	-0.59 ± 0.07	126.1 ± 2.5
Pseudo (11)	-0.67 ± 0.05	127.3 ± 3.5
Poor Learners (7)	-0.76 ± 0.14	126.2 ± 6.4
Good Learners (8)	-0.72 ± 0.12	148.4 ± 4.2#

Data are mean ± SE. LTP, long-term potentiation; fEPSP, field excitatory postsynaptic potential; pseudo, pseudoconditioned. Statistically different between good learners and all other groups (# $p <$ 0.01)
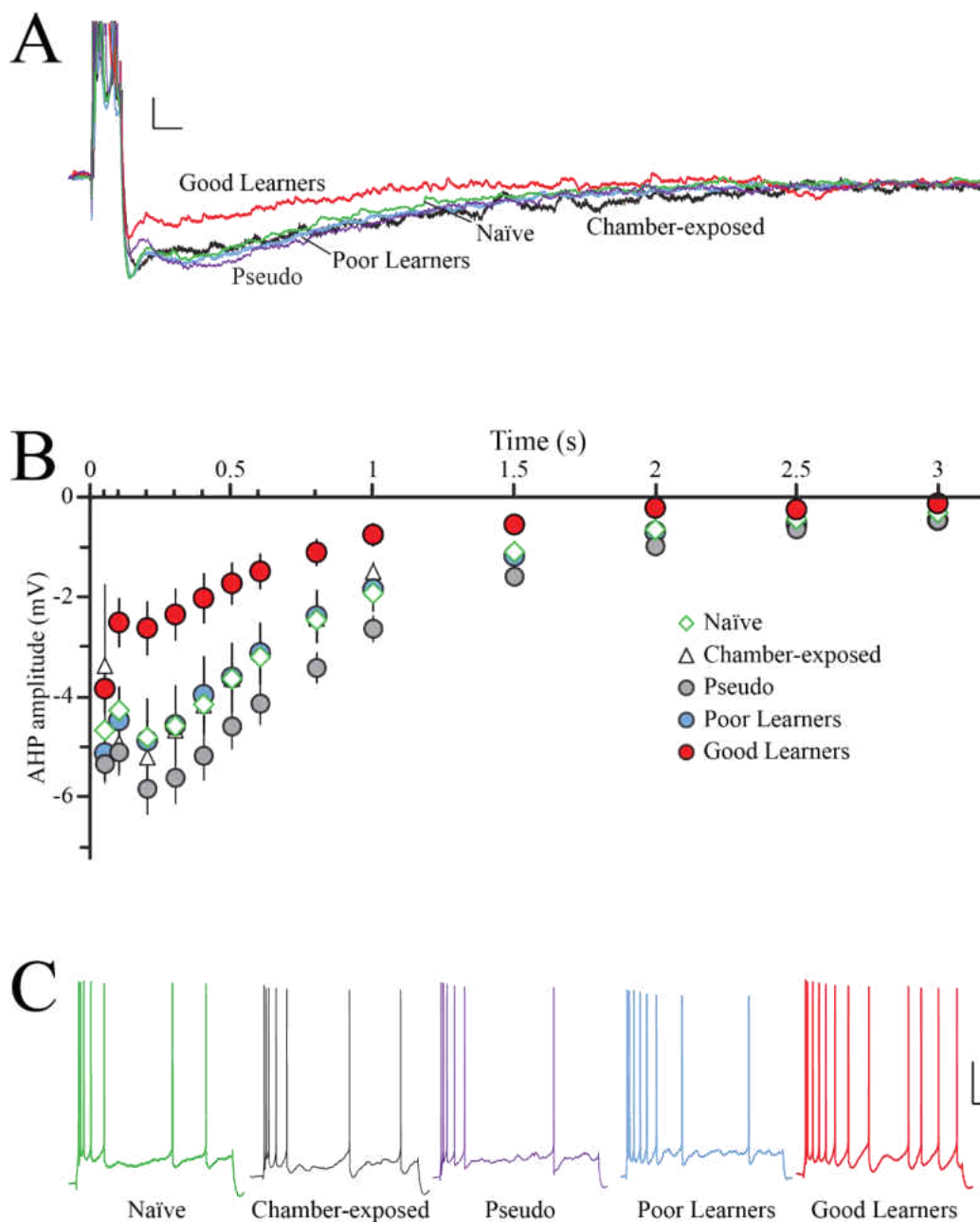
Figure 10. Acquisition of trace fear conditioning increased the intrinsic excitability of hippocampal CA1 pyramidal neurons. A, Representative traces of the post-burst AHP illustrating that CA1 neurons from good learners had smaller AHPs compared to those from poor learners, pseudoconditioned, chamber-exposed, and naïve rats. Scale bar, 2 mV, 100 ms. B, Plot showing the time course of the post-burst AHP amplitude as a function of training condition. Neurons from good learners had a significantly smaller AHP compared to all other groups when measured at $0.1 - 0.8$ s following current offset ($p < 0.05$). C, Action potential output of CA1 neurons in response to a prolonged 1 s current injection. Notice that CA1 pyramidal neurons from good learners fired more action potentials than did CA1 neurons from poor learners, pseudoconditioned, chamber-exposed, or naïve rats. Scale bar, 20 mV, 100 ms. (Adapted from Song *et al.*, 2012).
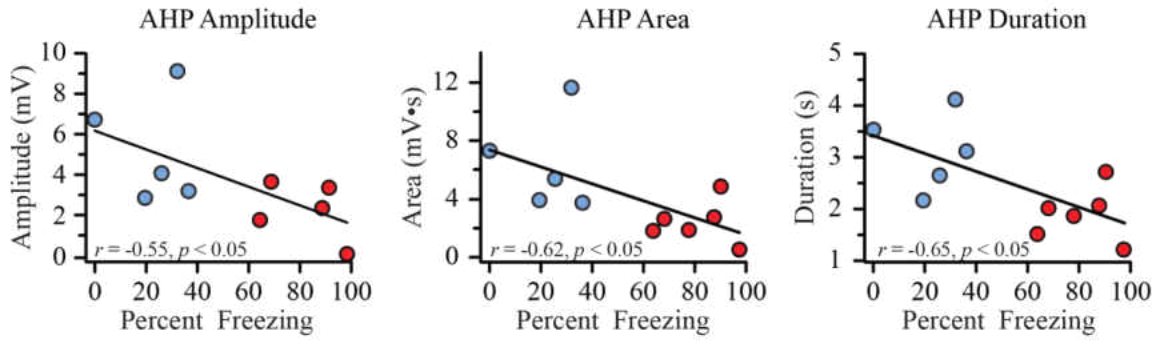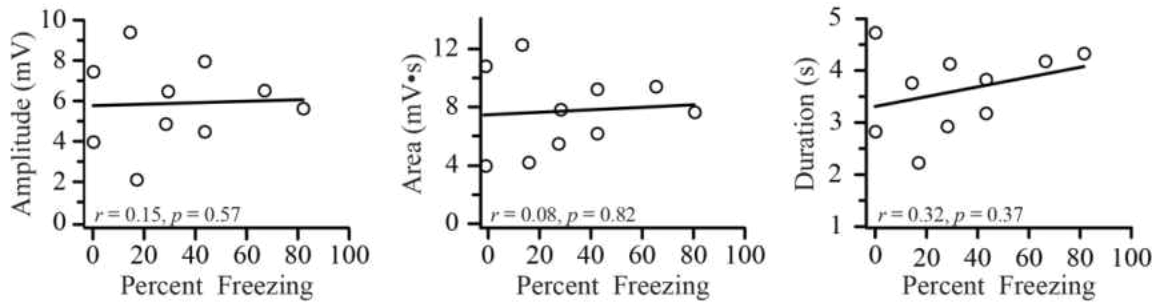
Figure 11. Behavioral performance is correlated with intrinsic excitability. Percent freezing during the probe test is significantly correlated with the AHP amplitude, area, and duration in trace conditioned (A) but not pseudoconditioned (B) rats. (Adapted from Song *et al.*, 2012).

successful acquisition of trace fear conditioning results in a significant decrease in the amplitude of the post-burst AHP of hippocampal CA1 neurons. Similar findings were also observed during analysis of the area and the duration of the post-burst AHP (see Table 2).

Percent freezing during the CS test was negatively correlated with the amplitude, area, and duration of the AHP in trace fear conditioned rats, such that better behavioral performance was associated with a smaller AHP (Figure 11A). In contrast, percent freezing during the CS test was not significantly correlated with the amplitude, area, or duration of the AHP in CA1 neurons from pseudoconditioned rats (Figure 11B). The significant correlation between behavioral performance and the AHP in trace fear conditioned but not pseudoconditioned rats further demonstrates that the enhancement of intrinsic excitability after trace fear conditioning is learning-specific.

In addition to altering the size and duration of the post-burst AHP, trace fear conditioning also altered spike-frequency adaptation (or accommodation), another index of intrinsic neuronal excitability. To quantify spike-frequency adaptation, the somatic current injection used to study the AHP was extended to deliver a 1 s depolarizing current injection and the number of action potentials was counted. Accommodation was significantly reduced after acquisition of trace fear conditioning [$F(3,52) = 5.62$, $p < 0.01$ see Figure 10C and Table 2]. *Post hoc* analysis revealed that CA1 neurons from good learners fired significantly more action potentials in response to the prolonged current injection than those of poor learners ($p < 0.05$), pseudoconditioned rats ($p < 0.01$), chamber-exposed rats ($p < 0.05$), or naïve rats ($p < 0.01$; see Table 2). Similar reductions in spike-frequency adaptation have been reported in hippocampal neurons following acquisition of other hippocampus-dependent tasks (e.g., see McKay *et al.*, 2009; Moyer et

Table 2. Summary of learning-related changes in CA1 neurons after trace fear conditioning

Group (number of rats)	Postburst afterhyperpolarization, AHP (*n*)			Accommodation (*n*)
	Amplitude (mV)	Duration (s)	Area (mV·s)	# of Action Potentials
Naïve (12)	-4.82 ± 1.50 (18)	3.13 ± 0.17 (18)	-5.56 ± 1.55 (18)	6.8 ± 0.5 (18)
Chamber-exposed (3)	-5.22 ± 0.46 (6)	3.29 ± 0.33 (6)	-6.25 ± 0.80 (6)	7.8 ± 0.4 (6)
Pseudo (10)	-5.85 ± 0.52 (16)	3.57 ± 0.21 (16)	-7.43 ± 0.74 (16)	6.3 ± 0.4 (16)
Poor Learners (5)	-4.89 ± 0.85 (8)	3.05 ± 0.26 (8)	-5.88 ± 1.00 (8)	7.8 ± 0.8 (8)
Good Learners (6)	-2.64 ± 0.54 (9) †§	2.10 ± 0.22 (9) †§	-2.85 ± 0.81 (9) †§	10.0 ± 0.8 (9) †§

Data are mean ± SE for number of cells in parentheses.

For AHP amplitude: significantly different from all controls († poor learners, $p < 0.05$; § naïve, chamber-exposed and pseudo, $p < 0.01$). For AHP duration: significantly different from all controls († poor learners, $p < 0.05$; § naïve, chamber-exposed and pseudo, $p < 0.01$). For AHP area: significantly different from all controls († naïve, chamber-exposed and poor learners, $p < 0.05$; § pseudo, $p < 0.01$). For Accommodation: significantly different from all controls († poor learners and chamber-exposed, $p < 0.05$; § naïve and pseudo, $p < 0.01$)

al., 2000; Moyer *et al.*, 1996; Thompson *et al.*, 1996b; Zelcer *et al.*, 2006), suggesting that in the present study acquisition of trace fear conditioning results in a more efficient neuronal input-output function in CA1 neurons. Furthermore, the learning-specific increase in CA1 pyramidal cell excitability was observed in the absence of any changes in resting membrane potential, input resistance, depolarizing sag, or action potential properties (see Table 3). These changes were also unlikely to result from any bias in cell selection for several reasons. First, all recordings were conducted by an individual who was blind to the training condition. Second, the cell selection criteria were established *a priori* (see Methods). Lastly, the percentage of cells lost during a recording was comparable between groups, $F(4,31) = 1.35$, $p = 0.27$. Taken together, these data suggest that acquisition of trace fear conditioning enhances intrinsic excitability in a learning-specific manner.

Table 3. Properties of CA1 neurons that do not change after trace fear conditioning

Group (number of rats)	V_{rest} (n) Mean (mV)	R_N (n) Mean (MΩ)	AP characteristics (n) AP_{amp} (mV)	AP_{width} (msec)	Sag (n) Mean (mV)
Naïve (12)	-68.6 ± 0.8 (18)	38.9 ± 2.1 (18)	90.4 ± 0.8 (18)	1.03 ± 0.01 (18)	5.9 ± 0.5 (18)
Chamber-exposed (3)	-66.3 ± 2.1 (6)	38.4 ± 4.1 (6)	88.2 ± 2.7 (6)	1.00 ± 0.02 (6)	6.1 ± 0.7 (6)
Pseudo (10)	-68.9 ± 1.0 (16)	42.5 ± 2.1 (16)	90.4 ± 0.8 (16)	1.04 ± 0.03 (16)	5.8 ± 0.4 (16)
Poor Learners (5)	-69.7 ± 2.2 (8)	46.2 ± 3.5 (8)	89.0 ± 1.6 (8)	1.08 ± 0.05 (8)	7.4 ± 0.9 (8)
Good Learners (6)	-70.5 ± 2.0 (9)	41.8 ± 3.5 (9)	88.4 ± 0.8 (9)	1.00 ± 0.04 (9)	5.6 ± 0.5 (9)

Data are mean ± SE for number of cells in parentheses.

Abbreviations: V_{rest} resting membrane potential; R_N input resistance; AP action potential; AP_{amp} action potential amplitude; AP_{width} action potential halfwidth

Discussion

The present data suggest that acquisition of trace fear conditioning induces learning-specific changes in hippocampal synaptic plasticity and intrinsic excitability. By using a single, brief CS test, we showed that trace fear memory was correlated with hippocampal intrinsic excitability as well as synaptic plasticity *in the same animals*. Recordings in brain slices from rats that were classified as good learners revealed not only a learning-specific facilitation of LTP but also a learning-specific reduction in both the post-burst AHP and spike-frequency adaptation. These data suggest that both intrinsic excitability and synaptic plasticity are integrally involved in shaping the efficiency of hippocampal processing during acquisition of trace fear conditioning.

Acquisition of trace fear conditioning is correlated with synaptic plasticity

Percentage of time spent freezing in trace fear conditioned rats was positively correlated with synaptic plasticity (Figure 9A). Although this is the first report of a learning-related enhancement in synaptic plasticity following trace fear conditioning, these data are consistent with other *in vivo* or *in vitro* synaptic plasticity studies using other hippocampus-dependent learning paradigms. For example, in adult rats the magnitude of LTP in hippocampus was strongly correlated with behavioral performance in the Morris water maze (Boric *et al.*, 2008). Similarly, *in vivo* recordings from hippocampal CA1 neurons in behaving mice demonstrated that LTP induced during (but not before) trace eyeblink conditioning lasted longer and was more resistant to extinction-induced depotentiation (Gruart *et al.*, 2006). Other manipulations that either impair or enhance learning have also resulted in a corresponding impairment or enhancement of LTP. For example, mice exposed to environmental enrichment not only performed better in

hippocampus-dependent contextual fear conditioning, but also exhibited greater LTP in hippocampal slices (e.g., Duffy, Craddock, Abel, & Nguyen, 2001). Conversely, exposure to stress resulted in both impaired hippocampal LTP and impaired retention of spatial learning in the Morris water maze (e.g. Kim, Lee, Han, & Packard, 2001). The current finding of a positive correlation between acquisition of trace fear conditioning and amount of hippocampal LTP suggests that the enhanced synaptic plasticity is learning-specific. This is supported by the fact that hippocampal LTP was highest in the good learners whereas LTP in the poor learners was comparable with the other control groups (Figure 8). These data are in line with a recent study showing that inducing LTP to the auditory input to lateral amygdala following fear conditioning specifically activate the conditioned memory whereas inducing LTD deactivate the conditioned memory (Nabavi *et al.*, 2014). Furthermore, although some of our pseudoconditioned rats exhibited high levels of freezing following CS offset, LTP was not significantly correlated with freezing levels in pseudoconditioned rats (Figure 9B). Other studies have observed high freezing levels in pseudoconditioned rats following CS offset (e.g., Gilmartin & Helmstetter, 2010; Majchrzak *et al.*, 2006). Since *trace interval* freezing (i.e., freezing following CS offset) is of particular interest in trace fear conditioning studies, care should be taken to minimize post-CS freezing (for further discussion of this topic see Smith, Gallagher, & Stanton, 2007). That LTP was not correlated with freezing in our pseudoconditioned rats suggests that the relatively high freezing levels observed in some of these animals did not result from hippocampal plasticity. Taken together, these data suggest that acquisition of trace fear conditioning facilitates synaptic plasticity in hippocampal neurons in a learning-specific manner.

Acquisition of trace fear conditioning is correlated with intrinsic excitability

Trace fear conditioning induced a learning-specific increase in the intrinsic excitability of CA1 pyramidal neurons, which was due to reductions in the post-burst AHP and spike-frequency adaptation (Figure 10). Furthermore, the percentage of time spent freezing in the trace fear conditioned rats was negatively correlated with the amplitude, area and duration of the post-burst AHP (see Figure 11A). The fact that these correlations were not observed in neurons recorded from pseudoconditioned rats (see Figure 11B) further supports that these intrinsic changes were learning-specific and not a general result of the training or testing procedures.

Numerous studies have investigated intrinsic plasticity following learning using both invertebrate and vertebrate preparations (for reviews, see Disterhoft & Oh, 2006; Zhang & Linden, 2003). Our observed AHP reductions following trace fear conditioning are reminiscent of intrinsic plasticity in CA1 observed following acquisition of trace eyeblink conditioning (e.g., de Jonge, Black, Deyo, & Disterhoft, 1990; Moyer *et al.*, 1996; Oh, McKay, Power, & Disterhoft, 2009). Furthermore, a recent study by McKay et al (McKay *et al.*, 2009) reported reduced AHPs in CA1 neurons from rats that received 3 trials of trace fear conditioning. Although the present data also observed reduced AHPs after trace fear conditioning, one major difference between the two studies is the number of training trials. The present study used 10 training trials and found that freezing during the test session was significantly correlated with the size of the AHP, and that this correlation was observed in trace fear conditioned but not pseudoconditioned rats (see Figure 11A). In contrast, McKay and colleagues used very few training trials and demonstrated the labile nature of these learning-related AHP reductions through the use of

3 extinction trials. Although rats did not receive an extinction session in the present study, our prior work suggests that extinction does not begin to emerge until at least 3 or more CS presentations (see Figure S1 of Kaczorowski *et al.*, 2012). Thus, our use of two test trials did not obscure our ability to observe learning-related changes in CA1 excitability – we observed reduced AHPs in CA1 neurons from trace fear conditioned but not pseudoconditioned rats.

Our studies employed a brief CS test session in order to relate freezing behavior to measures of hippocampal physiology. This test, although essential for getting a read-out of fear memory, is also likely to engage brain mechanisms associated with the well-described phenomenon of reconsolidation (for review, see Nader, Schafe, & Le Doux, 2000). Much has been learned about the cellular and molecular mechanisms of reconsolidation (e.g., Clem & Huganir, 2010; Miller & Marshall, 2005; Nader & Einarsson, 2010), but exactly how this process may influence our observed electrophysiological changes is unclear and beyond the scope of the present study. Although we cannot rule out an important influence of this CS test, we believe it is unlikely that our use of a brief test session substantially influenced our electrophysiological measurements for several reasons. First, using rats that received a test session 1-hr prior to slice preparation, Quirk and colleagues (Santini *et al.*, 2008) demonstrated electrophysiological changes in prefrontal neurons – changes that could be reversed by an interposed extinction session. Thus, the only variable was the presence of an extinction session as all rats received the same test session prior to slice preparation. Similarly, Restivo and colleagues (2009) demonstrated changes in spine density in hippocampal neurons following context fear conditioning – changes that were independent of whether the rat received a test session or

not. Perhaps the most compelling data come from a study by McKay and colleagues (2009) who demonstrated that changes in the intrinsic excitability of CA1 neurons after trace fear conditioning were similar between rats that *did* and those that *did not* receive a test trial prior to slice preparation. Taken together, these data suggest that acquisition of trace fear conditioning enhances intrinsic plasticity in a learning-specific manner.

Putative interaction between synaptic and intrinsic plasticity during learning

The current study found that acquisition of trace fear conditioning induced both an increase in the intrinsic excitability of CA1 neurons and a facilitation of LTP. The observed enhancement of LTP following acquisition of trace fear conditioning can be accomplished in a variety of ways. First, drugs or other treatments that reduce the AHP have been found to facilitate the induction of LTP. For example, the adrenergic agonist isoprenaline reduces the slow AHP and converts short term potentiation (STP) into LTP (Sah & Bekkers, 1996). Similarly, pharmacological stimulation of metabotropic glutamate receptors reduces the AHP of hippocampal CA1 neurons (Cohen & Abraham, 1996) and also facilitates LTP induction, without affecting basal synaptic transmission (Cohen, Coussens, Raymond, & Abraham, 1999). Thus, the AHP may act as an adjustable gain control where larger AHPs (or even the presence of the AHP) can shunt synaptic inputs (Sah & Bekkers, 1996). Indeed, a recent study demonstrated that the larger postsynaptic AHP observed in aged CA1 neurons significantly impairs synaptic throughput in a frequency-dependent manner (Gant & Thibault, 2009). Second, enhancement of synaptic plasticity can also be achieved by downregulation of transient A-type potassium channels. These transient K^+ channels are highly expressed in distal dendrites and shape action potential backpropagation through the dendrites. Furthermore, pharmacological down-regulation or deletion of A-type

potassium channels has been associated with an enhancement of both dendritic excitability and LTP (X. Chen *et al.*, 2006; Hoffman & Johnston, 1998). Third, LTP can be enhanced by application of brain-derived neurotrophic factor (BDNF). BDNF facilitates LTP induction (e.g., Figurov, Pozzo-Miller, Olafsson, Wang, & Lu, 1996) by enhancing intrinsic excitability (reduced AHP), which involves the activation of small-conductance Ca^{2+}-activated potassium (SK2) channels in hippocampal neurons (Kramar *et al.*, 2004).

Another line of evidence illustrating an interaction between synaptic stimulation and intrinsic plasticity comes from a recent report demonstrating that intrinsic plasticity can be induced independent of synaptic plasticity. For example, Barkai and colleagues (Cohen-Matsliah, Motanis, Rosenblum, & Barkai, 2010) recorded from CA1 pyramidal neurons and demonstrated that high frequency synaptic stimulation (e.g., 20 stimuli at 50 Hz), which alone was incapable of inducing LTP, was able to cause a significant reduction of the post-burst AHP. That we saw reduced AHPs in the absence of a significant alteration in baseline synaptic responses suggests the possibility that acquisition of trace fear conditioning may alter intrinsic neuronal excitability, which might then facilitate synaptic plasticity. Although this is highly speculative, support for this possibility comes from our within-animal analyses of the relationship between the size of the AHP and the amount of LTP. Figure 12 shows that there was a negative correlation between the size of the AHP and the amount of LTP such that hippocampal LTP was greater in animals whose CA1 neurons had smaller AHPs. This correlation was not only significant for the amplitude ($r = -0.38$, $p < 0.05$; Figure 12A), but also for the area ($r = -0.41$, $p < 0.05$; Figure 12B), and the duration ($r = -0.37$, $p < 0.05$; Figure 12C) of the post-burst AHP. Interestingly, if good learners are removed from the plots, the correlation is no longer significant (Figure 12,
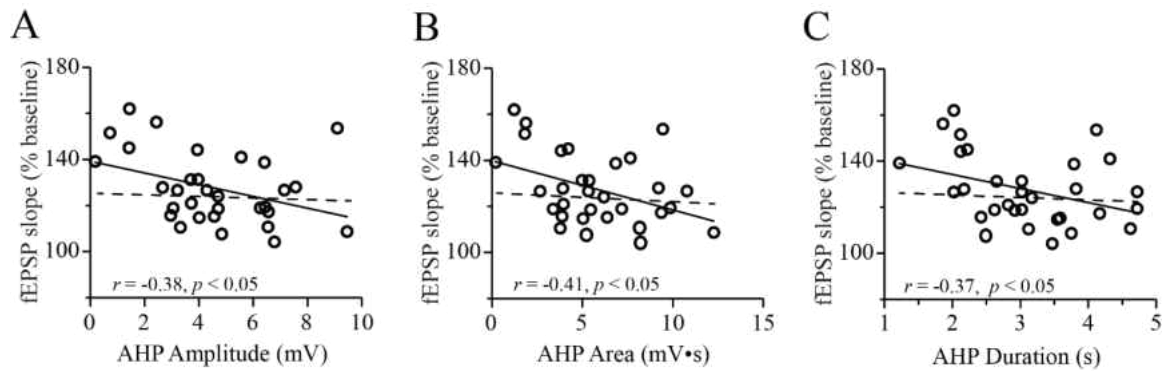
Figure 12. Synaptic plasticity is correlated with intrinsic excitability. The magnitude of LTP was significantly correlated with the amplitude (A), area (B) and duration (C) of the post-burst AHP (solid lines). Data are mean values for each animal where both intrinsic excitability and synaptic plasticity were studied in the same slice. Interestingly, when good learners are removed from the plot, the correlation is no longer significant (dashed line indicates slope of the line in the absence of good learners). (Adapted from Song *et al.*, 2012).

dashed lines). Thus, the data suggest that under baseline conditions (e.g., in the absence of learning-related changes), the AHP and LTP are not correlated. This correlation only emerges when there is a perturbation, such as a learning-related AHP reduction. Additional experiments, beyond the scope of this study, involving multiple time points (e.g., monitoring intrinsic and synaptic plasticity at different times throughout training) would be required to further address this complex relationship.

Implications of learning-induced synaptic and intrinsic plasticity

The current study demonstrated an increase in both intrinsic excitability and synaptic plasticity in hippocampal CA1 neurons following trace fear conditioning. Our data (see also review by Zhang & Linden, 2003) suggest that both intrinsic and synaptic plasticity play important roles in trace fear learning. These are dynamic and time-dependent processes. For example, it is known from prior studies that learning can rapidly induce, within an hour, an LTP-like enhancement of synaptic transmission (Power *et al.*, 1997; Rumpel, LeDoux, Zador, & Malinow, 2005; Whitlock *et al.*, 2006), which has been shown to occlude subsequent induction of LTP. In hippocampus, this LTP-like enhancement of basal synaptic transmission has been shown to result from a rapid and transient delivery of AMPA receptors at activated synapses (see Nabavi *et al.*, 2014; Whitlock *et al.*, 2006). However, in contrast, this enhancement of basal synaptic transmission has not been consistently observed in hippocampus 24 h after learning (LoTurco, Coulter, & Alkon, 1988; Power *et al.*, 1997; Zelcer *et al.*, 2006), suggesting that, at least in hippocampus, this learning-related LTP-like phenomenon is short lived. Furthermore, it has also been shown that intrinsic excitability is altered in hippocampus as early as 1 h after learning (Moyer *et al.*, 1996; Thompson *et al.*, 1996b) and that this change

persists for several days (Moyer *et al.*, 1996; Thompson *et al.*, 1996b; Zelcer *et al.*, 2006). Interestingly, it has recently been shown that synaptic activity, even activity that does not induce LTP, can cause a protein synthesis-dependent increase in intrinsic excitability, as measured by AHP reductions (Cohen-Matsliah *et al.*, 2010). Thus, it is possible (albeit speculative at this point) that as the animal learns the trace fear conditioning task, pairing of the CS and US transiently increases basal transmission at hippocampal synapses that leads to increased intrinsic excitability (e.g., a smaller AHP), and that this increased excitability contributes to our observed facilitation of LTP.

How does learning-induced intrinsic and synaptic plasticity impact further learning? Few studies have directly addressed this issue. However, a learning-related increase in CA1 excitability may facilitate learning of another hippocampus-dependent task. Support for this hypothesis comes from rule learning studies, where rats show an increased learning capacity in discriminating between new pairs of odors once they have learned to discriminate the first pair (Saar & Barkai, 2003; Saar, Grossman, & Barkai, 1998). In addition, odor discrimination also facilitates acquisition of hippocampus-dependent Morris water maze, but only within a brief time window of $1-2$ days following rule learning, while the AHP is reduced (Zelcer *et al.*, 2006). Thus, learning-induced intrinsic and synaptic modifications of postsynaptic neurons are capable of facilitating subsequent learning. In contrast, prior training in trace eyeblink conditioning *did not* enhance learning of hippocampus-dependent Morris water maze; however simultaneous training in both tasks facilitated trace eyeblink but not water maze learning (Kuo, Lee, & Disterhoft, 2006). Additional studies will be required to determine the extent to which intrinsic and/or synaptic changes following trace fear conditioning impact learning of other

hippocampus-dependent learning tasks or whether learning of other tasks affects the acquisition of trace fear conditioning.

Conclusions

The current data are the first to demonstrate that trace fear conditioning is significantly correlated with both synaptic plasticity and intrinsic excitability in the hippocampus. Acquisition of trace fear conditioning enhanced intrinsic excitability and facilitated the induction of LTP in the absence of significant changes in basal synaptic transmission. These observations were learning-specific because they were not observed in pseudoconditioned, chamber-exposed, or naïve rats. In addition, there was a negative correlation between the size of AHP and the amount of LTP such that animals whose CA1 neurons had smaller AHPs tended to display greater LTP. Thus, the data suggest a model whereby as acquisition occurs, hippocampal intrinsic excitability increases, which then leads to a facilitation of synaptic plasticity, which occurs during memory consolidation.

CHAPTER THREE: electrophysiological properties of mPFC-BLA projection neurons

Abstract

Medial prefrontal cortex (mPFC) is critical for the expression of long term conditioned fear memory. Growing evidence suggests the opposite roles of the two subregions (PL and IL) within the mPFC but some results are controversial. Such subregion-specific regulation of fear memory and the conflicting results may be associated with the heterogeneity of cortical projection neurons because different subtypes of neurons are distributed across the cortical layers and subregions. However, mPFC neurons have distinct morphological and electrophysiological properties that vary as a function of their long-range projection targets. In order to better understand how the heterogeneity of the mPFC neurons affects fear memory expression, the current study used visually-guided WCRs to characterize both randomly selected mPFC neurons (i.e., those whose projections are unknown) and neurons with known projections to the basolateral nucleus of amygdala (BLA). Recordings from randomly selected neurons suggest that L2/3 neurons were more hyperpolarized and less excitable than L5 neurons, which may be due to their differential expression of *h*-channels (more *h*-current was expressed in L5 neurons). Furthermore, L5 mPFC-BLA projection neurons displayed characteristics of HCN2-mediated *h*-current in response to hyperpolarization. We further demonstrated that HCN channels were involved in shaping the basic membrane properties, and that blocking HCN channels greatly affects the intrinsic excitability and dendritic signal integration of mPFC-BLA projection neurons. These data lay the foundation for a circuit-specific study of mPFC neurons in fear conditioning.

Introduction

Much of our understanding of the neurobiology of fear learning and memory expression comes from the study of Pavlovian fear conditioning and extinction, in which mPFC is critical for expression of long-term memory (Morgan, Schulkin, & LeDoux, 2003). Specifically, two subregions within mPFC that have received a lot of attention are the prelimbic (PL) and infralimbic (IL) cortices. Although these two subregions are adjacent, growing evidence suggests that the PL and IL play distinct roles during fear memory expression. However, the previous reports are not all consistent with each other, which obscures our understanding of the neural basis underlying fear memory expression (for review, see Kim & Jung, 2006). For example, it has been shown that PL activation facilitates the expression of conditioned fear (Burgos-Robles *et al.*, 2009; Vidal-Gonzalez *et al.*, 2006) whereas IL activation facilities extinction and reduces conditioned fear (Burgos-Robles *et al.*, 2007; Chang & Maren, 2011; Milad & Quirk, 2002; Milad *et al.*, 2004; Vidal-Gonzalez *et al.*, 2006). However, studies from LeDoux's group (Morgan & LeDoux, 1995) and Thompson's group (Garcia *et al.*, 1999) suggest that fear conditioning suppresses the activity of PL neurons, and studies from Grace's group suggest that fear conditioning excites those IL neurons that receive monosynaptic inputs from the basolateral nucleus of amygdala (Laviolette *et al.*, 2005) as well as those IL neurons that project to the nucleus accumbens (McGinty & Grace, 2008).

One possible reason for the conflicting data is the heterogeneity of mPFC neurons. For example, PL neurons that project to the pons express larger *h*-current (I_h) carried by hyperpolarization-activated and cyclic nucleotide-gated (HCN) channels and display lower steady-state input resistance thus are less excitable than neurons that project to the

contralateral PL (Dembrow *et al.*, 2010). Furthermore, these two groups of neurons also react differentially to neurotransmitters such as serotonin (5-HT): neurons that project to the pons are inhibited by 5-HT through activation of 1A receptors whereas the neurons that project to the contralateral mPFC are excited by 5-HT through activation of 2A receptors (Avesar & Gulledge, 2012). Thus, the current study was carried out to evaluate the heterogeneity of mPFC neurons. We used a combination of retrograde tracing and WCRs to characterize both randomly selected mPFC neurons and those mPFC neurons that project to BLA (mPFC-BLA projection neurons).

Methods

Subjects. Subjects were 11 adult male Sprague Dawley (4.9 ± 0.9 mo) and 14 adult male Fischer F344 rats (4.7 ± 0.2 mo). Data from different strains were combined because no significant difference was found in all measurements. Rats were maintained in an Association for Assessment and Accreditation of Laboratory Animal Care (AAALAC) accredited facility on a 14 h light–10 h dark cycle and housed individually with free access to food and water. Procedures were conducted in accordance with the University of Wisconsin-Milwaukee animal care and use committee (ACUC) and NIH guidelines.

Retrobeads^TM injection. Twelve of the 25 rats (4 Sprague, 8 Fischer) received unilateral pressure infusion of a fluorescent retrograde tracer (red Retrobeads^TM, Lumafluor) into the amygdala, targeting basolateral (BL) nucleus of the amygdala (relative to Bregma, -3 mm AP, ± 5 mm ML; - 8.3 mm DV; see Figure 13A), with deep anesthetization under stereotaxic. The infusion was made with a pipette (20 – 30 μm) pulled from borosilicate glass (VWR Micropipets) using a Sutter Instruments P97 puller. The pipette was connected to a 2 μl syringe (Hamilton) driven by an infusion pump
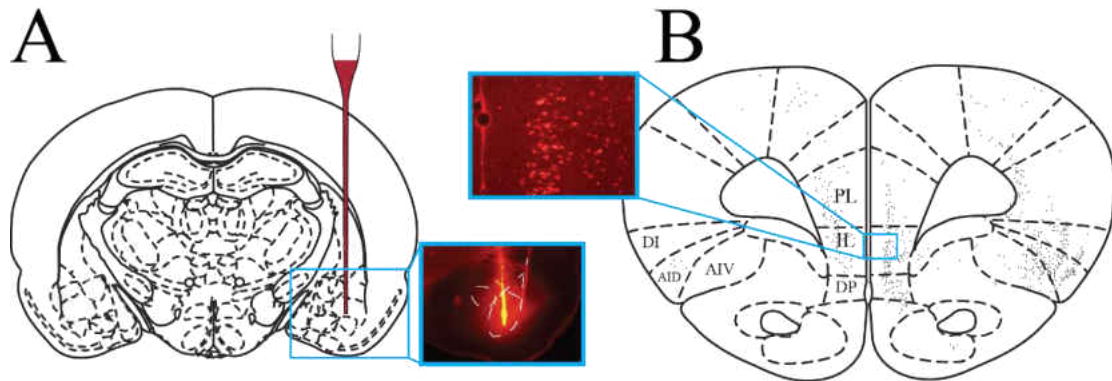
Figure 13. Unilateral infusion of a retrograde tracer into BLA used to characterize the electrophysiological properties of the mPFC-BLA projection neurons. A, Schematic diagram of rat coronal section (illustration modified from Paxinos & Watson, 1998, with permission from *Elsevier*) showing that a glass pipette was used for the unilateral infusion of red fluorescent microspheres (Retrobeads[TM]) into the BLA. Inset, a representative fluorescent image showing that red Retrobeads[TM] were injected into BLA. B, Distribution of the fluorescently labeled cortico-BLA somata in a coronal section (illustration modified from Paxinos & Watson, 1998, with permission from Elsevier). Each mark represents one neuron. In the ipsilateral hemisphere, intense distributions of corticoamygdala neurons were found in both mPFC and insular cortices. In the contralateral hemisphere, the corticoamygdala neurons were primarily distributed within the mPFC. Inset, a representative fluorescent image showing the fluorescently labeled neurons in IL. Abbreviations: AID, agranular insular cortex, dorsal part; AIV, agranular insular cortex, ventral part; DI, dysgranular insular cortex; IL, infralimbic cortex; PL, prelimbic cortex.

(Harvard Apparatus, model 975). The infusion lasted 5-10 min and the pipette was withdrawn 10 min after infusion. A total of $0.1 - 0.3$ µl red Retrobeads^{TM} were infused into the BLA.

PFC slice preparation for electrophysiological recording. After a minimum of 2 days of recovery from the Retrobeads^{TM} infusion, rats were anesthetized and decapitated. The brain was quickly removed and PFC was cut at the level of optic chiasm. Coronal PFC slices (300 µm) from both hemispheres were prepared in ice-cold aCSF using a vibrating tissue slicer (VT1200, Leica). The rest of the brain was then blocked and coronal slices that contain the amygdala were cut to confirm the location of the injection. PFC slices were incubated in oxygenated aCSF (32-36°C) whereas amygdala slices were temporarily kept in oxygenated aCSF at room temperature. The injection site was quickly verified by using fluorescent microscope (Olympus BX51WI) equipped with mercury lamp and a Texas Red epifluorescent filter cube immediately after cutting. Some PFC slices were used to examine the distribution of fluorescently labeled neurons and thus photoimaged with an Olympus DP70 camera and DP Controller software (version 2.1). Images were stitched together and individual cortico-BLA projection neurons were marked on a PFC diagram using Photoshop software (Adobe Systems; see Figure 13B).

Electrophysiological recordings. PFC slices were transferred to a submerged recoding chamber mounted on an Olympus BX51WI upright microscope where they were continuously perfused with oxygenated aCSF at a rate of 2 ml/min, maintained at 32-36°C using an inline temperature controller. WCRs were obtained under visual guidance from the soma of layer 5 (L5) pyramidal neurons (either fluorescently labeled or randomly selected) located in either infralimbic (IL) or prelimbic (PL) subregions of the mPFC. The

fluorescently labeled pyramidal cells in mPFC (i.e., mPFC-BLA projection neurons) were visualized using an Olympus microscope (BX51WI) equipped with mercury lamp and a Texas Red epifluorescent filter cube. A Hamamatsu CCD camera (Hamamatsu Camera Ltd., Tokyo, Japan) was used to visualize and take photograph of the brain slices and neurons. After fluorescently labeled neurons were recognized, the microscope was switched to IR-DIC mode to guide whole-cell recording (WCRs) on these cells. For WCRs, electrodes (5–8 MΩ) were prepared from thin-walled capillary glass and filled with the following solution (in mM): 110 K-gluconate, 20 KCl, 10 Di-TrisPCr, 10 HEPES, 2 $MgCl_2$, 2 Na_2ATP, 0.3 Na_2GTP, 0.10% Biocytin, pH to 7.3, osmolarity 285. All recordings were obtained in current-clamp mode using a HEKA EPC10 amplifier system (HEKA Instruments Inc. Bellmore, New York). Experiments were controlled by PatchMaster software (HEKA Instruments) running on a PC. All electrodes were pulled from thin-walled capillary glass (A-M Systems, Carlsborg, WA) using a Sutter Instruments P97 puller. Cells were held at -67 mV by manually adjusting the holding current. Voltages were not corrected for the liquid-liquid junction potential (~+13 mV, see Moyer and Brown, 2007). The electrode capacitance and series resistance (R_s) were monitored, compensated, and recorded frequently throughout the duration of the recording. Cells were only accepted for analysis if the initial series resistance was ≤ 30 MΩ and did not change by > 30% throughout the recording period. In some experiments, the effect of *h*-current on active and passive membrane properties was studied by bath applying HCN channel blockers ZD7288 (50 µM) or 3 mM CsCl to the aCSF for at least 10 min.

Intrinsic properties of mPFC neurons were recorded under current clamp according to the following protocols: *(1)* I-V relations were obtained from a series of 500 ms current

injections (range -300 to 50 pA) and plotting the plateau voltage deflection against current amplitude. Neuronal input resistance (R_N) was determined from the slope of the linear fit of the portion of the V-I plot where the voltage sweeps did not exhibit sags or active conductance (see Figure 14A). The sag ratio during hyperpolarizing membrane responses was expressed as $[(1 - \Delta V_{ss} / \Delta V_{min}) \times 100\%]$, where $\Delta V_{ss} = MP - V_{ss}$, $\Delta V_{min} = MP - V_{min}$, MP is the membrane potential before current step, V_{ss} is the steady-state potential and V_{min} is the initial minimum potential. For each neuron, sag ratio was calculated from -300 pA, -250 pA, and -200 pA current steps and averaged. *(2)* AP properties, including $I_{threshold}$ (the minimum current necessary to elicit an AP), were studied with an ascending series of 500 ms depolarizing pulses with a step of 10 pA (the step size was reduced whenever necessary). *(3)* Neuronal excitability was studied by injecting a series of 1 s current at 50 − 300 pA with an intertrial interval of 20 s and a step of 50 pA, and the number of APs evoked was counted (see Figure 14B). *(4)* Post-burst AHP was measured by injecting 10 suprathreshold current injections (2 ms; 1-3 nA) at 50 Hz (3X, at 20 sec intervals; see Figure 14C).

To study synaptically-evoked EPSPs, parallel stimulating electrodes with PTFE-coated Platinum-Iridium wires in glass pipettes (a tip size of < 60 μm) were custom made in the laboratory. The small diameter tip allowed for the placement of two stimulating electrodes within a small space. The synaptic properties of mPFC-BLA projection neurons were studied according to the following protocol: *(1)* Single EPSPs were evoked by stimulating layer 2/3 pathway. *(2)* Temporal summation was studied by stimulating the layer 2/3 pathway to elicit a train of EPSPs at 20 Hz, 50 Hz, and 100 Hz. *(3)* Signal integration (coincidence detection) was studied by stimulating both layer 2/3 and layer 5
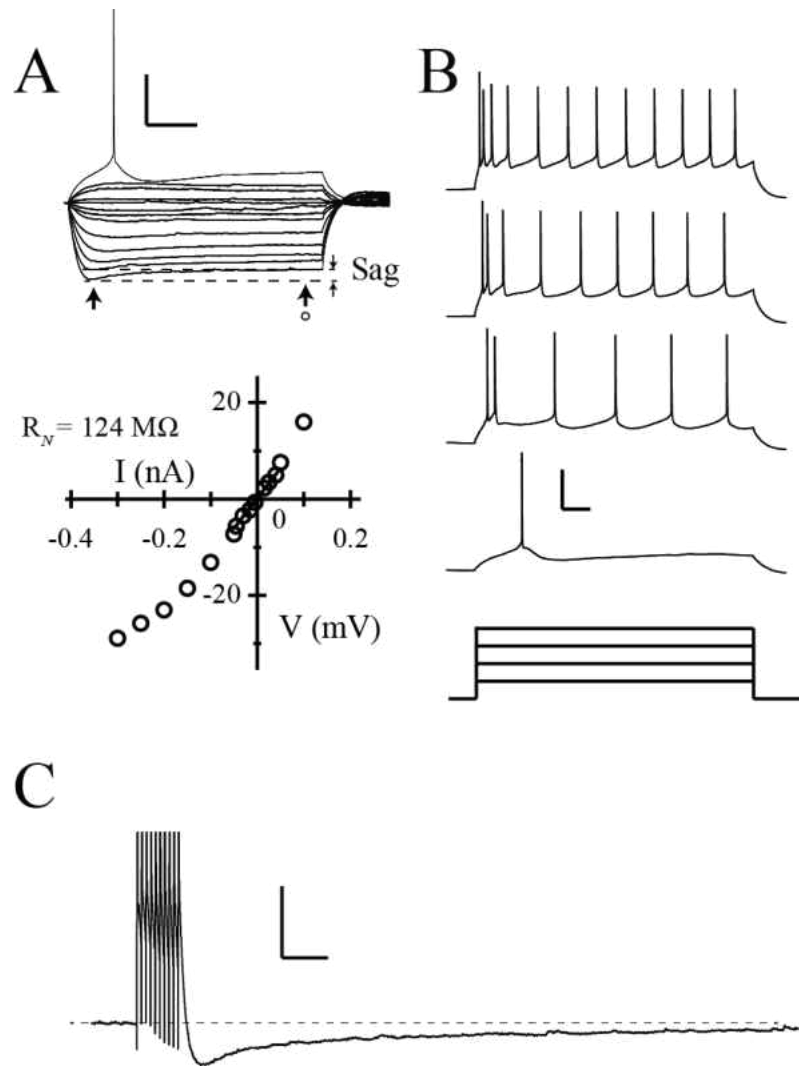
Figure 14. Electrophysiological study of IL-BLA projection neurons. A, Voltage responses to a series of current injections and the accompanying V-I plot used to measure neuronal input resistance (R_N). Arrows show the peak voltage deflection and the steady-state voltage near the end of the current injection (used in measuring the depolarizing sag). The amplitude of sag was calculated as the different membrane potential between the peak and the steady state. Scale bar, 40 mV, 0.1 s. B, Neuronal excitability was studied by injecting a series of depolarizing currents and the number of spikes evoked was counted. Scale bar, 40 mV/100 pA, 0.1 s. C, Post-burst AHP was studied by evoking 10 action potentials at 50 Hz. The amplitude of the post-burst AHP was measured from baseline at different time points following the last action potential. Scale bar, 10 mV, 0.2 s.

inputs and varying the delay between the two stimuli. Stimulation intensities were adjusted so that the cells only fired APs when the two stimulations were delivered simultaneously.

For the rats that did not receive Retrobeads^{TM} injection, slice preparation and recording procedures were the same as above except that the neurons were randomly selected in both L2/3 and L5.   In addition, before terminating any recording, a photomicrograph of the slice showing the location of recording electrode in the brain slice was taken with the CCD camera for offline verification of the somatic location (IL vs. PL) and measurement of the somatic depth from the pial surface.

Biocytin staining. Neurons filled with biocytin (0.1% in internal solution) during recording were fixed in formalin for 1 to 4 weeks before they were processed for visualization by using streptavidin Alexa Flour 488 reaction. Slices were mounted, and labeled neurons were visualized and imaged using a fluorescence microscope (BX51WI, Olympus) or laser scanning confocal fluorescence microscope (FV-1200, Olympus). Confocal image stacks were used for 3D reconstructions (see Figure 15A and 15B) using Neurolucida software (MBF bioscience).   All neurons displayed characteristics of pyramidal cells according to both morphological and electrophysiological criteria.

Statistical Analyses.   All statistical analyses were performed with the aid of Microsoft Excel and IBM SPSS statistics software (version 22; SPSS). For randomly selected neurons, although 4 groups of neurons were presented, comparisons were always conducted between two distinct groups.   Thus, neuronal comparisons were made as follows: L2/3 vs. L5 of IL; L2/3 vs. L5 of PL; L2/3 of IL vs. L2/3 of PL; L5 of IL vs. L5 of PL.   Two-tailed independent samples *t* test, paired *t* test, and a one-way repeated-

measures ANOVA were conducted wherever appropriate. All results were reported as mean ± SEM.
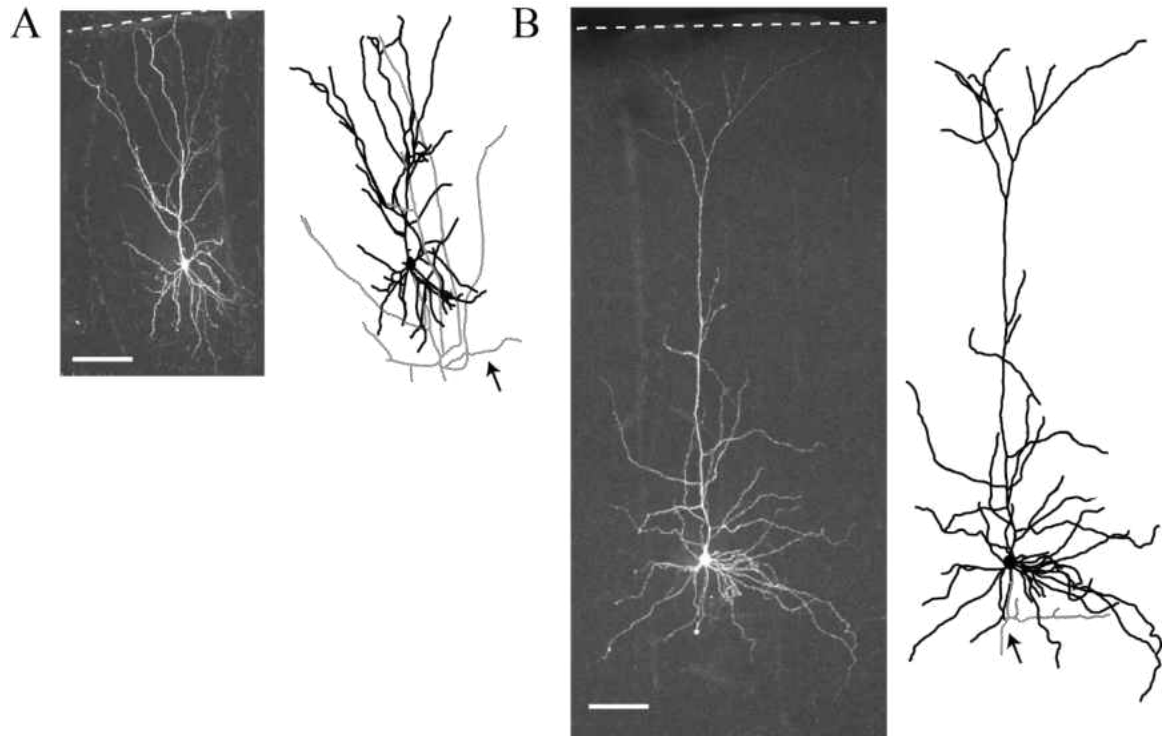
Figure 15. Confocal images of biocytin-filled neurons in L2/3 (A) and in L5 (B) of medial prefrontal cortex. Alexa Fluor 488 was conjugated to the biocytin reaction product to produce green fluorescence. Note that the axons (arrows) are represented in gray in the 3D reconstructions. Scale bars in both A and B are 100 μm.

Results

The current study first evaluated the heterogeneity of mPFC neurons (n = 108) by recording from pyramidal neurons with unknown projection targets in both L2/3 and L5. We then studied the mPFC-BLA projection neurons (n = 37) in L5 by recording the fluorescently labeled neurons after the rats received unilateral injection of Retrobeads™ into the BLA.

Layer- and region-specific properties of randomly selected neurons in mPFC

mPFC boundary definition. The location of the recorded neuron was determined from online image snapshots and drawn on the corresponding plates of the rat atlas (see Figure 16A). The boundary between L2/3 and L5 was defined according to the somatic depth (measured from the soma to the pial surface). Neurons with somatic depth that were 400 µm or less were defined as L2/3 neurons and the deeper neurons were defined as L5 neurons (Gabbott & Bacon, 1996; Perez-Cruz, Muller-Keuker, Heilbronner, Fuchs, & Flugge, 2007). L6 was recognized as it contains a high density of fibers (Gaillard & Sauve, 1995). Analysis with independent t test indicated the somatic depth was significantly different between L2/3 and L5 in both IL [$t(51) = 9.1$, $p < 0.01$] and PL [$t(30) = 8.8$, $p < 0.01$].

Layer-specific morphological characteristics of mPFC neurons. To correlate morphological and electrophysiological properties, neurons were filled with biocytin during recording and visualized with streptavidin Alexa Fluor 488. Neurons that showed strong biocytin signals were 3D reconstructed and analyzed (see representative neurons in Figure 16B). All these neurons displayed typical pyramidal architecture with multiple basal dendrites and a single tufted apical dendrite projecting to the pia. Specifically, L5
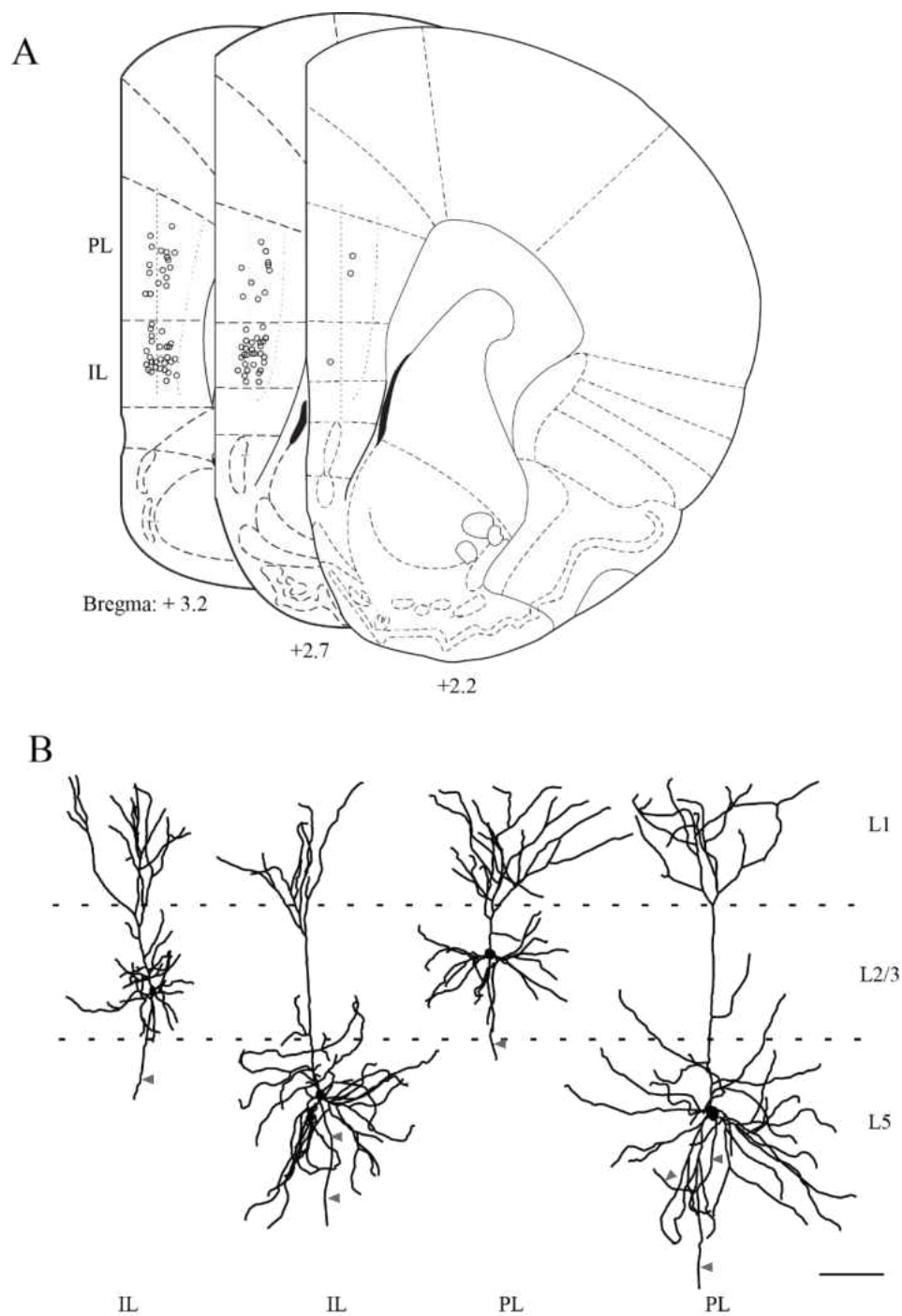
Figure 16 Location and morphology of randomly selected neurons recorded in mPFC. A, The location of each recorded neurons was obtained from a snapshot taken after each experiment and indicated as individual circles in brain stereotaxic atlases (Paxinos & Watson, 1998). B, Representative neurons reconstructed from laser scanned confocal images in different layers in IL and PL. Arrow heads point to axons. Scale bar, 100 μm.

neurons had a prominent apical dendrite, which rarely bifurcated or branched in L2/3 until they entered L1 where it was developed into dendritic tuft. The basal dendrites of L5 neurons were primarily located in L5. In contrast, the basal dendrites of L2/3 neurons were localized within L2/3 whereas the apical dendrite also bifurcated in L1.

      Subthreshold properties of randomly selected mPFC neurons. L2/3 neurons and L5 neurons were not only different in morphological properties, but also display distinct basic membrane properties, such as resting membrane properties, input resistance, and hyperpolarization-activated current (h-current or I_h).

      Resting membrane potential (RMP). In both IL and PL, RMP was slightly but significantly more negative in neurons obtained from L2/3 than that from L5 [see Table 4; $t(63) = 4.3$, $p < 0.01$ for IL and $t(41) = 4.7$, $p < 0.01$ for PL respectively]. In addition, there was a significant correlation between the RMP and the somatic depth such that neurons in superficial layers had more negative resting potentials than neurons in deep layers (see Figure 17; $p < 0.01$ for neurons in both IL and PL). Thus, to compensate the depth dependence of RMP, all cells were held at -67 mV during the rest of the recording unless noted. The average holding current was positive in L2/3 neurons and negative in L5 neurons (see Table 4) and they were significantly different in both IL [$t(59) = 3.6$, $p < 0.01$] and PL [$t(14) = 2.7$, $p < 0.05$; equal variances not assumed].

      Input resistance (R_N). The input resistance was significantly different between neurons from IL and PL. As shown in Figure 18B and Table 4, in both L2/3 and L5, IL neurons had significantly larger input resistance than that of PL neurons [$t(35) = 2.7$, $p < 0.05$ for L2/3 and $t(69) = 2.9$, $p < 0.01$ for L5 respectively]. The input resistance was not

Table 4. Basic membrane properties of mPFC neurons are layer- and subregion-specific

	Somatic Depth (μm)	RMP (mV)	I_{hold} (pA)	R_N (MΩ)	Sag (%)
IL					
L2/3	352 ± 13 (21)	-68.5 ± 1.3 (24)	19 ± 20 (22)	127 ± 11 (24) †	5.9 ± 0.8 (23)
L5	534 ± 14 (32)#	62.1 ± 0.8 (41)#	-53 ± 10 (39)#	137 ± 9 (41) §	10.3 ± 0.7 (36)#
PL					
L2/3	325 ± 20 (11)	-69.5 ± 1.2 (13)	55 ± 34 (13)	83 ± 9 (13)	6 ± 1.3 (13)
L5	623 ± 22 (21)#	-63.3 ± 0.7 (30)#	-40 ± 9 (28)#	104 ± 6 (30)	11.1 ± 0.8 (25)#

Data are mean ± SE for number of cells in parentheses. I_{hold}, the current used to hold neurons at -67 mV; IL, infralimbic cortex; PL, prelimbic cortex; R_N, neuronal input resistance; RMP, resting membrane potential. Soma depth is the distance measured from the soma to the pial surface. Statistically different between L2/3 and L5, # $p < 0.01$. Statistically different between IL and PL: † $p < 0.05$, § $p < 0.01$.
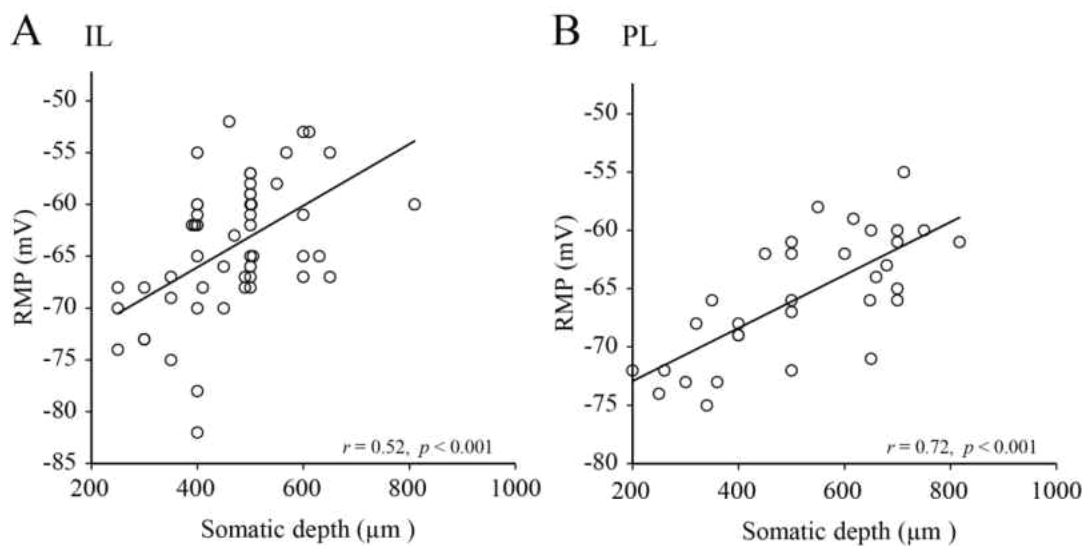
Figure 17. Resting membrane potential (RMP) is significantly correlated with the somatic depth in both IL (A) and PL (B). The somatic depth was measured as the distance of the soma from the pial surface. RMP was measured as the membrane potential when whole-cell recording was obtained.

significantly different between L2/3 and L5 in either IL or PL (see Figure 18B and Table 4; for all values, $p > 0.05$).

Depolarizing sag. In response to hyperpolarizing current injections, the membrane voltage of mPFC neurons showed depolarizing sags that are characteristics of h current (I_h) activation (see Figure 18A). Cells in deep layer (L5) displayed larger depolarizing sags than those in superficial layers (L2/3) in both IL and PL (Figure 18B and Table 4; $t(57) = 4.1$, $p < 0.01$ for IL and $t(36) = 3.4$, $p < 0.01$ for PL respectively). In addition, there was a significant correlation between the sag ratio and the somatic depth (see Figure 18C; $p < 0.01$), suggesting that more HCN channels are expressed in deep layers than in superficial layers.

L2/3 neurons are less excitable than L5 neurons in mPFC. Although held at the same membrane properties, neurons in different layers had distinct passive membrane properties. We then continued to examine the active membrane properties such as action potential properties and intrinsic excitability.

AP characteristics. AP characteristics were studied by injecting a threshold current (500 ms) to evoke one single action potential (see Figure 19A). As shown in Table 5 and Figure 19B, L2/3 IL neurons had significantly more hyperpolarized spike threshold [$t(55) = 3.8$, $p < 0.01$] than both L5 IL and L2/3 PL neurons (for both values, $p < 0.01$), suggesting they are more excitable. In addition, L2/3 PL neurons had significantly larger $I_{threshold}$ (the minimum current necessary to evoke an AP) than both L2/3 IL and L5 PL neurons (for both values, $p < 0.01$), suggesting they are less excitable. No significant differences were found when compared between different layers or subregions.

Table 5. Action potential characteristics of mPFC neurons

	AP_{amp} (mV)	AP_{width} (s)	AP_{thresh} (mV)	fAHP (mV)	$I_{threshold}$ (pA)
IL					
L2/3	86 ± 2 (23)	0.85 ± 0.04 (23)	-36.7 ± 0.9 (23)†#	10.9 ± 0.5 (23)	136 ± 9 (23)
L5	78 ± 2 (34)	0.94 ± 0.04 (34)	-31.6 ± 0.9 (34)	11.2 ± 0.6 (34)	131 ± 9 (34)
PL					
L2/3	81 ± 4 (13)	0.83 ± 0.06 (13)	-33.6 ± 1.3 (13)	10.8 ± 0.9 (13)	202 ± 21 (13) §#
L5	82 ± 2 (28)	0.77 ± 0.03 (28)	-32.8 ± 1 (28)	11.6 ± 0.7 (28)	34 ± 8 (28)

Data are mean ± SE for number of cells in parentheses. IL, infralimbic cortex; PL, prelimbic cortex; AP_{amp}, action potential amplitude; AP_{width}, action potential half-width; AP_{thresh}, action potential threshold; fAHP, fast AHP. Statistically different between L2/3 and L5, # $p < 0.01$. Statistically different between IL and PL: † $p < 0.05$, § $p < 0.01$.
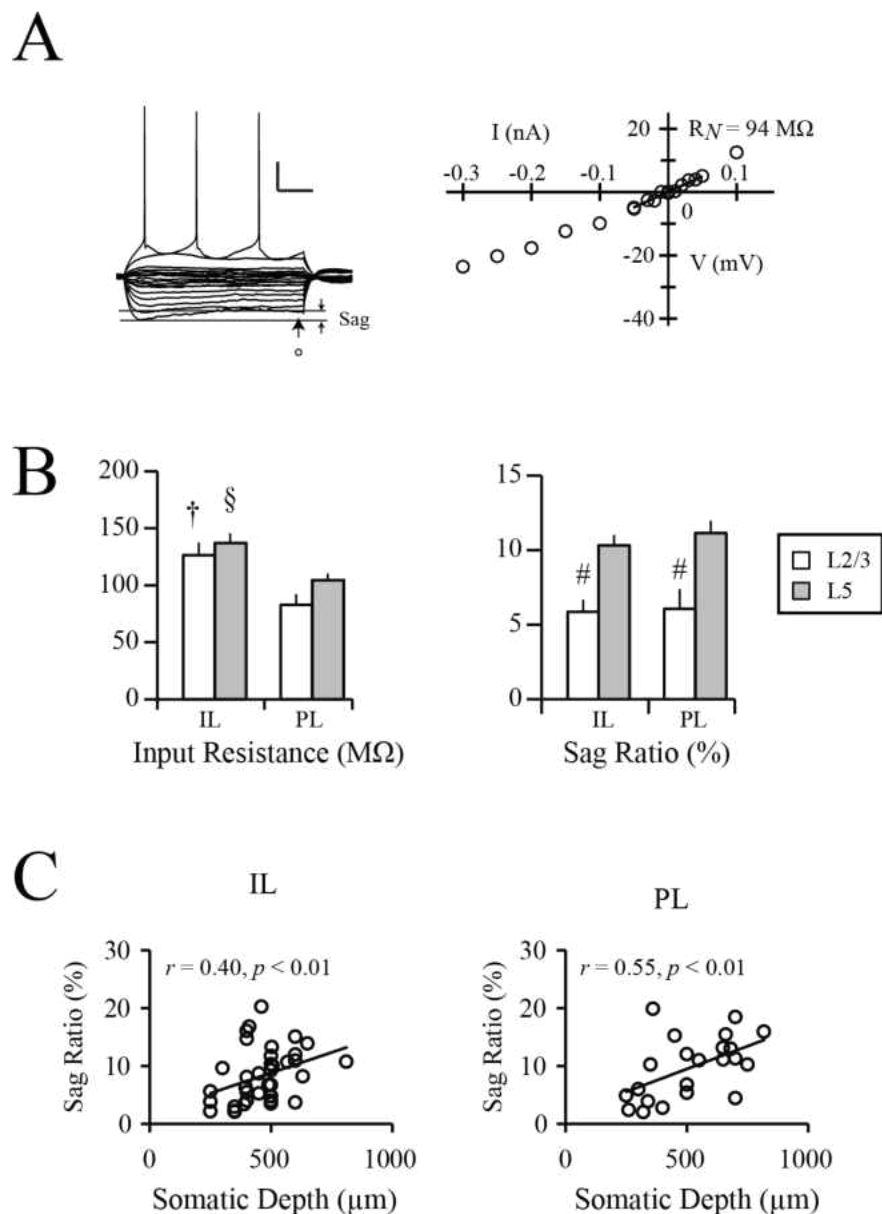
Figure 18. Basic membrane properties of mPFC neurons. A, Representative traces of V-I relations (left). The sag ratio was calculated from the depolarizing sag (between the thin arrows) in response to hyperpolarization. Input resistance (R_N) was calculated from the slope of the linear fit of the steady-state voltage responses (right). Thick arrow indicates the location where steady-state voltage response was measured. Scale bar, 50 mV, 100 ms. B, Bar graphs showing different membrane properties between layers and subregions. In both L2/3 and L5, IL neurons had significantly higher input resistance than PL neurons (statistically different between L2/3 and L5: # $p < 0.01$; statistically different between IL and PL: † $p < 0.05$, § $p < 0.01$). C, Sag ratio was significantly correlated with somatic depth in both IL and PL.

Intrinsic excitability. The intrinsic excitability of mPFC neurons was evaluated by counting the number of spikes evoked by a series of depolarizing current when held at -67 mV (see an example trace in Figure 20A and averaged data in Figure 20C). A repeated-measures ANOVA revealed that the excitability was significantly different between L2/3 and L5 neurons in PL [$F(1,39) = 7.2$, $p < 0.05$] but not in IL [$F(1,52) = 0.2$, $p = 0.69$]. Further analysis with independent t test in PL neurons revealed that L2/3 neurons fired significantly fewer spikes than L5 neurons in response to depolarizing currents ranging from 150 – 300 pA (for all values, $p < 0.05$; see Figure 20C and Table 6). Thus, these data suggest that L2/3 neurons are less excitable than L5 neurons in PL but not in IL. However, the fact that L2/3 IL neurons were held with a positive current during recording suggests that they may be less excitable at rest. To test this hypothesis, the excitability of L2/3 IL neurons was evaluated from a subset of L2/3 neurons (n = 4) when held at rest (-75 mV) and at -67 mV. As shown in Figure 20E, these neurons fired comparable number of spikes with the average of all L2/3 IL neurons when held at -67 mV (Figure 20C) but fired significantly less at rest (paired t test, $p < 0.01$ for 200 pA and $p < 0.05$ for 250 pA and 300 pA current injections). Thus, these results suggest that L2/3 neurons are generally less excitable than L5 neurons in both IL and PL.

Post-burst AHP. The size of post-burst AHP is another measurement of intrinsic excitability (Kaczorowski & Disterhoft, 2009; Moyer *et al.*, 1996; Oh *et al.*, 2003; Song *et al.*, 2012). We studied the post-burst AHPs by injecting 10 brief (2 ms) depolarizing currents to evoke 10 APs at 50 Hz (see Figure 20B). A repeated-measures ANOVA revealed that the post-burst AHP was significantly different between L2/3 and L5 neurons in PL [$F(1,41) = 10.6$, $p < 0.01$)] but not in IL [$F(1,56) = 0.01$, $p = 0.91$] when held at -67

Table 6. Excitability of mPFC neurons

	mAHP (mV)	sAHP (mV)	Number of spikes
IL			
L2/3	-3.8 ± 0.3 (23)	-1.2 ± 0.1 (23)	12.4 ± 1.1 (24)
L5	-4.4 ± 0.3 (36)	-0.9 ± 0.1 (36)	11.3 ± 1.3 (30)
PL			
L2/3	-2.9 ± 0.3 (13)#	-0.5 ± 0.1 (13)*	4.9 ± 1.6 (13)*§
L5	-4.9 ± 0.3 (30)	-1.0 ± 0.1 (30)	10.0 ± 1.0 (28)

Data are mean ± SE for number of cells in parentheses. IL, infralimbic cortex; PL, prelimbic cortex; mAHP, medium afterhyperpolarization; sAHP slow afterhyperpolarization. mAHP was measured at the peak of the AHP following a burst of 10 APs relative to baseline. sAHP was measured at 1 s following the offset of the current injection. Number of spikes was counted in response to a 1-s 300-pA depolarizing current injection. Statistically different between L2/3 and L5: * $p < 0.05$, # $p < 0.01$. Statistically different between IL and PL: § $p < 0.01$.
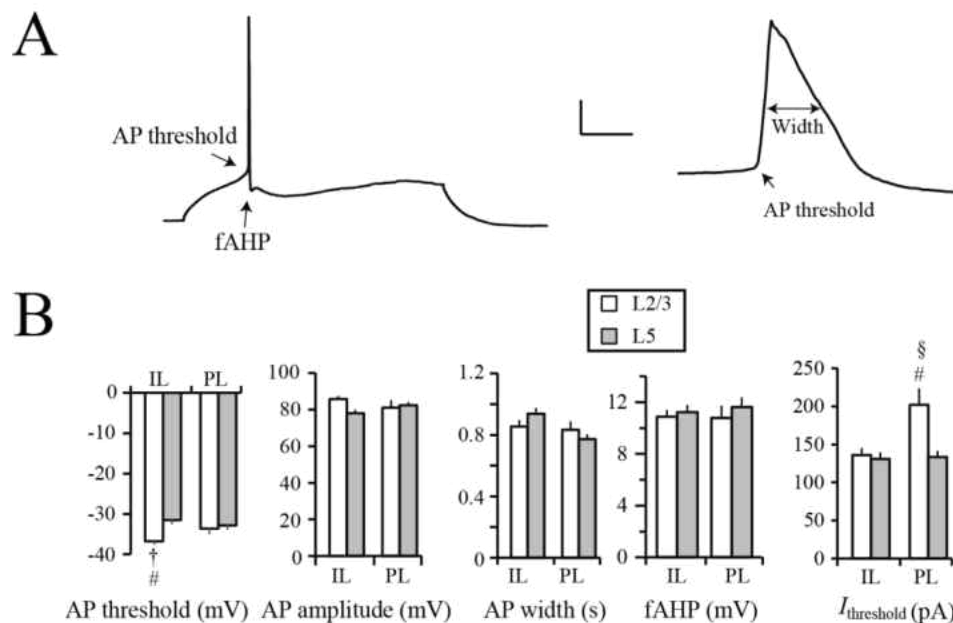
Figure 19. AP characteristics of mPFC neurons. A, Sample traces of a single AP evoked by a threshold current ($I_{threshold}$). AP threshold was defined as the voltage when dv/dt first exceeded 28 mV/ms. AP amplitude was measured from threshold. fAHP was defined as the different potential between the AP threshold and the initial negativity that followed the repolarization of the AP. AP width was measured as the width at half of the AP amplitude (from threshold). Scale bar, 20 mV, 1/100 ms. B, Bar graphs showing the AP characteristics of mPFC neurons. IL L2/3 neurons had significantly lower AP threshold, whereas PL L2/3 neurons had significantly higher $I_{threshold}$ (statistically different between L2/3 and L5: # $p < 0.01$; statistically different between IL and PL: † $p < 0.05$, § $p < 0.01$).

mV (see Table 3 and Figure 20D). We thus further examined post-burst AHP at RMP in a subset of L2/3 IL neurons (n = 4). Analysis with a paired *t* test revealed that post-burst AHP was significantly smaller at rest than at - 68 mV when measured $0.1 - 0.5$ s as well as 1 s following the AP burst (for all values, $p < 0.05$; see Figure 20F). Taken together, these data suggest that L2/3 neurons have smaller post-burst AHP but lower excitability than L5 neurons.

IL neurons are more excitable than PL neurons in layer 2/3. Previous studies have shown different roles of IL and PL in conditioned fear memory expression (Burgos-Robles *et al.*, 2009; Burgos-Robles *et al.*, 2007; Chang & Maren, 2011; Milad *et al.*, 2004; Vidal-Gonzalez *et al.*, 2006). We therefore compared the properties of the neurons between IL and PL in naïve animals. In L2/3, IL neurons fired significantly more spikes than PL neurons in response to depolarizing current injections [Table 6 and Figure 20C; for all values, $p < 0.01$ when depolarizing current was $200 - 300$ pA], perhaps due to lower spike threshold [Table 5 and Figure 19B; $t(34) = 2.0$, $p < 0.05$], larger input resistance [Table 4 and Figure 18B; $t_{(35)} = 2.7$, $p < 0.05$], and smaller $I_{threshold}$ [Table 5 and Figure 19B; $t(34) = 3.3$, $p < 0.01$]. In addition, these two groups of neurons had comparable RMP and sag (Table 4 and Figure 18B). Taken together, these data suggest that IL neurons are more excitable than PL neurons in L2/3.

Within L5, both IL and PL neurons fired comparable number of spikes (see Figure 20C and Table 6) in response to the depolarizing current injection and had comparable RMP, fAHP, post-burst AHPs, or AP threshold, (for all measurement, $p > 0.05$), although IL neurons displayed a larger input resistance [see Table 4, $t(69) = 2.9$, $p < 0.01$] than that of
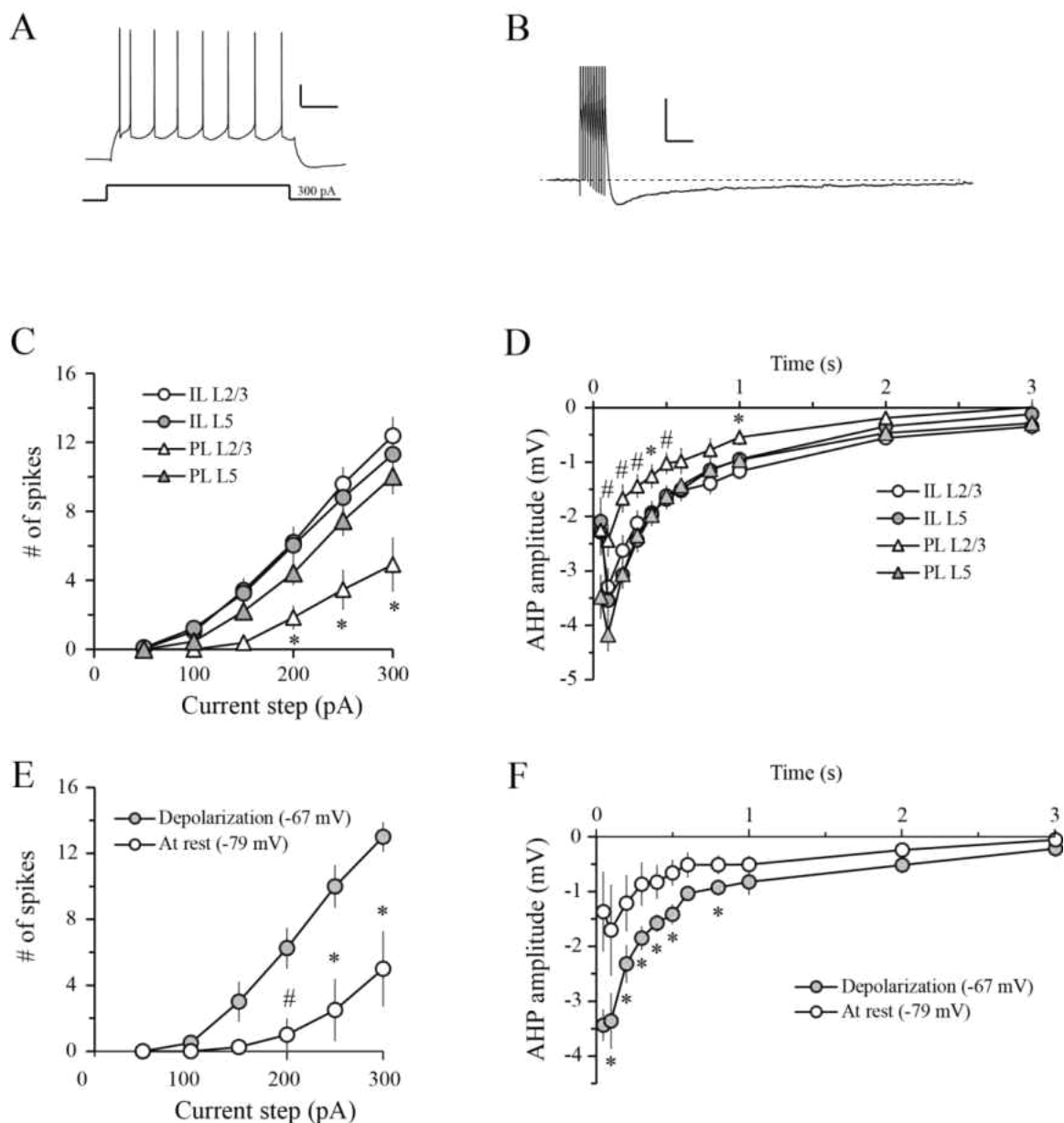
Figure 20. Medial prefrontal cortex pyramidal neurons in L2/3 neurons are less excitable than L5 neurons. Intrinsic excitability was studied by counting the number of spikes evoked by a series of depolarizing currents (see a representative trace in A; scale bar, 20 mV, 0.2 s). Post-burst AHP was measured from different time points following a burst of 10 APs evoked by brief current injections at 50 Hz (see a representative trace in B; scale bar, 10 mV, 0.2 s). PL pyramidal neurons in L2/3 showed the least excitability (C) and smallest post-burst AHP (D) compared to PL pyramidal neurons in L5 and IL pyramidal neurons in L2/3. Although IL pyramidal neurons in L2/3 displayed comparable excitability and post-burst AHP when held at -67 (C & D), they were significantly less excitable (E) and displayed smaller post-burst AHP (F) at rest.

PL neurons. Thus, these data suggest that in L5, the excitability of IL and PL neurons are comparable.

Different levels of HCN expression partially account for the layer-specific properties. To test the possible contributions of ion channels that account for the variability of excitability in mPFC neurons, we blocked HCN channels by bath applying either ZD7288 (50 μM) or CsCl (3 mM) and investigated the contribution of HCN channels on the electrophysiological properties of L5 mPFC neurons. Neurons from IL (n = 11) and from PL (n = 4) were combined because no significant differences between these two groups of neurons were observed. As shown in Figure 21A-C, blocking HCN channels dramatically changed the basic membrane properties and AP characteristics including RMP, input resistance, Sag ratio, $I_{threshold}$, fAHP, $AP_{threshold}$, and AP_{width} (for all measurements, $p < 0.01$). Furthermore, blocking HCN channels significantly reduced the medium portion of the post-burst AHP but slightly enhanced the slow portion (see Figure 22A). However, no significant effect of HCN channel blockade was observed on L2/3 neurons (n = 4, data not shown), which is consistent with previous studies showing that L2/3 neurons have less I_h and that HCN channels are primarily expressed in L5 neurons (Boudewijns *et al.*, 2013; Lorincz, Notomi, Tamas, Shigemoto, & Nusser, 2002). In addition, blocking HCN channels significantly increased the number of spikes evoked by depolarization when the neurons were held at -67 mV (see Figure 22B; $p < 0.05$ in response to 100, 150, and 200 pA current injections), perhaps due to the dramatic effects of I_h blockade on the mAHP, input resistance, and AP threshold. Thus, these observations
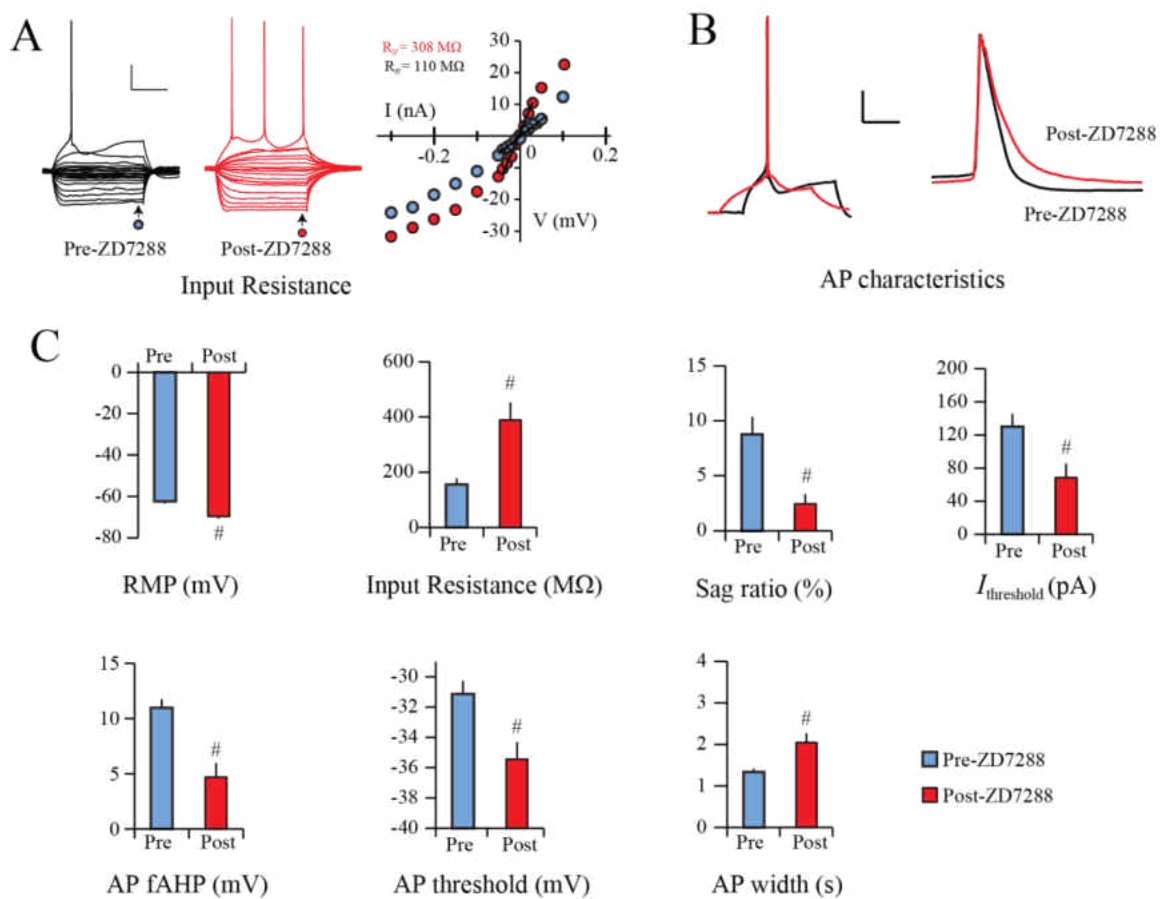
Figure 21. Blocking HCN channels significantly affects both passive and active membrane properties of L5 mPFC neurons. A – C, Blocking HCN channels significantly changed passive membrane properties and AP characteristics (statistically different between pre- and post-application of HCN channel blocker ZD7288: * $p < 0.05$, # $p < 0.05$). Scale bars: A, 20 mV, 200 ms; B, 20 mV, 2/200 ms.
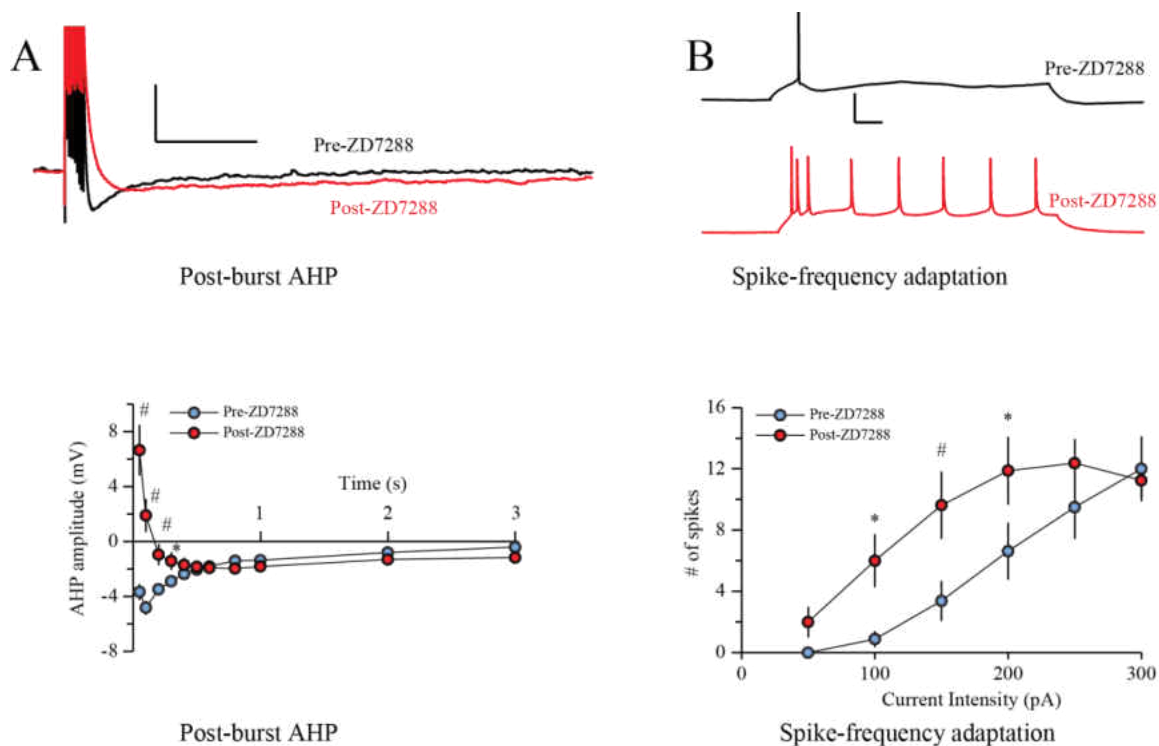
Figure 22. Blocking HCN channels significantly enhances intrinsic excitability of L5 pyramidal neurons in medial prefrontal cortex. A, The medium AHP was diminished but slow AHP was enhanced after blocking HCN channels (top, raw traces showing the response of an mPFC neuron to a 50 mM HCN channel blocker ZD 7288; bottom, average data showing the effect of HCN channel blockade on post-burst AHP). Scale bar, 10 mV, 1 s. B. Blocking HCN channels significantly increased the number of spikes evoked by current injections (statistically different between pre- and post-application of HCN channel blocker ZD7288: * $p < 0.05$, # $p < 0.05$). Scale bar, 40 mV, 100 ms.

suggest that the different expression levels HCN channels account, at least partially for the observed differential membrane properties between L2/3 and L5 neurons.

Properties of mPFC-BLA projection neurons

  Distribution of mPFC-BLA projection neurons. To study mPFC-BLA projection neurons, fluorescently labeled microspheres (Retrobeads™) were unilaterally injected into BLA. When injected, the microspheres displayed little lateral diffusion and thus produced a small, sharply defined injection site (see Figure 13A). Consistent with previous data (Katz, Burkhalter, & Dreyer, 1984), the beads had no obvious cytotoxicity as assessed by behavioral observation and electrophysiological recordings. There were also no obvious morphological changes observed in the Retrobeads™-labeled neurons (see Figure 23A) as compared with non-labeled neurons (Figure 23B). In PFC, the Retrobeads™-labeled neurons were differentially distributed between the ipsilateral and contralateral side relative to the injection site (see Figure 13B). On the ipsilateral side, the cortical-BLA projection neurons were primarily located in dorsal peduncular (DP) cortex, IL, PL, agranular insular cortex [AI, including ventral and dorsal subdivisions (AIV and AID)], and dysgranular insular cortex (DI). Within mPFC, the Retrobeads™ labeled neurons were distributed throughout L2/3 to L5, with more intensive labeling in L2/3. In addition, there were more fluorescently labeled neurons in IL than PL within the ipsilateral mPFC (Figure 13B). On the contralateral side, most Retrobeads™-labeled neurons were located in mPFC, with much fewer labeled neurons in the insular cortices. Furthermore, most Retrobeads™ labeled neurons were located in L5 of the contralateral mPFC (Figure 13B).

  The mPFC-BLA projection neurons are more depolarized than randomly selected neurons. To study the characteristics of mPFC-BLA projection neurons, we recorded
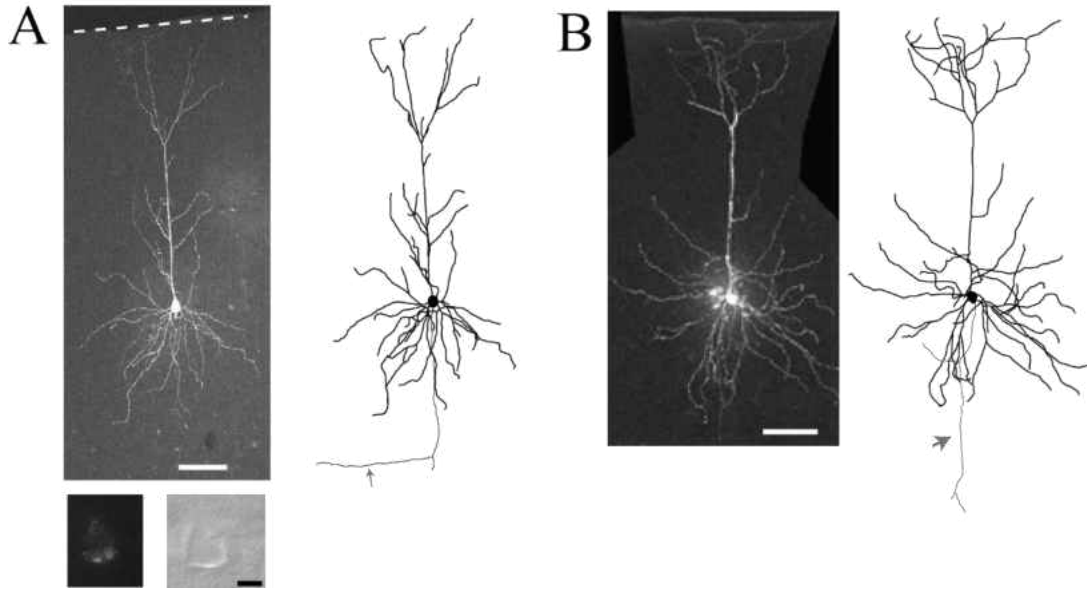
Figure 23. Retrobeads^{TM} does not affect morphology of pyramidal neurons in medial prefrontal cortex. A, Representative confocal image (top left) and 3D reconstruction (right) of a pyramidal neuron that was fluorescently labeled with Retrobeads^{TM} (bottom). Scale bars: top, 100 μm, bottom, 10 μm. B, Representative confocal image (left) and 3D reconstruction (right) of a pyramidal neuron with unknown projection target. Both neurons were from layer 5 in infralimbic cortex. The arrows point to axons. Scale bar, 100 μm

fluorescently labeled L5 neurons in both IL and PL from the rats that received Retrobeads^{TM} infusion, and compared with neurons that were selected at random (non-labeled neurons) from rats that didn't receive Retrobeads^{TM} infusion. As shown in Table 7, the mPFC-BLA projection neurons had significantly more depolarized resting membrane potential (RMP) compared with non-labeled neurons ($p < 0.05$ in both IL and PL). Other membrane properties, including AP characteristics, post-burst AHP, and intrinsic excitability were not significantly different from non-labeled neurons (see Table 7).

Properties of I$_h$ in mPFC-BLA projection neurons. Although not statistically significant ($p > 0.05$ in both IL and PL), the *h*-current was 10% percent larger in mPFC-BLA projection neurons than that in non-labeled neurons in both IL and PL (see Table 7). Because HCN channels are critical for dendritic signal integration (Magee, 1998; I. Pavlov, Scimemi, Savtchenko, Kullmann, & Walker, 2011) and PFC-dependent working memory (Wang *et al.*, 2007), we further studied the role of HCN channels on the electrophysiological properties L5 IL-BLA projection neurons by bath application of an HCN channel blocker – ZD7288. We focused on IL neurons only because IL and PL neurons share same membrane properties in L5. Analysis of the data with paired *t* test revealed a strong effect of HCN blockade on basic membrane, intrinsic, and synaptic properties of mPFC-BLA projection neurons (see below).

Blocking I$_h$ enhances intrinsic excitability of mPFC-BLA projection neurons. Blocking HCN channels also had strong effects on both passive and active membrane properties of mPFC-BLA projection neurons (see Figure 24 and Table 8). Furthermore,

Table 7. Properties of mPFC-BLA projection and randomly selected neurons

	IL		PL	
	Non-labeled	Labeled	Non-Labeled	Labeled
RMP (mV)	-64.6 ± 1 (13)*	-60.5 ± 1.2 (23)	-65.7 ± 1.1 (10)*	-61.7 ± 0.9 (14)
R_N (MΩ)	137 ± 16 (13)	128 ± 9 (23)	100 ± 14 (10)	108 ± 7 (14)
Sag (%)	9.1 ± 1.3 (11)	10.1 ± 0.9 (20)	11.2 ± 1.6 (9)	12.9 ± 1.2 (10)
$I_{threshold}$ (pA)	111 ± 11 (10)	147 ± 12 (20)	129 ± 9 (10)	142 ± 11 (12)
AP_{thresh} (mV)	-35.0 ± 1.3 (10)	-29.5 ± 1.2 (20)	-34.7 ± 1.9 (10)	-30.6 ± 1.6 (12)
AP_{amp} (mV)	81.5 ± 3.7 (10)	76.7 ± 2.4 (20)	82.7 ± 2.6 (10)	79.5 ± 3.0 (12)
AP_{width} (ms)	0.92 ± 0.07 (10)	0.97 ± 0.05 (20)	0.76 ± 0.06 (10)	0.82 ± 0.04 (12)
# of spikes	12.6 ± 2.2 (7)	8.1 ± 1.4 (10)	14.2 ± 2.6 (9)	9.4 ± 1.6 (11)
mAHP (mV)	-4.2 ± 0.5 (10)	-4.4 ± 0.3 (22)	-5.3 ± 0.5 (10)	-4.9 ± 0.3 (14)
sAHP (mV)	-0.9 ± 0.3 (10)	-1.0 ± 0.1 (22)	-0.9 ± 0.2 (10)	-1.0 ± 0.2 (14)

Data are mean ± SE for number of cells in parentheses. IL, infralimbic cortex; PL, prelimbic cortex; AP_{amp}, action potential amplitude; AP_{thresh}, action potential threshold; AP_{width}, action potential half-width; $I_{threshold}$, threshold current required to elicit an action potential;. mAHP, medium afterhyperpolarization; sAHP slow afterhyperpolarization. mAHP was measured at the peak of the AHP following a burst of 10 APs relative to baseline. sAHP was measured at 1 s following the offset of the current injection. Number of spikes was counted in response to a 1-s 300-pA depolarizing current. Statistically different between labeled and non-labeled neurons:* $p < 0.05$.

Table 8. Effects of HCN channel blockade on the properties of IL-BLA projection neurons

	Pre-ZD7288	Post-ZD7288
RMP (mV)	-61.8 ± 0.9 (9)	-68.0 ± 1.3 (9)#
R_N (MΩ)	189 ± 28 (9)	468 ± 84 (9)#
$I_{threshold}$ (pA)	103 ± 9 (7)	49 ± 11 (7)#
AP_{thresh}	-31.0 ± 1.4 (7)	-33.9 ± 1.5 (7)
AP_{amp} (mV)	81.8 ± 2.4 (7)	75.1 ± 4.4 (7)
AP_{width} (ms)	0.9 ± 0.1 (7)	1.4 ± 0.2 (6)#
# of spikes	1.4 ± 0.7 (5)	8.2 ± 1.4 (5)*
mAHP (mV)	-5.8 ± 0.6 (5)	-2.6 ± 0.5 (5)#
sAHP (mV)	-1.5 ± 0.3 (5)	-1.7 ± 0.5 (5)
Sag (%)	8.5 ± 2.8 (5)	2.0 ± 1.1 (5)*

Data are mean ± SE for number of cells in parentheses. AP_{amp}, action potential amplitude; AP_{thresh}, action potential threshold; AP_{width}, action potential half-width; $I_{threshold}$, threshold current required to elicit an action potential;. mAHP, medium afterhyperpolarization; sAHP slow afterhyperpolarization. mAHP was measured at the peak of the AHP following a burst of 10 APs relative to baseline. sAHP was measured at 1 s following the offset of the current injection. Number of spikes was counted in response to a 1-s 100-pA depolarizing current. Statistically different between pre- and post-ZD7288 application: * $p < 0.05$, # $p < 0.01$.
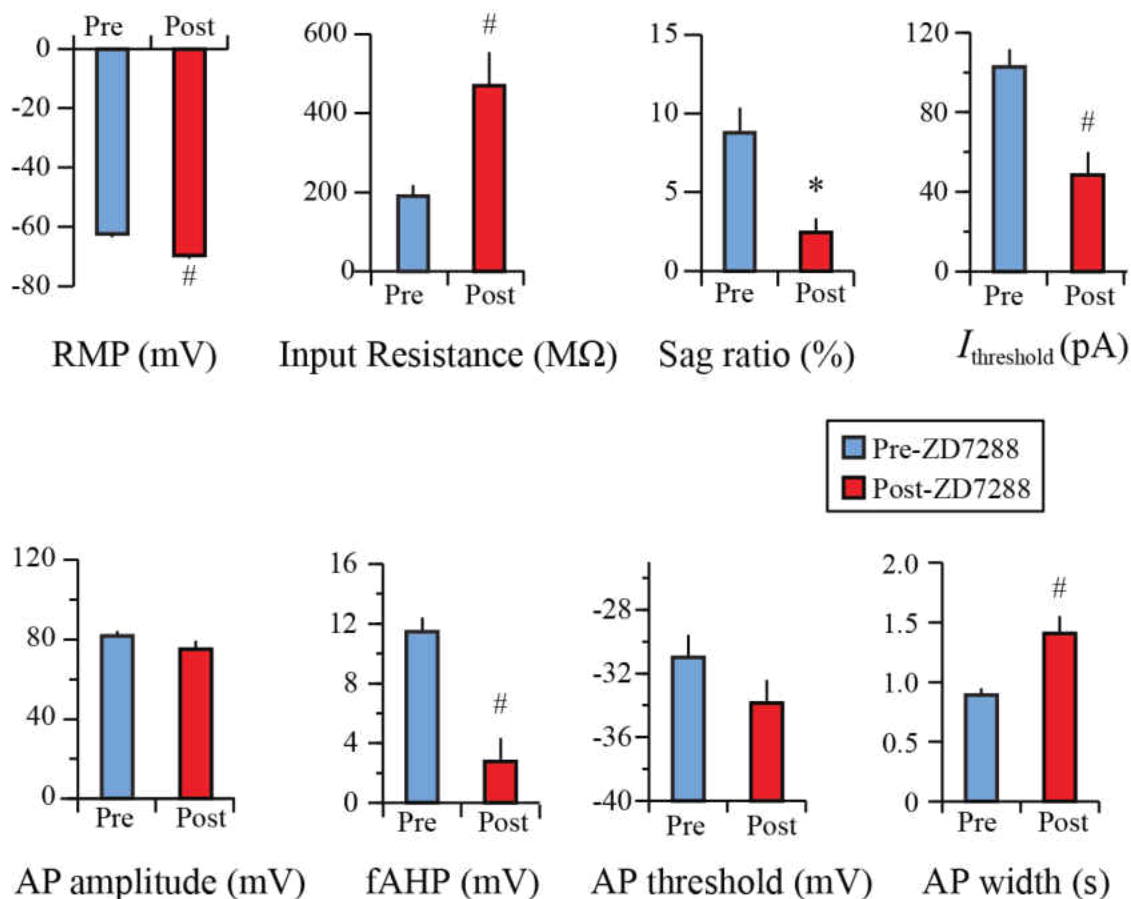
Figure 24. Blocking I_h changes basic membrane properties and AP characteristics of mPFC-BLA projection neurons. Blocking HCN channels significantly changed resting membrane potential (RMP), input resistance, sag, $I_{threshold}$, fAHP, and AP width (statistically different between pre- and post-application of HCN channel blocker ZD7288: * $p < 0.05$, # $p < 0.01$), but didn't significantly change the AP amplitude. The AP threshold was reduced following the blockade of HCN channels but this difference was not statistically significant.
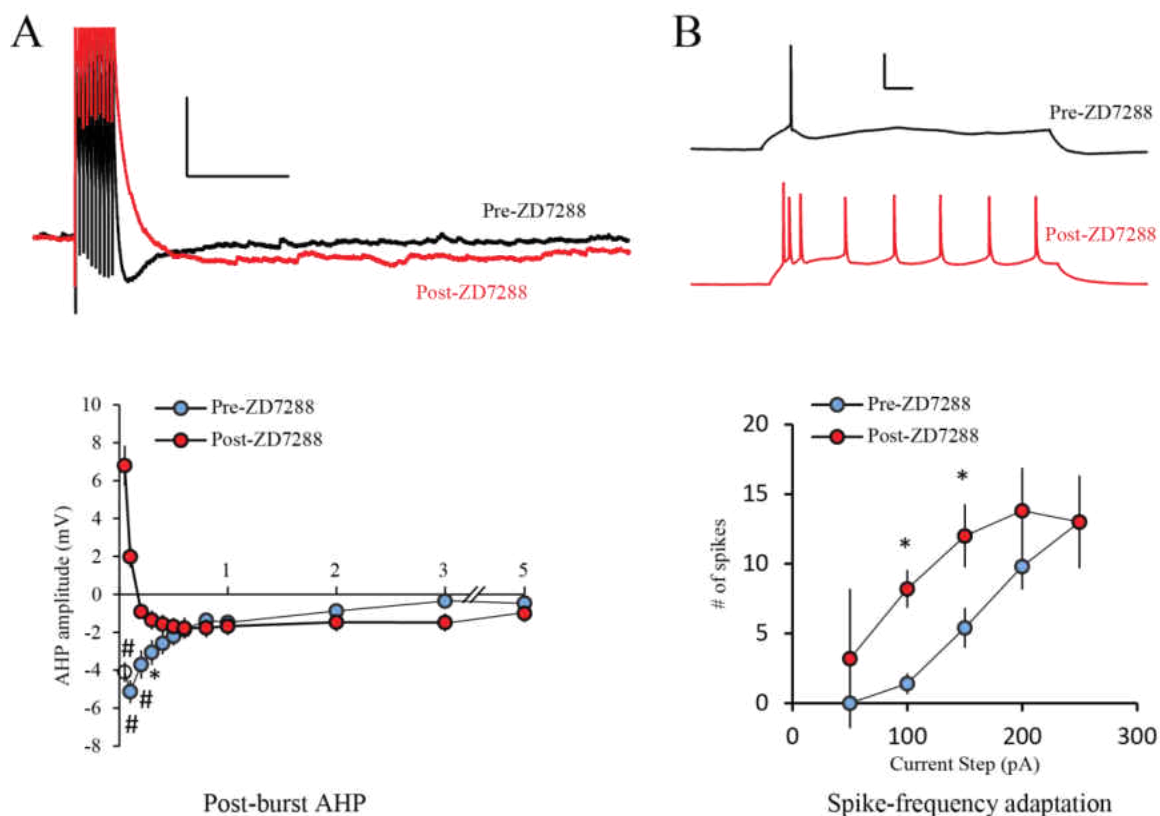
Figure 25. Blocking I_h enhances intrinsic excitability of mPFC-BLA projection neurons. A, Representative traces (top) and averaged data (bottom) showing the time course of post-burst AHP before and after bath application of ZD7288. Blocking HCN channels significantly reduced median AHP measured from 50 – 300 ms following the AP burst (statistically different between pre- and post-application of HCN channel blocker ZD7288: * $p < 0.05$, # $p < 0.01$). Scale bar, 10 mV, 0.5 s. B, Representative traces (top) and averaged data (bottom) showing the blockade of I_h significantly enhances intrinsic excitability. The neurons fired significantly more spikes in response to moderate (100 – 150 pA) current injections after blocking HCN channels (statistically different between pre- and post-ZD7288 application: * $p < 0.05$, # $p < 0.01$). Scale bar, 40 mV, 100 ms.

blockade of I_h significantly enhanced intrinsic excitability, as evidenced by a significant reduction in the mAHP (0.05 – 0.5 s following the AP train; see Figure 25A) and an increase in the number of spikes evoked by a series of 1-s depolarizing current injection (Figure 25B and Table 8).

Blocking I_h facilitates signal integration. HCN channels are more densely expressed in distal dendrites than proximal dendrites (Magee, 1998) and greatly affect temporal summation (Magee, 1999), as well as coincidence detection (I. Pavlov *et al.*, 2011). We therefore studied the role of HCN channels on dendritic signal integration in IL-BLA projection neurons. We first studied the effect of blocking HCN channels on single EPSPs by stimulating L2/3 pathway (see Figure 26A) while the cells were hold at -67 mV. As shown in Figure 26B, bath application of 50 μM ZD7288 increased the duration of single EPSPs on the mPFC-BLA projection neurons, suggesting that blocking HCN channels increases the time window for signal integration. This was tested by stimulating layer 2/3 inputs and evoking a train of 5 EPSPs at frequencies of 20 Hz, 50 Hz, or 100 Hz. As shown in Figure 26C, blocking HCN channels facilitated signal integration, with it's maximal effects at the lower frequency stimulation of 20 Hz. This suggests that under normal conditions, *h*-current restricts signal integration at low frequencies but allows integration for high-frequency stimuli.

Blocking I_h facilitates coincidence detection. Blockade of I_h has been shown to facilitate coincidence detection in hippocampal neurons (I. Pavlov *et al.*, 2011). In contrast to temporal summation that occurred on the same synaptic input, coincidence detection is the process by which the neurons integrate input signals that are temporally close but spatially distributed. We thus examined the effect of ZD7288 on coincidence detection of
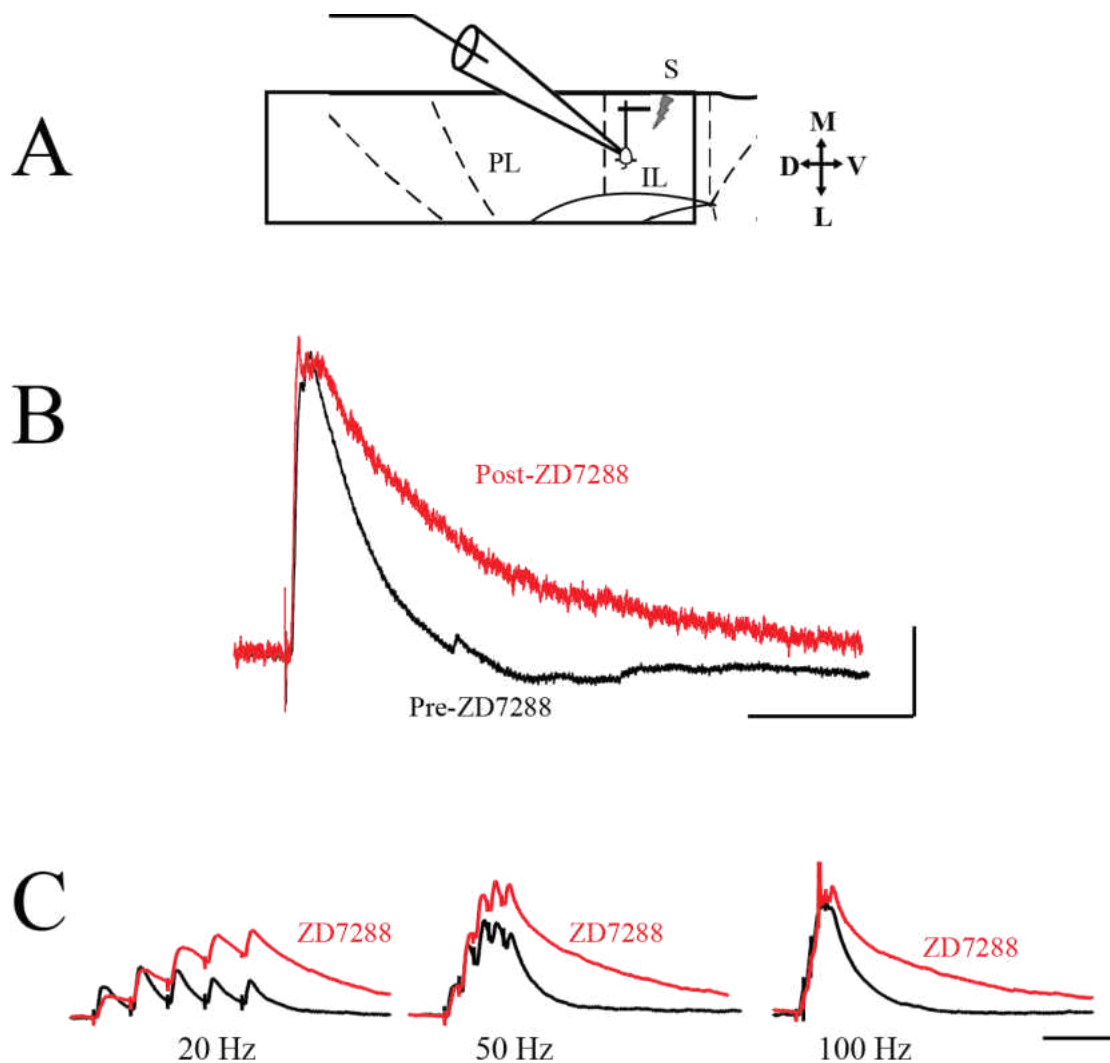
Figure 26. Blocking I_h facilitates temporal summation of mPFC-BLA projection neurons. A, Schematic showing the experimental set-up used to study the effect of ZD7288 on dendritic signal integration. Whole-cell recording was performed on L5 mPFC-BLA projection neurons and dendritic EPSPs were evoked by stimulating L2/3 fibers using an electrode located within 100 μm of the apical dendrites. B, Blocking I_h increased the width of single EPSPs evoked by stimulating L2/3. Scale bar, 5 mV, 100 ms. C: Blocking I_h facilitated temporal summation of dendritic EPSP, especially at lower frequencies. AP was truncated in the 100 Hz traces for clarity. Scale bar, 10 mV, 100 ms.

mPFC-BLA projection neurons by stimulating L2/3 and L5 to represent two afferent pathways (see Figure 27A). The stimulating intensities were adjusted so that the neurons consistently fired APs only when the two stimulations were delivered simultaneously. We then observed the firing activities of the neurons while systematically varying the interstimulus interval (ISI). As shown in Figure 27B, under control conditions, the neuron fired APs when the ISI was between $0 – 9$ ms (except at 18 ms). However, after blocking HCN channels, the neuron readily fired action potentials even when the ISI ranged from -12 ms to 39 ms (except 27 ms). Thus, under physiological conditions, the role of HCN channels is to restrict signal integration so that different afferent information can be integrated only when they occurred within a very short period of time (i.e., coincidence detection). Blocking HCN channels significantly broadened the time course over which inputs can be integrated within a neuron.
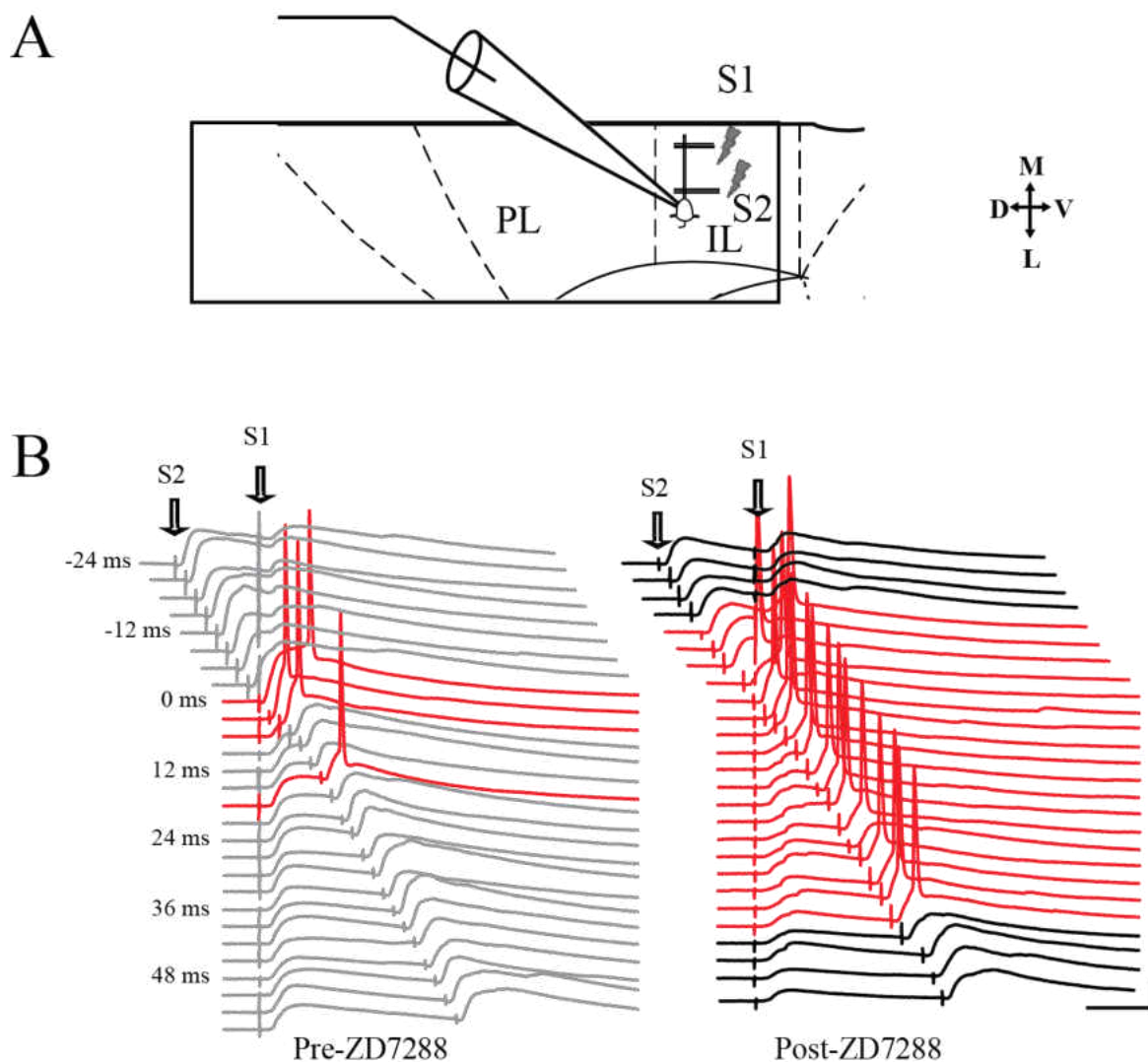
Figure 27. Blocking I_h facilitates coincidence detection. A, Schematic showing the experimental set-up used to study the effect of ZD7288 on coincidence detection. EPSPs were evoked by stimulating L2/3 and L5 within 100 μm of the apical dendrites of the recorded neuron. B, Bath application of ZD7288 facilitates coincidence detection. Under both control condition (left) and in the presence of ZD7288 (right), threshold stimulation intensities were found to reliably evoke a spike when there was no delay between the two stimuli. The interstimulus interval was then systemically varied with 3 ms step. Compare to pre-ZD7288 application (left), APs were more easily evoked by the two stimulations even when the interstimulus interval became larger. Scale bar, 20 mV, 20 ms.

Discussion

The current study found distinctive electrophysiological properties of pyramidal neurons between different layers and subdivisions within the mPFC. In both IL and PL, L2/3 neurons were more hyperpolarized and less excitable than L5 neurons. Such layer-specific properties of mPFC neurons is likely to be a result of differential dendritic architecture and differential ion channel expression. For example, the differential expression of HCN channels may be responsible for the different RMP, input resistance, and I_h. Furthermore, there was also a subregion-specific intrinsic excitability in L2/3 mPFC such that IL neurons were more excitable than PL neurons due to differential spike threshold and input resistance. Finally, we demonstrated that mPFC-amygdala projection neurons were distributed in both L2/3 and L5. HCN channels are important for shaping the basic membrane properties, intrinsic excitability, and dendritic signal integration of L5 mPFC-BLA projection neurons. Thus, these data may lay the foundation for understanding the region-specific contribution of mPFC in emotional responses and other cognitive processes.

L2/3 neurons are less excitable than L5 neurons

In both IL and PL, L2/3 neurons were significantly more hyperpolarized than L5 neurons. Although a significant difference in intrinsic excitability between L2/3 and L5 was only observed in PL but not in IL when held at the same membrane potential (-67 mV), the excitability of L2/3 neurons in IL was significantly reduced at rest (-75 mV). We conclude that L2/3 neurons are generally less excitable than L5 neurons at RMP. Furthermore, the RMP was significantly correlated with the somatic depth such that the neurons in superficial layers were more hyperpolarized. In addition, L5 neurons had

significantly larger depolarizing sags, suggesting that they express more HCN channels than L2/3 neurons. These observations are consistent with previous reports in that L2/3 neurons are more hyperpolarized and lack of *h*-current in both visual cortical (Mason & Larkman, 1990; Medini, 2011) and PL neurons (Boudewijns *et al.*, 2013). Thus, elucidating how such layer-specific excitability contributes to information processing in mPFC may be critical for understanding the mechanisms of mPFC-dependent cognitive processes.

One functional importance of the layer-specific membrane potential is the involvement of cortical neurons in slow oscillation (< 1 Hz), which is observed during quiet wakefulness or sleep and manifested by a bistability of resting membrane potential (Metherate, Cox, & Ashe, 1992; Steriade, Contreras, Curro Dossi, & Nunez, 1993; Steriade, Nunez, & Amzica, 1993). Such slow oscillation is observed in neocortex including mPFC and is thought important for memory consolidation (Eschenko, Magri, Panzeri, & Sara, 2012; Steriade, Nunez, *et al.*, 1993). Interestingly, a recent study by Beltramo and colleagues (2013) revealed that periodic activation of L5 but not L2/3 neurons resulted in almost complete entrainment of ongoing slow frequency field potential at the stimulation frequency (1 Hz). Furthermore, Beltramo's and other's studies indicate that the slow oscillations originate in deep layers and then spread to more superficial cortical layers (Beltramo *et al.*, 2013; Sakata & Harris, 2009; Sanchez-Vives & McCormick, 2000). In addition, there is evidence showing that slow oscillation only occurs at a specific range of membrane potential in thalamic neurons and when *h*-current is present (Luthi & McCormick, 1998; McCormick & Pape, 1990). Thus, the current

observations of different RMP and of I_h levels across layers suggest that neurons in different layers may play distinct functions for information processing.

IL neurons are more excitable than PL neurons

The current study found that within L2/3, IL neurons were more excitable than PL neurons, as evidenced by firing more spikes in response to current injections, which is associated with lower AP threshold, higher input resistance and smaller $I_{threshold}$ in IL neurons compared to that of PL neurons. Such different excitability of L2/3 neurons between IL and PL is consistent with our previous report (Kaczorowski *et al.*, 2012), where we also found that the disruption of the differential excitability between IL and PL in aged animals may underlie the observed extinction deficits (Kaczorowski *et al.*, 2012). Thus, the maintenance of the subregion-specific intrinsic excitability in mPFC is critical for conditioned fear memory expression, whereas abnormal intrinsic excitability in mPFC may lead to extinction deficits which is associated with anxiety disorders.

Although no significant difference was found between IL and PL neurons in L5, previous work has shown distinct roles of IL and PL in behavioral control, especially in conditioned fear memory expression. For example, lesion studies and *in vivo* electrophysiological recordings suggest that activation of PL is critical for the expression of conditioned fear (Blum *et al.*, 2006; Burgos-Robles *et al.*, 2009; Gilmartin & McEchron, 2005) whereas activation of IL is critical for the expression of extinction memory (Gilmartin & McEchron, 2005; Lebron *et al.*, 2004; Quirk *et al.*, 2000). Such subregion-specific roles of mPFC in fear expression may be related to their different projection targets. For example, IL and PL project to different subregions in the amygdala (McDonald

et al., 1996). However, there is still a lack of strong evidence of how such region-specific projection pattern facilitates the different roles of IL and PL in fear memory control.

I_h modulates intrinsic properties of mPFC-BLA projection neurons

mPFC-BLA projection neurons express I_h that is characteristic of HCN2 current. The strong effect of ZD7288 on the membrane properties of mPFC-BLA projection neurons suggests that I_h is critical for basic neuronal function. I_h is carried by HCN channels, which have 4 subunits (HCN1-HCN4). HCN1-HCN3 subunits have been detected in mPFC with HCN1 and HCN2 being most abundant (Day *et al.*, 2005). Based on the slow kinetics of the depolarizing sag observed in the current study, the *h*-current expressed in the mPFC-BLA projection neurons is most likely mediated by HCN2 homomers or HCN1 and HCN2 heteromers (S. Chen, Wang, & Siegelbaum, 2001). This is in contrast to the fast I_h (carried by HCN1 subunit) observed in corticopontine projection neurons and lack of I_h in corticocortical projection neurons in mPFC (Dembrow *et al.*, 2010). Considering the critical role of I_h in dendritic signal integration (Magee, 1998, 1999), the special expression profile of HCN channels in mPFC-BLA projection neurons may be important for circuit-specific information processing.

Although the mPFC-BLA projection neurons displayed unique HCN expression profile, the I_h carried by these channels share same functions with the I_h carried in other neurons such as regulating membrane potential, input resistance, the duration of synaptic EPSPs and signal integration (Dembrow *et al.*, 2010; Luthi & McCormick, 1998; Magee, 1998, 1999; Pape, 1996). The enhancement of intrinsic excitability following blockade of HCN channels with ZD7288 in mPFC-BLA projection neurons is also consistent with pharmacological blockade or genetic deletion of HCN channels in hippocampal CA1

pyramidal neurons (Li *et al.*, 2012), entorhinal cortical L3 neurons (Huang, Walker, & Shah, 2009), reticular thalamic neurons (Ying *et al.*, 2007), cerebellar Purkinje neurons (S. R. Williams, Christensen, Stuart, & Hausser, 2002); but see the study by Thuault *et al.* (2013) who didn't find a change in intrinsic excitability after HCN1 genetic deletion. Interestingly, genetic deletion of HCN1 but not HCN2 channel subtype produces phenotype that leads to provoked seizures and accelerates epileptogenesis (Huang *et al.*, 2009; Ludwig *et al.*, 2003; Poolos, 2012). Thus, these data suggest that the slightly different properties between the HCN subtypes may provide delicate modulatory factors that contribute to the heterogeneity in neuronal functions.

I_h shapes AP waveform of mPFC-BLA projection neurons. HCN channels are also involved in shaping AP waveform of mPFC-BLA neurons, as evidenced by an increase in spike width following the blockade of I_h with ZD7288. This is in line with the observation that blocking I_h with Zd7288 slightly but significantly increased spike half-width in rat inner hair cell afferent synapses, where HCN1, HCN2 and HCN4 subunits were detected (Yi, Roux, & Glowatzki, 2010). In contrast, in the Sinoatrial node where HCN4 channels are expressed, application of ZD7288 reduced spontaneous firing rate but did not affect action potential characteristics (Liu, Dobrzynski, Yanni, Boyett, & Lei, 2007; Nikmaram, Boyett, Kodama, Suzuki, & Honjo, 1997). Thus, it is possible that the HCN2 but not HCN4 subunit is involved in shaping AP waveforms. It is not clear, however, whether or not HCN1 and HCN3 also shape AP waveform because most studies have not reported such an effect.

***I*_h shapes dendritic EPSP and inhibits signal integration**

Blocking *I*_h increases the duration of EPSP and facilitates signal integration. Furthermore, blocking *I*_h facilitated temporal summation more strongly at low frequency (e.g., 20 Hz) but weakly at high frequency (e.g., 100 Hz), suggesting *I*_h specifically restrains the integration of low-frequency afferent signal but allow the integration of high-frequency afferent signals. Furthermore, blocking *I*_h with ZD7288 facilitated coincidence detection of mPFC neurons. These observations are consistent with previous reports in other neurons such as in hippocampal CA1 and superior colliculus (Endo *et al.*, 2008; Nolan *et al.*, 2004; I. Pavlov *et al.*, 2011; Vaidya & Johnston, 2013). Such a filter effect may manifest a mechanism of *I*_h through which mPFC-BLA neurons can selectively respond to salient environment stimuli (e.g., high frequency signals) whereas other stimuli (e.g., low frequency signals) are filtered out. On the contrary, restricted genetic deletion of HCN1 subunit in the forebrain (Nolan *et al.*, 2004) or moderate pharmacological blockade of HCN channels have been found to facilitate spatial learning and PFC-dependent working memory (Wang *et al.*, 2007). However, such enhancement of learning after blockade of HCN channels may occur at the expense of loss of temporal discrimination of inputs (I. Pavlov *et al.*, 2011) and impair the performance of certain executive functions associated with working memory (Thuault *et al.*, 2013). In addition, genetic deletion of HCN1 subunit has been found to induce phenotypes that induce altered nociception, impaired motor learning (Nolan *et al.*, 2003), as well as epilepsy (Huang *et al.*, 2009; Santoro *et al.*, 2010). Thus, maintaining at an optimal level of *I*_h is critical for normal physiological functions, given the neuropathology induced by hyper- or hypo- *I*_h

activity (Lewis, Estep, & Chetkovich, 2010). However, it remains unclear how I_h is involved in conditioned fear memory recall in mPFC-BLA projection neurons.

Mechanisms and implications of layer- and subregion-specific electrophysiological properties of mPFC neurons

In the current study, we found that the differential expression of HCN channels between L2/3 and L5 may account for the layer-specific properties, whereas the different input resistance between IL and PL partially accounts for the subregion-specific membrane properties. It has been well established that HCN channels are the determinants of RMP, R_N, and membrane time constant in cortical neurons (Luthi & McCormick, 1998; Magee, 1998; Pape, 1996). Our observation that L2/3 neurons are not affected by HCN channel blockers is consistent with previous reports that HCN channels are not detectable in L2/3 (Lorincz *et al.*, 2002). The different input resistance between IL and PL neurons is also consistent with our previous study in L2/3 neurons, where we also showed that maintaining the differential excitability between IL and PL may be important for extinction learning (Kaczorowski *et al.*, 2012).

In addition to intrinsic properties, cortical neurons also display layer-specific response to the same pharmacological stimulation. For example, activation of nicotinic acetylcholine receptors (nAchRs) in prefrontal cortex directly excite L5/6 pyramidal neurons but indirectly inhibits L2/3 pyramidal neurons, because only GABAergic interneurons express nAchRs in L2/3 (Poorthuis *et al.*, 2013). Furthermore, L2/3 and L5 neurons play distinct roles within the neural microcircuit. For example, in the same brain region, L2/3 pyramidal cells selectively innervate and excite L5 pyramidal cells whereas L5 pyramidal cell rarely have direct synaptic connections with L2/3 pyramidal cells

(Otsuka & Kawaguchi, 2008; Thomson & Bannister, 1998; Thomson, West, Wang, & Bannister, 2002). Finally, even within a single layer, cortical neurons may display distinct morphological and electrophysiological properties depending upon their long-range projection targets (Dembrow *et al.*, 2010; Otsuka & Kawaguchi, 2008; Yamashita *et al.*, 2013). For example, in L5 visual cortex, neurons that project to contralateral cortex express more voltage-gated K^+ channel subunit Kv4.3 and had smaller sag (I_h) compared to neurons that project to superior colliculus (Christophe *et al.*, 2005). Thus, the cortical neurons are highly heterogeneous in morphology, interconnectivity, and physiological properties depending upon the location of the soma and the long-range projection targets.

Intrinsic excitability is critical for a neuron in that it translates synaptic inputs to the particular output function (Schulz, 2006). Recordings from randomly selected neurons have found learning related increase in intrinsic excitability in the multiple brain regions such as hippocampus (Moyer *et al.*, 1996; Song *et al.*, 2012) and amygdala (Sehgal, Ehlers, & Moyer, 2014). Furthermore, dysregulation of the intrinsic excitability of L2/3 neurons in mPFC may underlie the aging-related extinction deficits (Kaczorowski *et al.*, 2012). However, studies recorded from randomly selected neurons may generate conflicting results regarding learning-related physiological changes from both *in vivo* and *in vitro* preparations (for review, see Kim & Jung, 2006). In contrast, more recent studies have shown that presentation of previously Pavlovian fear conditioned odor to anesthetized rats selectively excites the IL neurons that receive monosynaptic inputs from the amygdala (Laviolette *et al.*, 2005) and the IL neurons that project to the nucleus accumbens but not the neurons that project to the contralateral mPFC (McGinty & Grace, 2008). Taken together, although studies from randomly selected neurons are helpful, further focus on the

same population of neurons at microcircuit and target-specific level is necessary to fully

uncover the mechanisms underlying learning and memory.

Conclusions

The current study demonstrates that the mPFC neurons are highly heterogeneous in

a layer- and subregion-specific manner. L2/3 neurons are significantly hyperpolarized and

less excitable than L5 neurons. IL neurons are more excitable than PL neurons in L2/3 but

not in L5. Furthermore, within mPFC the L2/3 neurons have less *h*-current than do L5

neurons. Such layer-specific expression of HCN channels may underlie the laminar

differences in neuronal intrinsic properties. These data suggest that such layer- and

subregion-specific properties may underlie distinct functional roles of IL and PL in the fear

conditioning and extinction.

CHAPTER FOUR: effect of trace fear conditioning on intrinsic excitability of mPFC-BLA projection neurons

Abstract

The effect of trace fear conditioning on the medial prefrontal cortex (mPFC) to basolateral amygdala (BLA) projection neurons was studied by using a combination of retrograde labeling with *in vitro* whole-cell recordings in layer 5 neurons in adult rats. Trace fear conditioning significantly enhanced the intrinsic excitability of regular spiking infralimbic (IL) projection neurons, via a reduction in spike threshold and activation of hyperpolarization-activated current (*h*-current, or I_h). In contrast, intrinsic excitability was reduced in regular spiking prelimbic (PL) projection neurons through a decrease in input resistance. Behavior performance was positively correlated with intrinsic excitability in IL-BLA projection neurons following conditioning, but negatively correlated with the intrinsic excitability in PL-BLA projection neurons after extinction, suggesting different roles of IL and PL neurons in trace fear memory expression. In both IL and PL, these changes were observed in neurons from the conditioned but not in the pseudoconditioned rats, suggesting they were learning-specific. Furthermore, the conditioning-induced effects were transient, lasting up to 10 days following conditioning and they were reversed by extinction regardless of when extinction memory was probed. Trace fear conditioning significantly increased the input resistance of burst spiking neurons in PL, which enhanced their intrinsic excitability. This effect was also reversed by extinction. Taken together, these data suggest that trace fear conditioning and extinction differentially modulates the intrinsic excitability of mPFC-BLA projection neurons in a subregion- and cell type-specific manner.

Introduction

Although neuronal activity in medial prefrontal cortex (mPFC) influences the expression of long-term conditioned fear memories, few studies have investigated mPFC contributions to the acquisition and extinction of trace fear memories (where CS and US are separated by a trace interval). A growing body of literature has shown that the acquisition and storage of trace fear conditioning depends on the neuronal activity in the mPFC and hippocampus (Blum *et al.*, 2006; Clark & Squire, 1998; Gilmartin & Helmstetter, 2010; Gilmartin, Miyawaki, Helmstetter, & Diba, 2013; Han *et al.*, 2003; Runyan *et al.*, 2004). Our own and other recent studies have revealed that the acquisition of trace fear conditioning enhances intrinsic excitability of hippocampal neurons (Kaczorowski & Disterhoft, 2009; McKay *et al.*, 2009; Song *et al.*, 2012). Although previous studies have shown that delay fear conditioning significantly modulates the intrinsic excitability of IL neurons (Santini & Porter, 2010; Santini *et al.*, 2008), it is not clear how trace fear conditioning affects the intrinsic excitability of mPFC neurons.

The mPFC has reciprocal innervation with a variety of cortical and subcortical brain regions including amygdala (Gabbott, Warner, Jays, Salway, & Busby, 2005; Hurley, Herbert, Moga, & Saper, 1991; Vertes, 2004). Interestingly, the different projection neurons display distinct morphological and electrophysiological properties (DeFelipe & Farinas, 1992; Dembrow *et al.*, 2010; Hattox & Nelson, 2007; Larkman, Hannay, Stratford, & Jack, 1992; Mason & Larkman, 1990), which may contribute to their ability to play distinct roles during cognitive behavior (McGinty & Grace, 2008). Thus, the current study investigated how trace fear conditioning affects the intrinsic excitability of mPFC-BLA projection neurons by injecting a retrograde tracer into the basolateral nucleus of amygdala,

which is a critical area for fear conditioning and extinction (LeDoux, 2000). By using a combination of retrograde tracing and whole-cell recording, we are the first to show that trace fear conditioning significantly changed the intrinsic excitability of mPFC-BLA projection neurons in a region- and cell type-specific manner. The conditioning-induced effect lasted up to 10 days, and it was reversed by extinction.

Methods

Subjects. Subjects were 49 adult male F344 rats (5.0 ± 0.1 mo). Rats were maintained in an Association for Assessment and Accreditation of Laboratory Animal Care (AAALAC) accredited facility on a 14 h light–10 h dark cycle and housed individually with free access to food and water. Procedures were conducted in accordance with the University of Wisconsin-Milwaukee animal care and use committee (ACUC) and NIH guidelines.

Retrobeads^{TM} infusion. All rats received unilateral pressure infusion of a red fluorescent retrograde tracer (Retrobeads^{TM}, Lumafluor) into the basolateral nucleus of the amygdala (relative to Bregma, -3 mm AP, ± 5 mm ML; - 8.3 mm DV), with deep anesthetization under stereotaxic. The infusion was made with glass pipettes (20 – 40 μm) pulled from borosilicate glass (VWR Micropipets) using a Sutter Instruments P97 puller. The pipette was connected to a 2 μl syringe (Hamilton) driven by an infusion pump (Harvard Apparatus, model 975). The infusion lasted 5-10 min and the pipette was withdrawn 10 min after infusion. A total volume of 0.1 - 0.3 μl red Retrobeads^{TM} were infused into BLA.

Apparatus. *Fear conditioning chambers.* Trace fear conditioning was conducted in a Plexiglas and stainless steel chamber (30.5 X 25.4 X 30.5 cm; Coulbourn Instruments,

Whitehall, PA), located in a sound-attenuating box. The chamber was rectangular and had a standard grid floor consisting of 26 parallel steel rods (5 mm diameter and 6 mm spacing). The floor was connected to a precision adjustable shock generator (Coulbourn Instruments) for delivery of a scrambled footshock US. Within the sound-attenuating box, a ventilation fan produced a constant background noise of about 58 dB (measured by a sound level meter, A scale; model #33-2050, Realistic, Fort Worth, TX). The chamber was illuminated by a miniature incandescent white lamp (28V, type 1819) and was wiped with a 5% ammonium hydroxide solution prior to each training session. During training, the room lights were left on (illumination 20.9 lux) for the entire session.

Extinction and CS testing chambers. An additional Plexiglas chamber was served as a novel context for the auditory cue test. This chamber was located within a separate sound-attenuating box located in the same room. The test chamber was physically different from the training chamber in that it was octagonal (instead of rectangular), the floor was black-painted Plexiglas (instead of grid bars), and was illuminated with an infrared light. In addition, the tray below the test chamber floor contained clean bedding and the test chamber was wiped with 2% acetic acid prior to each test session to provide a different olfactory stimulus from that used during training. The room lights were turned off (illumination 0.2 lux) for the entire testing session.

Fear conditioning and extinction. After a minimum of 7 days of recovery from surgery, rats were handled for at least one week before they were randomly assigned to naïve (NAÏVE, n = 10), pseudoconditioned (PSEUDO, n = 8), trace fear conditioned (TRACE, n = 9), trace fear conditioned-retention (TRACE-RET, n = 3), trace fear conditioned-extinction (EXT, n = 10), and trace fear conditioned extinction-retention

(EXT-RET, n = 9) groups (see Figure 28A). On day 1, TRACE, TRACE-RET, EXT, and EXT-RET rats received one 10-trial session of *auditory trace fear conditioning* using a 15 s CS (80 dB white noise) followed by a 30-s trace interval (stimulus-free period) and a 1-s footshock US (1.0 mA). A long (5.2 min ± 20 %) intertrial interval (ITI) was used to maximize CS and minimize context (i.e., training chamber) conditioning (Detert, Kampa, & Moyer, 2008). PSEUDO rats received the same amount of CS and US presentations but they were explicitly unpaired. Naïve rats remained in their home cages throughout the experiment. On days 2-3, rats in the TRACE, TRACE-RET and PSEUDO groups remained in their home cages, whereas EXT and EXT-RET rats received 2 consecutive sessions (1 session per day) of 10 CS-alone presentations in a novel context. These sessions were identical to the training except no US was presented. Following each extinction session, rats were returned to their home cages 2 min after the last extinction trial.

Behavioral testing. Twenty-four hours after extinction (day 4), PSEUDO, TRACE, and EXT rats received a brief CS test session in the extinction context. TRACE-RET and EXT-RET rats received the CS test on day 11. During this behavioral test, rats were first allowed to explore the new chamber for 2-min (baseline), followed by two 15-s CS presentations (2.9-min ITI), and they were removed 2 min after the second CS presentation. To assess memory, the amount of time spent freezing during the baseline, the CS, and the trace interval (defined as the first 30 sec after CS offset) was measured. Consistent with our earlier report (Detert *et al.*, 2008), the freezing levels during CS were less than during the trace interval and therefore were not shown and the freezing levels during trace interval were used as the measurement of behavioral performance (see
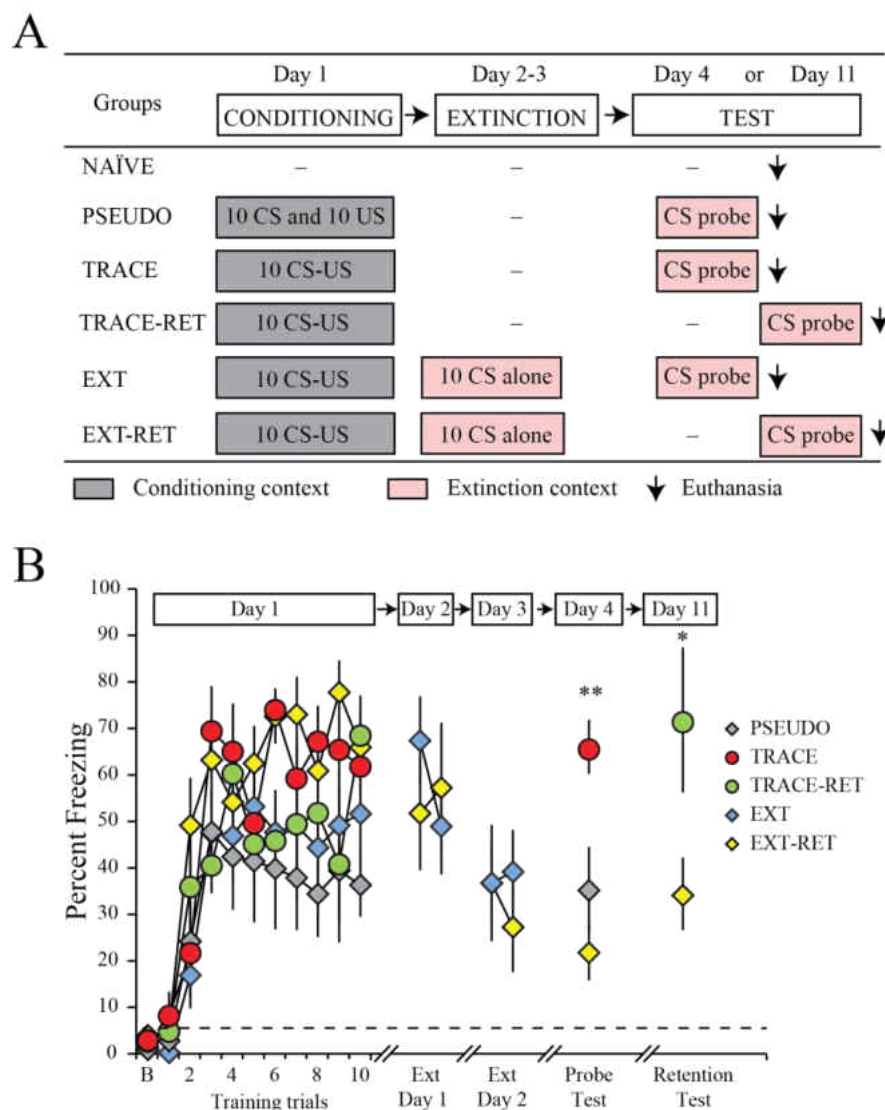
Figure 28.   Experimental design and behavioral performance during trace fear conditioning, extinction, and probe test. A, Experimental design.   Rats received one 10-trial session of trace fear conditioning or pseudoconditioning on day 1. EXT and EXT-RET rats received extinction on days 2-3 in a novel context. TRACE, PSEUDO, and EXT rats received a brief CS-alone probe test on day 4. TRACE-RET and EXT-RET rats received the probe test on day 11. Immediately following their last behavior test, brain slices were prepared for electrophysiological studies. NAÏVE rats remained in their homecage throughout the experiment. B, Behavioral responses of trace fear conditioned and pseudoconditioned rats during conditioning, extinction (first 2 trials), and testing. During conditioning, all rats displayed a rapid increase in freezing levels during the first three trials and then maintained high freezing levels. A repeated measures ANOVA of percent freezing revealed a significant main effect of training trials [$F(9,306) = 19.5$, $p < 0.01$; Greenhouse-Geisser corrected] and a significant effect of group [$F(4,34) =3.2$, $p < 0.05$] but no significant group by training trial interaction [$F(36,306) = 1.1$, $p = 0.34$; Greenhouse-Geisser corrected]. During the probe test, all rats displayed comparable levels of freezing during baseline (dashed line indicates the average baseline freezing of all groups). In contrast, TRACE rats froze significantly more than both PSEUDO and EXT rats during the trace interval following offset of the CS ($p < 0.01$). TRACE-RET rats froze significantly more than EXT-RET rats [$F(1,10) = 5.37$, $p <0.05$].

Figure 28B). In addition, the percent freezing during the 2 CS presentations during the probe test was averaged and used as the measurement of behavior performance (fear memory).

Analysis of behavioral data. A remote CCTV video camera (model #WV-BP334; Panasonic Corp., Suzhou, China), mounted to the top of each behavioral chamber, was used to record the activity of each rat during training and testing. The video data were fed to a PC running FreezeFrame 2.04 04 (Actimetrics Software, Coulbourn Instruments). Data were analyzed using FreezeView 2.04 (Actimetrics Software) where a 1 sec bout of immobility was scored as freezing. Freezing was defined as the absence of all movement except that required for respiration (Blanchard & Blanchard, 1969).

PFC slice preparation for electrophysiological recording. Immediately after CS test, rats were anesthetized and decapitated by an individual blind to training condition. The brains were quickly removed and placed into ice-cold artificial cerebral spinal fluid (aCSF, in mM): 124 NaCl, 2.8 KCl, 1.25 NaH_2PO_4, 2 $CaCl_2$, 2 $MgSO_4$, 26 $NaHCO_3$, 20 glucose (pH 7.5, bubbled with 95% O_2/5% CO_2). Coronal slices (300 μm) containing prefrontal cortex (AP + 3.2 – 2.2) were cut in ice-cold aCSF using a vibrating tissue slicer (VT1200, Leica). The slices were incubated at 32 – 36°C in oxygenated aCSF until use. The rest of the brain was then blocked and coronal slices that contained the amygdala were prepared to confirm infusion location. The injection site was inspected immediately after cutting by placing the slice on the stage of our upright microscope (Olympus BX51WI) equipped with fluorescence and photographing the section. All injection sites were within the basolateral complex of amygdala (BLA, including the basal, lateral, and accessory basal

nuclei) and intercalated cell masses (see a representative image in Figure 13A and the infusion location for all rats in Figure 29).

For whole-cell recordings (WCRs), electrodes (5–8 MΩ) were prepared from thin-walled capillary glass and filled with the following solution (in mM): 110 K-gluconate, 20 KCl, 10 Di-Tris-P-Creatine, 10 HEPES, 2 $MgCl_2$, 2 Na_2ATP, 0.3 Na_2GTP, 0.2% Biocytin, pH to 7.3. The osmolarity was 290 mOsmol. All chemicals were obtained from Sigma or Fisher unless noted.

Electrophysiological recordings. PFC slices were transferred to a submerged recoding chamber mounted on a fluorescence-equipped Olympus BX51WI upright microscope where they were continuously perfused with oxygenated aCSF at a rate of 2 ml/min, and maintained at 32 – 36°C using an inline temperature controller. The fluorescently labeled mPFC neurons were visualized using a Texas Red epifluorescent filter set. A Hamamatsu CCD camera (Hamamatsu Camera Ltd., Tokyo, Japan) was used to visualize and photograph the neuron and the brain slice for verification of recording location. Neurons with somata that were ≥ 400 μm from the pial surface were defined as layer 5 (L5) neurons (Gabbott & Bacon, 1996; Perez-Cruz *et al.*, 2007) and were recorded and analyzed. L6 was recognized as distinct from L5 because it contains a high density of fibers (Gaillard & Sauve, 1995). After positively labeled neurons were recognized, the microscope was switched to IR-DIC mode to guide whole-cell recording. Data were collected from those neurons whose RMP were more negative than -50 mV and held at -67 mV (mean holding current: -62 ± 4 pA). Series resistance was fully compensated and always monitored to ensure the stability of recording conditions. Cells were only accepted for analysis if the initial series resistance was ≤ 30 MΩ and did not change by > 30% throughout the recording period. The distribution of
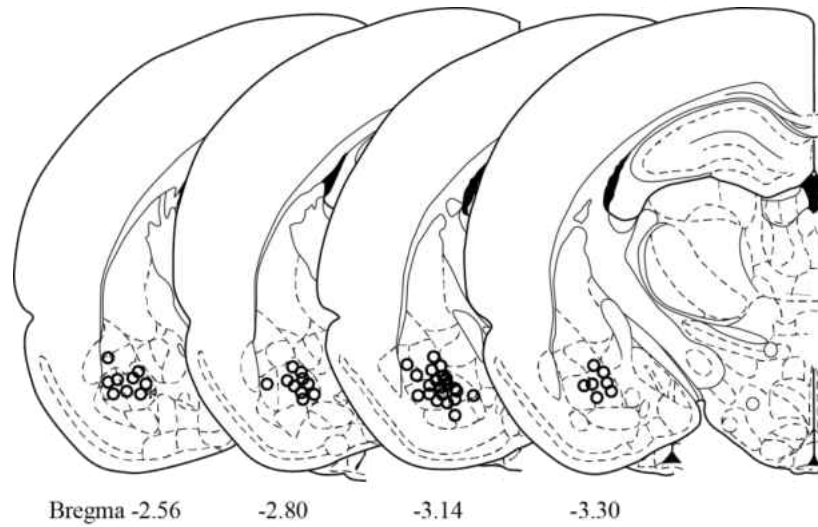
Figure 29. Schematic drawing of coronal sections of rat brain showing the location of pipette tips used for Retrobeads™ infusions in the amygdala (illustration modified from Paxinos & Watson, 1998, with permission from *Elsevier*). Retrobeads™ were infused into both hemispheres but all infusion locations are shown in left hemisphere for simplicity.

all recorded neurons included in this study are shown in Figure 30A (regular spiking) and Figure 30B (burst spiking).

Intrinsic properties of mPFC-BLA projection neurons were recorded under current clamp according to the following protocols: *(1)* I-V relations were obtained from a series of 500 ms current injections (range from -300 pA to 50 pA) and plotting the plateau voltage deflection against current amplitude. Neuronal input resistance (R_N) was determined from the slope of the linear fit of the portion of the V-I plot where the voltage sweeps did not exhibit sags or active conductance (see Figure 30E and 30G). The sag ratio during hyperpolarizing membrane responses was expressed as $[(1 - \Delta V_{ss} / \Delta V_{min}) \times 100\%]$, where $\Delta V_{ss} = MP - Vss$, $\Delta V_{min} = MP - V_{min}$, MP is the membrane potential before current step, V_{ss} is the steady-state potential and V_{min} is the initial minimum potential. For each neuron, sag ratio was calculated from -300 pA, -250 pA, and -200 pA current steps and averaged. *(2)* Action potential (AP) properties, including $I_{threshold}$ were studied with an ascending series of 500 ms depolarizing pulses necessary to elicit one single (regular spikers) or a burst of spikes (burst spikers). Neurons that generated two or more action potentials riding atop the $I_{threshold}$ depolarizing current in an all-or-none fashion were classified as burst spiking neurons (Connors, Gutnick, & Prince, 1982). For burst spiking neurons, AP properties were studied from the first spike. AP threshold (AP_{thresh}) was defined as the voltage when dV/dt first exceeded 28 mV/ms (Kaczorowski *et al.*, 2012). The AP amplitude (AP_{amp}) was measured relative to the AP_{thresh}. AP width (AP_{width}) was measured as the width at half of the AP amplitude. *(3)* Post-burst afterhyperpolarization (AHP) relative to baseline was measured at the peak (mAHP) or 1 s (sAHP) following a burst of 10 spikes evoked by brief (2 ms) suprathreshold current injections at 50 Hz (3X, at 20 sec
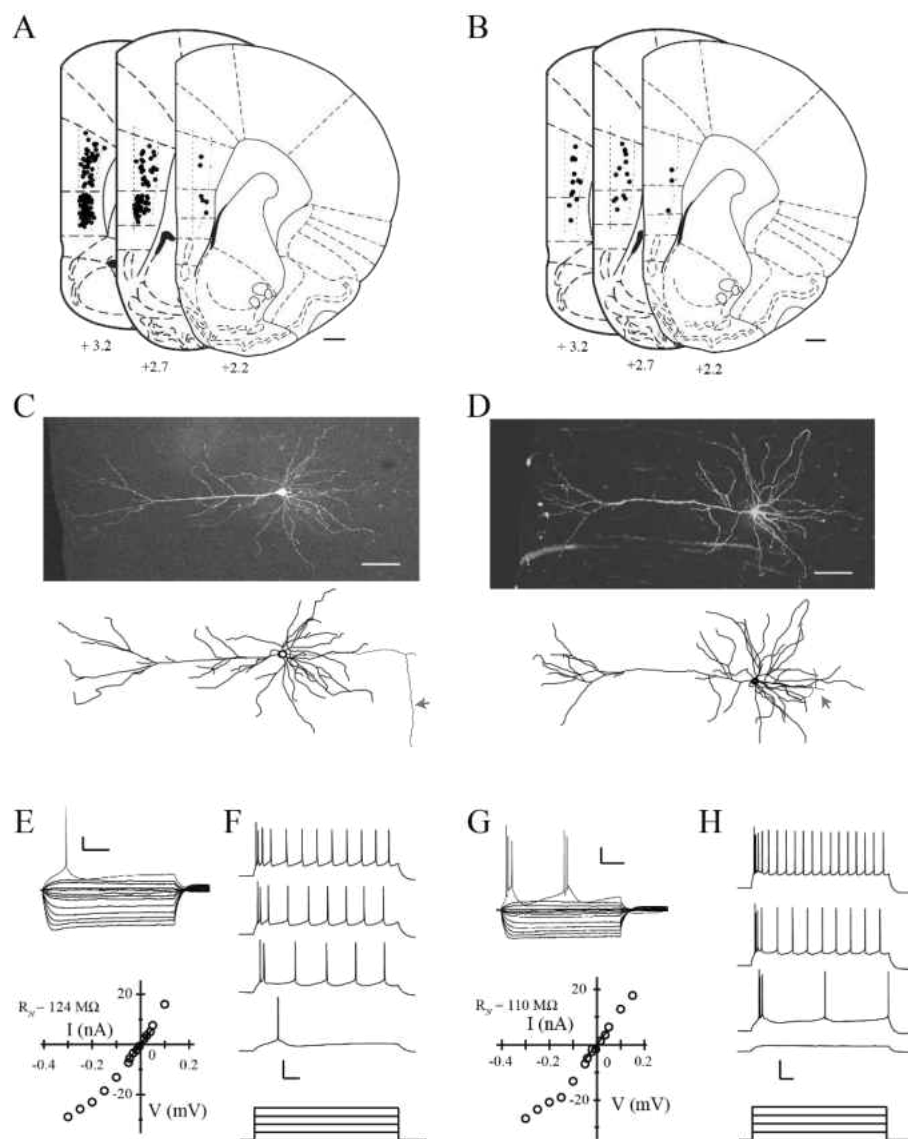
Figure 30. Location and basic properties of neurons in mPFC. Neurons with a somatic depth ≥ 400 μm were defined as layer 5 neurons. A and B, schematic diagrams of rat coronal sections (Paxinos & Watson, 1998) illustrating the distribution of all regular (A) and burst (B) spiking mPFC-BLA projection neurons obtained in this study. Neurons were recorded from either side but all were labeled in one hemisphere for simplicity. C and D, confocal images of representative regular spiking (C) and burst spiking (D) mPFC-BLA projection neurons and their 3D reconstructions. Arrows point to the axons (represented as gray) of the cells. E and G, voltage responses to a series of current injections and the accompanying V-I plot used to measure neuronal input resistance (R_N). F and H, Neuronal excitability was studied by injecting a series of depolarizing currents and the number of spikes evoked was counted. Scale bars: A and B, 500 μm; C and D, 100 μm; E and G, 20 mV, 100 ms; F and H, 40 mV/100 pA, 100 ms.

intervals). *(4)* Neuronal excitability was accessed by counting the number of spikes evoked in response to a series of 1-sec depolarizing steps (range 50 – 450 pA, 50 pA increments, 20 s ITI; see Figure 30F and 30H).

All recordings were obtained in current-clamp mode using a HEKA EPC10 amplifier system (HEKA Elektronik). Data were transferred to a PC computer using an ITC-16 digital-to-analog converter (HEKA Elektronik). The signals were filtered at 2.9 kHz and digitized at 20 kHz using Patchmaster software (HEKA Elektronik). Data were analyzed offline using Patchmaster and Igor Pro software (version 4.03; WaveMatrix). Voltages were not corrected for the liquid-liquid junction potential (~ +13 mV, see Moyer and Brown, 2007). Recordings were made from mPFC neurons located both ipsilateral and contralateral to the BLA injection site. Physiological data were combined because no significant differences were observed.

Biocytin staining. Neurons filled with biocytin (0.2% in internal solution) during recording were fixed in formalin for 1 to 4 weeks before they were processed for visualization by using streptavidin Alexa Flour 488 reaction. Slices were mounted, and labeled neurons were visualized and photoimaged using either a fluorescence microscope (BX51WI, Olympus) or laser scanning confocal fluorescence microscope (FV-1200, Olympus). Confocal image stacks were used for 3D reconstruction (see Figure 30C and 30D) using Neurolucida software (MBF Bioscience, Williston, VT). All neurons analyzed displayed characteristics of pyramidal cells according to morphology and electrophysiology. Confocal images and reconstructions of a representative regular spiking and a representative burst spiking neuron and their reconstructions are shown in Figure 30C and 30D respectively.

Statistical Analyses. All statistical analyses were performed with the aid of Microsoft Excel and IBM SPSS statistics software (version 22; SPSS). Data were analyzed using parametric statistics with two-tailed Student's t test, one-way ANOVA, or repeated measures ANOVA, as appropriate. For significant main effects (alpha 0.05), a Fisher's PLSD test was used for *post hoc* comparisons. All data are expressed as mean ± SEM.

Results

We examined the effect of trace fear conditioning and extinction on the intrinsic excitability of mPFC-BLA projection neurons by a combination of retrograde labeling with whole-cell recording. All rats received a unilateral injection of fluorescently labeled microspheres before they received behavioral training (except for NAÏVE rats, who received Retrobeads^{TM} injection but remained in home cages). Rats received conditioning or pseudoconditioning on day 1 followed by either extinction training or no treatment (i.e., they remained in their home cage) on days 2 and 3. Rats in the trace fear conditioned (TRACE), pseudoconditioned (PSEUDO), and extinction (EXT) groups received a brief CS-alone probe test on day 4. Rats in the trace fear conditioned-retention (TRACE-RET) and extinction-retention (EXT-RET) groups received the probe test on day 11 (see Figure 28A). Prefrontal cortical slices were prepared immediately (within one hour) after the probe test and the fluorescently labeled neurons in L5 of both IL and PL were recorded. The duration from the date of surgery to the date of slicing was not significantly different between groups [mean 30.8 ± 2.2 days; $F(5,43) = 0.19$, $p = 0.97$].

Analysis of behavioral performance during the trace interval indicated that all rats exhibited a rapid increase in percent freezing during the first 3 trials, after which they maintained a high level of freezing throughout the rest of the training trials (see Figure 28B). A repeated-measures ANOVA with *post hoc* tests showed that PSEUDO rats froze significantly less than TRACE ($p < 0.05$) or EXT-RET ($p < 0.01$) rats. Although EXT rats froze less than EXT-RET rats ($p < 0.05$), they displayed comparable levels of freezing during the first two trials of extinction, indicating the memory of conditioned fear was comparable between the two groups. When memory was tested on day 4, freezing levels

were comparably low [$F_{(2,26)} = 1.51$, $p = 0.24$] during the baseline among all the groups (average baseline freeze was shown as a dashed line in Figure 28B). As illustrated in Figure 28B, *post hoc* analyses indicated that TRACE rats froze significantly more than both PSEUDO ($p < 0.01$) and EXT rats ($p < 0.01$). During retention test on day 11, TRACE-RET rats froze significantly more than EXT-RET rats ($p < 0.05$), suggesting good memory retention for both conditioning and extinction.

Trace fear conditioning enhances intrinsic excitability of regular spiking IL-BLA projection neurons

To evaluate the effect of trace fear conditioning on the intrinsic excitability of mPFC-BLA projection neurons, PFC slices were prepared immediately after the memory test and WCRs were performed on the neurons that were labeled with fluorescent microspheres. Although both L2/3 and L5 neurons project to the amygdala (see Figure 13B), we restricted our studies to L5 neurons only because they were the major output neurons (Groh *et al.*, 2010) and have electrophysiological properties that are distinctly different from L2/3 neurons (Boudewijns *et al.*, 2013). To evaluate changes in neuronal intrinsic excitability, we counted the number of action potentials evoked by a series of depolarizing current pulses (50 – 450 pA) while the cells were held at -67 mV.

Trace fear conditioning significantly increased the intrinsic excitability of regular spiking IL-BLA projection neurons as evidenced by firing more APs in response to depolarizing steps compared to NAÏVE neurons (see Figure 31A and 31C). A repeated-measures ANOVA revealed significant main effects of group [$F_{(5,103)} = 3.0$, $p < 0.05$] and current intensity [$F_{(1.6, 162.1)} = 497.3$, $p < 0.01$; Greenhouse-Geisser corrected]. There was also a significant interaction of group by current intensity [$F_{(7.9,93.6)} = 2.4$, p
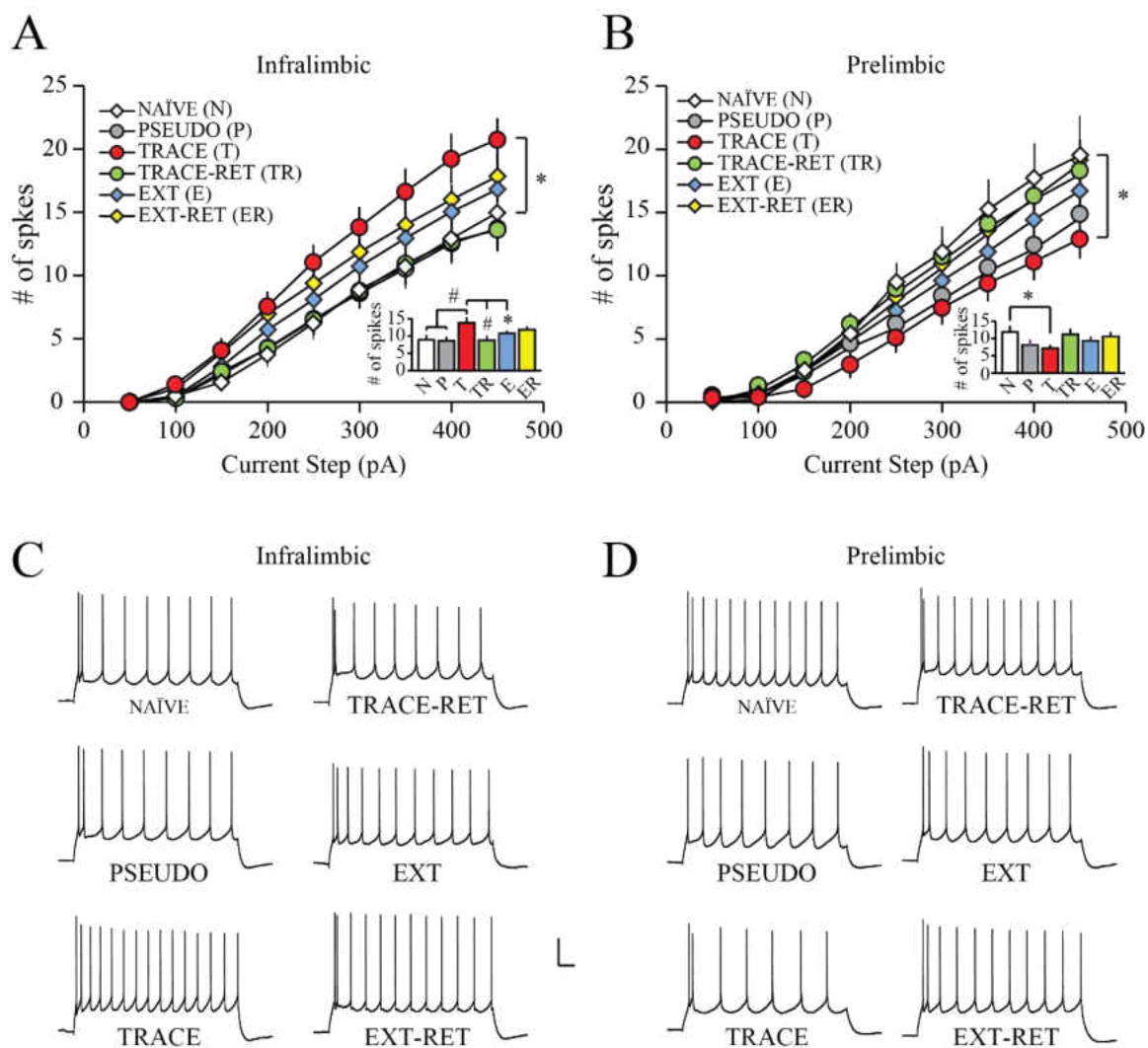
Figure 31. Trace fear conditioning differentially modulates the intrinsic excitability of regular spiking IL and PL neurons that project to BLA. A, Trace fear conditioning significantly enhanced the intrinsic excitability of IL-BLA projection neuron. Neurons from TRACE rats fired significantly more spikes than neurons from NAÏVE rats ($p < 0.05$). B, Trace fear conditioning significantly suppressed the intrinsic excitability of PL-BLA projection neurons. Neurons from TRACE rats fired significantly less spikes than neurons from NAÏVE rats ($p < 0.05$). In both IL and PL, extinction reversed the conditioning effect such that the intrinsic excitability in EXT neurons was comparable with neurons from other groups, and remained stable after extinction retention (EXT-RET). The conditioning-induced plasticity observed in TRACE rats was transient in both IL and PL as the intrinsic excitability returned to naïve level after memory retention (TRACE-RET). *Inset* in A and B are bar graphs showing the number of spikes evoked by a 300-pA current injection in mPFC-BLA projection neurons (statistically different between TRACE and other groups: * $p < 0.05$, # $p < 0.01$). C and D, Representative traces showing the number of spikes evoked by a 300-pA current injection. Scale bar, 20 mV, 100 ms.

< 0.05; Greenhouse-Geisser corrected]. Follow-up analyses using a one-way ANOVA revealed a significant group effect when the depolarizing currents that were greater than 250 pA (all values, $p < 0.05$). *Post hoc* comparisons confirmed that cells in TRACE rats fired significantly more action potentials than those in NAÏVE, PSEUDO, or TRACE-RET rats in response to the depolarizing currents ranged between 250 pA and 400 pA (see Figure 31A). Interestingly, the intrinsic excitability was not enhanced in TRACE-RET rats, although they displayed good retention memory 10 days after conditioning, suggesting the conditioning-induced effect was transient, which is consistent with previous studies in hippocampal neurons following trace eyeblink conditioning (Moyer *et al.*, 1996; Thompson, Moyer, & Disterhoft, 1996a). The enhancement of intrinsic excitability was also not observed in EXT or EXT-RET rats. In both groups intrinsic excitability was comparable to that of neurons from Naïve rats (see Figure 31A and 31C), suggesting that extinction reversed the effects of trace fear conditioning.

Although PSEUDO rats displayed an increase in freezing during the trace interval during conditioning and during probe test (see Figure 28B), the intrinsic excitability in IL-BLA projection neurons was not significantly changed (see Figure 31A and 31C), suggesting the enhancement of intrinsic excitability in conditioned rats was associative and learning-specific. Thus, our results indicate that acquisition of trace fear conditioning transiently enhances the intrinsic excitability of IL-BLA projection neurons and extinction reverses the effect of conditioning.

Trace fear conditioning modulates spike threshold and h-current in regular spiking IL-BLA projection neurons

Neuronal excitability is determined by the properties and distribution of ion channels within the plasma membrane. To examine which ion channels may underlie these learning-related changes, we further compared other membrane properties of regular spiking IL-BLA projection neurons between the various training groups. A planned comparison between neurons from naïve and conditioned animals suggests that the spike threshold was significantly hyperpolarized after conditioning [$t(40) = 2.4$, $p < 0.05$; see Figure 32A] and that there was a significant correlation between spike threshold and the number of spikes evoked by the depolarizing currents ($r = -0.46$, $p < 0.01$). Furthermore, conditioning significantly increased the depolarizing sag [$t(38) = 3.4$, $p < 0.01$; see Figure 32B and Table 9], suggesting the activation of h current (I_h) mediated by hyperpolarization-activated cyclic nucleotide-gated (HCN) channels. In addition, trace fear conditioning enhanced the mAHP (measured at the peak following a burst of 10 APs) but not sAHP (measured at 1 s following the burst of APs; see Figure 32C and Table 9), which is consistent with the activation of I_h (Kaczorowski, 2011; Oswald, Oorschot, Schulz, Lipski, & Reynolds, 2009). That activation of I_h contributed to the enhanced mAHP was also supported by the observation that the mAHP was significantly correlated with the sag ($r = -0.38$, $p < 0.05$). Other membrane properties (e.g., RMP, input resistance, $I_{threshold}$) were not significantly changed by conditioning (see Table 9). Taken together, these data suggest that trace fear conditioning specifically enhances intrinsic excitability of IL-BLA projection neurons through modulating the expression or properties of the ion channels that regulate spike threshold and I_h.
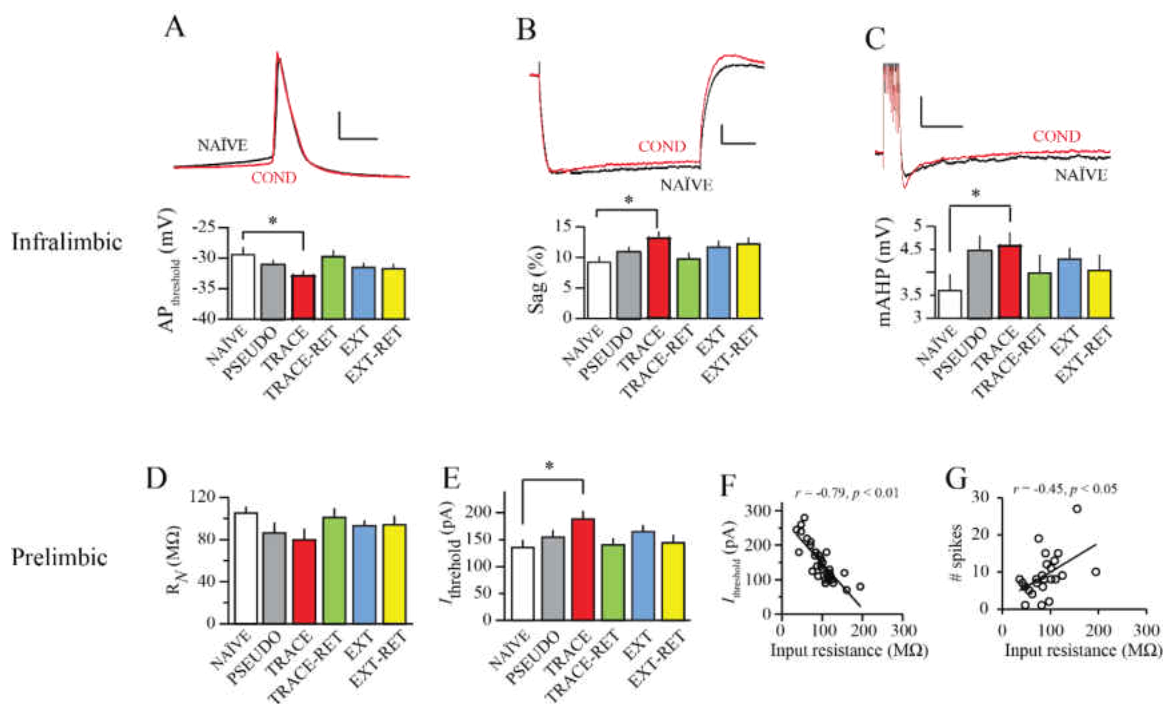
Figure 32. Distinct mechanisms underlying trace fear conditioning between IL and PL neurons. In IL, acquisition of trace fear conditioning reduced the AP threshold (A), depolarizing sag (B), and enhanced mAHP (C). Scale bars: A, 20 mV, 2 ms; B, 5 mV, 100 ms; C, 5 mV, 0.5 s. In PL, acquisition of trace fear conditioning reduced the neuronal input resistance (R_N) but the difference was not statistically significant (D). Conditioning significantly increased the minimal current ($I_{threshold}$) required to evoke one single AP (E), which may be caused by the reduction in R_N because these two measurements were significantly correlated (F). The conditioning-induced reduction in input resistance may have caused the decrease in the intrinsic excitability as the R_N was significantly correlated with excitability (G).

Table 9. Effect of trace fear conditioning and extinction on membrane properties of regular spiking mPFC-BLA projection neurons

Group (# of rats)	RMP (mV)	R_N (MΩ)	$I_{threshold}$ (pA)	AP_{thresh} (mV)	AP_{amp} (mV)	AP_{width} (µs)	mAHP (mV)	sAHP (mV)	Sag (%)
IL									
NAÏVE (10)	-60.7 ± 1.2 (21)	123 ± 9 (21)	147 ± 12 (20)	-29.5 ± 1.2 (20)	77 ± 2 (20)	971 ± 49 (20)	-4.2 ± 0.3 (20)	-0.9 ± 0.1 (20)	9.2 ± 1.0 (18)
PSEUDO (8)	-64.1 ± 1.3 (18)	104 ± 8 (18)	154 ± 14 (18)	-31.2 ± 0.9 (18)	78 ± 2 (18)	950 ± 36 (18)	-4.9 ± 0.4 (18)	-0.8 ± 0.1 (18)	10.8 ± 0.9 (18)
TRACE (8)	-62.5 ± 1.2 (22)	118 ± 9 (22)	137 ± 8 (22)	-32.8 ± 0.8 (22)*	78 ± 1 (22)	968 ± 42 (22)	-5.1 ± 0.3 (22)*	-0.7 ± 0.1 (22)	13.2 ± 1.0 (22)*
TRACE-RET (3)	-61.8 ± 1.2 (13)	99 ± 8 (13)	150 ± 15 (12)	-29.8 ± 1.1 (12)	75 ± 2 (12)	912 ± 26 (12)	-4.7 ± 0.4 (13)	-0.7 ± 0.2 (13)	9.7 ± 1.1 (13)
EXT (9)	-61.3 ± 1.1 (23)	107 ± 6 (23)	147 ± 10 (23)	-31.5 ± 0.7 (23)	78 ± 1 (23)	912 ± 34 (23)	-4.8 ± 0.2 (22)	1.0 ± 0.1 (22)	11.7 ± 1.1 (22)
EXT-RET (8)	-62.1 ± 1.0 (24)	108 ± 6 (24)	144 ± 12 (24)	-31.8 ± 0.8 (24)	81 ± 2 (24)	840 ± 29 (24)	-4.8 ± 0.3 (22)	0.9 ± 0.1 (22)	12.2 ± 1.1 (21)
PL									
NAÏVE (6)	-61.7 ± 0.4 (12)	105 ± 6 (12)	135 ± 14 (12)	-30.6 ± 1.6 (12)	80 ± 2 (12)	818 ± 37 (12)	-4.8 ± 0.3 (12)	-0.9 ± 0.1 (12)	11.7 ± 2.1 (9)
PSEUDO (5)	-62.0 ± 1.3 (9)	86 ± 10 (9)	154 ± 14 (9)	-30.9 ± 1.9 (9)	82 ± 1 (9)	780 ± 23 (9)	-6.0 ± 0.4 (9)	-1.0 ± 0.1 (9)	13.2 ± 2.3 (9)
TRACE (7)	-63.4 ± 0.9 (14)	80 ± 11 (14)	188 ± 15 (14)*	-32.2 ± 0.6 (14)	85 ± 2 (14)	846 ± 35 (14)	-4.8 ± 0.3 (14)	-0.9 ± 0.1 (14)	12.4 ± 1.1 (14)
TRACE-RET (3)	-63.0 ± 1.5 (15)	101 ± 9 (15)	140 ± 13 (14)	-31.5 ± 0.9 (14)	80 ± 2 (14)	750 ± 26 (14)	-4.9 ± 0.3 (15)	-1.0 ± 0.1 (13)	9.4 ± 1.0 (13)
EXT (8)	-61.3 ± 1.2 (22)	93 ± 5 (22)	165 ± 12 (22)	-31.3 ± 0.8 (22)	82 ± 2 (22)	829 ± 26 (22)	-4.6 ± 0.3 (22)	-0.6 ± 0.1 (22)	11.8 ± 1.0 (22)
EXT-RET (8)	-62.8 ± 1.5 (15)	94 ± 9 (15)	144 ± 15 (15)	-33.5 ± 0.9 (15)	85 ± 2 (15)	798 ± 31 (15)	-4.7 ± 0.4 (13)	-0.8 ± 0.1 (13)	11.4 ± 1.4 (13)

Data are mean ± SE for number of cells in parentheses. IL, infralimbic cortex; RMP, resting membrane potential; R_N, neuronal input resistance; $I_{threshold}$, threshold current required to elicit an action potential; AP_{thresh}, action potential threshold; AP_{amp}, action potential amplitude; AP_{width}, action potential half-width; mAHP, medium afterhyperpolarization. Rat groups: NAÏVE, rats that did not receive any behavioral training; PSEUDO, rats that received pseudoconditioning on day 1 and tested on day 4; TRACE, rats that received trace fear conditioning on day 1 and tested on day 4; TRACE-RET, rats that received trace fear conditioning on day 1 and tested on day 11; EXT, rats that received trace fear conditioning on day 1, extinction on days 2-3, and tested on day 4; EXT-RET, rats that received conditioning on day 1, extinction on days 2-3, and tested on day 11. AP_{amp} was relative to threshold. The mAHP was measured at the peak of the AHP following a burst of 10 APs relative to baseline. The sAHP was measured at 1 s following the burst of APs. Statistically different from Naïve: * $p < 0.05$.

Trace fear conditioning suppresses intrinsic excitability of regular spiking PL-BLA projection neurons

In contrast to IL neurons, acquisition of trace fear conditioning significantly reduced the intrinsic excitability of regular spiking neurons in PL (see Figure 31B and 31D). A planned repeated measures ANOVA between Naïve and Cond neurons revealed a significant main effects of group [$F(1,22) = 4.6$, $p < 0.05$] and current intensity [$F(1.2, 26.7) = 70.4$; $p < 0.01$; Greenhouse-Geisser corrected] but no significant group by current interaction [$F(1.2, 26.7) = 3.4$; $p = 0.07$; Greenhouse-Geisser corrected]. Further analysis with a one-way ANOVA revealed that conditioned rats fired significantly less spikes in response to the depolarizing currents of $250 - 400$ pA (all values, $p < 0.05$). However, the intrinsic excitability returned to naïve level after extinction or extinction retention, suggesting extinction reversed the effect of conditioning (see Figure 31B and 31D). Similar with IL neurons, the intrinsic excitability of PL-BLA projection neurons was not significantly changed between any other groups, suggesting the reduction of intrinsic excitability in conditioned rats was learning-specific, transient, and reversible.

Trace fear conditioning reduces input resistance of regular spiking PL-BLA projection neurons

Trace fear conditioning induced a subtle reduction in the input resistance (R_N) of PL-BLA projection neurons [$t(24) = 1.9$; $p = 0.07$; see Figure 32D]. However, such a subtle change in R_N significantly reduced the excitability of PL-BLA projection neurons such that the neurons from conditioned rats required a much larger threshold current ($I_{threshold}$) to evoke a single spike [$F(24) = 2.7$, $p < 0.05$; see Figure 32E]. The relationship between R_N and $I_{threshold}$ was supported by the strong correlation between the two

measurements ($r = -0.79$, $p < 0.0001$; see Figure 32F). Furthermore, the number of spikes evoked by depolarizing current was strongly correlated with both R_N ($p < 0.05$; see Figure 32G) and $I_{threshold}$ ($p < 0.001$). Moreover, the changes in R_N and $I_{threshold}$ were only observed in conditioned rats but not in pseudoconditioned rats (see Table 9 for other membrane properties that were not changed by conditioning), suggesting they are learning-specific. Thus, these data suggest that trace fear conditioning suppresses the intrinsic excitability of PL-BLA projection neurons through modulating ion channels that affect R_N and $I_{threshold}$.

Correlations between behavioral performance and intrinsic excitability after conditioning and extinction

We have previously reported that the amount of conditioned fear was significantly correlated with intrinsic excitability of hippocampal neurons in conditioned but not pseudoconditioned rats (Song *et al.*, 2012). We therefore examined if such correlations also exist in mPFC neurons after trace fear conditioning and extinction. As shown in Figure 33A, in IL, a significant correlation between the behavioral performance (percent freezing) and intrinsic excitability was only observed in trace fear conditioned group but not in any other groups or when all groups were combined. In contrast, in PL a significant correlation was only observed in extinction group, but not in any other groups or when all groups were combined (see Figure 33B). Thus, these data suggest that activity of regular spiking IL-BLA projection neurons is critical for the expression of conditioned fear memory whereas the activity of regular spiking PL-BLA projection neurons is critical the expression of extinction memory.
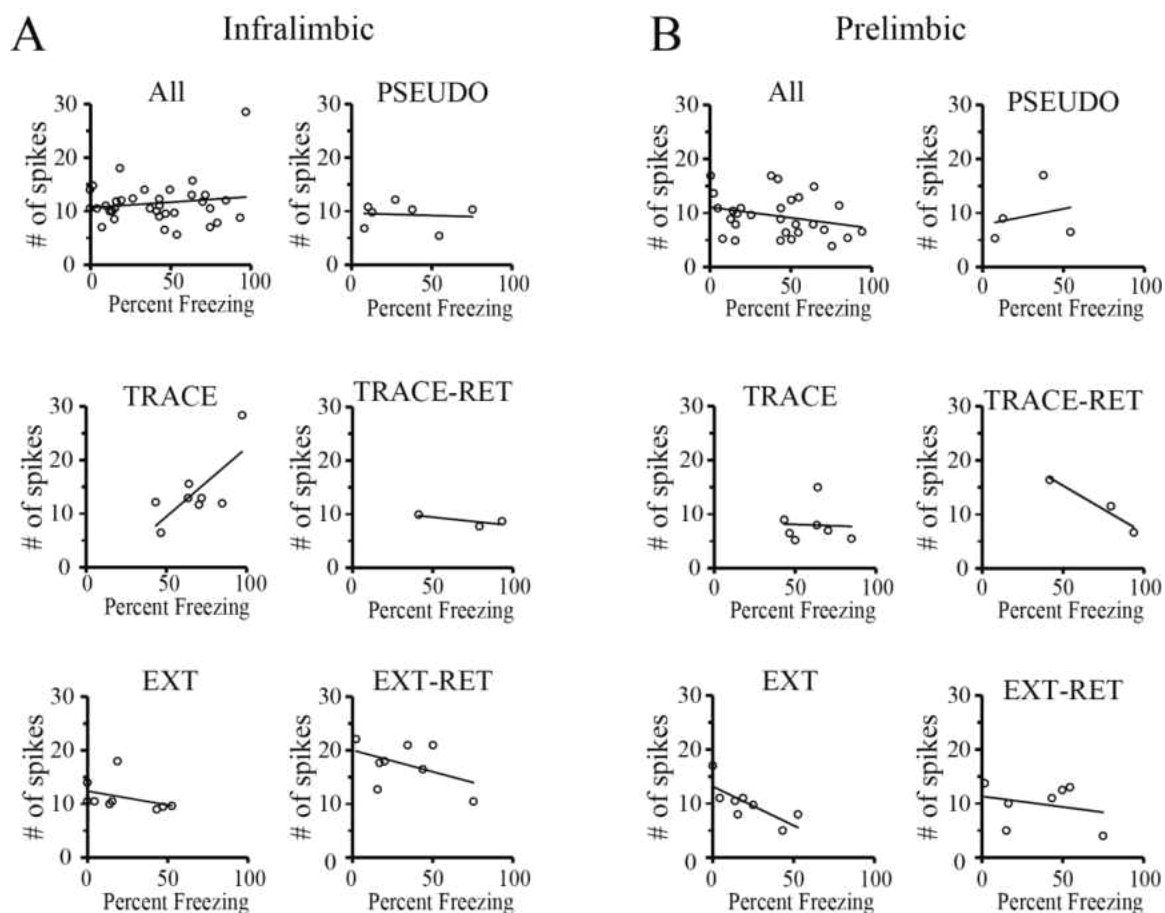
Figure 33. Correlations between behavioral performance and intrinsic excitability of regular spiking mPFC-BLA projection neurons. A, In IL, a significant correlation was observed in trace conditioned rats (TRACE; $r = 0.73$, $p < 0.05$) but not in any other groups or when all groups combined together. B, In PL, a significant correlation was observed in the rats that received extinction (EXT; $r = -0.72$, $p < 0.05$) but not any other groups. p values for other groups in A, All 0.40; PSEUDO 0.84; TRACE-RET 0.45; EXT 0.33; EXT-RET 0.25. p values that were not significant in B, All 0.15; PSEUDO 0.75 TRACE 0.92; TRACE-RET 0.16; EXT-RET 0.57.

Trace fear conditioning enhances the intrinsic excitability of bursting PL-BLA projection neurons

Neurons that generated two or more action potentials riding atop the $I_{threshold}$ depolarizing current in an all-or-none fashion were classified as burst spiking neurons (Connors *et al.*, 1982). A total of 30 bursting mPFC-BLA projection neurons were obtained in this study (see Figure 30B and Table 10). These represent 7% and 19% of total IL- and PL-BLA projection neurons respectively. Within IL, no burst spiking neurons were obtained from naïve or pseudoconditioned rats. Interestingly, there seems to be an increase in the percentage of burst spiking neurons following behavioral training, especially after extinction (percent burst spiking neurons in IL: TRACE, 8%; TRACE-RET, 7%; EXT, 15%; EXT-RET, 8%). No further statistics were performed in IL bursting neurons because of the small sample size. However, such a trend of increase in bursting activity following extinction is consistent with previous study within IL (Santini *et al.*, 2008). In PL, the intrinsic excitability was significantly enhanced in the neurons from conditioned rats compared to those from naïve rats (see Figure 34 and Table 10), suggesting that bursting activity is critical for the expression of conditioned fear in PL. In addition, there was a slight increase in R_N [$t(6) = 1.8, p = 0.12$; see Figure 35A] and a reduction in $I_{threshold}$ in bursting cells [$t(6) = -2.3, p = 0.059$; see Figure 35B]. Interestingly, this conditioning-induced plasticity in R_N and $I_{threshold}$ is the opposite direction with the effect on regular spiking cells. As a result, the R_N, the $I_{threshold}$ and the intrinsic excitability of bursting cells were significantly different from those of regular spiking neurons (see Figure 35C), and these phenomena were only observed in conditioned rats but not any other groups. These data suggest that trace fear conditioning differentially modulates the intrinsic excitability of regular spiking and burst spiking neurons in PL.
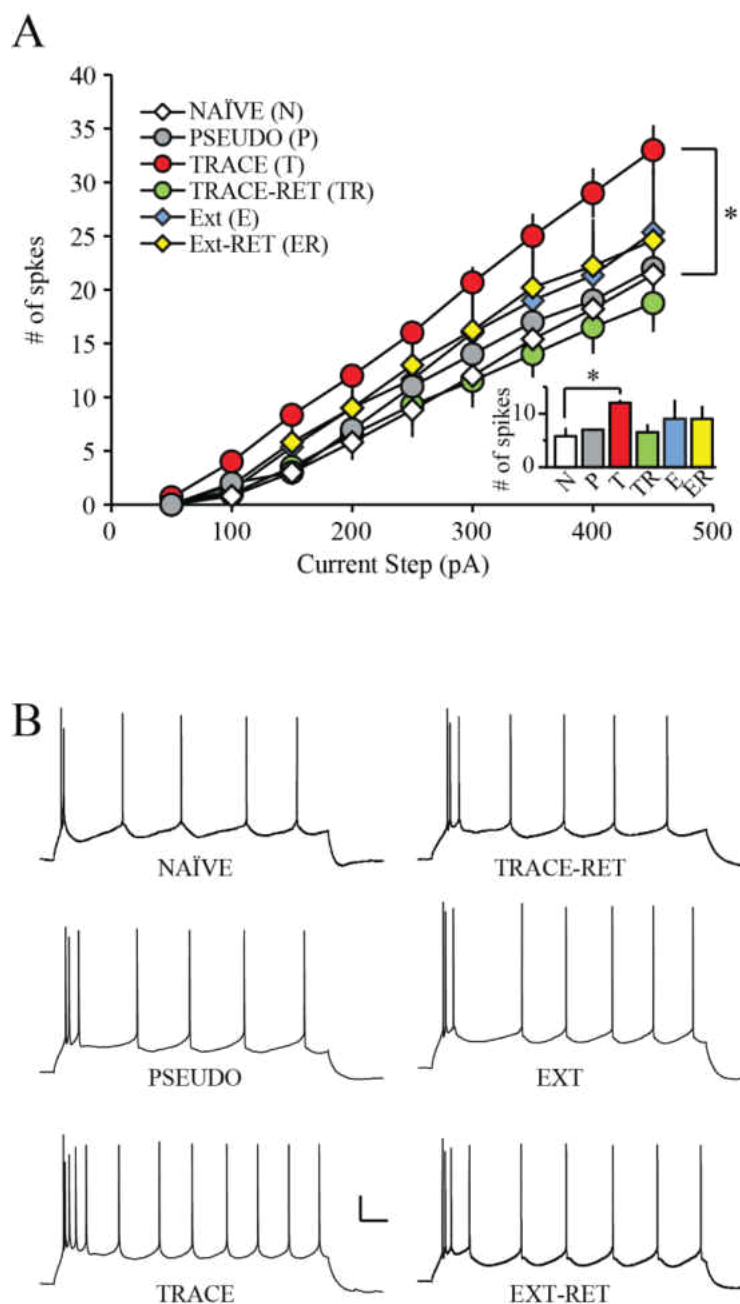
Figure 34. Trace fear conditioning enhances intrinsic excitability of burst spiking PL-BLA projection neurons. A, trace fear conditioning significantly enhanced the intrinsic excitability of burst spiking PL-BLA projection neuron [$F(1,6) = 6.1$, $p < 0.05$; repeated measures ANOVA]. *Inset*, bar graph showing the average number of spikes evoked by 200 pA depolarizing currents from all groups. Conditioning enhanced the intrinsic excitability of burst spiking PL-BLA projection neurons when compared to those from the naïve group [$F(1,6) = 7.6$, $p < 0.05$; planned comparison]. B, representative traces illustrating that PL-BLA projection neurons from trace conditioned rats fired more action potentials than neurons from naïve rats (scale bar 40 mV, 100 ms).
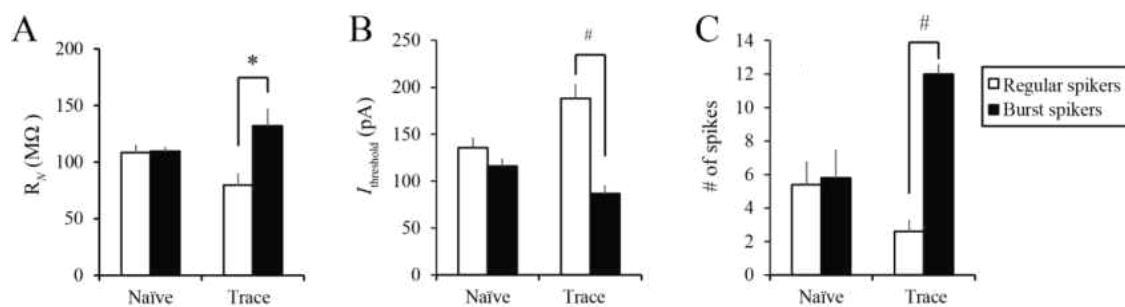
Figure 35. Differential effects of trace fear conditioning on regular and burst spiking neurons in PL. Trace fear conditioning specifically reduced the input resistance (R_N) of regular spikers but increased the R_N of burst spikers in PL (A). In contrast, trace fear conditioning increased the minimum current ($I_{threshold}$) required to evoke one action potential for regular spikers but reduced the $I_{threshold}$ for burst spikers (B). In PL, trace fear conditioning enhanced the excitability of burst spikers and decreased the excitability of regular spikers (C). All measurements (R_N, $I_{threshold}$, and number of spikes) in panels A – C were significantly different between regular spikers and burst spikers in trace conditioned rats but not naïve rats (* $p < 0.05$, # $p < 0.01$).

Table 10. Effect of trace fear conditioning on membrane properties of burst spiking IL-BLA projection neurons

Group (# of rats)	RMP (mV)	R_N (MΩ)	$I_{threshold}$ (pA)	AP_{thresh} (mV)	AP_{amp} (mV)	AP_{width} (ms)	# of spikes	mAHP (mV)	Sag (%)
IL									
NAÏVE (0)	-	-	-	-	-	-	-	-	-
PSEUDO (0)	-	-	-	-	-	-	-	-	-
TRACE (2)	-59.0 ± 3 (2)	84.7 ± 7 (2)	160 ± 40 (2)	-31.7 ± 5.4 (2)	88 ± 4 (2)	0.66 ± 0.04 (2)	2.0 (1)	-4.9 (1)	12.4 ± 8.3 (2)
TRACE-RET (1)	-62.0 (1)	79.7 (1)	180 (1)	-35.2 (1)	95 (1)	0.60 (1)	3.0 (1)	-4.3 (1)	5.4 (1)
EXT (3)	-66.3 ± 1.4 (4)	97 ± 15 (4)	133 ± 13 (4)	-34.2 ± 4 (4)	92 ± 9 (4)	0.72 ± 0.07 (4)	8.5 ± 3.4 (4)	-2.9 ± 0.4 (4)	3.5 ± 0.7 (4)
EXT-RET (2)	-59.5 ± 5.5 (2)	74 ± 33 (2)	170 ± 90 (2)	-39.1 ± 0.9 (2)	91 ± 3 (2)	0.73 ± 0.02 (2)	7.5 ± 7.5 (2)	-5.3 ± 1.7 (2)	16.1 ± 0.3 (2)
PL									
NAÏVE (4)	-66.0 ± 2.1 (5)	110 ± 4 (5)	116 ± 6 (5)	-35 ± 1.7 (5)	90 ± 3 (5)	0.66 ± 0.05 (5)	5.8 ± 1.6 (5)	-4.5 ± 0.8 (5)	8.2 ± 2.6 (4)
PSEUDO (1)	-63.0 (1)	101 (1)	120 (1)	-34.4 (1)	90 (1)	0.86 (1)	7.0 (1)	-5.0 (1)	9.7 (1)
TRACE (1)	-66.0 ± 1.2 (3)	132 ± 16 (3)	87 ± 9 (3)	-34.6 ± 0.3 (3)	93 ± 2 (3)	0.68 ± 0.04 (3)	12 ± 0.6 (3)*	-5.4 ± 0.5 (3)	8.0 ± 1.4 (3)
TRACE-RET (2)	-64.0 ± 0.9 (4)	85 ± 8 (4)	130 ± 20 (4)	-31.6 ± 0.9 (4)	80 ± 1 (4)	0.78 ± 0.02 (4)	6.5 ± 1.6 (4)	-5.4 ± 0.8 (4)	7.8 ± 1.3 (4)
EXT (3)	-60.3 ± 1.8 (3)	110 ± 106 (3)	113 ± 23 (3)	-32.9 ± 1.4 (3)	93 ± 2 (3)	0.60 ± 0.01 (3)	9.0 ± 3.6 (3)	-4.8 ± 0.4 (3)	9.4 ± 0.3 (3)
EXT-RET (4)	-66.0 ± 1.2 (5)	112 ± 10 (5)	112 ± 13 (5)	-32.5 ± 2.1 (5)	89 ± 6 (5)	0.70 ± 0.11 (5)	9.0 ± 2.5 (5)	-4.3 ± 0.3 (5)	5.3 ± 1.0 (5)

Data are mean ± SE for number of cells in parentheses. IL, infralimbic cortex; PL, prelimbic cortex; R_N, neuronal input resistance; RMP, resting membrane potential; $I_{threshold}$, threshold current required to elicit a burst of action potentials; AP_{thresh}, action potential threshold; AP_{amp}, action potential amplitude; AP_{width}, action potential half-width; mAHP, medium afterhyperpolarization. Rat groups: NAÏVE, rats that did not receive any behavioral training; PSEUDO, rats that received pseudoconditioning on day 1 and tested on day 4; TRACE, rats that received trace fear conditioning on day 1 and tested on day 4; TRACE-RET, rats that received trace fear conditioning on day 1 and tested on day 11; EXT, rats that received trace fear conditioning on day 1, extinction on days 2-3, and tested on day 4; EXT-RET, rats that received conditioning on day 1, extinction on days 2-3, and tested on day 11. AP_{amp} was relative to baseline. The mAHP was measured at the peak of the AHP following a burst of 10 APs relative to threshold. Number of spikes was counted from voltage response to a 200 pA depolarizing current injection. Statistically different from Naïve: * $p < 0.05$.

Discussion

With the combination of retrograde labeling and whole-cell patch clamp recordings, we first demonstrate that trace fear conditioning significantly affects the intrinsic excitability of mPFC-BLA projection neurons in a region-specific and cell type-specific manner. In IL, trace fear conditioning significantly enhanced the intrinsic excitability of regular spiking neurons through reducing the spike threshold and activation of h current. In PL, trace fear conditioning significantly suppressed the intrinsic excitability of regular spiking neurons whereas enhanced the intrinsic excitability of burst spiking neurons. The conditioning-induced changes in intrinsic excitability in PL were achieved through modulating the same membrane property – input resistance, but in the opposite direction – conditioning reduced the input resistance of regular spiking neurons whereas increased the input resistance of burst spiking neurons. In addition, the conditioning-induced effects were transient, and were reversed by extinction. Thus, our data suggest that within the IL, the activity of regular spiking neurons is critical for the expression of conditioned fear. In contrast, the balance between regular spiking and burst spiking neurons in PL affects the expression of conditioned fear.

Trace fear conditioning significantly affected the intrinsic excitability in a learning- and circuit-specific manner, suggesting mPFC-BLA neurons are critical for fear memory expression. These results are in agreement with previous work indicating the involvement of mPFC in the acquisition and expression of trace fear memory (Gilmartin & Helmstetter, 2010; Hylin, Orsi, Moore, & Dash, 2013; Runyan *et al.*, 2004; Sui, Wang, & Li, 2008), and that IL and PL play distinct roles (Burgos-Robles *et al.*, 2009; Burgos-Robles *et al.*, 2007; Chang & Maren, 2011; Milad & Quirk, 2002; Milad *et al.*, 2004; Vidal-Gonzalez *et*

al., 2006). These findings add to an increasing body of evidence suggesting that modulating intrinsic excitability is critical for the expression of trace fear memory (Kaczorowski *et al.*, 2012; Song *et al.*, 2012).

Trace fear conditioning enhances intrinsic excitability of IL neurons

Numerous studies have investigated the role of mPFC in fear conditioning and extinction but little is known how fear conditioning affects the intrinsic excitability of mPFC neurons. Previous studies using delay paradigm have shown that fear conditioning suppressed the intrinsic excitability of regular spiking IL neurons and that extinction revered the effect of conditioning (Santini *et al.*, 2008). This seems contradictory to the current study. However, there are a number of differences that may account for the different results. In addition to different conditioning paradigms, Santini and colleagues (1) used juvenile rats that were 25-30 days old; (2) used $KMeSO_4$-based internal solution that had 0.2 mM ATP; and (3) conducted their recordings at room temperature. Under these conditions, neurons might not be in optimal status because they only fired a maximum of 6 spikes and reached the asymptotic level in response to a 0.8-s depolarizing current, whereas single unit recordings have shown that mPFC neurons were able to spike at 10 Hz or more in response to stimuli (Febo, 2011; Ji & Neugebauer, 2012; Milad & Quirk, 2002). In contrast, we used a K-gluconate based internal solution that had 2 mM ATP and recorded from adult neurons using more physiological temperatures (32 – 35°C). Under these conditions, neurons fired more than 12 spikes in 1 s without reaching their asymptotic firing level. To validate these observations, we tried using Santini's internal solution and recorded from randomly selected neurons in IL. We found that neurons from juvenile rats (28 days old) did fire a maximum of 6 spikes in room temperature (n =5), whereas adult

neurons fired a maximum of 12 spikes in 32 – 35°C in response to the same current steps (n = 23). Thus, the different animal age and recording temperature may indeed have contributed to the different results between the current study and that of Santini's.

Another possible discrepancy is that we only recorded from L5 neurons that specifically project to the amygdala, whereas most other studies recorded neurons throughout the cortical layers without identifying their projection targets. Neurons in different cortical layers generally display distinct membrane properties, with L2/3 neurons often displaying a more hyperpolarized RMP and a relative lack of *h*-current (Boudewijns *et al.*, 2013; Mason & Larkman, 1990; Medini, 2011). Even within the same layer (e.g., L5), the mPFC neurons are highly heterogeneous in morphological and electrophysiological properties depending on their long-range projection targets (Brown & Hestrin, 2009; Dembrow *et al.*, 2010; Morishima & Kawaguchi, 2006; Otsuka & Kawaguchi, 2008). Moreover, different projection neurons may play different roles during learning. For example, a recent study demonstrated that presentation of a Pavlovian fear conditioned odor selectively activates those IL neurons that receive monosynaptic inputs from the basolateral nucleus of amygdala (Laviolette *et al.*, 2005) as well as those IL neurons that project to the nucleus accumbens but not the IL neurons that project to the contralateral mPFC (McGinty & Grace, 2008). Thus, it may be preferable to separate neurons into different layers as well as their different projection targets.

The enhanced intrinsic excitably of IL-BLA projection neurons suggests that a primary effect of IL is to facilitate fear memory expression through activation of BLA. This was supported by our observation that the behavioral performance in conditioned rats was positively correlated with intrinsic excitability. Although some discrepancies exist

(see Santini *et al.*, 2008), our IL data are in line with the results of Vouimba *et al.* (2011) showing that fear conditioning significantly enhanced the field potentials within the IL-BLA pathway and that the 24 h following conditioning these changes were positively correlated with freezing levels during the fear conditioning session. In agreement with our observations, Vouimba and colleagues have also shown that the conditioning effect diminished when the conditioned response was extinguished.

Cell type-specific effect of trace fear conditioning on PL neurons

In contrast to the enhancement in the intrinsic excitability of IL neurons, we observed a reduction in the excitability of PL regular spiking neurons after conditioning (Figure 31B). There was a negative correlation between the behavioral performance and intrinsic excitability, but this was only observed in the extinction group (see Figure 33). These results suggest that trace fear conditioning suppresses the excitability of PL-BLA neurons and that the activation of these neurons may facilitate extinction. Our observations agree with previous findings that PL lesions enhance the expression of conditioned fear and impair extinction (Morgan & LeDoux, 1995) and that fear conditioning suppresses firing activity of PL neurons during CS presentation (Garcia *et al.*, 1999; but see Burgos-Robles *et al.*, 2009; and Gilmartin & McEchron, 2005). Furthermore, it has been shown that the amount of freezing is negatively correlated with the level of firing activity after extinction, which fits well with our current data. These observations are also consistent with the reports showing that BLA stimulation predominantly inhibits PL activity (Perez-Jaranay & Vives, 1991) and that the synaptic plasticity in thalamus-PL pathway is depressed after conditioning but reversed or even potentiated after extinction (Herry & Garcia, 2002; Herry, Vouimba, & Garcia, 1999). These studies suggest that the

suppression of PL neural activity can be released by extinction, thereby reversing the conditioning effect in mPFC.

In contrast to the observed suppression of firing in regular spiking neurons, trace fear conditioning significantly enhanced the excitability of burst spiking neurons in PL (see Figure 34 and Table 10). This demonstrates a cell type-specific involvement of trace fear conditioning in mPFC neurons. Presumably these two types of neurons communicate before they send output to the amygdala because they both have axon collaterals in mPFC (see Figure 30C and 30D). It is also not known if they make synaptic connections with the same type of neurons in the BLA. Although out of the scope of the current study, answering these research questions may help to elucidate the involvement of mPFC in trace fear conditioning and extinction.

Subcellular mechanisms underlying trace fear conditioning-induced intrinsic plasticity

The current data indicate that different mechanisms underlie the conditioning-induced intrinsic plasticity in mPFC. In IL, the enhancement of intrinsic excitability in regular spiking neurons was associated with a reduction in AP threshold (see Figure 32A) and an enhancement in h current (see Figure 32B and 32C). The reduction in AP threshold is most likely caused by activation of voltage-gated sodium channels (VGSC), which underlie some forms of activity-dependent intrinsic plasticity (Ganguly, Kiss, & Poo, 2000; J. Xu, Kang, Jiang, Nedergaard, & Kang, 2005). I_h is mediated by HCN channels, which have 4 subtypes (HCN 1-4), with HCN1 and HCN2 are most abundant in mPFC (Day *et al.*, 2005). The *h*-current expressed in the mPFC-BLA projection neurons is most likely mediated by HCN2 homomers or HCN1 and HCN2 heteromers, based on the slow kinetics of the depolarizing sag (see Figure 32B) (S. Chen *et al.*, 2001). Although the functional

difference is not entirely clear, it has been well established that HCN channels are highly expressed in distal dendrites (Lorincz *et al.*, 2002; Magee, 1998) and are critical for coincidence detection (I. Pavlov *et al.*, 2011) that may underlie associative learning such as classical fear conditioning (Johnson, Ledoux, & Doyere, 2009), and cortical rhythmic oscillation during slow wave sleep, which potentiates memory consolidation (Luthi & McCormick, 1998; Marshall, Helgadottir, Molle, & Born, 2006; McCormick & Pape, 1990).

In PL, we found that input resistance was the primary modulator that influenced experience-dependent changes in neuronal intrinsic excitability. Our data demonstrated that after trace fear conditioning, input resistance was reduced in regular spiking but increased in burst spiking PL neurons. As a consequence, the intrinsic excitability was reduced in regular spiking neurons but enhanced in burst spiking neurons, such that the burst spiking neurons were significantly more excitable than regular spiking neurons (see Figure 35C). The activity-dependent modulation of input resistance has been observed in granule cells following high frequency stimulation of Mossy fiber in cerebellum (Armano, Rossi, Taglietti, & D'Angelo, 2000) and in amygdala neurons following fear conditioning (Rosenkranz & Grace, 2002). In both cases, the increase in input resistance significantly enhanced the intrinsic excitability, suggesting that modulating intrinsic excitability is one mechanism that underlies learning and memory.

Conditioning-induced plasticity is learning-specific, transient and flexible

The transient feature of learning-induced enhancement of intrinsic excitability suggests that some regulatory process exists for restoring excitability to the normal baseline state, such that the intrinsic excitability of cortical neurons remains largely constant. Such

transient learning-induced enhancement intrinsic plasticity has been observed in hippocampal CA1 and CA3 neurons following trace eyeblink conditioning (Moyer *et al.*, 1996; Thompson *et al.*, 1996a; Zelcer *et al.*, 2006). However, one difference between hippocampus and mPFC is that hippocampus is not required for long-term memory retrieval (Kim *et al.*, 1995; Kim & Fanselow, 1992) whereas long term conditioned fear is significantly attenuated when mPFC is inactivated during the memory retrieval (Blum *et al.*, 2006). Thus, an alternative mechanism that does not require the enhanced intrinsic excitability may exist during long-term memory retrieval. Elucidating such mechanism will be a great interest for future studies.

In the current study, we found that the intrinsic excitability and other membrane properties from extinction or extinction-retention rats were comparable to naïve levels, suggesting extinction reversed the effect of conditioning. This is consistent with a previous study by Baeg and colleagues (2001) who used single-unit recordings and showed that more than 70% of mPFC (both IL and PL) neurons were responsive to the CS during conditioning, and that some neurons showed an increase (44%) whereas others showed a decrease (55%) in firing rate to the CS. Although it is not clear whether or not the different responding cells were located in different subdivisions of mPFC, all the changes diminished following extinction training, suggesting that extinction reversed the conditioning-induced plasticity. Furthermore, these results are also consistent with morphological studies showing that extinction reverses conditioning-induced plasticity in spine density (Lai *et al.*, 2012; Vetere *et al.*, 2011). However, these results seem to support the view that extinction involves an "unlearning" process, which doesn't agree with the hypothesis that extinction involves a new learning to inhibit the acquired CR (Barrett *et*

al., 2003; Bouton, 1993; I. P. Pavlov, 1927; Quirk, 2002; Rescorla, 2001). In fact, there is evidence showing that extinction involves a subset of mPFC neurons that are only activated during extinction memory recall but not during conditioning (Milad & Quirk, 2002). Thus, it is likely that both mechanisms (unlearning and new learning) coexist in mPFC and may underlie the acquisition and retention of extinction memory.

Conclusions

The current data manifest a complicated effect of trace fear conditioning on mPFC-BLA projection neurons, in an area- and cell type-specific manner. Specifically, trace fear conditioning enhanced the intrinsic excitability of regular spiking projection neurons in IL. Whereas in PL, trace fear conditioning suppressed the intrinsic excitability of regular spiking neurons but enhanced the intrinsic excitability of bursting neurons. In both IL and PL, the conditioning effects were learning-specific, transient (lasted up to 10 days) and reversed by extinction.   In addition, the behavioral performance was significantly positively correlated with intrinsic excitability of IL neurons after conditioning, whereas negatively correlated with intrinsic excitability of PL neurons after extinction. These data suggest that the overall function of IL-BLA projection neurons is to facilitate fear expression whereas the function of PL-BLA projection neurons is to inhibit trace conditioned fear.

CHAPTER FIVE: effect of delay fear conditioning and extinction on intrinsic excitability of mPFC neurons

Abstract

It has been established that the activity of medial prefrontal cortex (mPFC) is critical for fear memory expression through its reciprocal interaction with the amygdala. Two subregions that are critical for fear conditioning and extinction are the infralimbic (IL) and prelimbic (PL) cortices. In experiment 4 we observed that acquisition of trace fear conditioning enhanced the intrinsic excitability of IL-BLA projection neurons but suppressed the PL-BLA projection neurons in a time-dependent manner, whereas extinction reversed the conditioning effect. Although these results are in line with some earlier *in vivo* studies (Laviollette 2005; McGinty 2008), they seem to be contradictory to the report that acquisition of delay fear conditioning suppresses the intrinsic excitability of IL neurons from juvenile rats (Santini 2008). To determine whether these conflicting results are due to differences between trace and delay fear conditioning paradigms, we performed whole-cell patch-clamp recordings from brain slices of adult rats that were naïve, delay fear conditioned, or delay fear conditioned-extinguished. Analysis of data from 125 regular spiking neurons (71 IL, 54 PL) indicated that acquisition of delay fear conditioning significantly enhanced intrinsic excitability of IL neurons ($p < 0.05$). The excitability was still high following extinction but not significantly different from Naïve. In addition, fear conditioning was associated with an enhancement of hyperpolarization-activated current (I_h; $p < 0.05$), which remained high after extinction ($p < 0.01$). Thus, delay fear conditioning enhanced the intrinsic excitability and I_h of randomly selected IL neurons, which are consistent with our observations following trace fear conditioning. We

conclude that in adult rats fear conditioning enhances intrinsic excitability of IL neurons following both delay and trace fear conditioning. Thus, these data rule out differences between the delay and trace fear paradigm as a factor contributing to the discrepancies between our data and those of Santini *et al.* (2008).

Introduction

The medial prefrontal cortex is critical for emotional responses, especially for the recall of conditioned fear memory (Corcoran & Quirk, 2007). In experiment 4, we observed that trace fear conditioning enhanced the intrinsic excitability of IL-BLA projection neurons but suppressed PL-BLA projection neurons in a timely manner, whereas extinction reversed the conditioning effect in both IL and PL. These data suggest that activation of IL-BLA pathway facilitates the expression of conditioned fear whereas activation of PL-BLA pathway facilities extinction. These observations are consistent with other studies showing that the spontaneous activity in PL neurons are negatively correlated with percent freezing during fear memory recall (Garcia *et al.*, 1999), and that a low dose infusion of GABA(A) agonist muscimol into PL facilitated extinction (Akirav, Raizel, & Maroun, 2006). In IL, *in vivo* recordings have also revealed that presenting the rats with a fear conditioned odor enhances the spontaneous activity of not only IL neurons that receive monosynaptic inputs from BLA (Laviolette *et al.*, 2005) but also the IL neurons that project to the nucleus accumbens (McGinty & Grace, 2008). These results also agree with more recent data showing that fear conditioning enhances the field potential within the IL-BLA pathway whereas extinction reverses this conditioning effect (Vouimba & Maroun, 2011). Although our observations are consistent with these studies in both IL and PL neurons, there are a number of studies showing contradictory results. For example, data from Quirk lab suggests that activation of PL facilitates the expression of conditioned fear (Burgos-Robles *et al.*, 2009; Corcoran & Quirk, 2007; Vidal-Gonzalez *et al.*, 2006) whereas activation of IL inhibits fear expression (Chang & Maren, 2011; Milad & Quirk, 2002; Milad *et al.*, 2004). These data also fit with their observations that acquisition of fear

conditioning suppressed the intrinsic excitability of IL neurons whereas extinction reversed the conditioning-induced effect (Santini & Porter, 2010; Santini *et al.*, 2008). Several critical differences between these studies and our data included their use of a delay paradigm, their use of a potassium methylsulfate recording solution, their use of room temperature recordings, and their use of juvenile rats (postnatal day 25 to P30; see also discussion in Chapter 4). Thus, the aim of the present study was to investigate how delay fear conditioning and extinction affect the intrinsic excitability of randomly selected mPFC neurons in adult rats.

Methods

Subjects. Subjects were 12 adult male Sprague-Dawley rats (3.5 – 4.2 mo). One additional juvenile Sprague-Dawley rat (27 day old) was used to compare the effect of internal solution on intrinsic excitability. Rats were maintained in an Association for Assessment and Accreditation of Laboratory Animal Care (AAALAC) accredited facility on a 14 h light–10 h dark cycle and housed individually with free access to food and water. All adult rats were handled at least one week prior to experiments. Procedures were conducted in accordance with the University of Wisconsin-Milwaukee animal care and use committee (ACUC) and NIH guidelines.

Apparatus. Delay fear conditioning were conducted in a Plexiglas and stainless steel chamber (30.5 X 25.4 X 30.5 cm; Coulbourn Instruments, Whitehall, PA), located in a sound-attenuating box. The chamber had a standard grid floor consisting of 26 parallel steel rods (5 mm diameter and 6 mm spacing). The floor was connected to a precision adjustable shock generator (Coulbourn Instruments) for delivery of a scrambled footshock US. Within the sound-attenuating box, a ventilation fan produced a constant background

noise of about 58 dB (measured by a sound level meter, A scale; model #33-2050, Realistic, Fort Worth, TX). The chamber was illuminated by a miniature incandescent white lamp (28V, type 1819) and was wiped with soap prior to each training session. During training, the room lights were left on (illumination 20.9 lux) for the entire session.

Fear conditioning and extinction. The behavioral procedure was modified from the study of Santini *et al* (2008). Rats were randomly assigned to naïve (NAÏVE, n = 4), conditioned (COND, n = 4), and conditioned-extinguished (EXT, n = 4). On day 1, COND and EXT rats received one 4-trial session of *auditory delay fear conditioning* using a 30 s CS (4 kHz tone with an intensity of 80 dB) and a 1 s footshock US (0.5 mA). A long (5.2 min ± 20 %) intertrial interval was used to maximize CS and minimize context (i.e., training chamber) conditioning (Detert *et al.*, 2008). On day 2, COND rats remained in their home cages whereas EXT rats were returned to the conditioning chamber and received one 10-trial session of CS-alone presentations with intertrial interval of 2 ± 20% min. Following the extinction session, rats were returned to their home cages 2 min after the last extinction trial.

Behavioral testing. On day 3, both COND and EXT rats were returned to the conditioning chamber where they received a brief CS session in the conditioning context. After a 2 min baseline, rats received 2 CS-alone presentations and were removed 2 min later. To assess memory, the amount of time spent freezing during the baseline and the CS was measured. Naïve rats also received the CS-alone presentations although they didn't receive conditioning on day one. Figure 36A and 36B illustrates the conditioning protocol and experimental procedure.

Analysis of behavioral data. A remote CCTV video camera (model #WV-BP334; Panasonic Corp., Suzhou, China), mounted to the top of each behavioral chamber, was used to record the activity of each rat during training and testing. The video data were fed to a PC running FreezeFrame 2.04. Data were analyzed using FreezeView 2.04 (Actimetrics Software, Coulbourn Instruments) where a 1-sec bout of immobility was scored as freezing. Freezing is defined as the absence of all movement except that required for respiration (Blanchard & Blanchard, 1969).

Slice preparation. Brain slices containing PFC were prepared within 1 h following the test session by an individual blind to training condition. Rats were deeply anesthetized with isoflurane and decapitated. The brains were quickly removed and placed in ice-cold oxygenated (95% O_2/5% CO_2) aCSF (composition in mM: 124 NaCl, 2.8 KCl, 1.25 NaH_2PO_4, 2 $MgSO_4$, 2 $CaCl_2$, 26 $NaHCO_3$, and 20 dextrose, pH 7.4). The brain was then blocked and coronal prefrontal brain slices (300 µm) were cut in aCSF at ~ 0°C aCSF using a vibrating tissue slicer (VT1200, Leica). Slices were then transferred to a holding chamber (Moyer *et al.,* 1996) containing oxygenated aCSF at 32-36°C.

Electrophysiological recordings. For experiments, slices were transferred to a submerged recording chamber mounted on an Olympus BX51WI upright microscope where they were perfused with oxygenated aCSF at a rate of 2 ml/min (maintained at 32-36°C using an inline temperature controller). Neurons were visualized with infrared differential video interference microscopy, and WCRs were obtained under visual guidance from the soma of layer 5 pyramidal neurons located in either the IL or PL subregions of the mPFC (Paxinos & Watson, 1998). For WCRs, electrodes (5–8 MΩ) were prepared

A

CS ⎯⎯⎯⎯⎯⌐‾‾‾‾‾‾‾‾‾‾‾‾‾‾‾‾‾‾⌐⎯⎯⎯⎯⎯⎯⎯⎯⎯
        30 s

US ⎯⎯⎯⎯⎯⎯⎯⎯⎯⎯⎯⎯⎯⎯⎯⎯⎯⎯⎯⎯⎯⌐⌐⎯⎯⎯⎯⎯⎯⎯
                              1 s

B

Groups	Day 1 CONDITIONING →	Day 2 EXTINCTION →	Day 3 TEST
NAÏVE	–	–	CS probe ↓
COND	4 CS-US	–	CS probe ↓
EXT	4 CS-US	10 CS alone	CS probe ↓

C
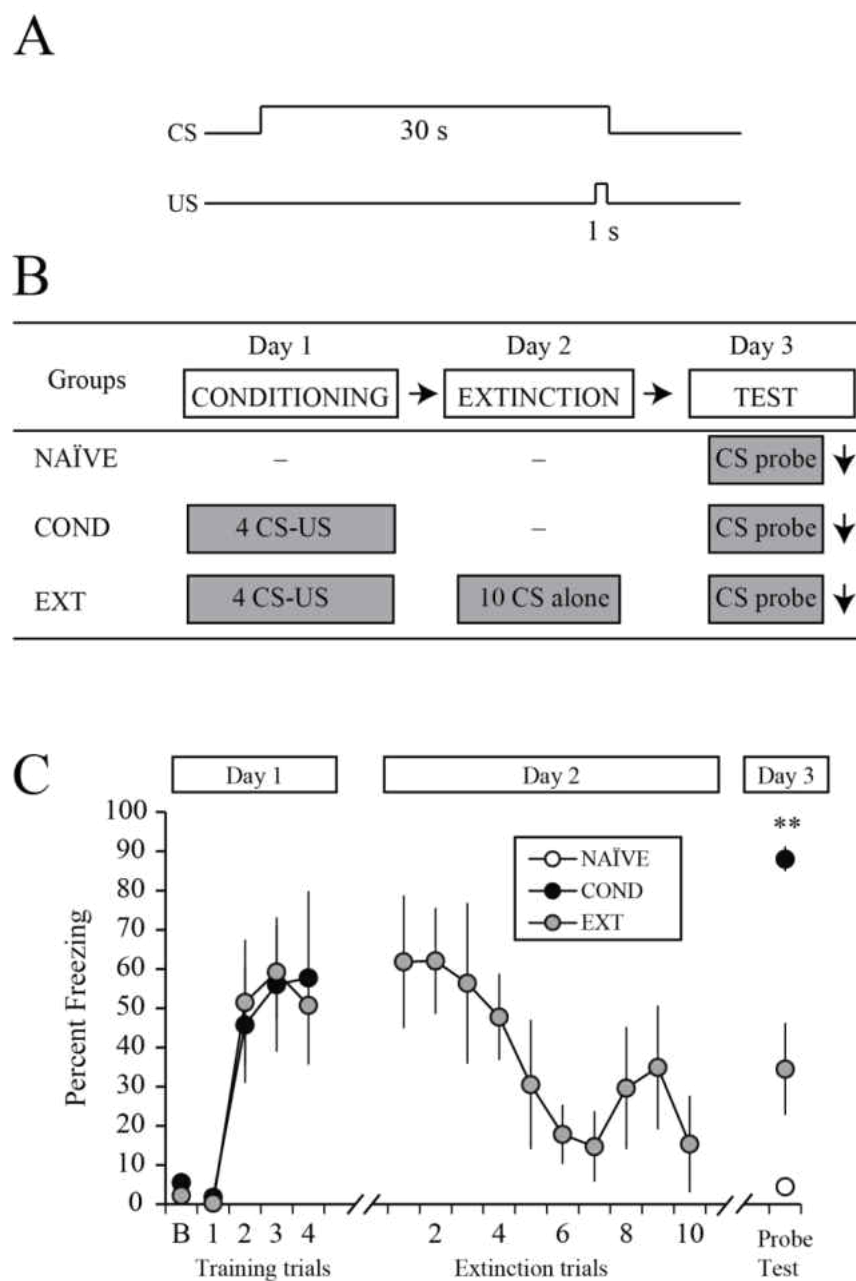
Figure 36. Experimental design and behavioral performance during delay fear conditioning, extinction, and probe test. A, Behavioral paradigm used in the current study. The conditioning consists a 30-s tone (CS) co-terminated with a 1-s footshock (US). B, Experimental design. On day 1, the COND and EXT rats received one 4-trial session of delay fear conditioning (mean ITI = 5.2 min). On day 2, EXT rats received one 10-trial session of extinction in the same context where they received conditioning. NAÏVE rats remained in their homecages without receiving any stimuli. On day 4, all rats received 2 CS-alone presentations to test memory. C, Percent freezing during conditioning, extinction and probe test. During the probe test, COND rats froze significantly more than both EXT ($p < 0.05$) and NAÏVE ($p < 0.01$) rats.

from thin-walled capillary glass and filled with the following solution (in mM): 150

$KMeSO_3$, 10 KCl, 0.1 EGTA, 10 HEPES, 0.3 GTP, and 0.2 ATP, pH 7.3 (292 mOsmol).

All recordings were obtained in current-clamp mode using a HEKA EPC10 amplifier

system (HEKA Instruments Inc. Bellmore, New York). Experiments were controlled by

PatchMaster software (HEKA Instruments) running on a PC. All electrodes were pulled

from thin-walled capillary glass (A-M Systems, Carlsborg, WA) using a Sutter Instruments

P97 puller. Cells were held at -67 mV by manually adjusting the holding current. The

electrode capacitance and series resistance (Rs) were monitored, compensated, and

recorded frequently throughout the duration of the recording. In some experiments, the

recording pipettes were filled with K-gluconate based solution (composition in mM: 110

K-gluconate, 20 KCl, 10 Di-Tris-P-Creatine, 10 HEPES, 2 $MgCl_2$, 2 Na_2ATP, 0.3 Na_2GTP,

0.2% Biocytin, pH to 7.3) to compare the effect of internal solutions on the excitability.

Intrinsic excitability studies. Neurons were recorded under current clamp using

the following protocol: (1) Voltage–current (V-I) relations were obtained by injecting a

series of 500 ms current steps (range -300 to +50 pA) and plotting the plateau voltage

deflection as a function of current amplitude. Neuronal input resistance (R_N) was

determined from the slope of the linear fit of that portion of the V-I plot where the voltage

sweeps did not exhibit sags or active conductances. The sag ratio during hyperpolarizing

membrane responses was expressed as $[(1 - \Delta V_{ss} / \Delta V_{min}) \times 100\%]$, where $\Delta V_{ss} = MP -$

Vss, $\Delta V_{min} = MP - V_{min}$, MP is the membrane potential before current step, V_{ss} is the steady-

state potential and V_{min} is the initial minimum potential. For each neuron, sag ratio was

calculated from -300 pA, -250 pA, and -200 pA current steps and averaged. (2) Postburst-

AHPs were measured by injecting 10 suprathreshold (1-3 nA for 2 ms) current injections

at 50 Hz. Post-burst AHPs were measured from somatic membrane potentials following the offset of the last current injection (3X, at 20 sec intervals). (3) Neuronal excitability was studied using a family of 1-s depolarizing current injection (from 100 to 1000 pA). For each sweep, the number of action potentials elicited were counted.

Statistical Analyses. The overall treatment effects were examined using a one-way ANOVA, or repeated measures ANOVA using IBM SPSS (version 22) whereas appropriate. For significant main effects (alpha 0.05), a Fisher's PLSD test was used for *post hoc* comparisons. All data were expressed as mean ± SEM.

Results

The current study was conducted to explore the possible factors that may have contributed to the different results observed between our trace fear conditioning data and others', especially the study by Quirk and colleagues (Santini *et al.*, 2008). We investigated whether the results of the Santini study using juvenile rats were applicable to those using adult rats by replicating their behavioral paradigm and recording methods. However, we performed whole-cell recordings in 32-36°C because it is more close to the biological state, instead of room temperature as in the Santini study. In addition, we used an internal recording solution ($KMeSO_3$-based) with which the neurons displayed comparable excitability as those from the Santini study ($KMeO_4$-based).

As shown in Figure 36C, both conditioned (COND) and conditioned-extinguished (EXT) rats displayed a rapid increase in freezing on day 1 during training [$F(2.1, 12.5) = 11.6$, $p < 0.01$; Greenhouse-Geisser corrected], but no significant difference between the two groups [$F(1,6) = 0$, $p = 0.99$]. On day 2, EXT rats showed a reduction of freezing within the extinction section (from 62% to 15%). On day 3, COND rats displayed a

significantly higher level of freezing than Ext ($p < 0.05$) and NAÏVE rats [$p < 0.01$]. These data suggest that COND rats displayed good conditioning memory whereas Ext rats displayed good extinction memory during the behavioral test.

Delay fear conditioning increased intrinsic excitability of IL neurons

To examine the effect of delay fear conditioning and extinction on the intrinsic excitability of mPFC neurons, PFC slices were prepared immediately after the behavioral test and whole-cell recordings were performed on L5 neurons in both IL and PL. Figure 37 shows the location of the neurons obtained in this study. As shown in Figure 38A, delay fear conditioning enhanced the excitability of IL neurons but only at high current intensities (0.9 – 1.0 nA; $p < 0.05$ for both values when tested with a planned two-tailed t-test). After extinction, the excitability was reduced but still higher than naïve although this effect did not reach statistical significance ($p = 0.16$ and $p = 0.06$ for 0.9 nA and 1.0 nA current injection respectively). This suggests the extinction did not completely reverse the effect of conditioning. In PL, neurons from COND rats fired a comparable number of spikes compared with those from Naïve rats. Extinction tended to reduce the excitability of PL neurons but not significantly (see Figure 38B). In addition, under our recording conditions, the Naïve neurons fired a maximum of 13 spikes in IL and 25 spikes in PL. This is in stark contrast to the maximum of 5 spikes in IL and 6 spikes in PL in the Santini study (see Figure 2 of Santini *et al.,* 2008).

Delay fear conditioning enhanced depolarizing sag in IL neurons

We observed an enhancement of depolarizing sag in IL-BLA projection neurons following trace fear conditioning in Chapter 5. Consistent with this, analysis of sag ratio

PL

IL

Bregma: + 3.2

+2.7
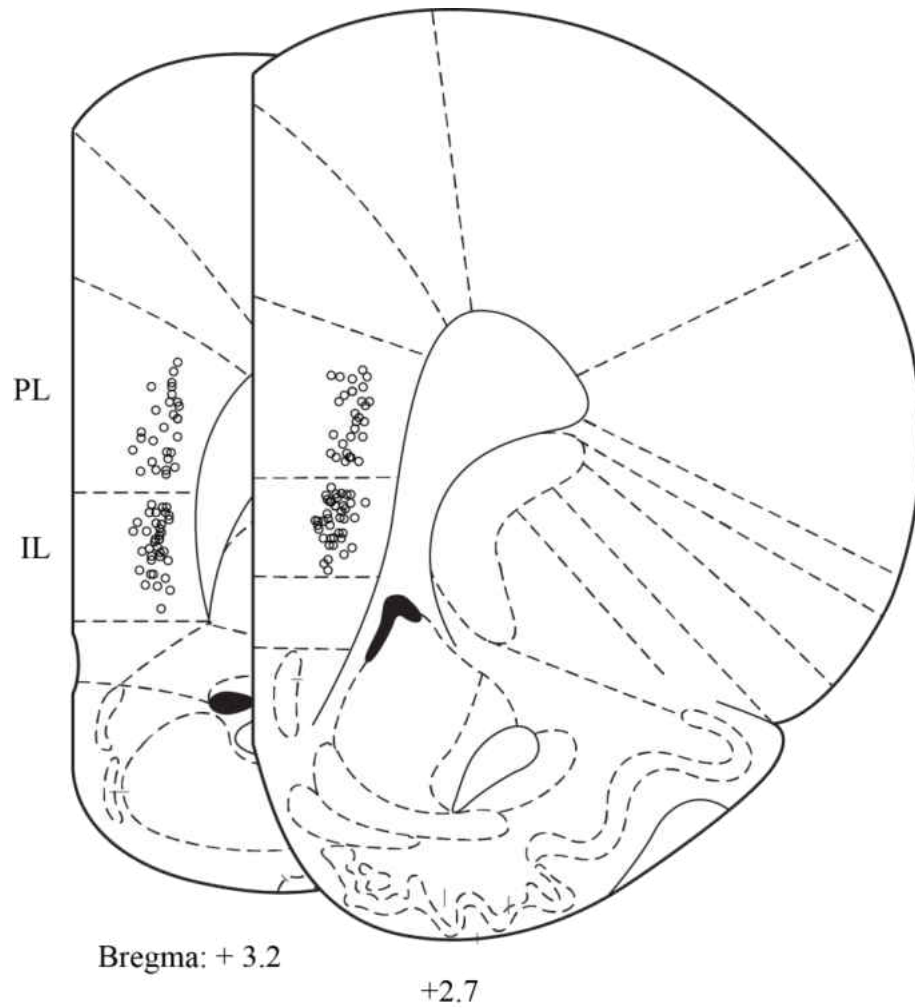
Figure 37. Location of L5 pyramidal neurons obtained in mPFC following delay fear conditioning and extinction. The location of each recorded neuron was obtained from a snapshot taken after each experiment and indicated as individual circles in brain stereotaxic atlases (Paxinos & Watson, 1998). Only regular spiking neurons in layer 5 were studied.
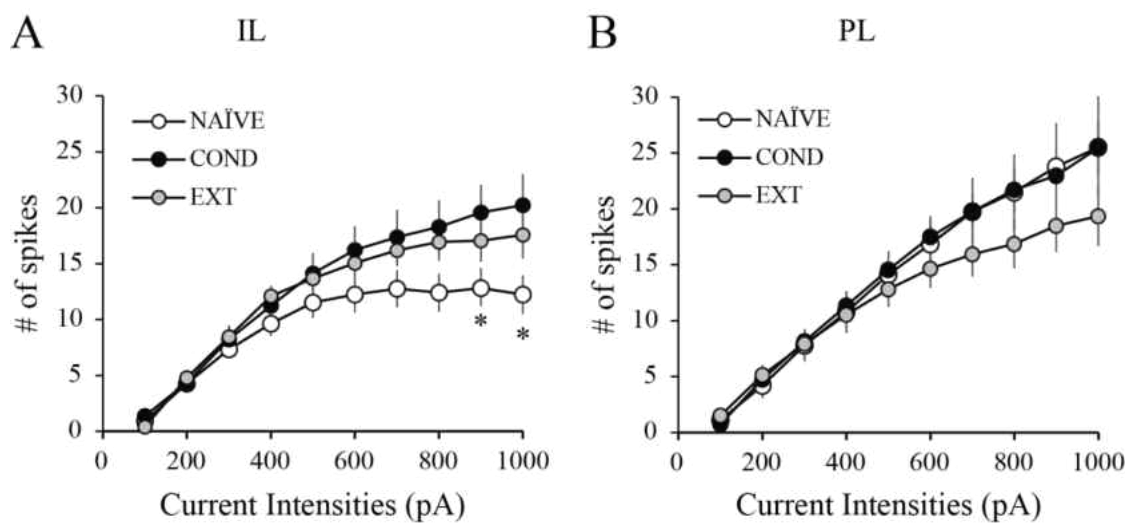
Figure 38. Effect of acquisition and extinction of delay fear conditioning on the intrinsic excitability of mPFC neurons. A, acquisition of delay fear conditioning significantly enhanced the intrinsic excitability of IL neurons ($p < 0.05$ between COND and NAÏVE). B, acquisition or extinction of delay fear conditioning didn't significantly change the intrinsic excitability of PL neurons.

(measured from - 300 to - 100 pA current injection) with a one-way ANOVA followed by *post hoc* test indicated that delay fear conditioning significantly enhanced the sag ($p <$ 0.01), which was still larger than naïve neurons following extinction ($p < 0.05$; see Figure 39A). In PL, the sag was not significantly changed after conditioning or extinction (see Figure 39B). Other membrane properties such as input resistance and AP characteristics were not significantly changed following conditioning or extinction (see Table 11).

Neurons recorded with KMeO$_3$-based internal solution are less excitable than those recorded using a K-gluconate based internal solution

We next examined whether the different pipette solution and animal age could account for the differential excitability of mPFC neurons observed between the current study and that of Santini and colleagues (2008). We recorded from L5 IL neurons from a juvenile rat (27d old) in room temperature ($\sim 22°C$) and compared the excitability between neurons obtained using either a KMeSO$_3$-based or a K-Gluconate-based internal solution. As shown in Figure 40, neurons are much more excitable when recordings were made using a K-Gluconate (a maximum of 15 ± 3 spikes, n = 2) rather than a KMeSO$_3$-based internal solution (a maximum of 5 ± 1 spikes, n = 5), and these differences were statistically significant (repeated measures ANOVA; $F(1,5) = 37.9$, $p < 0.01$, followed by an independent *t*-test where $p < 0.01$ for all values of 150 – 400 pA current steps. Thus, the excitability of neurons recorded with a K-Gluconate-based solution matches our study of trace fear conditioning in Chapter 4 and that the excitability of neurons recorded using KMeSO$_3$-based solution matches that of the Santini *et al.*, 2008 study. .
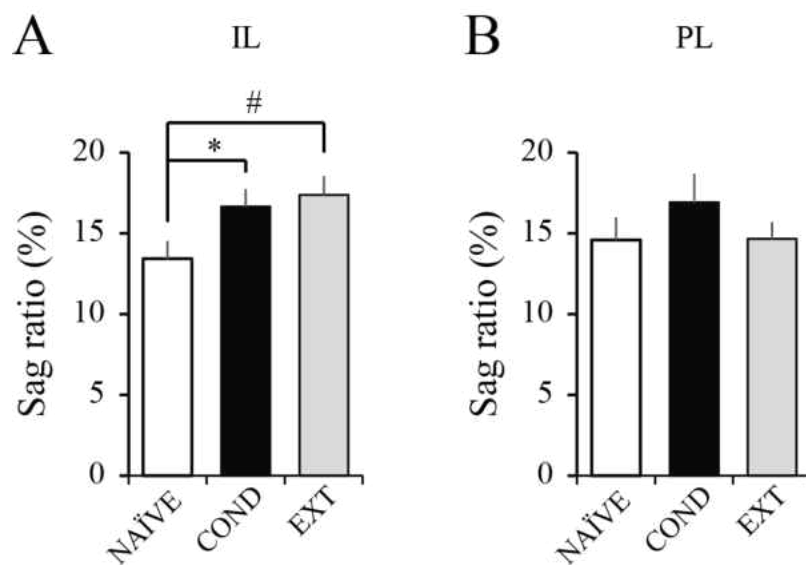
Figure 39. Acquisition of delay fear conditioning significantly enhanced depolarizing sag in IL (A) but not in PL (B) neurons. The voltage sag ratio in response to hyperpolarizing currents was calculated as the peak voltage deflection divided by the amplitude of the steady-state voltage deflection. In IL, the sag ratio was significantly increased in neurons from COND and EXT rats compared to neurons from NAÏVE rats (* $p < 0.05$, # $p < 0.01$).
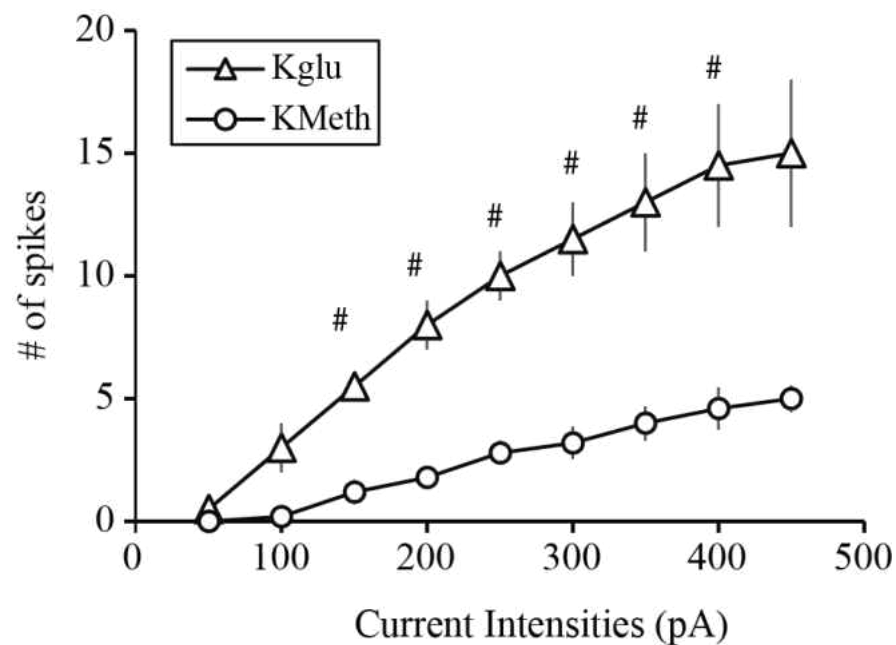
Figure 40. Effect of internal solutions on intrinsic excitability of mPFC neurons. Intrinsic excitability was evaluated in neurons from a young (27-d old) rat with K-gluconate (Kglu)-based and $KMeSO_3$ (KMeth)-based internal solutions at room temperature ($\sim 22°C$). Neurons recorded with a Kglu-based internal solution were more excitable than neurons recorded with a KMeth-based internal solution (# $p < 0.01$).

Table 11. Effect of delay fear conditioning on membrane properties of mPFC neurons

	RMP (mV)	R_N (MΩ)	$I_{threshold}$ (pA)	AP_{thresh} (mV)	AP_{amp} (mV)	AP_{width} (μs)	mAHP (mV)	sAHP (mV)	Number of spikes	Sag (%)
IL										
NAÏVE	-63.3 ± 0.9 (21)	110 ± 8 (21)	133 ± 10 (21)	-34.3 ± 0.7 (21)	79.2 ± 1.8 (21)	767 ± 33 (21)	-6.1 ± 0.4 (21)	-1.0 ± 0.1 (21)	12.2 ± 1.7 (17)	13.4 ± 1.1 (19)
COND	-62.4 ± 0.6 (28)	115 ± 9 (28)	154 ± 15 (27)	-33.0 ± 0.7 (27)	79.4 ± 2.2 (27)	843 ± 57 (27)	-5.9 ± 0.2 (27)	-0.8 ± 0.1 (27)	20.2 ± 2.8 (21)*	16.7 ± 1.1 (23)*
EXT	-62.6 ± 0.7 (22)	93 ± 7 (22)	151 ± 10 (22)	-35.2 ± 0.8 (22)	80.9 ± 2.1 (22)	747 ± 39 (22)	-5.1 ± 0.3 (22)	-0.6 ± 0.1 (22)	17.6 ± 2.1 (17)	17.4 ± 1.1 (20)#
PL										
NAÏVE	-65.4 ± 1.1 (14)	77 ± 10 (14)	181 ± 30 (14)	-36.5 ± 1.1 (14)	89.2 ± 2.1 (14)	623 ± 22 (14)	-5.9 ± 0.4 (14)	-0.8 ± 0.1 (14)	25.7 ± 4.6 (13)	14.6 ± 1.4 (14)
COND	-63.7 ± 0.8 (21)	83 ± 7 (21)	184 ± 23 (20)	-35.0 ± 0.7 (20)	87.3 ± 1.8 (20)	694 ± 27 (20)	-5.8 ± 0.2 (20)	-0.7 ± 0.1 (20)	25.6 ± 2.5 (16)	16.9 ± 1.8 (18)
EXT	-63.5 ± 0.7 (19)	92 ± 8 (19)	132 ± 10 (18)	-34.9 ± 0.7 (18)	84.6 ± 1.8 (18)	697 ± 26 (18)	-5.8 ± 0.3 (19)	-0.8 ± 0.1 (19)	19.4 ± 2.7 (16)	14.7 ± 1.0 (16)

Data are mean ± SE for number of cells in parentheses. IL, infralimbic cortex; PL, prelimbic cortex; R_N, neuronal input resistance; RMP, resting membrane potential; $I_{threshold}$, threshold current required to elicit an action potential; AP_{thresh}, action potential threshold; AP_{amp}, action potential amplitude; AP_{width}, action potential half-width; mAHP, medium afterhyperpolarization; sAHP, slow afterhyperpolarization. Rat groups: NAÏVE, rats that did not receive any behavioral training; COND, rats that received delay fear conditioning on day 1 and tested on day3; EXT, rats that received delay fear conditioning on day 1, extinction on day 2, and tested on day 3. The mAHP was measured at the peak of the AHP following a burst of 10 APs relative to baseline. Number of spikes was counted from voltage response to a 1-nA depolarizing current injection for 1 s. Statistically different from Naïve:*, $p < 0.05$; #, $p < 0.01$.

Discussion

We performed whole-cell patch-clamp recordings from naïve rats, or behaviorally characterized rats that received either conditioning or conditioning followed by extinction. Our data indicated that delay fear conditioning significantly enhances the intrinsic excitability of IL neurons. Although the excitability remained high after extinction, it was not significantly different from that of naïve neurons. Delay fear conditioning also significantly increased I_h, which remained high following extinction. In contrast, delay fear conditioning and extinction did not significantly affect the intrinsic excitability or I_h in PL neurons.

The current observations that delay fear conditioning enhances intrinsic excitability of IL neurons and activation of I_h are consistent with our data from IL-BLA projection neurons following trace fear conditioning. However, the effect on the delay conditioning is weaker compared with trace conditioning because it was only observed when the neuron reached its asymptotic level of firing, which occurred at higher current injections (e.g., 0.9 − 1.0 nA for 1 s). In contrast, in experiment 4 we observed a strong conditioning-induced enhancement of intrinsic excitability in IL-BLA projection neurons even when the neurons received a moderate level of stimulation (e.g., 200 − 400 pA for 1 s), which was not sufficient to saturate its firing capability (see Figure 32A). Thus, it is likely that a strong activation of IL neurons is not required for acquisition of delay fear conditioning, which agrees with previous reports (Lebron *et al.*, 2004; Quirk *et al.*, 2000). Another possible explanation is the heterogeneity of the randomly recorded neurons. It has been shown that the pyramidal neurons in mPFC have distinct electrophysiological properties depending on their long-range projection targets (Dembrow *et al.*, 2010) and are modified differently

following fear conditioning. For example, olfactory fear conditioning specifically enhances the spontaneous activity of IL neurons that receive monosynaptic inputs from the BLA (Laviolette *et al.*, 2005) and IL neurons that project to the nucleus accumbens but not the neurons that project to the contralateral mPFC (McGinty & Grace, 2008). In contrast neurons that do not have direct connection with nucleus of accumbens or BLA are not changed or even suppressed by fear conditioning (Laviolette *et al.*, 2005; McGinty & Grace, 2008). This agrees with our current observation that a small effect of delay fear conditioning occurred on randomly selected mPFC neurons.

At first glance, our results seem contradictory with an earlier study by Santini *et al.* (2008). This previous study reported that acquisition of delay fear conditioning significantly reduced the intrinsic excitability of randomly selected IL neurons whereas extinction reversed the conditioning effect. However, as was discussed in Chapter 4, there are many differences between our study and that of Santini and colleagues (2008). Although we have tried to match some of their experimental protocol (e.g., animal strain, fear conditioning paradigm, and pipette internal solution), there are still other differences (e.g., animal age, recording temperature, and recording procedure) that may have contributed to the dramatically different results.

One dramatically different result between the current and that of Santini *et al.* (2008) is the baseline excitability of mPFC neurons. In the Santini *et al.* 2008 study, both IL and PL neurons obtained from juvenile rats fired a maximum of 6 spikes in response to 0.8 s current injections. In contrast, in our current study, the IL neurons obtained from naïve rats fired a maximum of 13 spikes in response to 1-s depolarizing current injections. This difference is most likely caused by the different animal age and recording temperature

because we have demonstrated that IL neurons were much less excitable (fired a maximum of 5 spikes) when recorded from a young rats at room temperature (see Figure 40). Thus, the different results observed between our trace fear conditioning and that of Santini are likely caused by different experiment methods.

The current study also observed that the acquisition of delay fear conditioning significantly enhanced I_h, suggesting that activation of HCN channels is critical for the maintenance of conditioned fear. This is consistent with our observation that trace fear conditioning enhanced I_h in IL-BLA projection neurons (see Figure 32B). However, unlike in the study of trace fear conditioning, extinction of delay fear conditioning didn't reverse the conditioning effect. There may be several reasons for this difference. First, in the present study the rats received one-session extinction training, which might not be enough to reverse the conditioning effect. In contrast, in our trace conditioning study the rats received a 2-session extinction training which allowed the extinction memory consolidated. Second, the present study recorded from randomly selected neurons whereas in our trace fear conditioning study only mPFC-BLA projection neurons were recorded. The different effect observed following extinction between the two studies suggests that different projection neurons are involved in the acquisition and extinction of fear conditioning. The neurons that involved conditioning (e.g., mPFC-BLA projection neurons) were reversed by extinction, whereas additional neurons were activated during extinction and were obtained by the random recordings. Third but not last, it is also possible that delay and trace fear conditioning activated the mPFC neurons differently. It is interesting to explore how these different results were generated by similar experimental

procedures. However, it is out of the scope of the current study to completely elucidate the causes of these differences.

Conclusions

Delay fear conditioning significantly enhanced the intrinsic excitability of randomly selected L5 neurons in IL but not PL in adult rats. In addition, acquisition of delay fear conditioning was associated with enhanced *h*-current in IL neurons. These data are consistent with the results from Experiment 4 that IL is critical for expression of conditioned fear memory.

CHAPTER SIX: effect of trace fear conditioning and extinction on spine density of

mPFC-BLA projection neurons

Abstract

The activation of mPFC neurons is required for both acquisition and extinction of trace fear conditioning. Such activation may involve a temporal plasticity in neuronal excitability and a long-term plasticity in synaptic circuits. In experiment 3, we have shown that trace fear conditioning and extinction differentially modulate intrinsic excitability of mPFC-BLA projection neurons. Here, we further characterized the morphological properties of these neurons and examined how trace fear conditioning and extinction affect the spine density of these neurons. We found that the spine density was significantly correlated with the somatic depth in both IL and PL ($p < 0.01$ for both IL and PL) such that neurons in superficial layers had higher spine density than those in deep layers ($p < 0.01$ for both IL and PL). In L2/3, the spine density was not significantly changed after trace conditioning or pseudoconditioning but was significantly reduced after extinction. In L5, there was a trend that conditioning increased the spine density whereas extinction and extinction-retention reduced the spine density, such that the spine density was significantly lower after extinction-retention than after conditioning. Furthermore, the reduction in spine density in IL L2/3 neurons is primarily driven by mushroom spines, whereas in PL the reduction in spine density in L2/3 neurons was primarily driven by thin spines. Thus, such subtype- and subregion-specific modulation of spine density may underlie the different roles of IL and PL in the long-term expression of conditioned fear.

Introduction

Medial prefrontal cortex (mPFC) has reciprocal innervation with the amygdala (Bacon, Headlam, Gabbott, & Smith, 1996; Gabbott *et al.*, 2005; McDonald, 1998), through which the mPFC neurons affect the acquisition, consolidation, and extinction of conditioned fear (Burgos-Robles *et al.*, 2009; Corcoran & Quirk, 2007; Marek, Strobel, Bredy, & Sah, 2013). However, the mPFC also projects to a variety of other brain regions that involve multiple cognitive functions (Gabbott *et al.*, 2005), so it is possible that different projection neurons within the mPFC are differentially modulated during fear conditioning and extinction. This has been demonstrated in a recent study showing that stimulation of BLA (or presentation of a Pavlovian fear conditioned odor) selectively activates the IL neurons that project to the nucleus accumbens but not those that project to the contralateral mPFC (McGinty & Grace, 2008). Thus, a circuit-specific study of the neurons within mPFC may be necessary to uncover the mechanisms underlying Pavlovian fear conditioning.

Fear conditioning and extinction not only involve the modulation of electrophysiological properties of cortical neurons, but they also remodel the synaptic circuits, which may underlie the long-term fear/extinction memory. For example, a recent *in vivo* photoimaging study in frontal association cortex (FrA) in live animals has shown that fear conditioning significantly eliminated existing spines in layer 5 neurons, whereas extinction reversed the conditioning effect such that the spines being eliminated during conditioning were reformed (Lai *et al.,* 2012). This indicates that modulation of spine density is critical for the formation and expression of long-term conditioned fear memory. However, little is known about how fear conditioning affects spine density in mPFC. One

previous study found that the spine density was increased following contextual fear conditioning and remained high following extinction (Vetere *et al.*, 2011). Although it has been established that the acquisition of trace fear conditioning requires the activation of mPFC (Gilmartin & Helmstetter, 2010; Gilmartin & McEchron, 2005), it is still not clear how acquisition and extinction of trace fear affects the spine density in mPFC neurons, especially the neurons that project to amygdala. Thus, the current study was carried out to investigate the effect of trace fear conditioning and extinction on spine density of mPFC-BLA projection neuron. In order to study the dendritic spines, the mPFC-BLA projection neurons were labeled with florescent microspheres (Retrobeads^{TM}), followed later by Lucifer-Yellow injection into those individual neurons.

Methods

Subjects. Subjects were 19 adult male F344 rats (3.8 ± 0.1 mo). Rats were maintained in an Association for Assessment and Accreditation of Laboratory Animal Care (AAALAC) accredited facility on a 14 h light–10 h dark cycle and housed individually with free access to food and water. All rats were handled at least one week prior to experiments. Procedures were conducted in accordance with the University of Wisconsin-Milwaukee animal care and use committee (ACUC) and NIH guidelines.

Retrobeads^{TM} infusion. All rats received unilateral pressure infusion of a fluorescent retrograde tracer (Retrobeads^{TM}, Lumafluor) into the basolateral nucleus of the amygdala (relative to Bregma, -3 mm AP, ± 5 mm ML; - 8.3 mm DV), with deep anesthetization under stereotaxic. The infusion was made with glass pipettes (20 – 40 μm) pulled from borosilicate glass (VWR Micropipets) using a Sutter Instruments P97 puller. The pipette was connected to a 2 μl syringe (Hamilton) driven by an infusion pump

(Harvard Apparatus, model 975). The infusion lasted 5-10 min and the pipette was withdrawn 10 min after infusion. A total volume of 0.1 - 0.3 µl red Retrobeads^{TM} were infused into BLA.

Apparatus. Fear conditioning chambers. Trace fear conditioning was conducted in a Plexiglas and stainless steel chamber (30.5 X 25.4 X 30.5 cm; Coulbourn Instruments, Whitehall, PA), located in a sound-attenuating box. The chamber was rectangular and had a standard grid floor consisting of 26 parallel steel rods (5 mm diameter and 6 mm spacing). The floor was connected to a precision adjustable shock generator (Coulbourn Instruments) for delivery of a scrambled footshock US. Within the sound-attenuating box, a ventilation fan produced a constant background noise of about 58 dB (measured by a sound level meter, A scale; model #33-2050, Realistic, Fort Worth, TX). The chamber was illuminated by a miniature incandescent white lamp (28V, type 1819) and was wiped with a 5% ammonium hydroxide solution prior to each training session. During training, the room lights were left on (illumination 20.9 lux) for the entire session.

Extinction and CS testing chambers. An additional Plexiglas chamber was served as a novel context for the auditory cue test. This chamber was located within a separate sound-attenuating box located in the same room. The test chamber was physically different from the training chamber in that it was octagonal (instead of rectangular), the floor was black-painted Plexiglas (instead of grid bars), and was illuminated with an infrared light. In addition, the tray below the test chamber floor contained clean bedding and the test chamber was wiped with 2% acetic acid prior to each test session to provide a different olfactory stimulus from that used during training. The room lights were turned off (illumination 0.2 lux) for the entire testing session.

Fear conditioning and extinction. After a minimum of 7 days of recovery from Retrobeads™ infusion, rats were handled for at least a week before they were randomly assigned to naïve (NAÏVE, n = 2), pseudoconditioned (PSEUDO, n = 5), trace fear conditioned (TRACE, n = 3), trace fear conditioned-extinction (EXT, n = 5), and trace fear conditioned extinction-retention (EXT-RET, n = 4) groups (see Figure. 41). On day 1, TRACE, EXT, and EXT-RET rats received one 10-trial session of *auditory trace fear conditioning* using a 15 s CS (80 dB white noise) followed by a 30 s trace interval (stimulus-free period) and a 1 s footshock US (1.0 mA). A long (5.2 min ± 20 %) intertrial interval was used to maximize CS and minimize context (i.e., training chamber) conditioning (Detert *et al.*, 2008). PSEUDO rats received the same amount of CS and US presentations but explicitly unpaired. On days 2-3, rats in TRACE and PSEUDO groups remained in their home cages, whereas EXT and EXT-RET rats received 2 consecutive sessions (1 session per day) of 10 CS-alone presentations in the extinction chamber. These sessions were identical to training except no US was presented (i.e., 15 sec white noise CS; 30 sec trace interval; 5.2 min ITI). Following each extinction session, rats were returned to their home cages 2 min after the last extinction trial.

Behavioral testing. Twenty-four hours after extinction (day 4), PSEUDO, TRACE, and EXT rats received a brief CS test session in the extinction context. EXT-RET rats received the CS test on day 11. After a 2-min baseline, rats received two 15-s CS presentations with a 2.9-min intertrial interval, and were removed 2 min after the second CS presentation. To assess memory, the amount of time spent freezing during the baseline, the CS, and the trace interval (defined as the first 30 sec after CS offset) was measured. The percent freezing during the 2 CS presentations during the probe test was averaged and

used as the measurement of behavior performance (memory). A summary of experimental design and behavioral performance is shown in Figure 41.

Analysis of behavioral data. A remote CCTV video camera (model #WV-BP334; Panasonic Corp., Suzhou, China), mounted to the top of each behavioral chamber, was used to record the activity of each rat during training and testing. The video data were fed to a PC running FreezeFrame 2.04. Data were analyzed using FreezeView 2.04 (Actimetrics Software, Coulbourn Instruments) where a 1 sec bout of immobility was scored as freezing. Freezing was defined as the absence of all movement except that required for respiration (Blanchard & Blanchard, 1969).

Visualization of corticoamygdala projection neurons. Immediately after testing, rats were re-anaesthetized and perfused with 200 ml 1% paraformaldehyde in 0.1 M phosphate buffer (PB, pH 7.4) followed by 450 ml 4% paraformaldehyde 0.125% glutaraldehyde in 0.1 M PB with a speed of ~ 20 ml/min. Brains were removed and post-fixed for 2 h in the same fixative in 4°C (adapted from Radley *et al.*, 2006). After fixation, coronal sections (250 μm thick) were cut in 0.1 M PB with a vibratome (model 1000S, Vibratome, St. Louis, MO). Slices were stored in 0.1 M PB in 4°C until further use. An example of the bilateral distributions of corticoamygdala somata is shown in Figure 13B. The location of Retrobeads[TM] infusions for all rats included in this study is shown in Figure 42.

For Lucifer yellow (LY) injection, slices from the ipsilateral side of Retrobeads[TM] infusion were mounted on a nitrocellulose filter paper and submerged in 0.1 M PB, and visualized under DIC and epifluorescence. Sharp micropipettes with resistance of 100 – 400 MΩ (when filled with 5% LY in dH$_2$O and measured in 0.1 M PB) were used for
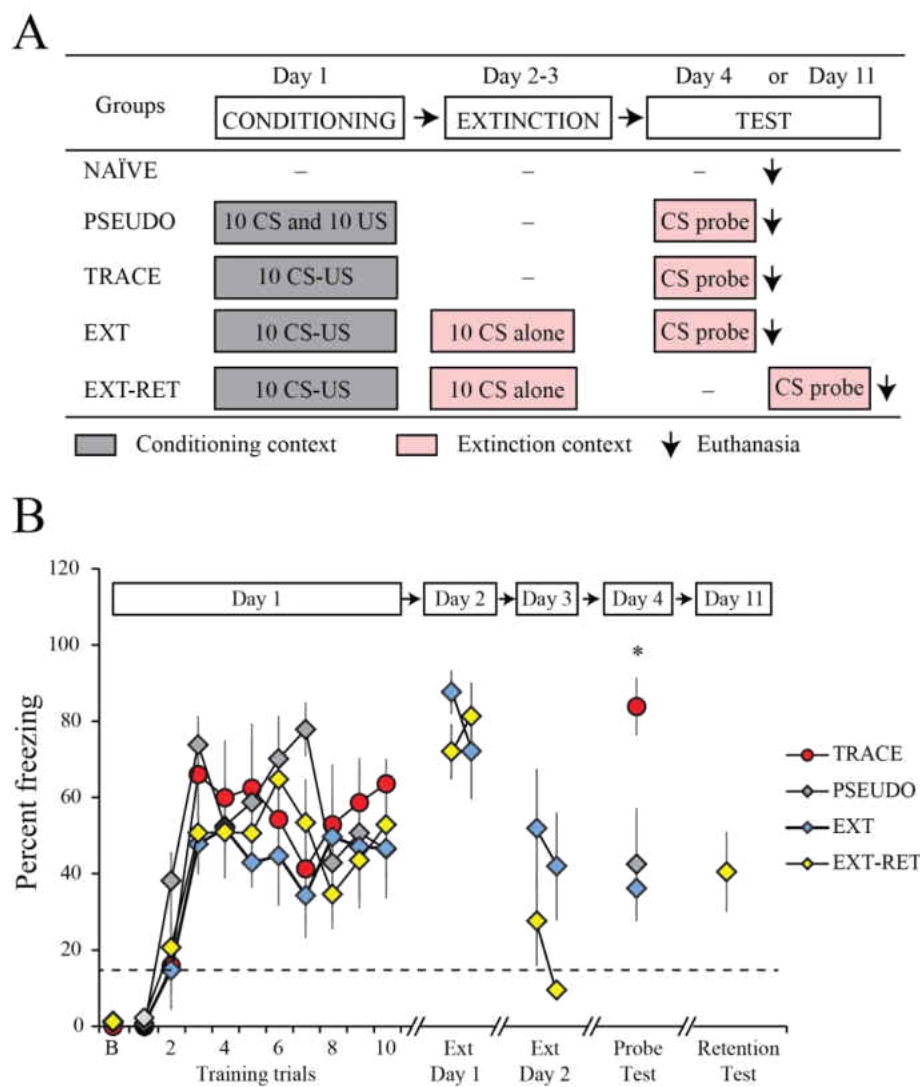
Figure 41. Experimental design and behavioral performance during trace fear conditioning, extinction, and probe test. A, Experimental design. Rats received one 10-trial session of trace fear conditioning or pseudoconditioning on day 1. EXT and EXT-RET rats received 2 sessions of extinction on days 2-3 in a novel context. TRACE, PSEUDO, and EXT rats received a brief CS-alone probe test on day 4 in the extinction context. EXT-RET rats received the probe test on day 11. Rats were euthanized immediately by perfusing with paraformaldehyde and glutaraldehyde following behavior test for morphological study. NAÏVE rats remained in their homecages throughout the experiment. B, Behavioral responses of trace fear-conditioned and pseudoconditioned rats during conditioning, extinction (first 2 trials), and testing. During conditioning, all rats displayed a rapid increase in freezing levels during the first three trials and maintained at high freezing levels. A repeated measures ANOVA of percent freezing revealed a significant main effect of training trials [$F(9,117) = 14.0$, $p < 0.01$] but no significant effect of group [$F(3,13) = 1.6$, $p = 0.24$] nor significant group by training trial interaction [$F(27,117) = 1.2$, $p = 0.22$]. On both extinction days, EXT and EXT-RET rats displayed comparable levels of freezing during extinction sessions. During the probe test, all rats displayed comparable levels of freezing during baseline (dashed line indicates the average baseline freezing of all groups). In contrast, TRACE rats froze significantly more than PSEUDO ($p < 0.05$), EXT ($p < 0.01$), and EXT-RET ($p < 0.05$) rats. All values are percent freezing during the trace interval (see Methods).

Bregma -2.56   -2.80   -3.14   -3.30
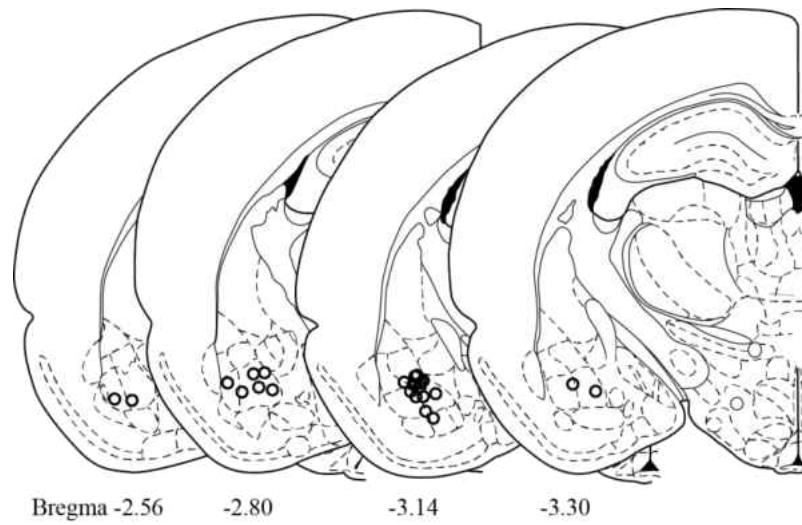
Figure 42. Schematic drawing of coronal sections of rat brain showing the location of pipette tips used for Retrobeads[TM] infusions in the amygdala. Retrobeads[TM] were infused into both hemispheres but all infusion locations were shown in left hemisphere for simplicity. Illustrations were modified from Paxinos & Watson (1998), with permission from *Elsevier*.

injection (Buhl & Lubke, 1989). Retrobeads[TM]-labeled neurons within mPFC were identified by exposing sections to ultraviolet light and the target cells were centered in the field of view. Successful impalement of a neuron was ascertained by applying a short negative current pulse, leading to rapid and intense filling with LY (see Figure 43). In contrast, when the pipette tip was still located extracellular, the dye spreads in a diffuse cloud. LY was iontophoretically injected by applying a negative constant current (1-8 nA) for 5-15 min until the distal dendrites appeared brightly fluorescent (Buhl, Schwerdtfeger, & Germroth, 1990). After injection, the slices were mounted, coverslipped with Ultra Cruz Mounting Medium (Santa Cruz Biotechnology, Santa Cruz, CA), and sealed with nail polish for visualization.

Reconstruction of mPFC-BLA projection neurons. An individual blind to the training condition analyzed both dendritic branching and spine density. LY injected neurons were visualized and imaged on an Olympus confocal laser scanning microscope (FV1200) using a 488 nm excitation wavelength. Stacks of images that contained the whole individual neuron were taken using a 10x objective [numerical aperture (NA), 0.4] at 0.62 μm increments. This method produced images with a voxel resolution of 0.621 x 0.621 x 0.62 μm in the x-, y-, and z- planes, respectively. Maximum intensity projections were prepared with the FV10-ASW viewer software (Olympus, v 4.0) to obtain 3D images of the mPFC-BLA projection neurons (see Figure 43B and 43 C).

Analysis of dendritic spines. In order to select dendritic segments from which to analyze spine density, concentric circles were drawn on the 3D image at radial increments of 50 μm relative to the soma (see Figure 43B and 43C). Segments were selected with a
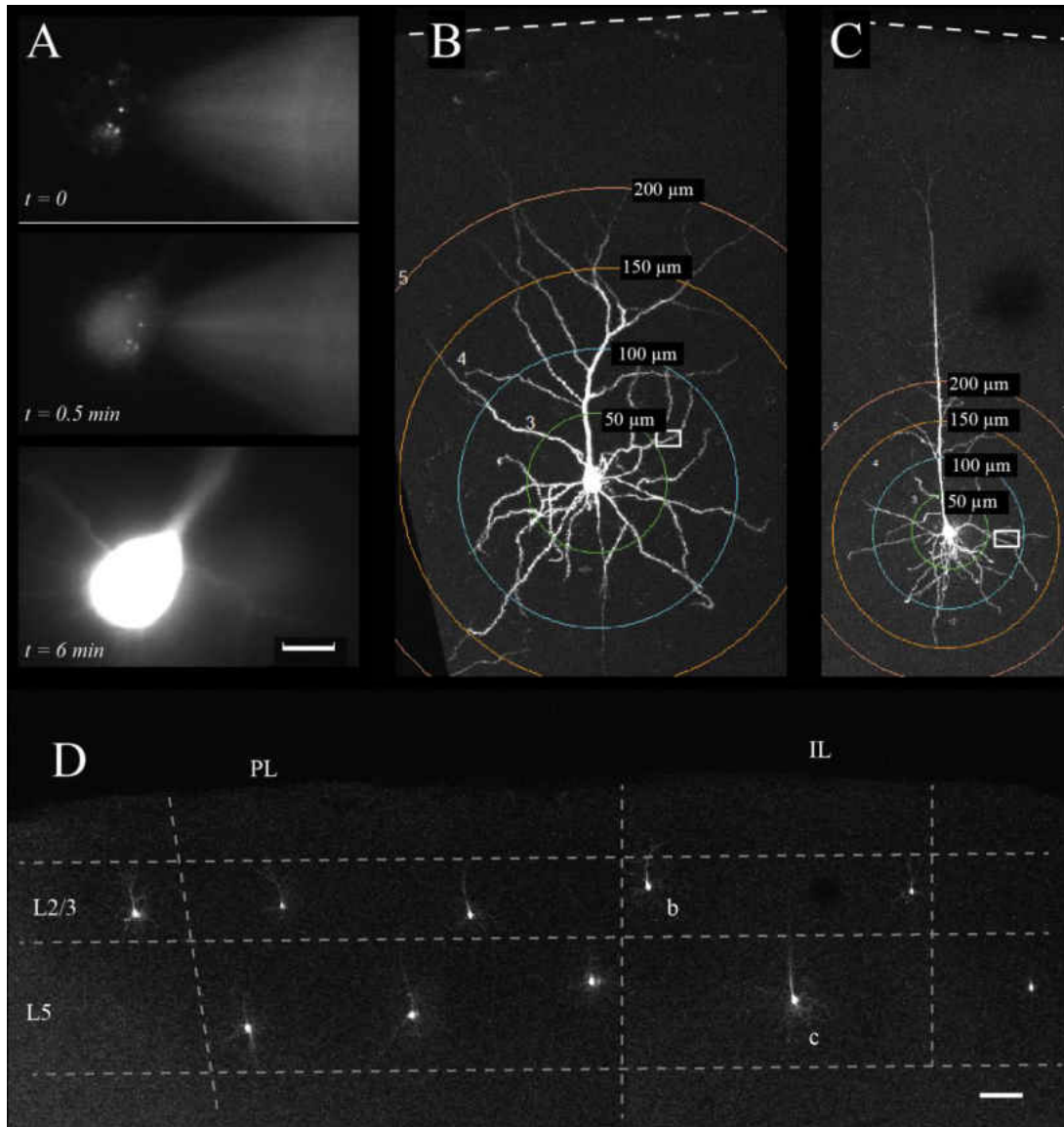
Figure 43. Visualization of dendritic arbor in L2/3 and L5 pyramidal neurons of the mPFC-BLA projection neurons. A, Photoimages showing before ($t = 0$), during ($t = 0.5$ min) and after ($t = 6$ min) iontophoretic injection of Lucifer Yellow (LY) into a Retrobeads[TM]-labeled pyramidal neuron (i.e., mPFC-BLA projection). B, Maximum z-projection of an LY-injected L2/3 neuron (see cell location in Db). C, Maximum z-projection of an LY injected L5 neuron (see cell location in Dc). The white rectangles in B and C indicate dendritic segments shown in Figure 44. The concentric circles in B and C were used to select dendritic segments at different radial distance for the analysis of dendritic spines. D, Confocal image showing multiple neurons being injected with LY in mPFC area (Bregma 3.2 mm). b and c in panel D indicate cells shown in B and C. As shown in panels B and C, the mPFC-BLA projections neurons displayed similar arborization patterns in basal dendrites between L2/3 and L5. The apical dendrite of L2/3 projection neuron was short and bifurcated within 200 μm from the soma. In contrast, the apical dendrite of L5 projection neurons was prominent and had a trunk, from which oblique dendrites emerge before bifurcating to form a tuft dendrite. Scale bars: A, 5 μm; D, 100 μm.

systematic-random design at 50, 100, and 150 µm from the soma (up to 4 segments at each distance) to provide a systematic sampling of proximal, intermediate, and distal dendritic segments. For apical dendrites, segments were selected from secondary or tertiary branches that have comparable diameter because the spine density is correlated with segment diameter (Larkman, 1991). Although additional distal segments were selected, segments within 150 µm yielded best fluorescent intensity for spine counting therefore were analyzed. Stacks of image that contain the selected dendritic segments (20 – 60 µm) were taken using a 60x oil immersion objective (NA, 1.42) at a zoom of 6.6 and at 0.1 µm increment. This method produced images with a voxel resolution of 0.1 x 0.1 x 0.1 µm in the x-, y-, and z-planes, respectively.

Spine analysis was performed using the semi-automated software NeuronStudio (http://research.mssm.edu/cnic/tools-ns.html), which analyzes dendritic length and spine number in 3D (see Figure 44; see also Rodriguez, Ehlenberger, Dickstein, Hof, & Wearne, 2008; Wearne *et al.*, 2005). NeuronStudio can automatically classify spines into different subtypes (stubby, thin, and mushroom) and has been validated by comparison with serial section electron microscopy (Dumitriu, Rodriguez, & Morrison, 2011). After NeuronStudio processing, a human operator, blind to the condition, manually corrected both dendritic reconstructions and spine detections. Spine density for each branch segment was expressed as spine number/µm.

Statistical Analyses. Total and subtype spine densities were calculated by dividing the total number of spines by the length of the dendritic segment. Spine densities were calculated for each segment, then averaged for each cell. Spines from apical and basal dendrites were combined because no significant difference were found from the same
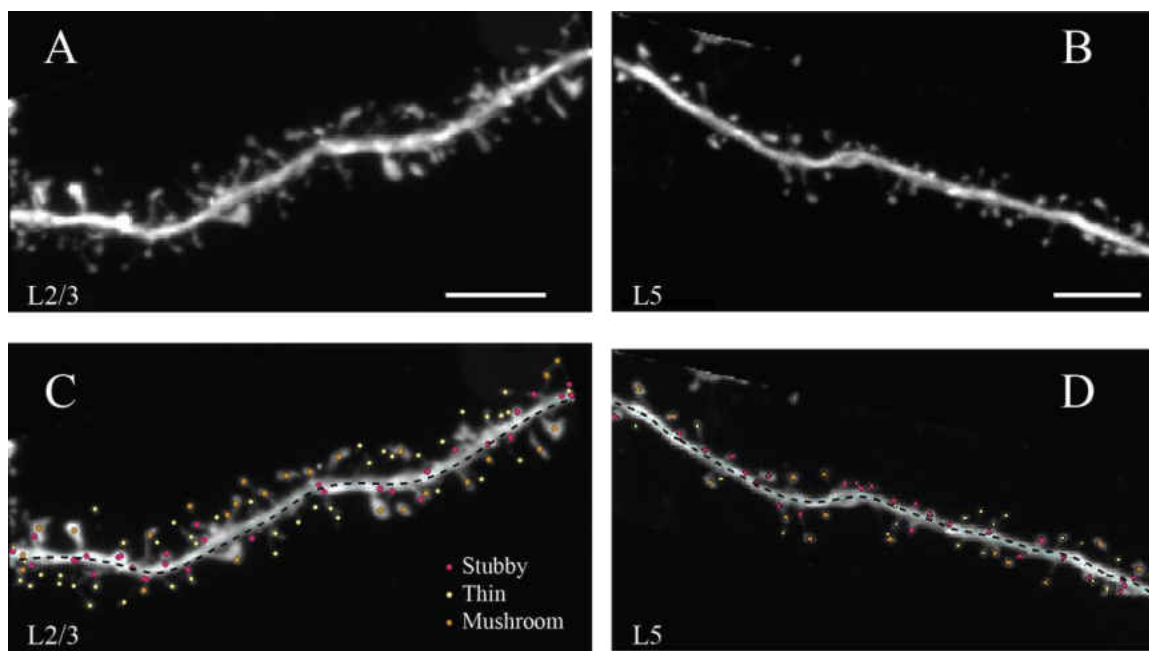
Figure 44. Analysis of dendritic spines in mPFC-BLA projection neurons. A and B, Maximum intensity projections of confocal images obtained from dendritic segments of L2/3 and L5 neurons respectively. The locations of the segments were indicated in the white rectangles in Figure 40B and 40C. The shape of the dendritic segments and spines was well preserved following Lucifer Yellow injection. Scale bar, 5 μm. C and D, analysis of dendritic spines with NeuronStudio (Rodriguez *et al.*, 2008). The spines were automatically identified and classified as stubby (purple), thin (yellow) and mushroom (orange) in NeuronStudio. Dashed lines in C and D are the traces of the dendritic segments. Scale bar, 5 μm.

radial distance in all groups. All statistical analyses were performed with the aid of Microsoft Excel and IBM SPSS statistics software (version 22; SPSS). A repeated measures ANOVA were used to compare freezing levels across training trials for each group of rats. Two-tailed *t*-test for independent samples were used to compare spine density between different cortical layers and subregions. Pearson's correlation coefficient was used to analyze the correlation between spine density and somatic depth from the pial surface. For significant main effects (alpha 0.05), a Fisher's PLSD test was used for *post hoc* comparisons. All data were expressed as mean ± SEM.

Results

To examine the effect of trace fear conditioning on spine density of mPFC-BLA projection neurons, rats received a unilateral infusion of a retrograde fluorescence tracer into BLA, followed by trace fear conditioning and extinction. Control rats were either pseudoconditioned or experimentally naïve. After a brief behavioral test, the rats were perfused and the brains were fixed. The fluorescently labeled neurons (i.e., mPFC-BLA projection neurons) were recognized and injected with Lucifer Yellow for later morphological analyses.

All rats exhibited a rapid increase in percent freezing during the first 3 trials and then maintained a high level of freezing throughout the rest of training trials (see Figure 41B). When memory was tested on day 4, freezing levels were comparably low [$F(3,13)$ = 1.27, p = 0.32] during the baseline among all the groups (average baseline freeze was shown as a dashed line in Figure 41B). As illustrated in Figure 41B, *post hoc* analyses indicated that TRACE rats froze significantly more than both PSEUDO ($p < 0.01$) and EXT rats ($p < 0.01$). EXT-RET rats were tested on day 11, and displayed significantly lower

level of freezing compared to conditioned rats but comparable to that of EXT rats, suggesting good extinction memory.

Layer 2/3 mPFC-BLA projection neurons have higher spine density than Layer 5 neurons

Individual fluorescently labeled mPFC-BLA projection neurons were microinjected with Lucifer yellow after the behavioral test. IL and PL neurons within both L2/3 and L5 were injected but analyzed separately. For most neurons, basal dendrites did not go beyond 150 µm. Both L2/3 and L5 neurons had apical dendrites that arborized in L1 and extended toward the pial surface (see Figure 43D). High-resolution confocal z-stacks of dendrites were obtained (see Materials and Methods). Individuals blind to the behavioral training condition used a semi-automatic approach to conduct unbiased spine morphometric analysis in 3D using NeuronStudio (Rodriguez *et al.*, 2008).

We first examined whether or not there were any layer- and region-specific differences of spine density in the mPFC neurons. For this purpose, we combined spines obtained in different groups together because behavioral training didn't change these properties. Analysis of 90,709 spines obtained from 1,030 dendritic segments revealed a significant correlation between the somatic depth and the spine density in both IL and PL such that neurons in the superficial layers have higher spine density than neurons in the deep layers (see Figure 45). Furthermore, such correlation between spine density and somatic depth is subtype- and region-specific. As shown in Table 12, in IL, the correlation between spine density and somatic depth was significant in both stubby and thin spines but not in mushroom spines. In PL, the correlation was significant in all spine types in all radial distances except mushroom spines at 150 µm. No significant difference was
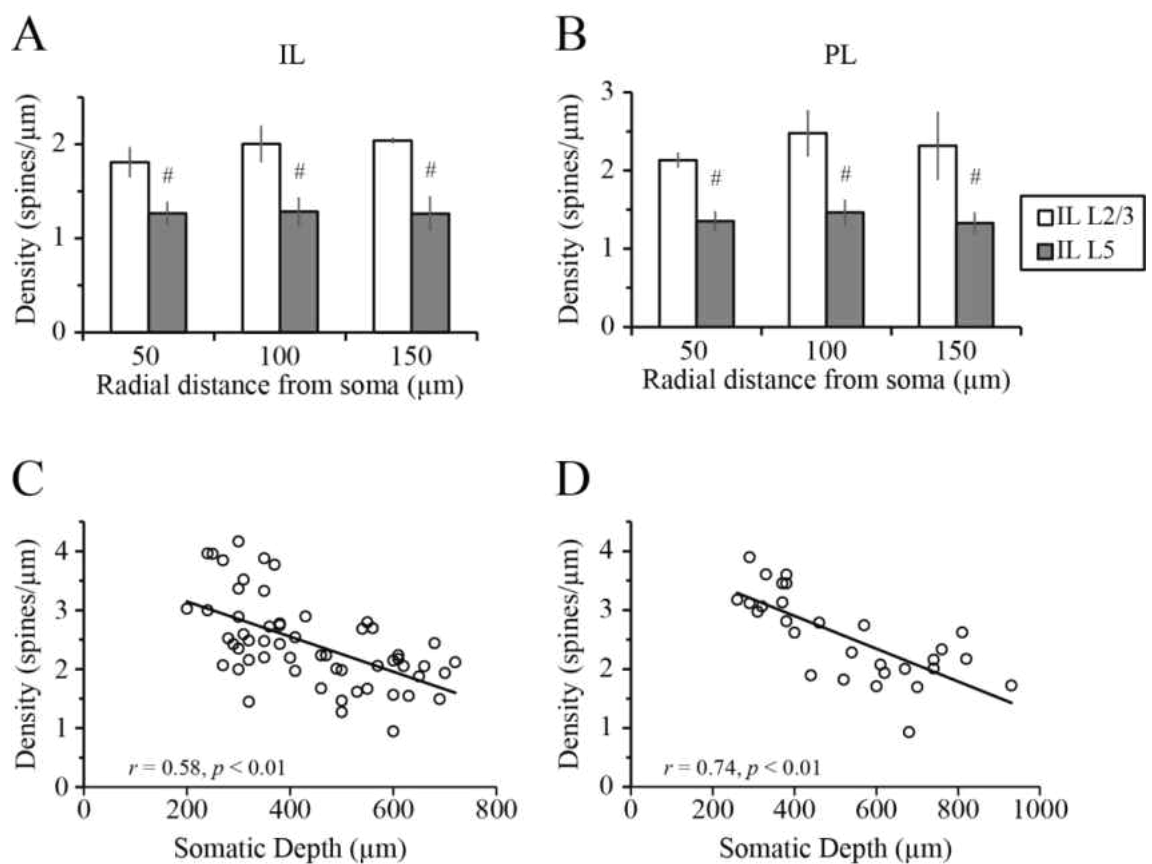
Figure 45. Medial prefrontal cortex pyramidal neurons in L2/3 have greater spine density than those in L5. A and B, The spine densities were significantly greater in L2/3 neurons than those in L5 neurons (#, $p < 0.01$) in all radial distances in both IL and PL. C and D, The spine density was significantly correlated with somatic depth in both IL and PL.

Table 12. Spine density is significantly correlated with somatic depth

Location (# of cells)	Total	Stubby	Thin	Mushroom
50 µm				
IL (57)	- 0.58#	- 0.60#	- 0.54#	- 0.23
PL (34)	- 0.72#	- 0.69#	- 0.74#	- 0.47#
100 µm				
IL (56)	- 0.60#	- 0.53#	- 0.64#	- 0.09
PL (34)	- 0.64#	- 0.51#	- 0.55#	- 0.34*
150 µm				
IL (49)	- 0.40#	- 0.45#	- 0.40#	0.07
PL (32)	- 0.62#	- 0.38#	- 0.62#	-0.20

Data are correlation coefficients between spine density and somatic depth. IL, infralimbic cortex; PL, prelimbic cortex.   Statistically significant correlation between spine density and somatic depth: *, $p < 0.05$; #, $p < 0.01$.

observed when comparing between IL and PL in either L2/3 or L5.

Extinction reduced spine density in L2/3 mPFC-BLA projection neurons

The spine density was not significantly changed following trace fear conditioning when compared with NAÏVE neurons. However, in distal dendrites (150 μm) in L5 neurons in IL, conditioning slightly increased whereas EXT and EXT-RET reduced the spine density (see Figure 46B). A planned *t*-test revealed that the spine density was significantly smaller in EXT-RET group than that of TRACE [$t(9) = 2.4$, $p < 0.05$]. In addition, planned comparisons revealed that extinction significantly reduced spine density in L2/3 neurons in both IL and PL compared to NAÏVE. In IL, the reduction was significant only in distal dendrites [$t(6) = 6.6$, $p < 0.01$]. Further analysis with the subtypes revealed that the reduction is primarily driven by the reduction in mushroom spines [$t(5) = 2.4$, $p = 0.062$; see Table 13]. In PL, extinction significantly reduced total spine density at proximal dendrites when compared to NAÏVE [$t(5) = 7.7$, $p < 0.01$], and remained low after extinction retention [$t(4) = 6.77$, $p < 0.01$]. The total spine density was also reduced in medium and distal dendrites after extinction but not significantly (see Figure 46C). Further analysis with the subtypes revealed that the reduction was primarily driven by the reduction in thin spines [$t(5) = 2.3$, $p = 0.066$; see Table 13]. In contrast, trace fear conditioning or extinction did not induce any significant change in spine density in L5 projection neurons (see Table 14). Thus, these data suggest that fear extinction facilitates spine elimination in mPFC-BLA projection neurons in L2/3.
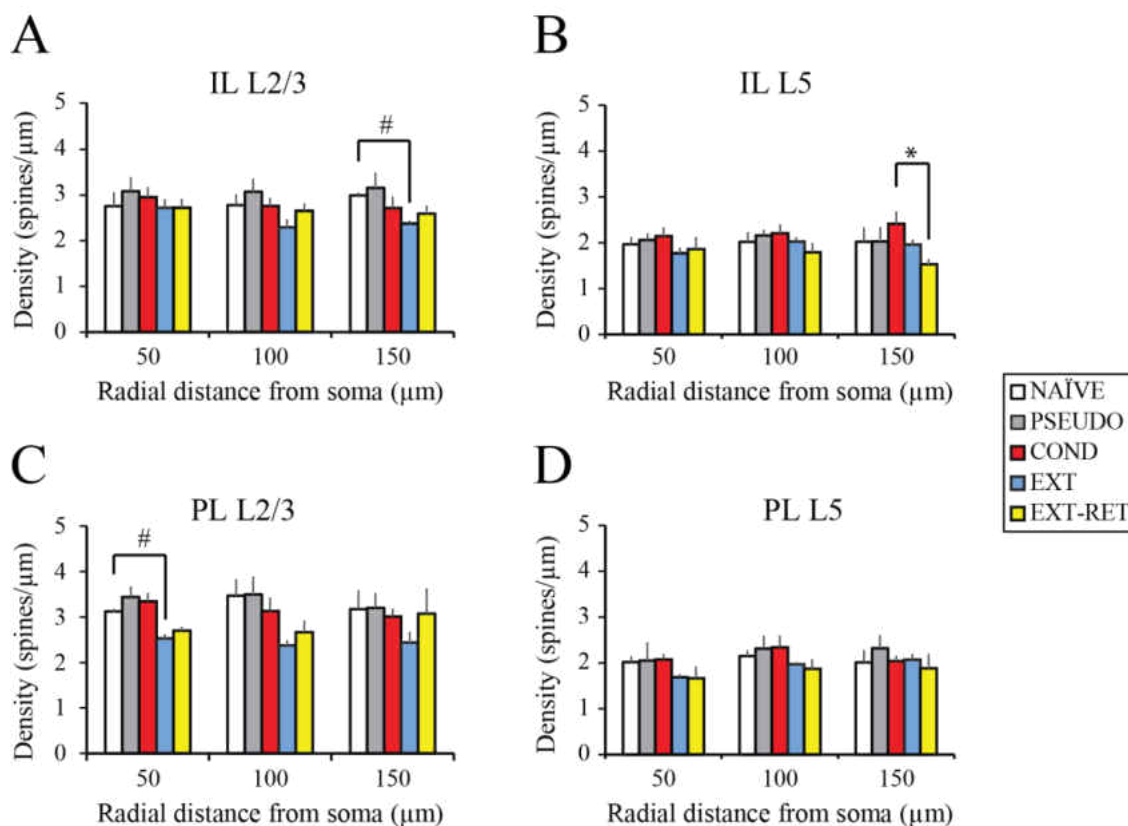
Figure 46. Fear extinction reduces spine density in L2/3 neurons but not L5 neurons in both IL and PL. A, Extinction significantly reduced total spine density in IL L2/3 neurons at distal dendrites (150 μm; $p < 0.01$) but not proximal dendrites (50 μm). B, Trace fear conditioning and extinction did not significantly change total spine density in L5 neurons in IL. However, the spine density between TRACE and EXT-RET was significantly different ($p < 0.05$). C, Extinction significantly reduced spine density of PL L2/3 neurons at proximal dendrites (50 μm; $p < 0.01$), which remained low after extinction retention. The spine density was also reduced after extinction in medium and distal dendrites but not significantly. D, Trace fear conditioning and extinction did not significantly change spine density in L5 neurons in PL.

Table 13. Subtype-specific modulation of spine density by extinction

Location (# of cells)	Spines/μm			
	Total	Stubby	Thin	Mushroom
IL L2/3 (150 μm from soma)				
NAÏVE (4)	3.0 ± 0.1	1.0 ± 0.1	1.5 ± 0.1	0.6 ± 0.2
PSEUDO (8)	3.2 ± 0.3	0.9 ± 0.1	1.8 ± 0.3	0.5 ± 0.1
TRACE (9)	2.7 ± 0.2	0.7 ± 0.1	1.5 ± 0.1	0.4 ± 0.1
EXT (6)	2.4 ± 0.1#	0.9 ± 0.1	1.3 ± 0.1	0.2 ± 0.1§
EXT-RET (8)	2.6 ± 0.2	0.8 ± 0.1	1.4 ± 0.1	0.4 ± 0.1
PL L2/3 (50 μm from soma)				
NAÏVE (4)	3.1 ± 0.1	1.0 ± 0.1	1.5 ± 0.1	0.6 ± 0.1
PSEUDO (4)	3.4 ± 0.2	1.1 ± 0.1	1.6 ± 0.1	0.7 ± 0.1
TRACE (3)	3.3 ± 0.2	1.0 ± 0.1	1.6 ± 0.1	0.8 ± 0.1
EXT (3)	2.5 ± 0.1#	0.8 ± 0.1	1.2 ± 0.1§	0.4 ± 0.1
EXT-RET (2)	2.7 ± 0.1	0.7 ± 0.1	1.3 ± 0.1	0.7 ± 0.1

Data are mean ± SE. IL, infralimbic cortex; PL, prelimbic cortex. Rat groups: NAÏVE, rats that did not receive any behavioral training; PSEUDO, rats that received pseudoconditioning on day 1 and tested on day 4; TRACE, rats that received trace fear conditioning on day 1 and tested on day 4; EXT, rats that received trace fear conditioning on day 1, extinction on days 2-3, and tested on day 4; EXT-RET, rats that received conditioning on day 1, extinction on days 2-3, and tested on day 11. Statistically significant from Naïve (# $p < 0.01$). Non-significant difference from naïve: § $p = 0.062$ for IL-BLA projection neurons in L2/3, and $p = 0.066$ for PL-BLA projection neurons in L2/3 respectively).

Table 14. Spine density in L5 neurons after trace fear conditioning or extinction

Location (# of cells)	Spines/μm Total	Stubby	Thin	Mushroom
IL L5 (150 μm from soma)				
NAÏVE (3)	2.0 ± 0.3	0.8 ± 0.1	0.8 ± 0.1	0.5 ± 0.2
PSEUDO (8)	2.1 ± 0.3	0.5 ± 0.2	1.1 ± 0.1	0.4 ± 0.1
TRACE (7)	2.4 ± 0.3	0.7 ± 0.1	1.2 ± 0.2	0.5 ± 0.1
EXT (13)	2.0 ± 0.1	0.6 ± 0.1	1.0 ± 0.1	0.4 ± 0.1
EXT-RET (6)	1.5 ± 0.1*	0.4 ± 0.1	0.8 ± 0.1	0.3 ± 0.1
PL L5 (50 μm from soma)				
NAÏVE (4)	2.0 ± 0.1	0.7 ± 0.1	1.0 ± 0.2	0.4 ± 0.1
PSEUDO (5)	2.1 ± 0.4	0.6 ± 0.2	1.0 ± 0.1	0.5 ± 0.1
TRACE (3)	2.1 ± 0.1	0.7 ± 0.1	1.0 ± 0.1	0.4 ± 0.1
EXT (3)	1.7 ± 0.1	0.7 ± 0.1	0.8 ± 0.1	0.2 ± 0.1
EXT-RET (4)	1.7 ± 0.3	0.5 ± 0.1	0.8 ± 0.1	0.4 ± 0.1

Data are mean ± SE for number of cells in parentheses. IL, infralimbic cortex; PL, prelimbic cortex. Rat groups: NAÏVE, rats that did not receive any behavioral training; PSEUDO, rats that received pseudoconditioning on day 1 and tested on day 4; TRACE, rats that received trace fear conditioning on day 1 and tested on day 4; EXT, rats that received trace fear conditioning on day 1, extinction on days 2-3, and tested on day 4; EXT-RET, rats that received conditioning on day 1, extinction on days 2-3, and tested on day 11. Statistically significant between TRACE and EXT-RET: * $p < 0.05$.

Discussion

The current study examined the morphological properties of mPFC-BLA projection neurons and the effect of trace fear conditioning and extinction on the spine density of these neurons. We found a significant correlation between the spine density and the somatic depth of the neurons such that the neurons in superficial layers have higher spine density than the neurons in deep layers. We further found that trace fear conditioning facilitated spine formation in distal L5 neurons in IL whereas extinction and extinction-retention reduced the spine density. In L2/3, extinction significantly facilitated spine elimination in both IL and PL. Furthermore, the reduction in spine density in IL primarily occurred in mushroom spines in distal dendrites. Whereas in PL, the reduction in spine density primarily occurred in thin spines in proximal dendrites.

Although we are the first to study the morphological properties of mPFC-BLA projection neurons, the total spine density in L2/3 neurons is comparable to randomly selected mPFC neurons in previous studies (Radley *et al.*, 2006; Radley *et al.*, 2008). Interestingly, we observed that the spine density is higher in L2/3 neurons than L5 neurons. This was unlikely an artifact caused by any experimental procedures or bias because neurons in L2/3 and L5 were obtained from the same slices and the spines were counted by individuals blind to the cell location. In addition, the correlation between the spine density and somatic depth strongly support our conclusion. However, such a laminar-different spine density was not observed in rat visual cortex (Larkman, 1991) and an opposite pattern was shown in monkey cortical area 7m and the superior temporal polysensory area (Elston, 2001). In addition, our observation of different spine density across cortical layers is not specific to mPFC-BLA projection neurons, because analysis of

randomly selected, biocytin-filled neurons revealed the same pattern – the L5 neurons are less spiny than those in L2/3 (see Figure 47). Thus, the specific distribution pattern of dendritic spines in mPFC may reflect a region-specific neuronal properties, and suggests that the afferent information is processed differently in L2/3 and L5 neurons.

The current data suggest that trace fear conditioning and extinction differentially affect the synaptic circuits in the mPFC – trace fear conditioning may facilitate spine formation whereas extinction facilitates spine elimination. However, this result seems to differ from previous studies. For example, an *in vivo* imaging study in frontal association cortex indicated that delay fear conditioning eliminates dendritic spines whereas subsequent extinction reverses this effect (Lai *et al.*, 2012). Another study using Golgi staining showed that contextual fear conditioning increased the spine density in IL L2/3 neurons. Extinction didn't change the spine density but reduced spine size (Vetere *et al.*, 2011). There are several possible explanations for these seemly conflicting results. First, the conditioning paradigms were different in each study. We used trace fear conditioning whereas Lai and colleagues used delay fear conditioning and Vetere *et al.* used contextual fear conditioning. The different paradigms of fear conditioning have been shown to recruit different brain circuits and therefore may yield different effects on the dendritic spines. Second, our current study focused on the neurons that only project to the BLA, which may be differently modulated by fear conditioning and extinction compared to randomly selected neurons in other studies. Finally, the sample size in the current study is relatively small. This was because we examined both L2/3 and L5 neurons in both IL and PL, which resulted in a small number of cells in each layer each subregion. However, our data still demonstrated a significant change in spine density following fear extinction and suggest a

layer- and subregion- specific modulation of spine density within the mPFC following fear conditioning and extinction, which may provide useful information for future study.

Conclusions

The current data are the first to study the morphological properties of mPFC-BLA projection neurons. The neurons in superficial layers have higher spine densities than that in deep layers, suggesting different computational functions of these projection neurons. Furthermore, extinction of trace fear memory specifically eliminates dendritic spines in both IL and PL neurons, especially in L2/3 neurons. These data provide further evidence that the mPFC is critical for the expression of conditioned fear memory.
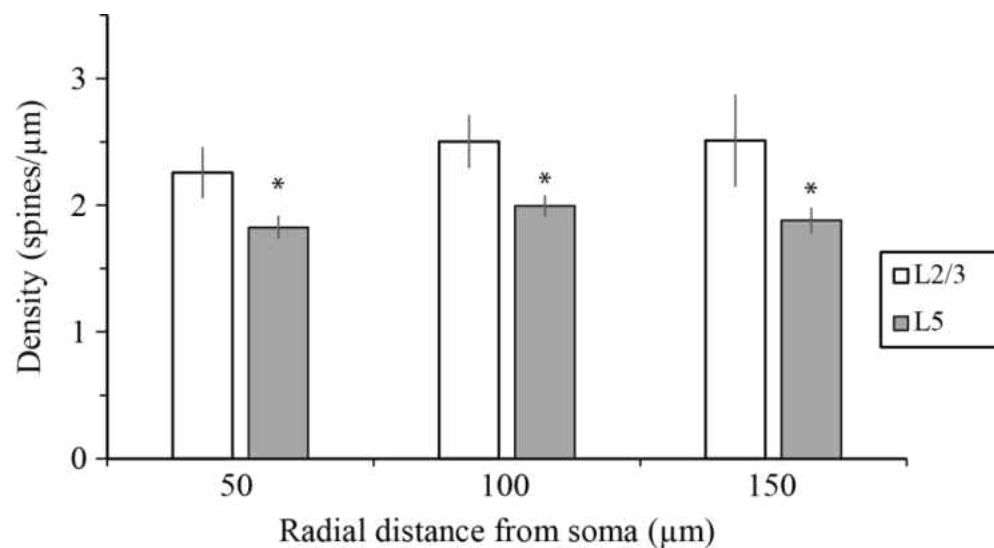
Figure 47. Laminar difference in spine density in mPFC pyramidal neurons with unknown projection targets. Graph depicting the mean and standard error of spine density calculated from dendritic segments. The spine density was significantly higher in L2/3 neurons than that in L5 neurons (* $p < 0.05$ for all values). Data were obtained from confocal images of biocytin-filled neurons and visualized with streptavidin Alexa Fluor 488.

Concluding remarks

The experiments described in this dissertation combined a series of behavioral, electrophysiological, and morphological techniques to study the cellular mechanisms underlying learning and memory. The current findings that trace fear conditioning induced neurophysiological and morphological plasticity in both hippocampus and mPFC are consistent with existing data that both of these brain areas are required for the acquisition of trace fear conditioning (McEchron *et al.*, 1998; Gilmartin & Helmstetter, 2010).

The increased intrinsic excitability of regular spiking neurons in both hippocampus and IL suggests that the activation of these neurons facilitates the expression of a conditioned fear memory. Such an effect is likely achieved through activation of the amygdala because both regions have intensive projections to the BLA (McDonald *et al.*, 1996; Gabbott *et al.*, 2005). However, it is not clear how the hippocampus and the mPFC interact in this process. Interestingly, unlike reciprocal innervations between the mPFC and other brain regions (see Figure 3), mPFC receives excitatory synaptic inputs from hippocampal CA1 neurons (Hoover & Vertes, 2007; Parent *et al.*, 2010) but mPFC does not send reciprocal projections back (Hurley *et al.*, 1991; Sesack, Deutch, Roth, & Bunney, 1989; Vertes 2004). In combination with the transient role of hippocampus in memory formation (e.g., Kim & Fanselow, 1992; Moyer *et al.*, 1996), these data suggest that the activation of hippocampal neurons facilitates the formation of long-term conditioned memory in the mPFC (e.g., Corcoran & Quirk, 2007; Quirk *et al.*, 2000) and other cortical areas (Lebron *et al.* 2004). In contrast, after memory has been stored in the cortex, hippocampus is no longer required for the memory retrieval.

The current study investigated three forms of plasticity as a function of trace fear conditioning and extinction. Our observation of a significant correlation between intrinsic excitability and the amount of LTP in CA1 neurons (Figure 12) and the fact that intrinsic plasticity can be induced in the absence of synaptic plasticity (Cohen-Matsliah *et al.* 2010) suggest that intrinsic plasticity facilitates synaptic plasticity. In addition, although not observed in the current study, the intrinsic plasticity may also facilitate morphological plasticity – the modulation of dendritic spine density, which is associated enhanced synaptic strength. One evidence that supports this point of view comes from the observation that animals raised in an enriched environment had higher spine density, increased excitablity, and greaer LTP in hippocampal neurons compared to control animals (Malik & Chattarji, 2012). Furthermore, environment enrichment facilitates contextual fear conditioning (Malik & Chattarji, 2012), suggesting that an interaction between all three forms of plasticity may contribute to the behavioral changes that occur following learning.

Previous studies suggest that the calcium influx through NMDA receptors may serve as a common path of the three types of plasticity. For example, the increase of intracellular caclium is capable of activating multiple signaling cascades that modulate the property and/or distribution of ion channels, as well as the phosphorylation and insertion of AMPA receptors to the postsynaptic membrane.. Such membrane insertion of AMPA receptors may not only enhance synaptic strength, but also lead to an increase in the size of postsynaptic density and eventually the production of perforated synapses, which then generate multi-spine synapses and induce synaptogenesis. Although this is an oversimplified model, there is strong evidence that supports this hypothesis, especially data

from LTP studies that showing a rapid synpse formation following LTP induction (for review, see Luscher *et al.*, 2000). In addition, there are many other intracellular cascades following calcium entry that are required during this process. For instance, the calcium entry may induce gene activation and protein synthesis, which are critical for the maintenance of long-term memory. All these processes require the activation of a variety of other intracellular signals, such as CaMKII, PKC, PKA, and CREB, which are critical for memory formation and expression (Impey *et al.*, 1998; Matsuzaki *et al.*, 2004; Ohno *et al.*, 2006; Sweatt, 2003).

In summary, the current set of experiments demonstrate that intrinsic, synaptic, and morphological plasticity occurs during acquisition and extinction of trace fear conditioning. Of critical significance remaining to be studied are the cellular cascades or molecular mechanisms that link these types of plasticity together. Although these studies suggest that synaptic signaling can lead to intrinsic changes, which can then facilitate circuit-specific synaptic plasticity, without a concrete way to selectively control intrinsic plasticity (and the myriad of ways intrinsic excitability can be altered), how these types of plasticity are interwoven to produce learning-related changes is likely to remain a significant neuroscientific challenge.

References

Abraham, W. C. (2008). Metaplasticity: tuning synapses and networks for plasticity. *Nat Rev Neurosci, 9*(5), 387. doi: 10.1038/nrn2356

Abraham, W. C., & Bear, M. F. (1996). Metaplasticity: the plasticity of synaptic plasticity. *Trends Neurosci, 19*(4), 126-130.

Akirav, I., Raizel, H., & Maroun, M. (2006). Enhancement of conditioned fear extinction by infusion of the GABA(A) agonist muscimol into the rat prefrontal cortex and amygdala. *Eur J Neurosci, 23*(3), 758-764. doi: 10.1111/j.1460-9568.2006.04603.x

Amano, T., Unal, C. T., & Pare, D. (2010). Synaptic correlates of fear extinction in the amygdala. *Nat Neurosci, 13*(4), 489-494. doi: 10.1038/nn.2499

American Psychiatric Association. (2000). *Diagnostic and statistical manual of mental disorders* (4th ed., text rev ed.). Arlington, VA: Author.

Anagnostaras, S. G., Maren, S., & Fanselow, M. S. (1999). Temporally graded retrograde amnesia of contextual fear after hippocampal damage in rats: within-subjects examination. *J Neurosci, 19*(3), 1106-1114.

Armano, S., Rossi, P., Taglietti, V., & D'Angelo, E. (2000). Long-term potentiation of intrinsic excitability at the mossy fiber-granule cell synapse of rat cerebellum. *J Neurosci, 20*(14), 5208-5216.

Artola, A., & Singer, W. (1987). Long-term potentiation and NMDA receptors in rat visual cortex. *Nature, 330*(6149), 649-652.

Avesar, D., & Gulledge, A. T. (2012). Selective serotonergic excitation of callosal projection neurons. *Front Neural Circuits, 6*, 12. doi: 10.3389/fncir.2012.00012

Bacon, S. J., Headlam, A. J., Gabbott, P. L., & Smith, A. D. (1996). Amygdala input to medial prefrontal cortex (mPFC) in the rat: a light and electron microscope study. *Brain Res, 720*(1-2), 211-219.

Baeg, E. H., Kim, Y. B., Jang, J., Kim, H. T., Mook-Jung, I., & Jung, M. W. (2001). Fast spiking and regular spiking neural correlates of fear conditioning in the medial prefrontal cortex of the rat. *Cereb Cortex, 11*(5), 441-451.

Bangasser, D. A., Waxler, D. E., Santollo, J., & Shors, T. J. (2006). Trace conditioning and the hippocampus: the importance of contiguity. *J Neurosci, 26*(34), 8702-8706. doi: 10.1523/JNEUROSCI.1742-06.2006

Baraban, J. M., Snyder, S. H., & Alger, B. E. (1985). Protein kinase C regulates ionic conductance in hippocampal pyramidal neurons: electrophysiological effects of phorbol esters. *Proc Natl Acad Sci U S A, 82*(8), 2538-2542.

Baratta, M. V., Zarza, C. M., Gomez, D. M., Campeau, S., Watkins, L. R., & Maier, S. F. (2009). Selective activation of dorsal raphe nucleus-projecting neurons in the ventral medial prefrontal cortex by controllable stress. *Eur J Neurosci, 30*(6), 1111-1116. doi: 10.1111/j.1460-9568.2009.06867.x

Barnes, C. A. (1979). Memory deficits associated with senescence: a neurophysiological and behavioral study in the rat. *J Comp Physiol Psychol, 93*(1), 74-104.

Barrett, D., Shumake, J., Jones, D., & Gonzalez-Lima, F. (2003). Metabolic mapping of mouse brain activity after extinction of a conditioned emotional response. *J Neurosci, 23*(13), 5740-5749.

Bast, T., Zhang, W. N., & Feldon, J. (2001). The ventral hippocampus and fear conditioning in rats. Different anterograde amnesias of fear after tetrodotoxin

inactivation and infusion of the GABA(A) agonist muscimol. *Exp Brain Res, 139*(1), 39-52.

Bear, M. F., & Abraham, W. C. (1996). Long-term depression in hippocampus. *Annu Rev Neurosci, 19*, 437-462.

Bechara, A., Tranel, D., Damasio, H., Adolphs, R., Rockland, C., & Damasio, A. R. (1995). Double dissociation of conditioning and declarative knowledge relative to the amygdala and hippocampus in humans. *Science, 269*(5227), 1115-1118.

Beck, H., & Yaari, Y. (2008). Plasticity of intrinsic neuronal properties in CNS disorders. *Nat Rev Neurosci, 9*(5), 357-369. doi: 10.1038/nrn2371

Beltramo, R., D'Urso, G., Dal Maschio, M., Farisello, P., Bovetti, S., Clovis, Y., . . . Fellin, T. (2013). Layer-specific excitatory circuits differentially control recurrent network dynamics in the neocortex. *Nat Neurosci, 16*(2), 227-234. doi: 10.1038/nn.3306

Bernard, J. F., & Besson, J. M. (1990). The spino(trigemino)pontoamygdaloid pathway: electrophysiological evidence for an involvement in pain processes. *J Neurophysiol, 63*(3), 473-490.

Blanchard, R. J., & Blanchard, D. C. (1969). Crouching as an index of fear. *J Comp Physiol Psychol, 67*(3), 370-375.

Bliss, T. V., & Lomo, T. (1973). Long-lasting potentiation of synaptic transmission in the dentate area of the anaesthetized rabbit following stimulation of the perforant path. *J Physiol, 232*(2), 331-356.

Blum, S., Hebert, A. E., & Dash, P. K. (2006). A role for the prefrontal cortex in recall of recent and remote memories. *Neuroreport, 17*(3), 341-344.

Bolshakov, V. Y., Golan, H., Kandel, E. R., & Siegelbaum, S. A. (1997). Recruitment of new sites of synaptic transmission during the cAMP-dependent late phase of LTP at CA3-CA1 synapses in the hippocampus. *Neuron, 19*(3), 635-651.

Bontempi, B., Laurent-Demir, C., Destrade, C., & Jaffard, R. (1999). Time-dependent reorganization of brain circuitry underlying long-term memory storage. *Nature, 400*(6745), 671-675.

Boric, K., Munoz, P., Gallagher, M., & Kirkwood, A. (2008). Potential adaptive function for altered long-term potentiation mechanisms in aging hippocampus. *J Neurosci, 28*(32), 8034-8039. doi: 10.1523/JNEUROSCI.2036-08.2008

Boudewijns, Z. S., Groen, M. R., Lodder, B., McMaster, M. T., Kalogreades, L., de Haan, R., de Kock, C. P. (2013). Layer-specific high-frequency action potential spiking in the prefrontal cortex of awake rats. *Front Cell Neurosci, 7*, 99. doi: 10.3389/fncel.2013.00099

Bouton, M. E. (1993). Context, time, and memory retrieval in the interference paradigms of Pavlovian learning. *Psychol Bull, 114*(1), 80-99.

Bremner, J. D., Narayan, M., Staib, L. H., Southwick, S. M., McGlashan, T., & Charney, D. S. (1999). Neural correlates of memories of childhood sexual abuse in women with and without posttraumatic stress disorder. *Am J Psychiatry, 156*(11), 1787-1795.

Bremner, J. D., Staib, L. H., Kaloupek, D., Southwick, S. M., Soufer, R., & Charney, D. S. (1999). Neural correlates of exposure to traumatic pictures and sound in Vietnam combat veterans with and without posttraumatic stress disorder: a positron emission tomography study. *Biol Psychiatry, 45*(7), 806-816.

Bremner, J. D., Vythilingam, M., Vermetten, E., Southwick, S. M., McGlashan, T., Nazeer, A., . . . Charney, D. S. (2003). MRI and PET study of deficits in hippocampal structure and function in women with childhood sexual abuse and posttraumatic stress disorder. *Am J Psychiatry, 160*(5), 924-932.

Brown, S. P., & Hestrin, S. (2009). Intracortical circuits of pyramidal neurons reflect their long-range axonal targets. *Nature, 457*(7233), 1133-1136. doi: 10.1038/nature07658

Buchel, C., Morris, J., Dolan, R. J., & Friston, K. J. (1998). Brain systems mediating aversive conditioning: an event-related fMRI study. *Neuron, 20*(5), 947-957.

Buhl, E. H., & Lubke, J. (1989). Intracellular lucifer yellow injection in fixed brain slices combined with retrograde tracing, light and electron microscopy. *Neuroscience, 28*(1), 3-16.

Buhl, E. H., Schwerdtfeger, W. K., & Germroth, P. (1990). Intracellular injection of neurons in fixed brain tissue combined with other neuroanatomical techniques at the light- and electron-microscopic level. In A. Bjorklund, T. Hokfelt, F. G. Wouterloud & A. N. van den Pol (Eds.), *Handbook of chemical neuroanatomy* (Vol. 8, pp. 273-304). Amsterdam: Elsevier.

Burgos-Robles, A., Vidal-Gonzalez, I., & Quirk, G. J. (2009). Sustained conditioned responses in prelimbic prefrontal neurons are correlated with fear expression and extinction failure. *J Neurosci, 29*(26), 8474-8482.

Burgos-Robles, A., Vidal-Gonzalez, I., Santini, E., & Quirk, G. J. (2007). Consolidation of fear extinction requires NMDA receptor-dependent bursting in the ventromedial prefrontal cortex. *Neuron, 53*(6), 871-880. doi: 10.1016/j.neuron.2007.02.021

Burstein, R., & Potrebic, S. (1993). Retrograde labeling of neurons in the spinal cord that project directly to the amygdala or the orbital cortex in the rat. *J Comp Neurol, 335*(4), 469-485.

Canteras, N. S., & Swanson, L. W. (1992). Projections of the ventral subiculum to the amygdala, septum, and hypothalamus: a PHAL anterograde tract-tracing study in the rat. *J Comp Neurol, 324*(2), 180-194.

Castro, C. A., Silbert, L. H., McNaughton, B. L., & Barnes, C. A. (1989). Recovery of spatial learning deficits after decay of electrically induced synaptic enhancement in the hippocampus. *Nature, 342*(6249), 545-548.

Cavus, I., & Teyler, T. (1996). Two forms of long-term potentiation in area CA1 activate different signal transduction cascades. *J Neurophysiol, 76*(5), 3038-3047.

Chang, C. H., & Maren, S. (2011). Medial prefrontal cortex activation facilitates re-extinction of fear in rats. *Learn Mem, 18*(4), 221-225. doi: 10.1101/lm.2070111

Chapman, P. F., Kairiss, E. W., Keenan, C. L., & Brown, T. H. (1990). Long-term synaptic potentiation in the amygdala. *Synapse, 6*(3), 271-278.

Chen, L. Y., Rex, C. S., Casale, M. S., Gall, C. M., & Lynch, G. (2007). Changes in synaptic morphology accompany actin signaling during LTP. *J Neurosci, 27*(20), 5363-5372. doi: 10.1523/JNEUROSCI.0164-07.2007

Chen, S., Wang, J., & Siegelbaum, S. A. (2001). Properties of hyperpolarization-activated pacemaker current defined by coassembly of HCN1 and HCN2 subunits and basal modulation by cyclic nucleotide. *J Gen Physiol, 117*(5), 491-504.

Chen, X., Yuan, L. L., Zhao, C., Birnbaum, S. G., Frick, A., Jung, W. E., . . . Johnston, D. (2006). Deletion of Kv4.2 gene eliminates dendritic A-type K+ current and

enhances induction of long-term potentiation in hippocampal CA1 pyramidal neurons. *J Neurosci, 26*(47), 12143-12151. doi: 10.1523/JNEUROSCI.2667-06.2006

Cheng, D. T., Knight, D. C., Smith, C. N., Stein, E. A., & Helmstetter, F. J. (2003). Functional MRI of human amygdala activity during Pavlovian fear conditioning: stimulus processing versus response expression. *Behav Neurosci, 117*(1), 3-10.

Chowdhury, N., Quinn, J. J., & Fanselow, M. S. (2005). Dorsal hippocampus involvement in trace fear conditioning with long, but not short, trace intervals in mice. *Behav Neurosci, 119*(5), 1396-1402. doi: 10.1037/0735-7044.119.5.1396

Christophe, E., Doerflinger, N., Lavery, D. J., Molnar, Z., Charpak, S., & Audinat, E. (2005). Two populations of layer v pyramidal cells of the mouse neocortex: development and sensitivity to anesthetics. *J Neurophysiol, 94*(5), 3357-3367. doi: 10.1152/jn.00076.2005

Clark, R. E., & Squire, L. R. (1998). Classical conditioning and brain systems: the role of awareness. *Science, 280*(5360), 77-81.

Clem, R. L., & Huganir, R. L. (2010). Calcium-permeable AMPA receptor dynamics mediate fear memory erasure. *Science, 330*(6007), 1108-1112.

Cohen-Matsliah, S. I., Motanis, H., Rosenblum, K., & Barkai, E. (2010). A novel role for protein synthesis in long-term neuronal plasticity: maintaining reduced postburst afterhyperpolarization. *J Neurosci, 30*(12), 4338-4342. doi: 10.1523/JNEUROSCI.5005-09.2010

Cohen, A. S., & Abraham, W. C. (1996). Facilitation of long-term potentiation by prior activation of metabotropic glutamate receptors. *J Neurophysiol, 76*(2), 953-962.

Cohen, A. S., Coussens, C. M., Raymond, C. R., & Abraham, W. C. (1999). Long-lasting increase in cellular excitability associated with the priming of LTP induction in rat hippocampus. *J Neurophysiol, 82*(6), 3139-3148.

Collingridge, G. L., Herron, C. E., & Lester, R. A. (1988). Frequency-dependent N-methyl-D-aspartate receptor-mediated synaptic transmission in rat hippocampus. *J Physiol, 399*, 301-312.

Collingridge, G. L., Kehl, S. J., & McLennan, H. (1983). Excitatory amino acids in synaptic transmission in the Schaffer collateral-commissural pathway of the rat hippocampus. *J Physiol, 334*, 33-46.

Colombo, P. J., Wetsel, W. C., & Gallagher, M. (1997). Spatial memory is related to hippocampal subcellular concentrations of calcium-dependent protein kinase C isoforms in young and aged rats. *Proc Natl Acad Sci U S A, 94*(25), 14195-14199.

Connors, B. W., Gutnick, M. J., & Prince, D. A. (1982). Electrophysiological properties of neocortical neurons in vitro. *J Neurophysiol, 48*(6), 1302-1320.

Corcoran, K. A., & Quirk, G. J. (2007). Activity in prelimbic cortex is necessary for the expression of learned, but not innate, fears. *J Neurosci, 27*(4), 840-844. doi: 10.1523/JNEUROSCI.5327-06.2007

Cormier, R. J., & Kelly, P. T. (1996). Glutamate-induced long-term potentiation enhances spontaneous EPSC amplitude but not frequency. *J Neurophysiol, 75*(5), 1909-1918.

Czerniawski, J., Yoon, T., & Otto, T. (2009). Dissociating space and trace in dorsal and ventral hippocampus. *Hippocampus, 19*(1), 20-32. doi: 10.1002/hipo.20469

Dalzell, L., Connor, S., Penner, M., Saari, M. J., Leboutillier, J. C., & Weeks, A. C. (2011). Fear conditioning is associated with synaptogenesis in the lateral amygdala. *Synapse, 65*(6), 513-519.

Davis, M., & Astrachan, D. I. (1978). Conditioned fear and startle magnitude: effects of different footshock or backshock intensities used in training. *J Exp Psychol Anim Behav Process, 4*(2), 95-103.

Davis, M., Redmond, D. E., Jr., & Baraban, J. M. (1979). Noradrenergic agonists and antagonists: effects on conditioned fear as measured by the potentiated startle paradigm. *Psychopharmacology (Berl), 65*(2), 111-118.

Day, M., Carr, D. B., Ulrich, S., Ilijic, E., Tkatch, T., & Surmeier, D. J. (2005). Dendritic excitability of mouse frontal cortex pyramidal neurons is shaped by the interaction among HCN, Kir2, and Kleak channels. *J Neurosci, 25*(38), 8776-8787. doi: 10.1523/JNEUROSCI.2650-05.2005

de Jonge, M. C., Black, J., Deyo, R. A., & Disterhoft, J. F. (1990). Learning-induced afterhyperpolarization reductions in hippocampus are specific for cell type and potassium conductance. *Exp Brain Res, 80*(3), 456-462.

DeFelipe, J., & Farinas, I. (1992). The pyramidal neuron of the cerebral cortex: morphological and chemical characteristics of the synaptic inputs. *Prog Neurobiol, 39*(6), 563-607.

Dembrow, N. C., Chitwood, R. A., & Johnston, D. (2010). Projection-specific neuromodulation of medial prefrontal cortex neurons. *J Neurosci, 30*(50), 16922-16937. doi: 10.1523/JNEUROSCI.3644-10.2010

Derkach, V. A., Oh, M. C., Guire, E. S., & Soderling, T. R. (2007). Regulatory mechanisms of AMPA receptors in synaptic plasticity. *Nat Rev Neurosci, 8*(2), 101-113. doi: 10.1038/nrn2055

Detert, J. A., Kampa, N. D., & Moyer, J. R., Jr. (2008). Differential effects of training intertrial interval on acquisition of trace and long-delay fear conditioning in rats. *Behav Neurosci, 122*(6), 1318-1327. doi: 10.1037/a0013512

Disterhoft, J. F., & Oh, M. M. (2006). Learning, aging and intrinsic neuronal plasticity. *Trends Neurosci, 29*(10), 587-599. doi: 10.1016/j.tins.2006.08.005

Donoghue, J. P., & Wise, S. P. (1982). The motor cortex of the rat: cytoarchitecture and microstimulation mapping. *J Comp Neurol, 212*(1), 76-88.

Doyere, V., Debiec, J., Monfils, M. H., Schafe, G. E., & LeDoux, J. E. (2007). Synapse-specific reconsolidation of distinct fear memories in the lateral amygdala. *Nat Neurosci, 10*(4), 414-416. doi: 10.1038/nn1871

Doyere, V., Redini-Del Negro, C., Dutrieux, G., Le Floch, G., Davis, S., & Laroche, S. (1995). Potentiation or depression of synaptic efficacy in the dentate gyrus is determined by the relationship between the conditioned and unconditioned stimulus in a classical conditioning paradigm in rats. *Behav Brain Res, 70*(1), 15-29.

Dudai, Y. (2004). The neurobiology of consolidations, or, how stable is the engram? *Annu Rev Psychol, 55*, 51-86. doi: 10.1146/annurev.psych.55.090902.142050

Dudek, S. M., & Bear, M. F. (1993). Bidirectional long-term modification of synaptic effectiveness in the adult and immature hippocampus. *J Neurosci, 13*(7), 2910-2918.

Duffy, S. N., Craddock, K. J., Abel, T., & Nguyen, P. V. (2001). Environmental enrichment modifies the PKA-dependence of hippocampal LTP and improves hippocampus-dependent memory. *Learn Mem, 8*(1), 26-34. doi: 10.1101/lm.36301

Dumitriu, D., Rodriguez, A., & Morrison, J. H. (2011). High-throughput, detailed, cell-specific neuroanatomy of dendritic spines using microinjection and confocal microscopy. *Nat Protoc, 6*(9), 1391-1411. doi: 10.1038/nprot.2011.389

Egorov, A. V., Hamam, B. N., Fransen, E., Hasselmo, M. E., & Alonso, A. A. (2002). Graded persistent activity in entorhinal cortex neurons. *Nature, 420*(6912), 173-178.

Eichenbaum, H. (1997). Declarative memory: insights from cognitive neurobiology. *Annu Rev Psychol, 48*, 547-572.

Elston, G. N. (2001). Interlaminar differences in the pyramidal cell phenotype in cortical areas 7 m and STP (the superior temporal polysensory area) of the macaque monkey. *Exp Brain Res, 138*(2), 141-152.

Endo, T., Tarusawa, E., Notomi, T., Kaneda, K., Hirabayashi, M., Shigemoto, R., & Isa, T. (2008). Dendritic Ih ensures high-fidelity dendritic spike responses of motion-sensitive neurons in rat superior colliculus. *J Neurophysiol, 99*(5), 2066-2076. doi: 10.1152/jn.00556.2007

Engert, F., & Bonhoeffer, T. (1999). Dendritic spine changes associated with hippocampal long-term synaptic plasticity. *Nature, 399*(6731), 66-70.

Eschenko, O., Magri, C., Panzeri, S., & Sara, S. J. (2012). Noradrenergic neurons of the locus coeruleus are phase locked to cortical up-down states during sleep. *Cereb Cortex, 22*(2), 426-435. doi: 10.1093/cercor/bhr121

Esclassan, F., Coutureau, E., Di Scala, G., & Marchand, A. R. (2009). Differential contribution of dorsal and ventral hippocampus to trace and delay fear conditioning. *Hippocampus, 19*(1), 33-44.

Ethell, I. M., & Pasquale, E. B. (2005). Molecular mechanisms of dendritic spine development and remodeling. *Prog Neurobiol, 75*(3), 161-205.

Eyre, M. D., Richter-Levin, G., Avital, A., & Stewart, M. G. (2003). Morphological changes in hippocampal dentate gyrus synapses following spatial learning in rats are transient. *Eur J Neurosci, 17*(9), 1973-1980.

Fanselow, M. S., & Dong, H. W. (2011). Are the dorsal and ventral hippocampus functionally distinct structures? *Neuron, 65*(1), 7-19.

Fanselow, M. S., & Poulos, A. M. (2005). The neuroscience of mammalian associative learning. *Annu Rev Psychol, 56*, 207-234.

Farber, J. L. (1981). The role of calcium in cell death. *Life Sci, 29*(13), 1289-1295.

Febo, M. (2011). Prefrontal cell firing in male rats during approach towards sexually receptive female: interactions with cocaine. *Synapse, 65*(4), 271-277. doi: 10.1002/syn.20843

Fedulov, V., Rex, C. S., Simmons, D. A., Palmer, L., Gall, C. M., & Lynch, G. (2007). Evidence that long-term potentiation occurs within individual hippocampal synapses during learning. *J Neurosci, 27*(30), 8031-8039.

Figurov, A., Pozzo-Miller, L. D., Olafsson, P., Wang, T., & Lu, B. (1996). Regulation of synaptic responses to high-frequency stimulation and LTP by neurotrophins in the hippocampus. *Nature, 381*(6584), 706-709.

Fortin, N. J., Agster, K. L., & Eichenbaum, H. B. (2002). Critical role of the hippocampus in memory for sequences of events. *Nat Neurosci, 5*(5), 458-462.

Foster, T. C. (2007). Calcium homeostasis and modulation of synaptic plasticity in the aged brain. *Aging Cell, 6*(3), 319-325.

Frankland, P. W., & Bontempi, B. (2005). The organization of recent and remote memories. *Nat Rev Neurosci, 6*(2), 119-130.

Frankland, P. W., Josselyn, S. A., Anagnostaras, S. G., Kogan, J. H., Takahashi, E., & Silva, A. J. (2004). Consolidation of CS and US representations in associative fear conditioning. *Hippocampus, 14*(5), 557-569.

Gabbott, P. L., & Bacon, S. J. (1996). Local circuit neurons in the medial prefrontal cortex (areas 24a,b,c, 25 and 32) in the monkey: I. Cell morphology and morphometrics. *J Comp Neurol, 364*(4), 567-608. doi: 10.1002/(SICI)1096-9861(19960122)364:4<567::AID-CNE1>3.0.CO;2-1

Gabbott, P. L., Warner, T. A., Jays, P. R., Salway, P., & Busby, S. J. (2005). Prefrontal cortex in the rat: projections to subcortical autonomic, motor, and limbic centers. *J Comp Neurol, 492*(2), 145-177.

Gaillard, F., & Sauve, Y. (1995). Fetal Tissue Allografts in the Central Visual System of Rodents. In H. Kolb, E. Fernandez & R. Nelson (Eds.), *Webvision: The Organization of the Retina and Visual System*. Salt Lake City (UT).

Ganguly, K., Kiss, L., & Poo, M. (2000). Enhancement of presynaptic neuronal excitability by correlated presynaptic and postsynaptic spiking. *Nat Neurosci, 3*(10), 1018-1026.

Gant, J. C., & Thibault, O. (2009). Action potential throughput in aged rat hippocampal neurons: regulation by selective forms of hyperpolarization. *Neurobiol Aging, 30*(12), 2053-2064.

Garcia, R., Vouimba, R. M., Baudry, M., & Thompson, R. F. (1999). The amygdala modulates prefrontal cortex activity relative to conditioned fear. *Nature, 402*(6759), 294-296.

Gasparini, S., & DiFrancesco, D. (1999). Action of serotonin on the hyperpolarization-activated cation current (Ih) in rat CA1 hippocampal neurons. *Eur J Neurosci, 11*(9), 3093-3100.

Geinisman, Y. (1993). Perforated axospinous synapses with multiple, completely partitioned transmission zones: probable structural intermediates in synaptic plasticity. *Hippocampus, 3*(4), 417-433.

Geinisman, Y. (2000). Structural synaptic modifications associated with hippocampal LTP and behavioral learning. *Cereb Cortex, 10*(10), 952-962.

Geinisman, Y., Berry, R. W., Disterhoft, J. F., Power, J. M., & Van der Zee, E. A. (2001). Associative learning elicits the formation of multiple-synapse boutons. *J Neurosci, 21*(15), 5568-5573.

Gilmartin, M. R., & Helmstetter, F. J. (2010). Trace and contextual fear conditioning require neural activity and NMDA receptor-dependent transmission in the medial prefrontal cortex. *Learn Mem, 17*(6), 289-296.

Gilmartin, M. R., & McEchron, M. D. (2005). Single neurons in the medial prefrontal cortex of the rat exhibit tonic and phasic coding during trace fear conditioning. *Behav Neurosci, 119*(6), 1496-1510.

Gilmartin, M. R., Miyawaki, H., Helmstetter, F. J., & Diba, K. (2013). Prefrontal activity links nonoverlapping events in memory. *J Neurosci, 33*(26), 10910-10914. doi: 10.1523/JNEUROSCI.0144-13.2013

Globus, A., & Scheibel, A. B. (1966). Loss of dendrite spines as an index of pre-synaptic terminal patterns. *Nature, 212*(5061), 463-465.

Gray, T. S., Carney, M. E., & Magnuson, D. J. (1989). Direct projections from the central amygdaloid nucleus to the hypothalamic paraventricular nucleus: possible role in stress-induced adrenocorticotropin release. *Neuroendocrinology, 50*(4), 433-446.

Groh, A., Meyer, H. S., Schmidt, E. F., Heintz, N., Sakmann, B., & Krieger, P. (2010). Cell-type specific properties of pyramidal neurons in neocortex underlying a layout that is modifiable depending on the cortical area. *Cereb Cortex, 20*(4), 826-836. doi: 10.1093/cercor/bhp152

Gruart, A., Munoz, M. D., & Delgado-Garcia, J. M. (2006). Involvement of the CA3-CA1 synapse in the acquisition of associative learning in behaving mice. *J Neurosci, 26*(4), 1077-1087.

Grutzendler, J., Kasthuri, N., & Gan, W. B. (2002). Long-term dendritic spine stability in the adult cortex. *Nature, 420*(6917), 812-816.

Gu, J., Lee, C. W., Fan, Y., Komlos, D., Tang, X., Sun, C., . . . Zheng, J. Q. (2010). ADF/cofilin-mediated actin dynamics regulate AMPA receptor trafficking during synaptic plasticity. *Nat Neurosci, 13*(10), 1208-1215.

Gulledge, A. T., Dasari, S., Onoue, K., Stephens, E. K., Hasse, J. M., & Avesar, D. (2013). A sodium-pump-mediated afterhyperpolarization in pyramidal neurons. *J Neurosci, 33*(32), 13025-13041. doi: 10.1523/JNEUROSCI.0220-13.2013

Gurvits, T. V., Shenton, M. E., Hokama, H., Ohta, H., Lasko, N. B., Gilbertson, M. W., . . . Pitman, R. K. (1996). Magnetic resonance imaging study of hippocampal volume in chronic, combat-related posttraumatic stress disorder. *Biol Psychiatry, 40*(11), 1091-1099.

Han, C. J., O'Tuathaigh, C. M., van Trigt, L., Quinn, J. J., Fanselow, M. S., Mongeau, R., Anderson, D. J. (2003). Trace but not delay fear conditioning requires attention and the anterior cingulate cortex. *Proc Natl Acad Sci U S A, 100*(22), 13087-13092. doi: 10.1073/pnas.2132313100

Hattox, A. M., & Nelson, S. B. (2007). Layer V neurons in mouse cortex projecting to different targets have distinct physiological properties. *J Neurophysiol, 98*(6), 3330-3340.

Hebb, D. O. (1949). *The organization of behavior*. New York: Wiley.

Heidbreder, C. A., & Groenewegen, H. J. (2003). The medial prefrontal cortex in the rat: evidence for a dorso-ventral distinction based upon functional and anatomical characteristics. *Neurosci Biobehav Rev, 27*(6), 555-579.

Herry, C., & Garcia, R. (2002). Prefrontal cortex long-term potentiation, but not long-term depression, is associated with the maintenance of extinction of learned fear in mice. *J Neurosci, 22*(2), 577-583.

Herry, C., Vouimba, R. M., & Garcia, R. (1999). Plasticity in the mediodorsal thalamo-prefrontal cortical transmission in behaving mice. *J Neurophysiol, 82*(5), 2827-2832.

Hoffman, D. A., & Johnston, D. (1998). Downregulation of transient K+ channels in dendrites of hippocampal CA1 pyramidal neurons by activation of PKA and PKC. *J Neurosci, 18*(10), 3521-3528.

Hongpaisan, J., & Alkon, D. L. (2007). A structural basis for enhancement of long-term associative memory in single dendritic spines regulated by PKC. *Proc Natl Acad Sci U S A, 104*(49), 19571-19576.

Hoover, W. B., & Vertes, R. P. (2007). Anatomical analysis of afferent projections to the medial prefrontal cortex in the rat. *Brain Struct Funct, 212*(2), 149-179.

Hosokawa, T., Rusakov, D. A., Bliss, T. V., & Fine, A. (1995). Repeated confocal imaging of individual dendritic spines in the living hippocampal slice: evidence for changes in length and orientation associated with chemically induced LTP. *J Neurosci, 15*(8), 5560-5573.

Huang, Z., Walker, M. C., & Shah, M. M. (2009). Loss of dendritic HCN1 subunits enhances cortical excitability and epileptogenesis. *J Neurosci, 29*(35), 10979-10988.

Hume, R. I., Dingledine, R., & Heinemann, S. F. (1991). Identification of a site in glutamate receptor subunits that controls calcium permeability. *Science, 253*(5023), 1028-1031.

Hurley, K. M., Herbert, H., Moga, M. M., & Saper, C. B. (1991). Efferent projections of the infralimbic cortex of the rat. *J Comp Neurol, 308*(2), 249-276.

Husi, H., Ward, M. A., Choudhary, J. S., Blackstock, W. P., & Grant, S. G. (2000). Proteomic analysis of NMDA receptor-adhesion protein signaling complexes. *Nat Neurosci, 3*(7), 661-669.

Hylin, M. J., Orsi, S. A., Moore, A. N., & Dash, P. K. (2013). Disruption of the perineuronal net in the hippocampus or medial prefrontal cortex impairs fear conditioning. *Learn Mem, 20*(5), 267-273. doi: 10.1101/lm.030197.112

Impey, S., Obrietan, K., Wong, S. T., Poser, S., Yano, S., Wayman, G., Storm, D. R. (1998). Cross talk between ERK and PKA is required for Ca2+ stimulation of CREB-dependent transcription and ERK nuclear translocation. *Neuron, 21*(4), 869-883.

Ji, G., & Neugebauer, V. (2012). Modulation of medial prefrontal cortical activity using in vivo recordings and optogenetics. *Mol Brain, 5*, 36. doi: 10.1186/1756-6606-5-36

Johnson, L. R., Ledoux, J. E., & Doyere, V. (2009). Hebbian reverberations in emotional memory micro circuits. *Front Neurosci, 3*(2), 198-205. doi: 10.3389/neuro.01.027.2009

Kaczorowski, C. C. (2011). Bidirectional pattern-specific plasticity of the slow afterhyperpolarization in rats: role for high-voltage activated Ca2+ channels and I h. *Eur J Neurosci, 34*(11), 1756-1765.

Kaczorowski, C. C., Davis, S. J., & Moyer, J. R., Jr. (2012). Aging redistributes medial prefrontal neuronal excitability and impedes extinction of trace fear conditioning. *Neurobiol Aging, 33*(8), 1744-1757.

Kaczorowski, C. C., & Disterhoft, J. F. (2009). Memory deficits are associated with impaired ability to modulate neuronal excitability in middle-aged mice. *Learn. Mem., 16*, 362-366.

Kaczorowski, C. C., Sametsky, E., Shah, S., Vassar, R., & Disterhoft, J. F. (2009). Mechanisms underlying basal and learning-related intrinsic excitability in a mouse model of Alzheimer's disease. *Neurobiol Aging*.

Kaczorowski, C. C., Sametsky, E., Shah, S., Vassar, R., & Disterhoft, J. F. (2011). Mechanisms underlying basal and learning-related intrinsic excitability in a mouse model of Alzheimer's disease. *Neurobiol Aging, 32*(8), 1452-1465.

Kandel, E. R. (2001). The molecular biology of memory storage: a dialogue between genes and synapses. *Science, 294*(5544), 1030-1038.

Katz, L. C., Burkhalter, A., & Dreyer, W. J. (1984). Fluorescent latex microspheres as a retrograde neuronal marker for in vivo and in vitro studies of visual cortex. *Nature, 310*(5977), 498-500.

Kennedy, M. B. (1998). Signal transduction molecules at the glutamatergic postsynaptic membrane. *Brain Res Brain Res Rev, 26*(2-3), 243-257.

Kennedy, M. B. (2000). Signal-processing machines at the postsynaptic density. *Science, 290*(5492), 750-754.

Kholodar-Smith, D. B., Boguszewski, P., & Brown, T. H. (2008). Auditory trace fear conditioning requires perirhinal cortex. *Neurobiol Learn Mem, 90*(3), 537-543.

Kim, J. J., Clark, R. E., & Thompson, R. F. (1995). Hippocampectomy impairs the memory of recently, but not remotely, acquired trace eyeblink conditioned responses. *Behav Neurosci, 109*(2), 195-203.

Kim, J. J., & Fanselow, M. S. (1992). Modality-specific retrograde amnesia of fear. *Science, 256*(5057), 675-677.

Kim, J. J., & Jung, M. W. (2006). Neural circuits and mechanisms involved in Pavlovian fear conditioning: a critical review. *Neurosci Biobehav Rev, 30*(2), 188-202.

Kim, J. J., Lee, H. J., Han, J. S., & Packard, M. G. (2001). Amygdala is critical for stress-induced modulation of hippocampal long-term potentiation and learning. *J Neurosci, 21*(14), 5222-5228.

Kjelstrup, K. G., Tuvnes, F. A., Steffenach, H. A., Murison, R., Moser, E. I., & Moser, M. B. (2002). Reduced fear expression after lesions of the ventral hippocampus. *Proc Natl Acad Sci U S A, 99*(16), 10825-10830.

Kleim, J. A., Barbay, S., Cooper, N. R., Hogg, T. M., Reidel, C. N., Remple, M. S., & Nudo, R. J. (2002). Motor learning-dependent synaptogenesis is localized to functionally reorganized motor cortex. *Neurobiol Learn Mem, 77*(1), 63-77.

Kleim, J. A., Hogg, T. M., VandenBerg, P. M., Cooper, N. R., Bruneau, R., & Remple, M. (2004). Cortical synaptogenesis and motor map reorganization occur during late, but not early, phase of motor skill learning. *J Neurosci, 24*(3), 628-633.

Knight, D. C., Cheng, D. T., Smith, C. N., Stein, E. A., & Helmstetter, F. J. (2004). Neural substrates mediating human delay and trace fear conditioning. *J Neurosci, 24*(1), 218-228.

Knight, D. C., Nguyen, H. T., & Bandettini, P. A. (2006). The role of awareness in delay and trace fear conditioning in humans. *Cogn Affect Behav Neurosci, 6*(2), 157-162.

Knight, D. C., Smith, C. N., Stein, E. A., & Helmstetter, F. J. (1999). Functional MRI of human Pavlovian fear conditioning: patterns of activation as a function of learning. *Neuroreport, 10*(17), 3665-3670.

Koike, H., Mano, N., Okada, Y., & Oshima, T. (1972). Activities of the sodium pump in cat pyramidal tract cell studied with intracellular injection of sodium ions. *Exp Brain Res, 14*(5), 449-462.

Kopec, C. D., Li, B., Wei, W., Boehm, J., & Malinow, R. (2006). Glutamate receptor exocytosis and spine enlargement during chemically induced long-term potentiation. *J Neurosci, 26*(7), 2000-2009.

Kozorovitskiy, Y., Gross, C. G., Kopil, C., Battaglia, L., McBreen, M., Stranahan, A. M., & Gould, E. (2005). Experience induces structural and biochemical changes in the adult primate brain. *Proc Natl Acad Sci U S A, 102*(48), 17478-17482.

Kramar, E. A., Lin, B., Lin, C. Y., Arai, A. C., Gall, C. M., & Lynch, G. (2004). A novel mechanism for the facilitation of theta-induced long-term potentiation by brain-derived neurotrophic factor. *J Neurosci, 24*(22), 5151-5161.

Krettek, J. E., & Price, J. L. (1978). A description of the amygdaloid complex in the rat and cat with observations on intra-amygdaloid axonal connections. *J Comp Neurol, 178*(2), 255-280.

Kumar, A., & Foster, T. C. (2004). Enhanced long-term potentiation during aging is masked by processes involving intracellular calcium stores. *J Neurophysiol, 91*(6), 2437-2444.

Kuo, A. G., Lee, G., & Disterhoft, J. F. (2006). Simultaneous training on two hippocampus-dependent tasks facilitates acquisition of trace eyeblink conditioning. *Learn Mem, 13*(2), 201-207.

LaBar, K. S., Gatenby, J. C., Gore, J. C., LeDoux, J. E., & Phelps, E. A. (1998). Human amygdala activation during conditioned fear acquisition and extinction: a mixed-trial fMRI study. *Neuron, 20*(5), 937-945.

LaBar, K. S., & LeDoux, J. E. (1996). Partial disruption of fear conditioning in rats with unilateral amygdala damage: correspondence with unilateral temporal lobectomy in humans. *Behav Neurosci, 110*(5), 991-997.

LaBar, K. S., LeDoux, J. E., Spencer, D. D., & Phelps, E. A. (1995). Impaired fear conditioning following unilateral temporal lobectomy in humans. *J Neurosci, 15*(10), 6846-6855.

Lai, C. S., Franke, T. F., & Gan, W. B. (2012). Opposite effects of fear conditioning and extinction on dendritic spine remodelling. *Nature, 483*(7387), 87-91.

Lang, C., Barco, A., Zablow, L., Kandel, E. R., Siegelbaum, S. A., & Zakharenko, S. S. (2004). Transient expansion of synaptically connected dendritic spines upon induction of hippocampal long-term potentiation. *Proc Natl Acad Sci U S A, 101*(47), 16665-16670.

Larkman, A. U. (1991). Dendritic morphology of pyramidal neurones of the visual cortex of the rat: III. Spine distributions. *J Comp Neurol, 306*(2), 332-343.

Larkman, A. U., Hannay, T., Stratford, K., & Jack, J. (1992). Presynaptic release probability influences the locus of long-term potentiation. *Nature, 360*(6399), 70-73.

Larkman, A. U., & Mason, A. (1990). Correlations between morphology and electrophysiology of pyramidal neurons in slices of rat visual cortex. I. Establishment of cell classes. *J Neurosci, 10*(5), 1407-1414.

Laroche, S., Jay, T. M., & Thierry, A. M. (1990). Long-term potentiation in the prefrontal cortex following stimulation of the hippocampal CA1/subicular region. *Neurosci Lett, 114*(2), 184-190.

Laviolette, S. R., Lipski, W. J., & Grace, A. A. (2005). A subpopulation of neurons in the medial prefrontal cortex encodes emotional learning with burst and frequency codes through a dopamine D4 receptor-dependent basolateral amygdala input. *J Neurosci, 25*(26), 6066-6075.

Lebron, K., Milad, M. R., & Quirk, G. J. (2004). Delayed recall of fear extinction in rats with lesions of ventral medial prefrontal cortex. *Learn Mem, 11*(5), 544-548. doi: 10.1101/lm.78604

LeDoux, J. E. (2000). Emotion circuits in the brain. *Annu Rev Neurosci, 23*, 155-184.

LeDoux, J. E., Cicchetti, P., Xagoraris, A., & Romanski, L. M. (1990). The lateral amygdaloid nucleus: sensory interface of the amygdala in fear conditioning. *J Neurosci, 10*(4), 1062-1069.

LeDoux, J. E., Farb, C., & Ruggiero, D. A. (1990). Topographic organization of neurons in the acoustic thalamus that project to the amygdala. *J Neurosci, 10*(4), 1043-1054.

LeDoux, J. E., Iwata, J., Cicchetti, P., & Reis, D. J. (1988). Different projections of the central amygdaloid nucleus mediate autonomic and behavioral correlates of conditioned fear. *J Neurosci, 8*(7), 2517-2529.

Lee, H. K., Barbarosie, M., Kameyama, K., Bear, M. F., & Huganir, R. L. (2000). Regulation of distinct AMPA receptor phosphorylation sites during bidirectional synaptic plasticity. *Nature, 405*(6789), 955-959.

Leuner, B., Falduto, J., & Shors, T. J. (2003). Associative memory formation increases the observation of dendritic spines in the hippocampus. *J Neurosci, 23*(2), 659-665.

Lewis, A. S., Estep, C. M., & Chetkovich, D. M. (2010). The fast and slow ups and downs of HCN channel regulation. *Channels (Austin), 4*(3), 215-231.

Li, B., Luo, C., Tang, W., Chen, Z., Li, Q., Hu, B., . . . Feng, H. (2012). Role of HCN channels in neuronal hyperexcitability after subarachnoid hemorrhage in rats. *J Neurosci, 32*(9), 3164-3175. doi: 10.1523/JNEUROSCI.5143-11.2012

Liu, J., Dobrzynski, H., Yanni, J., Boyett, M. R., & Lei, M. (2007). Organisation of the mouse sinoatrial node: structure and expression of HCN channels. *Cardiovasc Res, 73*(4), 729-738. doi: 10.1016/j.cardiores.2006.11.016

Llano, D. A., & Sherman, S. M. (2009). Differences in intrinsic properties and local network connectivity of identified layer 5 and layer 6 adult mouse auditory corticothalamic neurons support a dual corticothalamic projection hypothesis. *Cereb Cortex, 19*(12), 2810-2826.

Lorincz, A., Notomi, T., Tamas, G., Shigemoto, R., & Nusser, Z. (2002). Polarized and compartment-dependent distribution of HCN1 in pyramidal cell dendrites. *Nat Neurosci, 5*(11), 1185-1193. doi: 10.1038/nn962

LoTurco, J. L., Coulter, D. A., & Alkon, D. L. (1988). Enhancement of synaptic potentials in rabbit CA1 pyramidal neurons following classical conditioning. *Proc Natl Acad Sci U S A, 85*(5), 1672-1676.

Ludwig, A., Budde, T., Stieber, J., Moosmang, S., Wahl, C., Holthoff, K., . . . Hofmann, F. (2003). Absence epilepsy and sinus dysrhythmia in mice lacking the pacemaker channel HCN2. *Embo J, 22*(2), 216-224. doi: 10.1093/emboj/cdg032

Luscher, C., Nicoll, R. A., Malenka, R. C., & Muller, D. (2000). Synaptic plasticity and dynamic modulation of the postsynaptic membrane. *Nat Neurosci, 3*(6), 545-550.

Luthi, A., & McCormick, D. A. (1998). H-current: properties of a neuronal and network pacemaker. *Neuron, 21*(1), 9-12.

Lynch, G., Larson, J., Kelso, S., Barrionuevo, G., & Schottler, F. (1983). Intracellular injections of EGTA block induction of hippocampal long-term potentiation. *Nature, 305*(5936), 719-721.

Lynch, M. A. (2004). Long-term potentiation and memory. *Physiol Rev, 84*(1), 87-136.

Madison, D. V., & Nicoll, R. A. (1984). Control of the repetitive discharge of rat CA 1 pyramidal neurones in vitro. *J Physiol, 354*, 319-331.

Magee, J. C. (1998). Dendritic hyperpolarization-activated currents modify the integrative properties of hippocampal CA1 pyramidal neurons. *J Neurosci, 18*(19), 7613-7624.

Magee, J. C. (1999). Dendritic Ih normalizes temporal summation in hippocampal CA1 neurons. *Nat Neurosci, 2*(9), 848.

Majchrzak, M., Ferry, B., Marchand, A. R., Herbeaux, K., Seillier, A., & Barbelivien, A. (2006). Entorhinal cortex lesions disrupt fear conditioning to background context but spare fear conditioning to a tone in the rat. *Hippocampus, 16*(2), 114-124.

Malik, R., & Chattarji, S. (2012). Enhanced intrinsic excitability and EPSP-spike coupling accompany enriched environment-induced facilitation of LTP in hippocampal CA1 pyramidal neurons. *J Neurophysiol, 107*(5), 1366-1378.

Malinow, R., & Malenka, R. C. (2002). AMPA receptor trafficking and synaptic plasticity. *Annu Rev Neurosci, 25*, 103-126.

Marek, R., Strobel, C., Bredy, T. W., & Sah, P. (2013). The amygdala and medial prefrontal cortex: partners in the fear circuit. *J Physiol, 591*(Pt 10), 2381-2391. doi: 10.1113/jphysiol.2012.248575

Maren, S. (2011). Seeking a spotless mind: extinction, deconsolidation, and erasure of fear memory. *Neuron, 70*(5), 830-845.

Maren, S., Aharonov, G., & Fanselow, M. S. (1997). Neurotoxic lesions of the dorsal hippocampus and Pavlovian fear conditioning in rats. *Behav Brain Res, 88*(2), 261-274.

Maren, S., & Quirk, G. J. (2004). Neuronal signalling of fear memory. *Nat Rev Neurosci, 5*(11), 844-852.

Marshall, L., Helgadottir, H., Molle, M., & Born, J. (2006). Boosting slow oscillations during sleep potentiates memory. *Nature, 444*(7119), 610-613. doi: 10.1038/nature05278

Mason, A., & Larkman, A. U. (1990). Correlations between morphology and electrophysiology of pyramidal neurons in slices of rat visual cortex. II. Electrophysiology. *J Neurosci, 10*(5), 1415-1428.

Matsuzaki, M., Honkura, N., Ellis-Davies, G. C., & Kasai, H. (2004). Structural basis of long-term potentiation in single dendritic spines. *Nature, 429*(6993), 761-766.

Maviel, T., Durkin, T. P., Menzaghi, F., & Bontempi, B. (2004). Sites of neocortical reorganization critical for remote spatial memory. *Science, 305*(5680), 96-99.

McCormick, D. A., & Pape, H. C. (1990). Properties of a hyperpolarization-activated cation current and its role in rhythmic oscillation in thalamic relay neurones. *J Physiol, 431*, 291-318.

McDonald, A. J. (1991). Organization of amygdaloid projections to the prefrontal cortex and associated striatum in the rat. *Neuroscience, 44*(1), 1-14.

McDonald, A. J. (1998). Cortical pathways to the mammalian amygdala. *Prog Neurobiol, 55*(3), 257-332.

McDonald, A. J., & Augustine, J. R. (1993). Localization of GABA-like immunoreactivity in the monkey amygdala. *Neuroscience, 52*(2), 281-294.

McDonald, A. J., Mascagni, F., & Guo, L. (1996). Projections of the medial and lateral prefrontal cortices to the amygdala: a Phaseolus vulgaris leucoagglutinin study in the rat. *Neuroscience, 71*(1), 55-75.

McEchron, M. D., Bouwmeester, H., Tseng, W., Weiss, C., & Disterhoft, J. F. (1998). Hippocampectomy disrupts auditory trace fear conditioning and contextual fear conditioning in the rat. *Hippocampus, 8*(6), 638-646.

McGinty, V. B., & Grace, A. A. (2008). Selective activation of medial prefrontal-to-accumbens projection neurons by amygdala stimulation and Pavlovian conditioned stimuli. *Cereb Cortex, 18*(8), 1961-1972. doi: 10.1093/cercor/bhm223

McKay, B. M., Matthews, E. A., Oliveira, F. A., & Disterhoft, J. F. (2009). Intrinsic neuronal excitability is reversibly altered by a single experience in fear conditioning. *J Neurophysiol, 102*(5), 2763-2770. doi: 00347.2009 [pii] 10.1152/jn.00347.2009

McKernan, M. G., & Shinnick-Gallagher, P. (1997). Fear conditioning induces a lasting potentiation of synaptic currents in vitro. N*ature, 390(*6660), 607-611.

Medini, P. (2011). Layer- and cell-type-specific subthreshold and suprathreshold effects of long-term monocular deprivation in rat visual cortex. J *Neurosci, 31(*47), 17134-17148. doi: 10.1523/JNEUROSCI.2951-11.2011

Metherate, R., Cox, C. L., & Ashe, J. H. (1992). Cellular bases of neocortical activation: modulation of neural oscillations by the nucleus basalis and endogenous acetylcholine. J *Neurosci, 12(*12), 4701-4711.

Milad, M. R., & Quirk, G. J. (2002). Neurons in medial prefrontal cortex signal memory for fear extinction. N*ature, 420(*6911), 70-74.

Milad, M. R., Vidal-Gonzalez, I., & Quirk, G. J. (2004). Electrical stimulation of medial prefrontal cortex reduces conditioned fear in a temporally specific manner. B*ehav Neurosci, 118(*2), 389-394.

Miller, C. A., & Marshall, J. F. (2005). Molecular substrates for retrieval and reconsolidation of cocaine-associated contextual memory. N*euron, 47(*6), 873-884.

Miyake, A., Friedman, N. P., Emerson, M. J., Witzki, A. H., Howerter, A., & Wager, T. D. (2000). The unity and diversity of executive functions and their contributions to complex "Frontal Lobe" tasks: a latent variable analysis. C*ogn Psychol, 41(*1), 49-100.

Molnar, Z., & Cheung, A. F. (2006). Towards the classification of subpopulations of layer V pyramidal projection neurons. N*eurosci Res, 55(*2), 105-115. doi: 10.1016/j.neures.2006.02.008

Molyneaux, B. J., Arlotta, P., Fame, R. M., MacDonald, J. L., MacQuarrie, K. L., & Macklis, J. D. (2009). Novel subtype-specific genes identify distinct subpopulations of callosal projection neurons. J *Neurosci, 29(*39), 12343-12354.

Molyneaux, B. J., Arlotta, P., Menezes, J. R., & Macklis, J. D. (2007). Neuronal subtype specification in the cerebral cortex. N*at Rev Neurosci, 8(*6), 427-437.

Moore, A., & Malinowski, P. (2009). Meditation, mindfulness and cognitive flexibility. C*onscious Cogn, 18(*1), 176-186.

Morgan, M. A., & LeDoux, J. E. (1995). Differential contribution of dorsal and ventral medial prefrontal cortex to the acquisition and extinction of conditioned fear in rats. B*ehav Neurosci, 109(*4), 681-688.

Morgan, M. A., Schulkin, J., & LeDoux, J. E. (2003). Ventral medial prefrontal cortex and emotional perseveration: the memory for prior extinction training. B*ehav Brain Res, 146(*1-2), 121-130.

Morishima, M., & Kawaguchi, Y. (2006). Recurrent connection patterns of corticostriatal pyramidal cells in frontal cortex. J *Neurosci, 26(*16), 4394-4405. doi: 10.1523/JNEUROSCI.0252-06.2006

Morris, R. G., Anderson, E., Lynch, G., & Baudry, M. (1986). Selective impairment of learning and blockade of long-term potentiation by an N-methyl-D-aspartate receptor antagonist, AP5. N*ature, 319(*6056), 774-776.

Morris, R. G., Garrud, P., Rawlins, J. N., & O'Keefe, J. (1982). Place navigation impaired in rats with hippocampal lesions. N*ature, 297(*5868), 681-683.

Moseley, A. E., Williams, M. T., Schaefer, T. L., Bohanan, C. S., Neumann, J. C., Behbehani, M. M., . . . Lingrel, J. B. (2007). Deficiency in Na,K-ATPase alpha isoform genes alters spatial learning, motor activity, and anxiety in mice. J *Neurosci, 27(*3), 616-626. doi: 10.1523/JNEUROSCI.4464-06.2007

Moser, E. I., Krobert, K. A., Moser, M. B., & Morris, R. G. (1998). Impaired spatial learning after saturation of long-term potentiation. S*cience, 281(*5385), 2038-2042.

Moser, M. B., & Moser, E. I. (1998). Functional differentiation in the hippocampus. H*ippocampus, 8(*6), 608-619.

Moser, M. B., Moser, E. I., Forrest, E., Andersen, P., & Morris, R. G. (1995). Spatial learning with a minislab in the dorsal hippocampus. P*roc Natl Acad Sci U S A, 92(*21), 9697-9701.

Moyer, J. R., Jr., & Brown, T. H. (2006). Impaired trace and contextual fear conditioning in aged rats. B*ehav Neurosci, 120(*3), 612-624.

Moyer, J.R., Jr. & Brown, T.H. (2007). Visually-guided patch-clamp recordings in brain slices. In: Advanced Techniques for Patch-Clamp Analysis, 3rd ed. (Walz, W., ed.), pp. 169-227, Humana Press, Totowa, NJ.

Moyer, J. R., Jr., Deyo, R. A., & Disterhoft, J. F. (1990). Hippocampectomy disrupts trace eye-blink conditioning in rabbits. B*ehav Neurosci, 102(*2), 243-252.

Moyer, J. R., Jr., Power, J. M., Thompson, L. T., & Disterhoft, J. F. (2000). Increased excitability of aged rabbit CA1 neurons after trace eyeblink conditioning. J *Neurosci, 20(*14), 5476-5482.

Moyer, J. R., Jr., Thompson, L. T., & Disterhoft, J. F. (1996). Trace eyeblink conditioning increases CA1 excitability in a transient and learning-specific manner. J *Neurosci., 16(*17), 5536-5546.

Muller, W., Petrozzino, J. J., Griffith, L. C., Danho, W., & Connor, J. A. (1992). Specific involvement of Ca(2+)-calmodulin kinase II in cholinergic modulation of neuronal responsiveness. J *Neurophysiol, 68(*6), 2264-2269.

Nabavi, S., Fox, R., Proulx, C. D., Lin, J. Y., Tsien, R. Y., & Malinow, R. (2014). Engineering a memory with LTD and LTP. N*ature, 511(*7509), 348-352. doi: 10.1038/nature13294

Nader, K., & Einarsson, E. O. (2010). Memory reconsolidation: an update. A*nn N Y Acad Sci, 1191,* 27-41.

Nader, K., Schafe, G. E., & Le Doux, J. E. (2000). Fear memories require protein synthesis in the amygdala for reconsolidation after retrieval. N*ature, 406(*6797), 722-726.

Neafsey, E. J. (1990). Prefrontal cortical control of the autonomic nervous system: anatomical and physiological observations. P*rog Brain Res, 85,* 147-165; discussion 165-146.

Nguyen, P. V., Abel, T., & Kandel, E. R. (1994). Requirement of a critical period of transcription for induction of a late phase of LTP. S*cience, 265(*5175), 1104-1107.

Nicholson, D. A., Yoshida, R., Berry, R. W., Gallagher, M., & Geinisman, Y. (2004). Reduction in size of perforated postsynaptic densities in hippocampal axospinous synapses and age-related spatial learning impairments. J *Neurosci, 24(*35), 7648-7653.

Nikmaram, M. R., Boyett, M. R., Kodama, I., Suzuki, R., & Honjo, H. (1997). Variation in effects of Cs+, UL-FS-49, and ZD-7288 within sinoatrial node. A*m J Physiol, 272(*6 Pt 2), H2782-2792.

Nolan, M. F., Malleret, G., Dudman, J. T., Buhl, D. L., Santoro, B., Gibbs, E., . . . Morozov, A. (2004). A behavioral role for dendritic integration: HCN1 channels constrain spatial memory and plasticity at inputs to distal dendrites of CA1 pyramidal neurons. C*ell, 119(*5), 719-732.

Nolan, M. F., Malleret, G., Lee, K. H., Gibbs, E., Dudman, J. T., Santoro, B., . . . Morozov, A. (2003). The hyperpolarization-activated HCN1 channel is important for motor learning and neuronal integration by cerebellar Purkinje cells. C*ell, 115(*5), 551-564.

Nusser, Z., Lujan, R., Laube, G., Roberts, J. D., Molnar, E., & Somogyi, P. (1998). Cell type and pathway dependence of synaptic AMPA receptor number and variability in the hippocampus. N*euron, 21(*3), 545-559.

O'Keefe, J., & Dostrovsky, J. (1971). The hippocampus as a spatial map. Preliminary evidence from unit activity in the freely-moving rat. B*rain Res, 34(*1), 171-175.

O'Malley, A., O'Connell, C., Murphy, K. J., & Regan, C. M. (2000). Transient spine density increases in the mid-molecular layer of hippocampal dentate gyrus accompany consolidation of a spatial learning task in the rodent. N*euroscience, 99(*2), 229-232.

Oh, M. M., Kuo, A. G., Wu, W. W., Sametsky, E. A., & Disterhoft, J. F. (2003). Watermaze learning enhances excitability of CA1 pyramidal neurons. J *Neurophysiol, 90(*4), 2171-2179.

Oh, M. M., McKay, B. M., Power, J. M., & Disterhoft, J. F. (2009). Learning-related postburst afterhyperpolarization reduction in CA1 pyramidal neurons is mediated by protein kinase A. P*roc Natl Acad Sci U S A, 106(*5), 1620-1625.

Ohno, M., Sametsky, E. A., Silva, A. J., & Disterhoft, J. F. (2006). Differential effects of alphaCaMKII mutation on hippocampal learning and changes in intrinsic neuronal excitability. E*ur J Neurosci, 23(*8), 2235-2240.

Okamoto, K., Nagai, T., Miyawaki, A., & Hayashi, Y. (2004). Rapid and persistent modulation of actin dynamics regulates postsynaptic reorganization underlying bidirectional plasticity. N*at Neurosci, 7(*10), 1104-1112.

Ongur, D., & Price, J. L. (2000). The organization of networks within the orbital and medial prefrontal cortex of rats, monkeys and humans. C*ereb Cortex, 10(*3), 206-219.

Orr, S. P., Metzger, L. J., Lasko, N. B., Macklin, M. L., Peri, T., & Pitman, R. K. (2000). De novo conditioning in trauma-exposed individuals with and without posttraumatic stress disorder. J *Abnorm Psychol, 109(*2), 290-298.

Ostroff, L. E., Cain, C. K., Jindal, N., Dar, N., & Ledoux, J. E. (2012). Stability of presynaptic vesicle pools and changes in synapse morphology in the amygdala following fear learning in adult rats. J *Comp Neurol, 520(*2), 295-314.

Oswald, M. J., Oorschot, D. E., Schulz, J. M., Lipski, J., & Reynolds, J. N. (2009). IH current generates the afterhyperpolarisation following activation of subthreshold cortical synaptic inputs to striatal cholinergic interneurons. J *Physiol, 587(*Pt 24), 5879-5897. doi: 10.1113/jphysiol.2009.177600

Otsuka, T., & Kawaguchi, Y. (2008). Firing-pattern-dependent specificity of cortical excitatory feed-forward subnetworks. J *Neurosci, 28(*44), 11186-11195. doi: 10.1523/JNEUROSCI.1921-08.2008

Pape, H. C. (1996). Queer current and pacemaker: the hyperpolarization-activated cation current in neurons. A*nnu Rev Physiol, 58,* 299-327.

Pare, D., & Collins, D. R. (2000). Neuronal correlates of fear in the lateral amygdala: multiple extracellular recordings in conscious cats. J *Neurosci, 20(*7), 2701-2710.

Pare, D., & Smith, Y. (1993a). Distribution of GABA immunoreactivity in the amygdaloid complex of the cat. N*euroscience, 57(*4), 1061-1076.

Pare, D., & Smith, Y. (1993b). The intercalated cell masses project to the central and medial nuclei of the amygdala in cats. N*euroscience, 57(*4), 1077-1090.

Parent, M. A., Wang, L., Su, J., Netoff, T., & Yuan, L. L. (2010). Identification of the hippocampal input to medial prefrontal cortex in vitro. C*ereb Cortex, 20(*2), 393-403.

Park, M., Penick, E. C., Edwards, J. G., Kauer, J. A., & Ehlers, M. D. (2004). Recycling endosomes supply AMPA receptors for LTP. S*cience, 305(*5692), 1972-1975.

Pavlov, I., Scimemi, A., Savtchenko, L., Kullmann, D. M., & Walker, M. C. (2011). I(h)-mediated depolarization enhances the temporal precision of neuronal integration. N*at Commun, 2,* 199.

Pavlov, I. P. (1927). C*onditioned reflexes.* Oxford, England: Oxford University Press.

Paxinos, G., & Watson, C. (1998). T*he Rat Brain in Stereotaxic Coordinates* (4 ed.). San Diego: Academic Press.

Perez-Cruz, C., Muller-Keuker, J. I., Heilbronner, U., Fuchs, E., & Flugge, G. (2007). Morphology of pyramidal neurons in the rat prefrontal cortex: lateralized dendritic remodeling by chronic stress. N*eural Plast, 2007,* 46276. doi: 10.1155/2007/46276

Perez-Jaranay, J. M., & Vives, F. (1991). Electrophysiological study of the response of medial prefrontal cortex neurons to stimulation of the basolateral nucleus of the amygdala in the rat. B*rain Res, 564(*1), 97-101.

Peri, T., Ben-Shakhar, G., Orr, S. P., & Shalev, A. Y. (2000). Psychophysiologic assessment of aversive conditioning in posttraumatic stress disorder. B*iol Psychiatry, 47(*6), 512-519.

Peters, A., & Kaiserman-Abramof, I. R. (1970). The small pyramidal neuron of the rat cerebral cortex. The perikaryon, dendrites and spines. A*m J Anat, 127(*4), 321-355.

Phelps, E. A., Delgado, M. R., Nearing, K. I., & LeDoux, J. E. (2004). Extinction learning in humans: role of the amygdala and vmPFC. N*euron, 43(*6), 897-905.

Phillips, R. G., & LeDoux, J. E. (1992). Differential contribution of amygdala and hippocampus to cued and contextual fear conditioning. B*ehav Neurosci, 106(*2), 274-285.

Poolos, N. P. (2012). Hyperpolarization-Activated Cyclic Nucleotide-Gated (HCN) Ion Channelopathy in Epilepsy. In J. L. Noebels, M. Avoli, M. A. Rogawski, R. W. Olsen & A. V. Delgado-Escueta (Eds.), J*asper's Basic Mechanisms of the Epilepsies* (4th ed.). Bethesda (MD).

Poorthuis, R. B., Bloem, B., Schak, B., Wester, J., de Kock, C. P., & Mansvelder, H. D. (2013). Layer-specific modulation of the prefrontal cortex by nicotinic acetylcholine receptors. C*ereb Cortex, 23(*1), 148-161. doi: 10.1093/cercor/bhr390

Power, J. M., Thompson, L. T., Moyer, J. R., Jr., & Disterhoft, J. F. (1997). Enhanced synaptic transmission in CA1 hippocampus after eyeblink conditioning. J *Neurophysiol, 78(*2), 1184-1187.

Power, J. M., Wu, W. W., Sametsky, E., Oh, M. M., & Disterhoft, J. F. (2002). Age-related enhancement of the slow outward calcium-activated potassium current in hippocampal CA1 pyramidal neurons in vitro. J *Neurosci, 22(*16), 7234-7243.

Quinn, J. J., Oommen, S. S., Morrison, G. E., & Fanselow, M. S. (2002). Post-training excitotoxic lesions of the dorsal hippocampus attenuate forward trace, backward trace, and delay fear conditioning in a temporally specific manner. H*ippocampus, 12(4*), 495-504.

Quirk, G. J. (2002). Memory for extinction of conditioned fear is long-lasting and persists following spontaneous recovery. L*earn Mem, 9(6*), 402-407.

Quirk, G. J., Repa, C., & LeDoux, J. E. (1995). Fear conditioning enhances short-latency auditory responses of lateral amygdala neurons: parallel recordings in the freely behaving rat. N*euron, 15(5*), 1029-1039.

Quirk, G. J., Russo, G. K., Barron, J. L., & Lebron, K. (2000). The role of ventromedial prefrontal cortex in the recovery of extinguished fear. J *Neurosci, 20(16*), 6225-6231.

Racca, C., Stephenson, F. A., Streit, P., Roberts, J. D., & Somogyi, P. (2000). NMDA receptor content of synapses in stratum radiatum of the hippocampal CA1 area. J *Neurosci, 20(7*), 2512-2522.

Racine, R. J., Wilson, D. A., Gingell, R., & Sunderland, D. (1986). Long-term potentiation in the interpositus and vestibular nuclei in the rat. E*xp Brain Res, 63(1*), 158-162.

Radley, J. J., Rocher, A. B., Miller, M., Janssen, W. G., Liston, C., Hof, P. R., . . . Morrison, J. H. (2006). Repeated stress induces dendritic spine loss in the rat medial prefrontal cortex. C*ereb Cortex, 16(3*), 313-320.

Radley, J. J., Rocher, A. B., Rodriguez, A., Ehlenberger, D. B., Dammann, M., McEwen, B. S., . . . Hof, P. R. (2008). Repeated stress alters dendritic spine morphology in the rat medial prefrontal cortex. J *Comp Neurol, 507(1*), 1141-1150.

Ramirez-Amaya, V., Balderas, I., Sandoval, J., Escobar, M. L., & Bermudez-Rattoni, F. (2001). Spatial long-term memory is related to mossy fiber synaptogenesis. J *Neurosci, 21(*18), 7340-7348.

Ramirez-Amaya, V., Escobar, M. L., Chao, V., & Bermudez-Rattoni, F. (1999). Synaptogenesis of mossy fibers induced by spatial water maze overtraining. H*ippocampus, 9(*6), 631-636.

Rauch, S. L., Shin, L. M., Segal, E., Pitman, R. K., Carson, M. A., McMullin, K., . . . Makris, N. (2003). Selectively reduced regional cortical volumes in post-traumatic stress disorder. N*euroreport, 14(*7), 913-916.

Rauch, S. L., van der Kolk, B. A., Fisler, R. E., Alpert, N. M., Orr, S. P., Savage, C. R., . . . Pitman, R. K. (1996). A symptom provocation study of posttraumatic stress disorder using positron emission tomography and script-driven imagery. A*rch Gen Psychiatry, 53(*5), 380-387.

Rees, G. (2007). Neural correlates of the contents of visual awareness in humans. P*hilos Trans R Soc Lond B Biol Sci, 362(*1481), 877-886.

Rescorla, R. A. (2001). Are associative changes in acquisition and extinction negatively accelerated? J *Exp Psychol Anim Behav Process, 27(*4), 307-315.

Restivo, L., Vetere, G., Bontempi, B., & Ammassari-Teule, M. (2009). The formation of recent and remote memory is associated with time-dependent formation of dendritic spines in the hippocampus and anterior cingulate cortex. J *Neurosci, 29(*25), 8206-8214.

Richmond, M. A., Yee, B. K., Pouzet, B., Veenman, L., Rawlins, J. N., Feldon, J., & Bannerman, D. M. (1999). Dissociating context and space within the hippocampus:

effects of complete, dorsal, and ventral excitotoxic hippocampal lesions on conditioned freezing and spatial learning. B*ehav Neurosci, 113(*6), 1189-1203.

Roberts, T. F., Tschida, K. A., Klein, M. E., & Mooney, R. (2010). Rapid spine stabilization and synaptic enhancement at the onset of behavioural learning. N*ature, 463(*7283), 948-952.

Rodrigues, S. M., Schafe, G. E., & LeDoux, J. E. (2004). Molecular mechanisms underlying emotional learning and memory in the lateral amygdala. N*euron, 44(*1), 75-91.

Rodriguez, A., Ehlenberger, D. B., Dickstein, D. L., Hof, P. R., & Wearne, S. L. (2008). Automated three-dimensional detection and shape classification of dendritic spines from fluorescence microscopy images. P*LoS One, 3(*4), e1997.

Rogan, M. T., Staubli, U. V., & LeDoux, J. E. (1997). Fear conditioning induces associative long-term potentiation in the amygdala. N*ature, 390(*6660), 604-607.

Romanski, L. M., Clugnet, M. C., Bordi, F., & LeDoux, J. E. (1993). Somatosensory and auditory convergence in the lateral nucleus of the amygdala. B*ehav Neurosci, 107(*3), 444-450.

Romanski, L. M., & LeDoux, J. E. (1992). Equipotentiality of thalamo-amygdala and thalamo-cortico-amygdala circuits in auditory fear conditioning. J *Neurosci, 12(*11), 4501-4509.

Rosenkranz, J., & Grace, A. (2002). Dopamine-mediated modulation of odour-evoked amygdala potentials during pavlovian conditioning. N*ature, 417(*6886), 282-287.

Royer, S., Martina, M., & Pare, D. (1999). An inhibitory interface gates impulse traffic between the input and output stations of the amygdala. J *Neurosci, 19(*23)*, 10575-10583.

Rumpel, S., LeDoux, J. E., Zador, A., & Malinow, R. (2005). Postsynaptic receptor trafficking underlying a form of associative learning. S*cience, 308(*5718), 83-88.

Runyan, J. D., Moore, A. N., & Dash, P. K. (2004). A role for prefrontal cortex in memory storage for trace fear conditioning. J *Neurosci, 24(*6), 1288-1295.

Rusakov, D. A., Davies, H. A., Harrison, E., Diana, G., Richter-Levin, G., Bliss, T. V., & Stewart, M. G. (1997). Ultrastructural synaptic correlates of spatial learning in rat hippocampus. N*euroscience, 80(*1), 69-77.

Saar, D., & Barkai, E. (2003). Long-term modifications in intrinsic neuronal properties and rule learning in rats. E*ur J Neurosci, 17(*12), 2727-2734.

Saar, D., Grossman, Y., & Barkai, E. (1998). Reduced after-hyperpolarization in rat piriform cortex pyramidal neurons is associated with increased learning capability during operant conditioning. E*ur J Neurosci, 10(*4), 1518-1523.

Sah, P. (1996). Ca(2+)-activated K+ currents in neurones: types, physiological roles and modulation. T*rends Neurosci, 19(*4), 150-154.

Sah, P., & Bekkers, J. M. (1996). Apical dendritic location of slow afterhyperpolarization current in hippocampal pyramidal neurons: implications for the integration of long-term potentiation. J *Neurosci, 16(*15), 4537-4542.

Sakata, S., & Harris, K. D. (2009). Laminar structure of spontaneous and sensory-evoked population activity in auditory cortex. N*euron, 64(*3), 404-418. doi: 10.1016/j.neuron.2009.09.020

Sanchez-Vives, M. V., & McCormick, D. A. (2000). Cellular and network mechanisms of rhythmic recurrent activity in neocortex. N*at Neurosci, 3(*10), 1027-1034. doi: 10.1038/79848

Santini, E., & Porter, J. T. (2010). M-type potassium channels modulate the intrinsic excitability of infralimbic neurons and regulate fear expression and extinction. J *Neurosci, 30(*37), 12379-12386.

Santini, E., Quirk, G. J., & Porter, J. T. (2008). Fear conditioning and extinction differentially modify the intrinsic excitability of infralimbic neurons. J *Neurosci, 28(*15), 4028-4036.

Santoro, B., Lee, J. Y., Englot, D. J., Gildersleeve, S., Piskorowski, R. A., Siegelbaum, S. A., . . . Blumenfeld, H. (2010). Increased seizure severity and seizure-related death in mice lacking HCN1 channels. E*pilepsia, 51(*8), 1624-1627. doi: 10.1111/j.1528-1167.2010.02554.x

Schafe, G. E., & LeDoux, J. E. (2000). Memory consolidation of auditory pavlovian fear conditioning requires protein synthesis and protein kinase A in the amygdala. J *Neurosci, 20(*18), RC96.

Schulz, D. J. (2006). Plasticity and stability in neuronal output via changes in intrinsic excitability: it's what's inside that counts. J *Exp Biol, 209(*Pt 24), 4821-4827.

Scoville, W. B., & Milner, B. (1957). Loss of recent memory after bilateral hippocampal lesions. J *Neurol Neurosurg Psychiatry, 20(*1), 11-21.

Sehgal, M., Ehlers, V. L., & Moyer, J. R., Jr. (2014). Learning enhances intrinsic excitability in a subset of lateral amygdala neurons. L*earn Mem, 21(*3), 161-170. doi: 10.1101/lm.032730.113

Sehgal, M., Song, C., Ehlers, V. L., & Moyer, J. R., Jr. (2013). Learning to learn - Intrinsic plasticity as a metaplasticity mechanism for memory formation. N*eurobiol Learn Mem.* doi: 10.1016/j.nlm.2013.07.008

Sesack, S. R., Deutch, A. Y., Roth, R. H., & Bunney, B. S. (1989). Topographical organization of the efferent projections of the medial prefrontal cortex in the rat: an anterograde tract-tracing study with Phaseolus vulgaris leucoagglutinin. *J Comp Neurol, 290*(2), 213-242.

Shin, L. M., Orr, S. P., Carson, M. A., Rauch, S. L., Macklin, M. L., Lasko, N. B., . . . Pitman, R. K. (2004). Regional cerebral blood flow in the amygdala and medial prefrontal cortex during traumatic imagery in male and female Vietnam veterans with PTSD. A*rch Gen Psychiatry, 61(*2), 168-176.

Shin, L. M., Wright, C. I., Cannistraro, P. A., Wedig, M. M., McMullin, K., Martis, B., ... Rauch, S. L. (2005). A functional magnetic resonance imaging study of amygdala and medial prefrontal cortex responses to overtly presented fearful faces in posttraumatic stress disorder. A*rch Gen Psychiatry, 62(*3), 273-281.

Siegel, J. J., Kalmbach, B., Chitwood, R. A., & Mauk, M. D. (2011). Persistent activity in a cortical-to-subcortical circuit: bridging the temporal gap in trace eyelid conditioning. J *Neurophysiol, 107(*1), 50-64.

Sierra-Mercado, D., Corcoran, K. A., Lebron-Milad, K., & Quirk, G. J. (2006). Inactivation of the ventromedial prefrontal cortex reduces expression of conditioned fear and impairs subsequent recall of extinction. E*ur J Neurosci, 24(*6), 1751-1758.

Smith, D. R., Gallagher, M., & Stanton, M. E. (2007). Genetic background differences and nonassociative effects in mouse trace fear conditioning. L*earn Mem, 14(*9), 597-605.

Solomon, P. R., Vander Schaaf, E. R., Thompson, R. F., & Weisz, D. J. (1986). Hippocampus and trace conditioning of the rabbit's classically conditioned nictitating membrane response. B*ehav Neurosci, 100(*5), 729-744.

Song, C., Detert, J. A., Sehgal, M., & Moyer, J. R., Jr. (2012). Trace fear conditioning enhances synaptic and intrinsic plasticity in rat hippocampus. J *Neurophysiol, 107(*12), 3397-3408.

Squire, L. R. (1992). Memory and the hippocampus: a synthesis from findings with rats, monkeys, and humans. P*sychol Rev, 99(*2), 195-231.

Squire, L. R. (2009). The legacy of patient H.M. for neuroscience. N*euron, 61(*1), 6-9.

Steriade, M., Contreras, D., Curro Dossi, R., & Nunez, A. (1993). The slow (< 1 Hz) oscillation in reticular thalamic and thalamocortical neurons: scenario of sleep rhythm generation in interacting thalamic and neocortical networks. J *Neurosci, 13(*8), 3284-3299.

Steriade, M., Nunez, A., & Amzica, F. (1993). A novel slow (< 1 Hz) oscillation of neocortical neurons in vivo: depolarizing and hyperpolarizing components. J *Neurosci, 13(*8), 3252-3265.

Storm, J. F. (1989). An after-hyperpolarization of medium duration in rat hippocampal pyramidal cells. J *Physiol, 409,* 171-190.

Suh, J., Rivest, A. J., Nakashiba, T., Tominaga, T., & Tonegawa, S. (2011). Entorhinal cortex layer III input to the hippocampus is crucial for temporal association memory. S*cience, 334(*6061), 1415-1420.

Sui, L., Wang, J., & Li, B. M. (2008). Role of the phosphoinositide 3-kinase-Akt-mammalian target of the rapamycin signaling pathway in long-term potentiation and trace fear conditioning memory in rat medial prefrontal cortex. L*earn Mem, 15(*10), 762-776.

Sweatt, J. D. (2003). M*echanisms of Memory (*1 ed.). Burlington: Academic Press.

Sweatt, J. D. (2004). Hippocampal function in cognition. P*sychopharmacology (Berl), 174(*1), 99-110.

Takumi, Y., Ramirez-Leon, V., Laake, P., Rinvik, E., & Ottersen, O. P. (1999). Different modes of expression of AMPA and NMDA receptors in hippocampal synapses. N*at Neurosci, 2(*7), 618-624.

Teng, E., & Squire, L. R. (1999). Memory for places learned long ago is intact after hippocampal damage. N*ature, 400(*6745), 675-677.

Thompson, L. T., Moyer, J. R., Jr., & Disterhoft, J. F. (1996a). Trace eyeblink conditioning in rabbits demonstrates heterogeneity of learning ability both between and within age groups. N*eurobiol Aging, 17(*4), 619-629.

Thompson, L. T., Moyer, J. R., Jr., & Disterhoft, J. F. (1996b). Transient changes in excitability of rabbit CA3 neurons with a time course appropriate to support memory consolidation. J *Neurophysiol, 76(*3), 1836-1849.

Thomson, A. M., & Bannister, A. P. (1998). Postsynaptic pyramidal target selection by descending layer III pyramidal axons: dual intracellular recordings and biocytin filling in slices of rat neocortex. N*euroscience, 84(*3), 669-683.

Thomson, A. M., West, D. C., Wang, Y., & Bannister, A. P. (2002). Synaptic connections and small circuits involving excitatory and inhibitory neurons in layers 2-5 of adult rat and cat neocortex: triple intracellular recordings and biocytin labelling in vitro. C*ereb Cortex, 12(*9), 936-953.

Thuault, S. J., Malleret, G., Constantinople, C. M., Nicholls, R., Chen, I., Zhu, J., . . . Kandel, E. R. (2013). Prefrontal cortex HCN1 channels enable intrinsic persistent neural firing and executive memory function. J *Neurosci, 33(*34), 13583-13599. doi: 10.1523/JNEUROSCI.2427-12.2013

Tombaugh, G. C., Rowe, W. B., Chow, A. R., Michael, T. H., & Rose, G. M. (2002). Theta-frequency synaptic potentiation in CA1 in vitro distinguishes cognitively impaired from unimpaired aged Fischer 344 rats. J *Neurosci, 22(*22), 9932-9940.

Trachtenberg, J. T., Chen, B. E., Knott, G. W., Feng, G., Sanes, J. R., Welker, E., & Svoboda, K. (2002). Long-term in vivo imaging of experience-dependent synaptic plasticity in adult cortex. N*ature, 420(*6917), 788-794.

Tschida, K. A., & Mooney, R. (2012). Deafening drives cell-type-specific changes to dendritic spines in a sensorimotor nucleus important to learned vocalizations. N*euron, 73(*5), 1028-1039.

Turner, B. H., & Zimmer, J. (1984). The architecture and some of the interconnections of the rat's amygdala and lateral periallocortex. J *Comp Neurol, 227(*4), 540-557.

Urban, N. N., & Barrionuevo, G. (1996). Induction of hebbian and non-hebbian mossy fiber long-term potentiation by distinct patterns of high-frequency stimulation. J *Neurosci, 16(*13), 4293-4299.

Vaidya, S. P., & Johnston, D. (2013). Temporal synchrony and gamma-to-theta power conversion in the dendrites of CA1 pyramidal neurons. N*at Neurosci, 16(*12), 1812-1820. doi: 10.1038/nn.3562

Valverde, F. (1967). Apical dendritic spines of the visual cortex and light deprivation in the mouse. E*xp Brain Res, 3(*4), 337-352.

Van der Zee, E. A., Palm, I. F., O'Connor, M., Maizels, E. T., Hunzicker-Dunn, M., & Disterhoft, J. F. (2004). Aging-related alterations in the distribution of Ca(2+)-dependent PKC isoforms in rabbit hippocampus. H*ippocampus, 14(*7), 849-860.

Vertes, R. P. (2004). Differential projections of the infralimbic and prelimbic cortex in the rat. S*ynapse, 51(*1), 32-58.

Vetere, G., Restivo, L., Novembre, G., Aceti, M., Lumaca, M., & Ammassari-Teule, M. (2011). Extinction partially reverts structural changes associated with remote fear memory. L*earn Mem, 18(*9), 554-557.

Vidal-Gonzalez, I., Vidal-Gonzalez, B., Rauch, S. L., & Quirk, G. J. (2006). Microstimulation reveals opposing influences of prelimbic and infralimbic cortex on the expression of conditioned fear. L*earn Mem, 13(*6), 728-733.

Vouimba, R. M., & Maroun, M. (2011). Learning-induced changes in mPFC-BLA connections after fear conditioning, extinction, and reinstatement of fear. N*europsychopharmacology, 36(*11), 2276-2285. doi: 10.1038/npp.2011.115

Walikonis, R. S., Jensen, O. N., Mann, M., Provance, D. W., Jr., Mercer, J. A., & Kennedy, M. B. (2000). Identification of proteins in the postsynaptic density fraction by mass spectrometry. J *Neurosci, 20(*11), 4069-4080.

Wang, M., Ramos, B. P., Paspalas, C. D., Shu, Y., Simen, A., Duque, A., . . . Arnsten, A. F. (2007). Alpha2A-adrenoceptors strengthen working memory networks by inhibiting cAMP-HCN channel signaling in prefrontal cortex. C*ell, 129(*2), 397-410.

Wearne, S. L., Rodriguez, A., Ehlenberger, D. B., Rocher, A. B., Henderson, S. C., & Hof, P. R. (2005). New techniques for imaging, digitization and analysis of three-dimensional neural morphology on multiple scales. N*euroscience, 136(*3), 661-680.

Weike, A. I., Schupp, H. T., & Hamm, A. O. (2007). Fear acquisition requires awareness in trace but not delay conditioning. P*sychophysiology, 44(*1), 170-180.

Wessa, M., & Flor, H. (2007). Failure of extinction of fear responses in posttraumatic stress disorder: evidence from second-order conditioning. A*m J Psychiatry, 164(*11), 1684-1692. doi: 10.1176/appi.ajp.2007.07030525

Whitlock, J. R., Heynen, A. J., Shuler, M. G., & Bear, M. F. (2006). Learning induces long-term potentiation in the hippocampus. S*cience, 313(*5790), 1093-1097.

Williams, S., & Johnston, D. (1989). Long-term potentiation of hippocampal mossy fiber synapses is blocked by postsynaptic injection of calcium chelators. N*euron, 3(*5), 583-588.

Williams, S. R., Christensen, S. R., Stuart, G. J., & Hausser, M. (2002). Membrane potential bistability is controlled by the hyperpolarization-activated current I(H) in rat cerebellar Purkinje neurons in vitro. J *Physiol, 539(*Pt 2), 469-483.

Witter, M. P., Groenewegen, H. J., Lopes da Silva, F. H., & Lohman, A. H. (1989). Functional organization of the extrinsic and intrinsic circuitry of the parahippocampal region. P*rog Neurobiol, 33(*3), 161-253.

Xiao, D., Zikopoulos, B., & Barbas, H. (2009). Laminar and modular organization of prefrontal projections to multiple thalamic nuclei. N*euroscience, 161(*4), 1067-1081.

Xu, J., Kang, N., Jiang, L., Nedergaard, M., & Kang, J. (2005). Activity-dependent long-term potentiation of intrinsic excitability in hippocampal CA1 pyramidal neurons. J *Neurosci, 25(*7), 1750-1760.

Xu, T., Yu, X., Perlik, A. J., Tobin, W. F., Zweig, J. A., Tennant, K., . . . Zuo, Y. (2009). Rapid formation and selective stabilization of synapses for enduring motor memories. N*ature, 462(*7275), 915-919.

Yaffe, K., Vittinghoff, E., Lindquist, K., Barnes, D., Covinsky, K. E., Neylan, T., . . . Marmar, C. (2010). Posttraumatic stress disorder and risk of dementia among US veterans. A*rch Gen Psychiatry, 67(*6), 608-613.

Yamashita, T., Pala, A., Pedrido, L., Kremer, Y., Welker, E., & Petersen, C. C. (2013). Membrane potential dynamics of neocortical projection neurons driving target-specific signals. N*euron, 80(*6), 1477-1490. doi: 10.1016/j.neuron.2013.10.059

Yamasue, H., Kasai, K., Iwanami, A., Ohtani, T., Yamada, H., Abe, O., . . . Kato, N. (2003). Voxel-based analysis of MRI reveals anterior cingulate gray-matter volume reduction in posttraumatic stress disorder due to terrorism. P*roc Natl Acad Sci U S A, 100(*15), 9039-9043.

Yang, G., Pan, F., & Gan, W. B. (2009). Stably maintained dendritic spines are associated with lifelong memories. N*ature, 462(*7275), 920-924.

Yang, N., Higuchi, O., Ohashi, K., Nagata, K., Wada, A., Kangawa, K., . . . Mizuno, K. (1998). Cofilin phosphorylation by LIM-kinase 1 and its role in Rac-mediated actin reorganization. N*ature, 393(*6687), 809-812. doi: 10.1038/31735

Yankova, M., Hart, S. A., & Woolley, C. S. (2001). Estrogen increases synaptic connectivity between single presynaptic inputs and multiple postsynaptic CA1 pyramidal cells: a serial electron-microscopic study. P*roc Natl Acad Sci U S A, 98(*6), 3525-3530.

Yeckel, M. F., Kapur, A., & Johnston, D. (1999). Multiple forms of LTP in hippocampal CA3 neurons use a common postsynaptic mechanism. N*at Neurosci, 2(*7), 625-633.

Yi, E., Roux, I., & Glowatzki, E. (2010). Dendritic HCN channels shape excitatory postsynaptic potentials at the inner hair cell afferent synapse in the mammalian cochlea. J *Neurophysiol, 103(*5), 2532-2543. doi: 10.1152/jn.00506.2009

Ying, S. W., Jia, F., Abbas, S. Y., Hofmann, F., Ludwig, A., & Goldstein, P. A. (2007). Dendritic HCN2 channels constrain glutamate-driven excitability in reticular thalamic neurons. J *Neurosci, 27(*32), 8719-8732. doi: 10.1523/JNEUROSCI.1630-07.2007

Yuste, R., & Bonhoeffer, T. (2001). Morphological changes in dendritic spines associated with long-term synaptic plasticity. A*nnu Rev Neurosci, 24,* 1071-1089.

Yuste, R., & Bonhoeffer, T. (2004). Genesis of dendritic spines: insights from ultrastructural and imaging studies. N*at Rev Neurosci, 5(*1), 24-34.

Zelcer, I., Cohen, H., Richter-Levin, G., Lebiosn, T., Grossberger, T., & Barkai, E. (2006). A cellular correlate of learning-induced metaplasticity in the hippocampus. *Cereb Cortex, 16(*4), 460-468.

Zhang, W., & Linden, D. J. (2003). The other side of the engram: experience-driven changes in neuronal intrinsic excitability. N*at Rev Neurosci, 4(*11), 885-900.

Zola-Morgan, S. M., & Squire, L. R. (1990). The primate hippocampal formation: evidence for a time-limited role in memory storage. S*cience, 250(*4978), 288-290.

CURRICULUM VITAE

Chenghui Song

EDUCATION

Ph.D. student

University of Wisconsin – Milwaukee

Department of Psychology

Advisor: James R. Moyer, Jr. PhD

Departmental Major: Neuroscience

Departmental Minors: Neurobiology, Behavior Analysis

M.S., 2003

Third Military Medical University, Chongqing, China.

Major: Neurobiology

B.S., 1995

Military Medical University, Chongqing, China.

Major: Medical Laboratory Technology

RESEARCH/PROFESSIONAL EXPERIENCE

2006-present *Graduate research assistant*, UW-Milwaukee. Moyer Lab

2003-2006 *Research Assistant*, Center for Disease Control and Prevention (CDC)**,** Shenyang, China

2000-2003 *Graduate research assistant*, TMMU, Hu Lab

1995-2000 *Research Assistant*, Center for Disease Control and Prevention (CDC)**,** Shenyang, China

TEACHING EXPERIENCE

Spring 2013 *Guest Lecturer*, UW-Milwaukee

Physiological Psychology, 1 class (synaptic plasticity)

Spring 2013 *Teaching Assistant,* UW-Milwaukee

Physiological Psychology (Dr. Mary R Lonergan)

Fall 2012	*Teaching Assistant,* UW-Milwaukee
	Physiological Psychology (Dr. James R. Moyer, Jr.)
Spring 2012	*Teaching Assistant,* UW-Milwaukee
	Physiological Psychology (Dr. James R. Moyer, Jr.)
Fall 2011	*Teaching Assistant,* UW-Milwaukee
	Physiological Psychology (Dr. James R. Moyer, Jr.)
Spring 2011	*Teaching Assistant,* UW-Milwaukee
	Physiological Psychology (Dr. James R. Moyer, Jr.)
2006-2011	*Grader* for 3-4 courses per semester

AWARDS AND HONORS

2012	Department of Psychology Graduate Research Award at UWM for top peer-reviewed manuscript
2011	Graduate Student Travel Award at UWM
2010	Graduate Student Travel Award at UWM
2009	Graduate Student Travel Award at UWM
2008	Graduate Student Travel Award at UWM

PUBLICATIONS

Sehgal, M., **Song, C**., Ehler, V.L., & Moyer, J.R., Jr. (2013). Learning to learn – intrinsic plasticity as a metaplasticity mechanism for memory formation. *Neurobiol Learn Mem.* Doi:10.1016/j.nlm.2013.07.008.

Song, C., Detert, J. A., Sehgal, M., & Moyer, J. R., Jr. (2012). Trace Fear Conditioning Enhances Synaptic and Intrinsic Plasticity in Rat Hippocampus. *J Neurophysiol.,* 107(12):3397-3408.

Song, C., Chen, X., Xia, J., Yu, Z., and Hu, Z. (2006). Modulatory Effects of Hypocretin-1/orexin-A with Glutamate and Gamma-aminobutyric Acid on Freshly Isolated Pyramidal Neurons from the Rat Prefrontal Cortex. *Neurosci Lett.,*399, 101-105.

Song C., Xia, J.., Ye, J., Chen, X., Zhang, C., Gao, E., and Hu, Z. (2005). Signaling Pathways of Hypocretin-1 Actions on Pyramidal Neurons in the Rat Prefrontal Cortex. *Neuroreport*, 16, 1529-1533.

Xia, J., Chen, X. **Song, C.,** Ye, J., Yu, Z., and Hu, Z. (2005). Postsynaptic Excitation of Prefrontal Cortical Pyramidal Neurons by Hypocretin-1/orexin A through the Inhibition of Potassium Currents. *J Neurosci Res.,* 82, 729-736.

Song C., Hu, Z, Ruan, H., *et al.* (2003). Effects of Glutamic Acid and GABA on Spontaneous Activity of Pyramidal Cells of Frontal Cortex in Rats. *Acta Academiae Medicinae Militaris Tertiae*; 25(10): 858-861.

Song C., Hu, Z. (2003). Orexin: an Important Neuropeptide of Arousal Pathway from Hypothalamus. *Acta Academiae Medicinae Militaris Tertiae,* 25(13): 1207-1209.

Song C., Liu, X. (2001). Mechanisms and Disinfection Effect of TiO2-mediated Photocatalytic Oxidation. *Chinese Journal of Disinfection,* 18(3) 169-173.

Chen, C., Liu, X., **Song, C.**, *et al.* (2000). Comparison of Performance between Two Formulations of Chlorine Dioxide. *Chinese Journal of Disinfection*, 17(3):168-170.

MANUSCRIPTS IN PREPARATION

Song, C. & Moyer, J.R., (in preparation). Layer- and region-specific electrophysiological properties of mPFC neurons.

Song, C. Ehlers V.L., Aitken, J. C., Bula, T., & Moyer, J.R., (in preparation). Trace fear conditioning and extinction differentially modulate intrinsic excitability of mPFC-amygdala projection neurons.

Song, C. Ehlers V.L., Aitken, J. C., Bula, T., & Moyer, J.R., (in preparation). Effect of trace fear conditioning and extinction on spine density of mPFC-amygdala projection neurons.

ABSTRACTS AND POSTER PRESENTATIONS

Song, C., Ehlers, V. L., Aitken, J. C., Bula, T., Moyer, J. R., Jr. (2014) Trace fear conditioning and extinction differentially modulate intrinsic excitability of mPFC neurons that project to the amygdala. 44th annual meeting of the *Society for Neuroscience, abstract.*

Moyer, J. R., Jr., Ehlers, V. L., **Song, C.**, Layer- and region-specific differences in the neurophysiological properties of medial prefrontal cortical neurons. 44th annual meeting of the *Society for Neuroscience, abstract.*

Song, C., Ehlers, V. L., Aitken, J. C., Bula, T., Moyer, J. R., Jr. (2014) Effect of trace fear conditioning and extinction on mPFC-amygdala projection neurons. 43th annual meeting of the *Society for Neuroscience, abstract and poster presentation 93.12.*

Song, C., Ehlers, V. L., Aitken, J. C., Bula, T., Moyer, J. R., Jr. (2013) Effect of trace fear conditioning and extinction on mPFC-amygdala projection neurons. 12th annual meeting of *the Molecular and Cellular Cognition Society, abstract and poster presentation.*

Song, C., Ehlers, V. L., Aitken, J. C., Bula, T., Moyer, J. R., Jr. (2013) Effect of trace fear conditioning and extinction on mPFC-amygdala projection neurons *Society for Neuroscience Milwaukee Area Chapter Meeting, poster presentation 93.12.*

Song, C., Ehlers V.L., Aitken, J. C., Bula, T., Moyer, J. R., jr. (2012). Circuit-specific study of fear conditioning and extinction in mPFC neurons. *Society for Neuroscience Milwaukee Area Chapter Meeting, poster presentation 12.*

Song, C., Aitken, J. C., Hilty, B. W., Moyer, J. R., jr. (2012). Electrophysiological properties of medial prefrontal cortex-amygdala projection neurons. 42th annual meeting of the *Society for Neuroscience meeting, abstract and poster presentation 291.05.*

Song, C., Moyer, J. R., jr. (2011). Characteristics of Medial Prefrontal Cortex – Basal Lateral Amygdala Projection Neurons. 41th annual meeting of the *Society for Neuroscience meeting, abstract and poster presentation 727.10.*

Song, C., Detert, J.A., Sehgal, M., Moyer, J. R., jr. (2011). Trace Fear Conditioning Enhances Synaptic and Intrinsic Plasticity in Rat Hippocampus. *Pavlovian Society annual meeting, poster presentation 28.*

Song, C., Detert, J.A., O'Hara, D.T., Sehgal, M., Moyer, J. R., jr. (2010). Enhancement of synaptic and intrinsic plasticity in hippocampus after trace fear conditioning. *Society for Neuroscience Milwaukee Area Chapter Meeting, poster presentation.*

Song, C., O'Hara, D. T., Detert, J. A., Sehgal, M., Moyer, J. R., jr. (2009). Learning-induced synaptic and intrinsic plasticity in hippocampus. 39th annual meeting of the *Society for Neuroscience, abstract and poster presentation 319.19.*

Song, C., O'Hara, D. T., Detert, J. A., Moyer, J. R., jr. (2009). Learning - Induced Synaptic and Intrinsic Plasticity in Hippocampus. *The Milwaukee Chapter for the Society for Neuroscience & 26th Midwest Neurobiology Meeting, poster presentation P31.*

Song, C., O'Hara, D. T., Detert, J. A., Moyer, J. R., jr. (2008). Effects of Trace Fear Conditioning on Hippocampal CA1 Synaptic Plasticity. 38th annual meeting of the *Society for Neuroscience, abstract and poster presentation 539.6.*

INVITED SYMPOSIUM PRESENTATION

Nanosymposium: "*Associative Learning and Fear Conditioning*", 40th annual meeting of the Society for Neuroscience, 11/17/2010.

COLLOQUIA AND SYMPOSIA

Effect of Trace fear conditioning and Extinction on mPFC-amygdala Projection neurons. Presented in part of a Data Blitz for Dr. Robert Sutherland (Univ. of Lethbridge). October 2013.

Long-term Extinction of Conditioned Fear Enhances Intrinsic Excitability of mPFC-Amygdala Projection Neurons. Neuroscience Group Seminar, UW-Milwaukee. September 2013.

Circuit-specific Study of Fear Conditioning and Extinction in mPFC Neurons. Presented at the 15th Annual Graduate Research Symposium. April 2013.

Characteristics of mPFC-Amygdala projection Neurons. Presented in part of a Data Blitz for Dr. Charan Ranganath (UC-Davis). March 2013.

Characteristics of mPFC-Amygdala projection Neurons. Presented in part of a Data Blitz for Dr. Jarrod Lewis-Peacock (Princeton University). January 2013.

Electrophysiological Properties of Medial Prefrontal Cortex-Amygdala Projection Neurons. Neuroscience Group Seminar, UW-Milwaukee. October 2012.

Electrophysiological Properties of Medial Prefrontal Cortex-Amygdala Projection Neurons. Presented at the 14th Annual Graduate Research Symposium. April 2012.

Characteristics of Medial Prefrontal Cortex - Amygdala Projection Neurons. Neuroscience Group Seminar, UW-Milwaukee. February2012.

Investigating Medial Prefrontal Cortical Contributions to Aging-related deficits in Cognitive Flexibility. Presented at the 13th Annual Graduate Research Symposium. April 2011.

Learning-specific Enhancement of Intrinsic and Synaptic Plasticity after Trace Fear conditioning. Presented in part of a Data Blitz for Dr. Gregory Quirk (Univ. of Puerto Rico). March 2011.

Trace Fear Conditioning Enhances Synaptic and Intrinsic Plasticity in Hippocampus. Presented at the 12th Annual Graduate Research Symposium. April 2010.

Trace Fear conditioning Enhances Synaptic and Intrinsic Plasticity in Hippocampus. Presented in part of a Data Blitz for Dr. Tom Carew (UC-Irvine). March 2010.

Trace Fear Conditioning Enhances Synaptic and Intrinsic Plasticity in Hippocampus. Neuroscience Group Seminar, UW-Milwaukee. December 2009.

Learning-induced Synaptic and Intrinsic Plasticity in Hippocampus. Presented at the 11th Annual Graduate Research Symposium. April 2009.

Learning-induced Synaptic and Intrinsic Plasticity in Hippocampus. Neuroscience Group Seminar, UW-Milwaukee. February 2009.

RELEVANT TECHNIQUES

Electrophysiology

Whole-cell somatic & dendritic patch clamp recording
Sharp intracellular recording
Field recording (LTP)
Proficient with both pClamp 10 and Patchmaster software for data acquisition & analysis

Confocal Laser Scanning Microscopy
Confocal imaging in brain sections
3D reconstruction with Neurolucida

Stereotaxic Brain surgery
Cannulae implantation and microinjections
Microinjections with glass pipettes

RT-PCR

Immunohistochemistry

PROFESSIONAL MEMBERSHIPS

2006-present	Society for Neuroscience
2006-present	The Milwaukee Chapter for the Society for Neuroscience
2006-present	Association for Graduate Students in Psychology
2006-present	Graduate Students in Behavioral Neuroscience
2009-present	Northwestern Psychological Association
2011-present	Pavlovian Society